



RETURNING MATERIALS:  
Place in book drop to  
remove this checkout from  
your record. FINES will  
be charged if book is  
returned after the date  
stamped below.

--	--	--

ASYMMETRIC HYDROGENATION OF PROCHIRAL OLEFINS  
WITH LAYERED SILICATE INTERCALATION CATALYSTS  
AND SYNTHESIS AND CHARACTERIZATION OF NEW  
FUNCTIONALIZED CHIRAL DIPHOSPHINE LIGANDS

By

Han-Min Chang

A DISSERTATION

Submitted to

Michigan State University

in partial fulfillment of the requirements

for the degree of

DOCTOR OF PHILOSOPHY

Department of Chemistry

1982

## ABSTRACT

### ASYMMETRIC HYDROGENATION OF PROCHIRAL OLEFINS WITH LAYERED SILICATE INTERCALATION CATALYSTS AND SYNTHESIS AND CHARACTERIZATION OF NEW FUNCTIONALIZED CHIRAL DIPHOSPHINE LIGANDS

By

Han-Min Chang

Cationic rhodium(I) complexes of the type  $\text{Rh}(\text{diene})(\text{diphos}^*)^+$ , where  $\text{diphos}^*$  is a chiral diphosphine ligand, (+)-2,3-*O*-isopropylidene-2,3-dihydroxy-1,4-bis(diphenylphosphino)butane [DIOP(+)], SPIPHOS, (*R*)-1,2-bis(diphenylphosphino)propane [(*R*)-Prophos] or (*R*)-1,2-bis(di-4'-methylphenylphosphino)propane [(*R*)-4-Me-Prophos] and where diene is norbornadiene (NBD) or 1,5-cyclooctadiene (COD), were intercalated into mica-type swelling layer silicates such as Na-hectorite. The preparations of the intercalation catalysts were readily achieved through simple cationic exchange. The intercalated rhodium(I) chiral diphosphine complexes were highly effective asymmetric hydrogenation catalysts for the hydrogenation of dehydroamino acids to the corresponding amino acids at ambient conditions. The effect of intercalation on optical yields as a function of substrate size, interlayer swelling and chelate ring size was studied.

Seven amino acid precursors of alanine, phenylalanine, tyrosine and DOPA were studied in the silicate and homogeneous systems. For the intercalated  $[\text{Rh}(\text{NBD})\text{DIOP}(+)]^+$  catalyst, the optical yields of the corresponding amino acids were comparable to the homogeneous results. When the ligand was SPIPHOS, (*R*)-Prophos or (*R*)-4-Me-Prophos, the optical yields were comparable to or lower than those obtained with the homogeneous analogues. The results obtained with the intercalated catalysts are comparable to those reported by others using rhodium diphos\* complexes immobilized on polymers.

The new, functionalized diphos\* ligand, 4-(1'-tetrahydropyranloxy)-1,2-(*R*)-bis(diphenylphosphino)butane [THP-butaphos], 4-hydroxy -1,2-(*R*)-bis(diphenylphosphino)butane [(*R*)-Hydroxylbutaphos] and 4-[[(*tert*-butoxy)carbonyl]-isobutylamino]-1,2-(*R*)-bis(di-4'-methylphenylphosphino)butane [*N*-BOC-butaphos] were synthesized from L-malic acid. The *N*-BOC-butaphos was highly effective for asymmetric hydrogenation of dehydroamino acids. The optical yields of the corresponding amino acids with homogeneous  $[\text{Rh}(\text{NBD})\text{N-BOC-butaphos}]^+\text{ClO}_4$  catalyst were in the range of 86-96%. The homogeneous catalyst was more effective and stereoselective in THF than in 95% EtOH.



© 1982

HAN-MIN CHANG

**All Rights Reserved**

TO MY PARENTS AND MICHELE

## ACKNOWLEDGEMENTS

I would like to sincerely thank Professor Thomas J. Pinnavaia for his guidance, support, and valuable advice throughout my graduate study. I would also like to extend my appreciation to Professor Carl H. Brubaker for editorial assistance as a second reader.

Thanks goes to my research committee and Professor William H. Reusch for his generosity in making laboratory equipment available.

I would like to acknowledge the financial support of the National Science Foundation and Michigan State University.

Special thanks to my parents and parents-in-law, and to my wife.

## TABLE OF CONTENTS

Chapter	Page
LIST OF TABLES . . . . .	viii
LIST OF FIGURES . . . . .	xv
INTRODUCTION	
I. The Historical Development of Asymmetric Hydrogenation . . . . .	4
II. Chiral Diphosphine Ligands and Their Application to Asymmetric Hydrogenation . . . . .	10
A. Rigid Ligands . . . . .	10
1. Ligands Chiral at Carbon Backbone . . . . .	10
2. Ligand Chirality at Phosphorus. .	16
B. DIOP and DIOP Analogues . . . . .	18
C. Pyrrolidinephosphines . . . . .	20
D. Ferrocenylphosphines . . . . .	24
E. Atropisomeric Ligands . . . . .	29
F. Bis-aminophosphines . . . . .	30
G. Polymeric Chiral Diphosphines . . . . .	35
III. Asymmetric Hydrogenation Mechanism Study . . . . .	40
A. Enamide Bonding Structure . . . . .	41
B. Proposed Mechanisms and Asymmetric Induction Steps . . . . .	41
C. <u>E-Z</u> Dehydroamino Acids Isomerization . . . . .	47

Chapter	Page
IV. Catalyst Supports . . . . .	47
V. Research Objectives . . . . .	51

## RESULTS AND DISCUSSION

I. Asymmetric Hydrogenation of Prochiral Olefins with Layered Silicate Intercalation Catalysts . . . . .	54
A. Diphosphine Ligands . . . . .	54
B. General Method for the Preparation of Cationic Catalysts . . . . .	60
C. Intercalation Catalysts and Interlayer Spacings . . . . .	62
D. Preparation of Dehydroamino Acid Derivatives via Unsaturated Azlactones . . . . .	63
E. Hydrogenation Conditions . . . . .	64
F. Characterization of Dehydroamino Acids and Their Corresponding $\alpha$ -Amino Acids . . . . .	67
G. Optical Yields . . . . .	71
1. (R)-Prophos (6) and (R)-4- Me-Prophos (49) Systems . . . . .	72
2. SPIPHOS (48) System . . . . .	77
3. DIOP(+) (3) System . . . . .	79
4. Solvent Effect on the Optical Yields . . . . .	82
5. The Effect of Rhodium Complex Precursor on Optical Yields . . . . .	83
6. Asymmetric Hydrogenation with Recycled Catalysts . . . . .	84



Chapter	Page
H. The Observed Hydrogenation Rates . . . .	87
I. A Comparison of Intercalated Rh(I)-DIOP ( <u>3</u> ) System with Other Rh(I)-DIOP Systems . . . . .	111
J. The Probable Asymmetric Hydrogenation Mechanism <sup>31</sup> P NMR Spectra of the Solution Structures of ( <u>R</u> )-4-Me- Prophos ( <u>49</u> ) and its Rhodium Complexes .	119
II. Synthesis and Characterization of New Functionalized Chiral Diphosphine Ligands . . . . .	132
A. Synthesis of the Key Synthetic Precursor . . . . .	135
B. Synthesis of 4-(1'-Tetrahydro- pyranloxy)-1,2-( <u>R</u> )-bis(diphenyl- Phosphino)butane, [THP-butaphos ( <u>51</u> )] and 4-Hydroxy -1,2-( <u>R</u> )- (diphenylphosphino)butane [( <u>R</u> )-Hydroxylbutaphos ( <u>52</u> )] . . . . .	137
C. Characterization of THP-butaphos ( <u>51</u> ) and ( <u>R</u> )-Hydroxylbutaphos ( <u>52</u> ) . . .	139
D. Synthesis of 4-{[( <i>tert</i> -Butyloxy) carbonyl]-isobutylamino}-1,2-( <u>R</u> )- bis(di-4'-methylphenylphosphino) butane [ <i>N</i> -BOC-butaphos ( <u>53</u> )] . . . . .	141
E. Characterization of 4-{[( <i>tert</i> - Butyloxy)carbonyl]-isobutylamino} 1,2-( <u>R</u> )-bis(di-4'-methylphenyl- phosphino)butane [ <i>N</i> -BOC-butaphos ( <u>53</u> )] . . . . .	144
F. The Observed Hydrogenation Rates and Optical Yields in the <i>N</i> -BOC- butaphos ( <u>53</u> ) System . . . . .	149
G. Suggested Future Work . . . . .	157
EXPERIMENTAL	
A. General . . . . .	160

Chapter	Page
B. Substrates . . . . .	162
C. Identification of $\alpha$ -Amino Acid Derivatives (Hydrogenated Products) . . . . .	165
D. Preparation of ( <i>R</i> )-Prophos ( <u>6</u> ) and ( <i>R</i> )-4-Me-Prophos ( <u>49</u> ) . . . . .	166
E. Preparation of the Synthetic Precursor, Acetonide-triol ( <u>58</u> ) . . . . .	170
F. Synthesis of THP-butaphos ( <u>51</u> ) and ( <i>R</i> )-Hydroxylbutaphos ( <u>52</u> ) . . . . .	170
G. Synthesis of <i>N</i> -BOC-butaphos ( <u>53</u> ) . . . . .	175
H. Hectorite . . . . .	180
I. Catalyst Precursors . . . . .	180
J. X-ray Powder Diffraction Measure- ments . . . . .	183
K. Hydrogenation Procedure . . . . .	184
L. Production Isolation . . . . .	185
M. Chemical Conversions . . . . .	185
N. Optical Yields . . . . .	186
APPENDIX . . . . .	187
BIBLIOGRAPHY . . . . .	205



## LIST OF TABLES

Table		Page
1	Asymmetric Hydrogenation of Prochiral Olefins Using a Rh(I)-PMePh- <i>n</i> -Pr (1) Catalyst Precursor . . . . .	5
2	Asymmetric Hydrogenation of Prochiral Olefins with Rh (-)DIOP (3) Catalyst Precursor . . . . .	7
3	Asymmetric Hydrogenation of ( <i>Z</i> )-Dehydroamino Acids with Rh(I)-ACMP (4) Catalyst Precursor . . . . .	9
4	Asymmetric Hydrogenation of Dehydroamino Acids Using DIOP (3) and Carbocyclic Analogues . . . . .	20
5	Asymmetric Hydrogenation of ( <i>Z</i> )-Dehydroamino Acids with <i>In-situ</i> Rh(I)-BPPM (23) Complex at 20°C and 50 atm . . . . .	22

Table		Page
6	Optical Yields of (R)-(-) Pantolactone by Using PPM (25) and its Analogues . . . . .	24
7	Asymmetric Hydrogenation Catalyzed by Rh(I)-(S)-(R)- BPPFA (27) Complex . . . . .	26
8	Asymmetric Hydrogenation of Carbonyl Compounds R <sup>1</sup> -CO-R <sup>2</sup> with (R)-(S)-BPPFOH (29) or (R)-(S)-BPPFA (28) . . . . .	27
9	Asymmetric Hydrogenation of Aminomethyl Aryl Ketones with (R)-(S)-BPPFOH (29) . . . . .	29
10	Asymmetric Hydrogenation of (Z)-Dehydroamino Acid Derivatives . . . . .	34
11	Asymmetric Hydrogenation of Itaconic Acid and (Z)-α- Acetamidocinnamic Acid with Polymer Supported Rh(I)- 4VB-PPM-HEMA (47) Catalysts and Homogeneous Analogues . . . . .	39
12	Spectra Parameters and Their Physical Properties of (R)- Prophos (6) and (R)-4-Me- Prophos (49) . . . . .	59

Table		Page
13	Preparation of ( <u>Z</u> )-Dehydro- Amino Acids . . . . .	65
14	<sup>13</sup> C NMR Chemical Shifts of Dehydroamino Acids and Their Corresponding α-Amino Acids in D <sub>6</sub> -DMSO Solution at 20.03 MHz and 25°C . . . . .	68
15	<sup>13</sup> C NMR Chemical Shifts of Dehydroamino Acids and Their Corresponding α-Amino Acids in D <sub>6</sub> -DMSO Solution at 20.03 MHz and 25°C . . . . .	69
16	<sup>13</sup> C NMR Chemical Shifts of Dopa Precursor and L-DOPA in D <sub>6</sub> -DMSO Solution at 20.05 MHz and 25°C . . . . .	70
17	Asymmetric Hydrogenation of Dehydroamino Acids with Intercalated and Homogeneous [Rh(NBD)( <u>R</u> )-Prophos ( <u>6</u> )] <sup>+</sup> Catalysts . . . . .	73
18	Asymmetric Hydrogenation of Dehydroamino Acids with Intercalated and Homogeneous [Rh(NBD)( <u>R</u> )-4-Me-Prophos ( <u>49</u> )] <sup>+</sup> Catalysts . . . . .	74

Table		Page
19	Difference in Optical Yields ( $Y_I - Y_H$ ) for Intercalated and Homogeneous Cationic [Rh(NBD)(diphos*)] <sup>+</sup> Precursors . . . . .	76
20	Asymmetric Hydrogenation of Dehydroamino Acids with Intercalated and Homogeneous [Rh(NBD)SPIPHOS (48)] <sup>+</sup> Catalysts . . . . .	78
21	Asymmetric Hydrogenation of Dehydroamino Acids with Intercalated and Homogeneous [Rh(NBD)DIOP(+)(3)] <sup>+</sup> Catalysts . . . . .	80
22	Solvent Effect on the Optical Yields of Hydrogenation Product of 1-Acetamino- 1-phenylethene with DIOP(+)(3) . . . . .	81
23	Asymmetric Hydrogenation of ( <u>Z</u> )- $\alpha$ -Benzamidocinnamic Acid with Intercalated and Homogeneous [Rh(NBD)( <u>R</u> )-Prophos (6)] <sup>+</sup> Catalysts . . . . .	82
24	Asymmetric Hydrogenation of Dehydroamino Acids with Intercalated and Homogeneous [Rh(diene)( <u>R</u> )-Prophos (6)] <sup>+</sup> Catalysts . . . . .	85

Table		Page
25	Asymmetric Hydrogenation of ( <u>Z</u> )- $\alpha$ -Acetamidocinnamic Acid with Recycled Intercalated [Rh(NBD)(diphos*)] <sup>+</sup> Catalysts . . . . .	86
26	Hydrogenation Rates for Intercalated [Rh(NBD)( <u>R</u> )-Prophos (6)] <sup>+</sup> Catalyst and Its Homogeneous Analogue . . . . .	100
27	Hydrogenation Rates for Intercalated [Rh(NBD)( <u>R</u> )- 4-Me-Prophos (49)] <sup>+</sup> Catalyst and Its Homogeneous Analogue . . . . .	101
28	Hydrogenation Rates for Intercalated [Rh(NBD)SPIPHOS (48)] <sup>+</sup> Catalyst and Its Homogeneous Analogue . . . . .	103
29	Hydrogenation Rates for Intercalated [Rh(NBD)DIOP(+) (3)] <sup>+</sup> Catalyst and Its Homogeneous Analogue . . . . .	105
30	Hydrogenation Rates of ( <u>Z</u> )- $\alpha$ -Acetamidocinnamic Acid with <i>In-situ</i> Rhodium Diphosphine Catalysts . . . . .	107

Table	Page
31	Asymmetric Hydrogenation of Prochiral Olefins with Polymer Supported Rh DIOP Catalyst and Homogeneous Analogue . . . . . 112
32	Optical Yields for the Intercalated [Rh(NBD)DIOP(+) ( <u>3</u> )] <sup>+</sup> System Compared with Other Rh(I)-DIOP Systems . . . . . 116
33	<sup>31</sup> P NMR Parameters of Chiral Diphosphines (L) and Their Rhodium(I) Complexes . . . . . 129
34	Hydrogenation Rates for Intercalated [Rh(NBD)- <i>N</i> -BOC- butaphos ( <u>53</u> )] <sup>+</sup> Catalyst and Its Homogeneous Analogue . . . . . 152
35	Asymmetric Hydrogenation of Dehydroamino Acids with Homogeneous [Rh(NBD)- <i>N</i> -BOC- butaphos ( <u>53</u> )] <sup>+</sup> Catalyst . . . . . 153
36	Asymmetric Hydrogenation of Dehydroamino Acids with Intercalated and Homogeneous [Rh(NBD)- <i>N</i> -BOC-butaphos ( <u>53</u> )] <sup>+</sup> Catalyst . . . . . 155

Table		Page
37	Basal Spacings of [Rh(NBD)diphos*] <sup>+</sup> - hectorite . . . . .	184
38	Specific Rotations of Pure Amino Acid Derivatives . . . . .	186
39	High Resolution Mass Spectrum of ( <u>R</u> )-4-Me-Prop <sup>h</sup> os (4 <u>9</u> ) . . . . .	202
40	High Resolution Mass Spectrum of <i>N</i> -BOC-butaphos (5 <u>3</u> ) . . . . .	202
41	High Resolution Mass Spectrum of Benzyl-di <sup>h</sup> ol (5 <u>9</u> ) . . . . .	203
42	High Resolution Mass Spectrum of (6 <u>4</u> ) . . . . .	203
43	High Resolution Mass Spectrum of <i>N</i> -BOC-aminodi <sup>h</sup> ol (6 <u>6</u> ) . . . . .	204

# LIST OF FIGURES

Figure		Page
1	X-ray structure of $[\text{Rh}(\text{DIPHOS})(\text{MAC})]^+$ . . . . .	42
2	Hydrogenation catalytic cycle by unsaturate route . . . . .	43
3	Hydrogenation catalytic cycle by the hydride route . . . . .	46
4	Structure of the mica-type swelling silicates such as montmorillonite or hectorite . . . . .	48
5	$^1\text{H}$ NMR spectrum of ( <i>R</i> )-4-Me- Prophos (49) in $\text{CDCl}_3$ at 25°C (60 MHz) . . . . .	61
6	Hydrogen uptake plots for reduction of 5 mmol of <i>N</i> -acetyldehydrophenylalanine with homogeneous and inter- calated $[\text{Rh}(\text{NBD})(\text{R})\text{-Prophos}$ $(\underline{6})]^+$ catalysts . . . . .	88
7	Hydrogen uptake plots for reduction of <i>N</i> -acetyldehydro- phenylalanine with intercalated $[\text{Rh}(\text{NBD})(\text{R})\text{-Prophos}(\underline{6})]^+$ catalyst and recycled catalyst . . . . .	90





Figure		Page
8	Hydrogen uptake plots for reduction of <i>N</i> -acetyldehydro- phenylalanine with homogeneous and intercalated [Rh(NBD) ( <u>R</u> )-4-Me-Prophos (49)] <sup>+</sup> catalyst . . . . .	92
9	Hydrogen uptake plots for reduction of <i>N</i> -acetyldehydro- phenylalanine with homogeneous and intercalated [Rh(NBD) SPIPHOS (48)] <sup>+</sup> catalyst . . . . .	94
10	Hydrogen uptake plots for reduction of <i>N</i> -acetyldehydro- phenylalanine with homogeneous and intercalated [Rh(NBD) DIOP(+) ( <u>3</u> )] <sup>+</sup> catalyst . . . . .	96
11	Hydrogen uptake plots for reduction of <i>N</i> -acetyldehydro- phenylalanine with intercalated [Rh(NBD)DIOP(+) ( <u>3</u> )] <sup>+</sup> catalyst and recycled catalyst . . . . .	98
12	Asymmetric hydrogenation catalytic cycle using the unsaturate route . . . . .	121

Figure		Page
13	The probable mechanism of asymmetric hydrogenation of dehydroamino acids (enamides) using cationic rhodium(I) chiral diphosphine catalysts . . . . .	123
14	The $^{31}\text{P}$ NMR spectrum of ( <u>R</u> )- 4-Me-Prophos ( <u>49</u> ) in $\text{CDCl}_3$ at $25^\circ\text{C}$ . . . . .	127
15	The $^{31}\text{P}$ NMR spectrum of 0.01 M solution of $[\text{Rh}(\text{NBD})(\text{R})\text{-}$ 4-Me-Prophos ( <u>49</u> )] $^+\text{ClO}_4^-$ in $\text{CDCl}_3$ at $-16^\circ\text{C}$ . . . . .	128
16	The $^{31}\text{P}$ NMR of 0.01 M of $[\text{Rh}(\text{Z-ester})(\text{R})\text{-4-Me-Prophos}$ ( <u>49</u> )] $^+\text{ClO}_4^-$ in $\text{CH}_3\text{OD}$ at $-30^\circ\text{C}$ . . . . .	130
17	The $^{31}\text{P}$ NMR spectrum of THP- butaphos ( <u>51</u> ) in $\text{CDCl}_3$ , at $25^\circ\text{C}$ . . . . .	140
18	$^{31}\text{P}$ NMR spectrum of ( <u>R</u> )- Hydroxy1butaphos ( <u>52</u> ) in $\text{EtOD}$ , at $25^\circ\text{C}$ . . . . .	142
19	$^1\text{H}$ NMR spectrum of <i>N</i> -BOC- butaphos ( <u>53</u> ) in $\text{CDCl}_3$ , at $25^\circ\text{C}$ (250 MHz) . . . . .	145

Figure		Page
20	$^1\text{H}$ NMR spectrum of <i>N</i> -BOC-butaphos ( <u>53</u> ) in $\text{CDCl}_3$ , at 25°C (250 MHz) . . . . .	147
21	$^{31}\text{P}$ NMR spectrum of <i>N</i> -BOC-butaphos ( <u>53</u> ) in $\text{CDCl}_3$ , at 0°C . . . . .	148
22	Hydrogen uptake plots for reduction of <i>N</i> -acetyldehydro- phenylalanine with homogeneous and intercalated $[\text{Rh}(\text{NBD})$ <i>N</i> -BOC-butaphos ( <u>53</u> )] $^+$ catalyst . . . . .	150
23	$^1\text{H}$ NMR spectrum of Acetonide- triol ( <u>58</u> ) in $\text{CDCl}_3$ , at 25°C (250 MHz) . . . . .	187
24	$^1\text{H}$ NMR spectrum of Benzyl- ether-ditosylate ( <u>60</u> ) in $\text{CDCl}_3$ , at 25°C (60 MHz) . . . . .	188
25	$^1\text{H}$ NMR spectrum of Acetonide- toyslate ( <u>63</u> ) in $\text{CDCl}_3$ , at 25°C (250 MHz) . . . . .	189
26	$^1\text{H}$ NMR spectrum of 4-Iso- butylamino-1,2- <i>O</i> -isopropy- lidene-1,2-( <u>5</u> )-butanediol ( <u>64</u> ) in $\text{CDCl}_3$ , at 25°C (250 MHz) . . . . .	190

Figure		Page
27	$^1\text{H}$ NMR spectrum of Aminodiol (65) in $\text{CDCl}_3$ at $25^\circ\text{C}$ (250 MHz) . . . . .	191
28	$^1\text{H}$ NMR spectrum of <i>N</i> -BOC- aminodiol (66) in $\text{CDCl}_3$ , at $25^\circ\text{C}$ (250 MHz) . . . . .	192
29	$^1\text{H}$ NMR spectrum of <i>N</i> -BOC- aminoditosylate (67) in $\text{CDCl}_3$ at $25^\circ\text{C}$ (250 MHz) . . . . .	193
30	Mass spectrum of ( $\underline{\text{R}}$ )-Prophos (6) . . . . .	194
31	Mass spectrum of ( $\underline{\text{R}}$ )-4-Me- Prophos (49) . . . . .	195
32	Mass spectrum of <i>N</i> -BOC- butaphos (53) . . . . .	196
33	Mass spectrum of <i>N</i> -BOC- aminodiol (66) . . . . .	197
34	$^{31}\text{P}$ NMR spectrum of ( $\underline{\text{R}}$ )-Prophos (6) in $\text{CDCl}_3$ at $25^\circ\text{C}$ . . . . .	198
35	$^{31}\text{P}$ NMR spectrum of $[\text{Rh}(\text{NBD})(\underline{\text{R}})\text{-}$ Prophos (6)] $\text{ClO}_4$ in $\text{CDCl}_3$ at $-20^\circ\text{C}$ . . . . .	199-
36	$^{31}\text{P}$ NMR spectrum of $[\text{Rh}(\text{NBD})\text{SPIPHOS} (48)]^+$ $\text{ClO}_4$ in $\text{CDCl}_3$ at $25^\circ\text{C}$ . . . . .	200
37	$^{31}\text{P}$ NMR spectrum of Rh SPIPHOS (48) $\text{PPh}_3\text{Cl}$ in $\text{CDCl}_3$ at $10^\circ\text{C}$ . . . . .	201

## LIST OF SYMBOLS AND ABBREVIATIONS

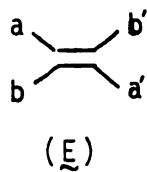
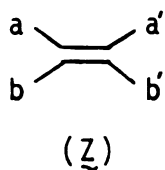
AIBN	azobisisobutyronitril
Ar	aromatic group
br	broad
brs	broad singlet
brm	broad multiplet
COD	1,5-cyclooctadiene
d	doublet
dd	doublet of doublets
diphos*	any chiral or achiral diphosphine
DOPA	$\beta$ -3,4-dihydroxyphenyl- $\alpha$ -alanine
dt	doublet of triplets
e.e.	enantiomeric excess
m	multiplet
M <sup>+</sup>	parent ion peak
Me	methyl
MS	mass spectrum
NBD	norboradiene
NMR	Nuclear Magnetic Resonance
O.Y.	optical yield
Ph	phenyl group
s	singlet
S	solvent
t	triplet
THF	tetrahydrofuran

TMS

tetramethylsilane

(Z) and (E)

The prefix Z (from zusammen,  
German = together) and E  
(entegen, German = opposite)



$\delta$

chemical shift

## INTRODUCTION

Recently, asymmetric synthesis has become very important in organic synthesis, because a great number of the new synthetic methods have been developed to control the stereochemistry of reactions and produce highly optically pure products in high yields.<sup>1</sup> New developments in this field offer great opportunities for food, pharmaceutical and agricultural industries to adopt these new methodologies to produce the pure optically active commercial products. In many important chiral compounds only one enantiomer is active for pharmaceuticals, food additives, perfumes and insecticides; the other isomer is inactive or even toxic. For example, (S)-asparagine is bitter, whereas the (R)-isomer is sweet; 3-chloro-1,2-(R)-propanediol is toxic, but the (S)-enantiomer is under study as a male antifertility agent. However, there are drawbacks in most of the new methods of asymmetric synthesis. Optically active starting materials are needed or stoichiometric chiral reagents are necessary to mediate the reactions. It is also difficult to recycle the chiral reagents.

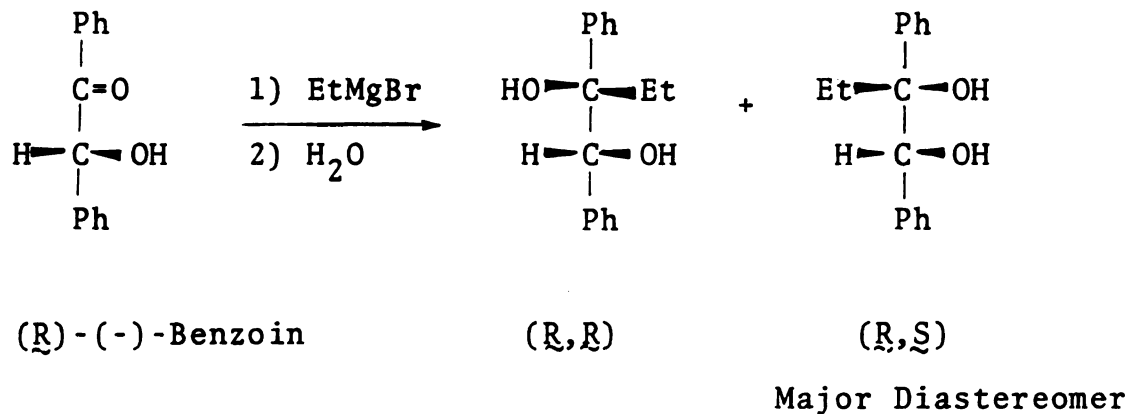
Asymmetric catalysis is the most effective way to perform asymmetric synthesis, since only a catalytic amount of chiral reagent is needed to produce large quantities of optically pure product without resolution. Asymmetric



catalysis with transition metal complexes has been an exciting research area for the last ten years. The catalysts which contain chiral phosphines have proved to be especially useful for a variety of catalytical asymmetric reactions.<sup>1,2</sup> In this introduction, the recent advances in asymmetric hydrogenation catalysis are surveyed. The focus of the study is asymmetric hydrogenation with rhodium chiral phosphine complexes and synthetic development of chiral phosphine ligands.

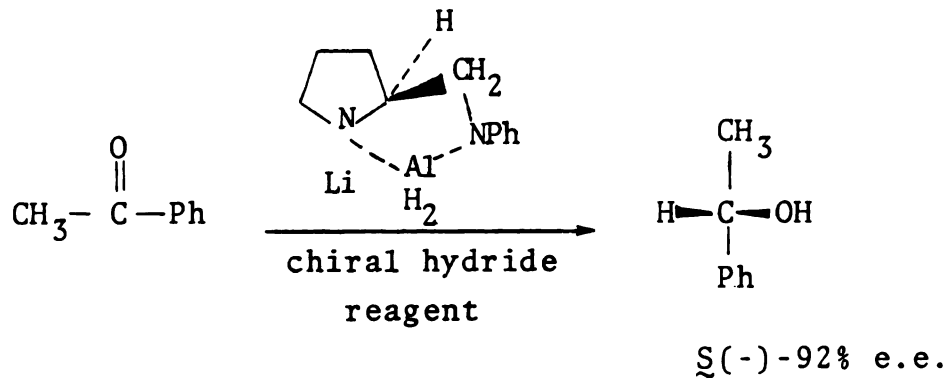
Asymmetric synthesis occurs as a result of a reagent reacting with a substrate to form diastereomeric transition states. One of the reactants must have a chiral center. The free energy difference between the diastereomeric transition states  $\Delta\Delta G^\ddagger$  determines the excess of one enantiomer over the other. For example,  $\Delta\Delta G^\ddagger$  of approximately 2 kcal of 0°C is considered essential to provide one of the enantiomers at 80% excess (90:10 mixture).

According to Morrison's classification,<sup>1a</sup> asymmetric synthesis can be carried out in one of two ways, either by intramolecular or by intermolecular chiral mediation. In intramolecular mediation, a second chiral center is created in a molecule under the influence of an existing chiral center in that same molecule (Scheme 1).



Scheme 1

In intermolecular chiral mediation, a chiral reagent interacts with a prochiral substrate to mediate the creation of a new chiral center (Scheme 2).



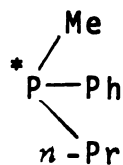
Scheme 2

The definition of enantiomeric excess (e.e.) or optical yield (O.Y.) is the ratio of actual specific rotation  $[\alpha]$  to the absolute rotation  $[\alpha]_{\text{abs}}$ , i.e., to the specific rotation of the pure enantiomer.

$$\text{e.e.} = \text{O.Y.} = \frac{[\alpha]}{[\alpha]_{\text{abs}}} \times 100\%$$

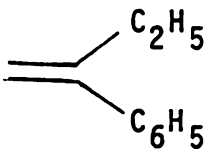
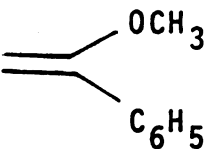
## I. The Historical Development of Asymmetric Hydrogenation

In 1964, Wilkinson discovered that  $\text{Rh}(\text{PPh}_3)_3\text{Cl}$  and its related derivatives were effective homogeneous catalysts in hydrogenation for a variety of olefin substrates. Four years later, Horner<sup>3</sup> was the first to point out that modified Wilkinson catalysts which contained chiral phosphine ligands should effect the asymmetric hydrogenation of prochiral olefins. At the same time (1968) two groups, Horner<sup>4</sup> and Knowles<sup>5</sup> independently confirmed that prediction: Horner and co-workers prepared a rhodium complex *in situ* from the precursor  $[\text{Rh}(\text{1,5-hexadiene})\text{Cl}]_2$  and (S)-(+)-methyl-phenyl-*n*-propylphosphine<sup>4</sup> (1) (69% optical purity) to hydrogenate  $\alpha$ -ethyl styrene and  $\alpha$ -methoxystyrene to (S)-(+)-2-phenylbutane (7-8% optical purity) and (R)-(+)-1-methoxy-1-phenylethane (3-4% optical purity) (Table 1).

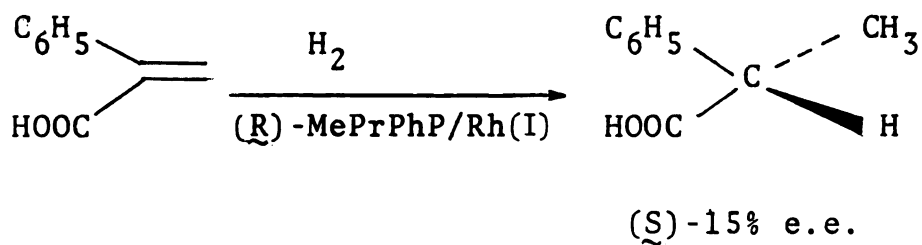


(1)

Table 1. Asymmetric Hydrogenation of Prochiral Olefins Using a Rh(I)-PMePh- $\tilde{n}$ -Pr (1) Catalyst Precursor.

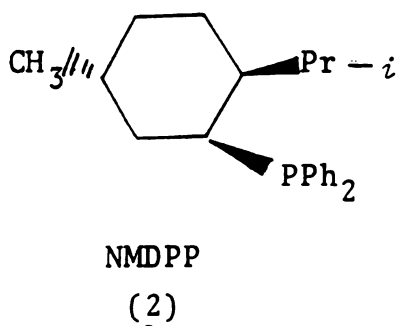
Substrate	Optical yield (%)
	7-8% ( $\tilde{S}$ )
	3-4% ( $\tilde{R}$ )

Knowles' group used a similar catalyst<sup>5</sup> to hydrogenate  $\alpha$ -phenylacrylic acid to ( $\tilde{S}$ )-hydratropic acid (Scheme 3).

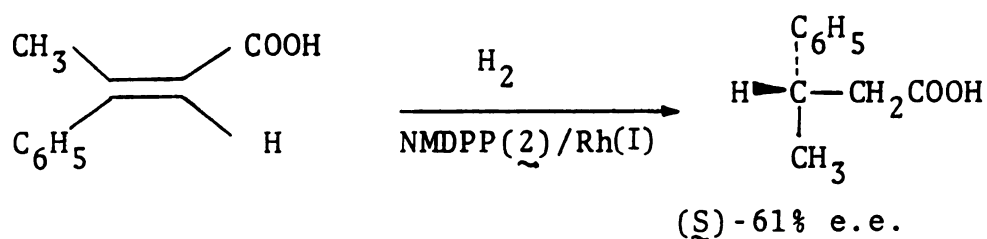


Scheme 3

Also, the hydrogenation rates and optical yields were increased by using salts of the olefinic acids. This was rationalized by more effective coordination of the carboxylate. In 1971, Morrison and co-workers synthesized a chiral neomenthyldiphenylphosphine, (+)-NMDPP<sup>6</sup> (2), from (-) menthol.



With Rh(I)-NMDPP (2) as catalyst the optical yield was greatly improved (Scheme 4)



Scheme 4

At the same time, Kagan and co-workers had synthesized a bidentate diphosphine ligand, (-)DIOP (3), from tartaric acid. A (-)DIOP (3)/Rh(I) catalyst precursor was obtained *in situ* from [Rh(cyclo-octene)<sub>2</sub>Cl]<sub>2</sub> and (-)DIOP (3) in benzene-ethanol. The optical yields obtained from asymmetric

hydrogenations of prochiral olefins are shown in Table 2.

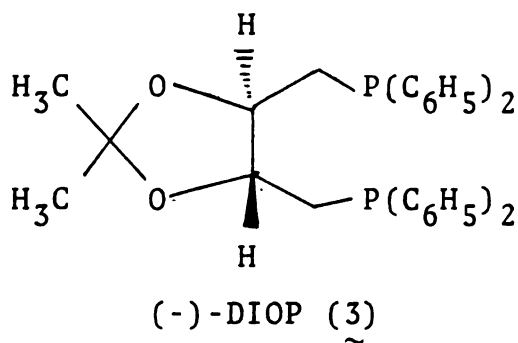
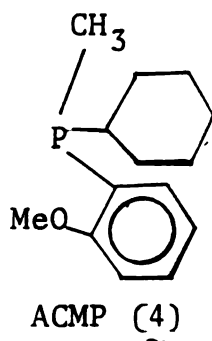


Table 2. Asymmetric Hydrogenation of Prochiral Olefins with Rh/(-)DIOP (3) Catalyst Precursor.

Substrate	Optical yield (%)
	63 ( <u>S</u> )
	7 ( <u>R</u> )
	72 ( <u>R</u> )
	68 ( <u>R</u> )

High optical yields observed using this catalyst were accredited to conformational rigidity of the chelating diphosphine and the functionalized groups of the substrates NMDPP (2) and (-)DIOP (3), were demonstrated to be effective ligands, however, for both ligands the chirality was not at the phosphorous atom. This new concept was a big breakthrough for the design of new chiral phosphine ligands.

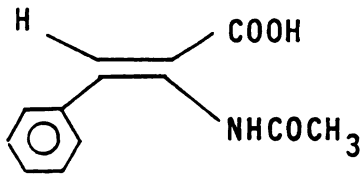
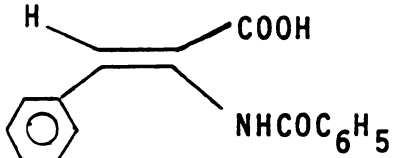
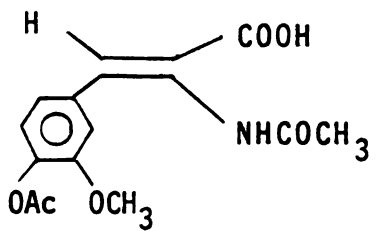
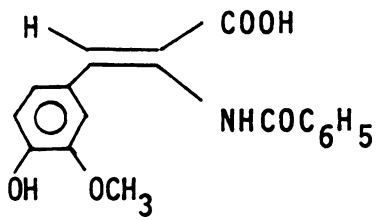
Another major development was the design of a new chiral phosphine with a different synthetic path. A chiral phosphine, ACMP<sup>8</sup> (4) containing methyl, cyclohexyl, and *O*-anisyl groups (95% optically pure) proved to be an excellent ligand for asymmetric hydrogenation of (*Z*)-dehydro-amino acids (Table 3).



In this case, almost complete stereospecific hydrogenation could be achieved, since the oxygen atoms of the *O*-anisyl groups of the ligands could coordinate partially with rhodium, resulting in the reduction of the conformation flexibility and the fixation of the chirality of the complex. This successful development led Monsanto to adopt the process for the manufacture of L-DOPA (a

drug used for the treatment of Parkinson's disease).

Table 3. Asymmetric Hydrogenation of (*Z*)-Dehydroamino Acids with Rh(I)-ACMP (4) Catalyst Precursor

Substrate	Solvent	Optical Yield (%)
	95% Ethanol	85
	95% Ethanol	85
	Isopropanol	88
	Isopropanol	90

Since 1972 asymmetric hydrogenation has become one of the most exciting research areas in chemistry. Many new chiral phosphine ligands for asymmetric hydrogenation have been synthesized and studied. Their catalytic applications for other asymmetric reactions; hydroformylation, hydrosilylation, and alkylation also have begun to be explored.



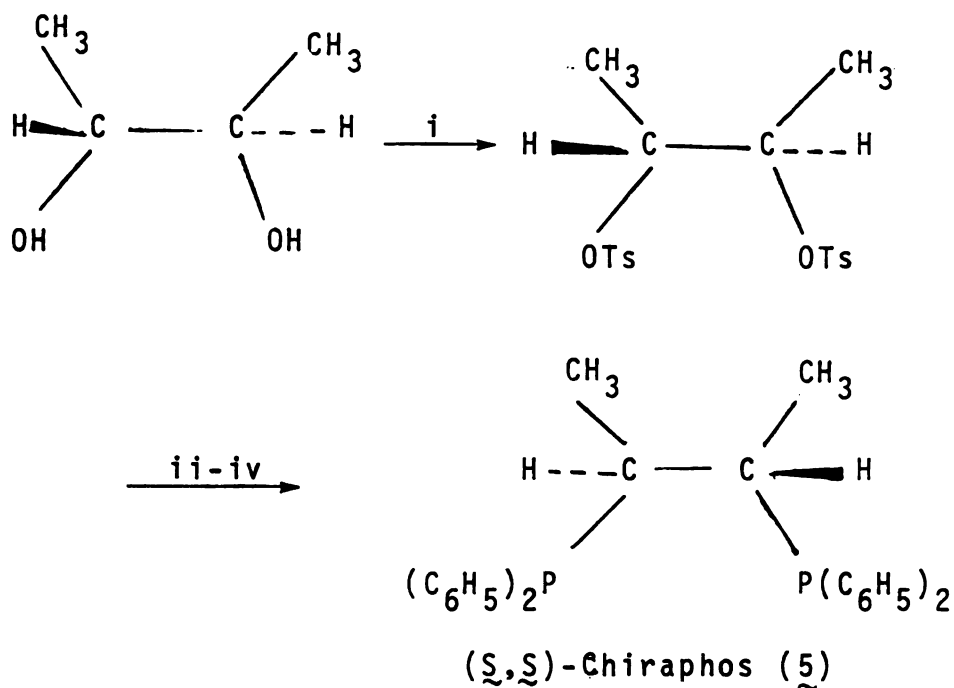
## II. Chiral Diphosphine Ligands and Their Application to Asymmetric Hydrogenation

### A. Rigid Ligands

The optical yields from asymmetric hydrogenation of (Z)-dehydroamino acids are extremely high when chiral diphosphines form rigid five-membered chelating rings.

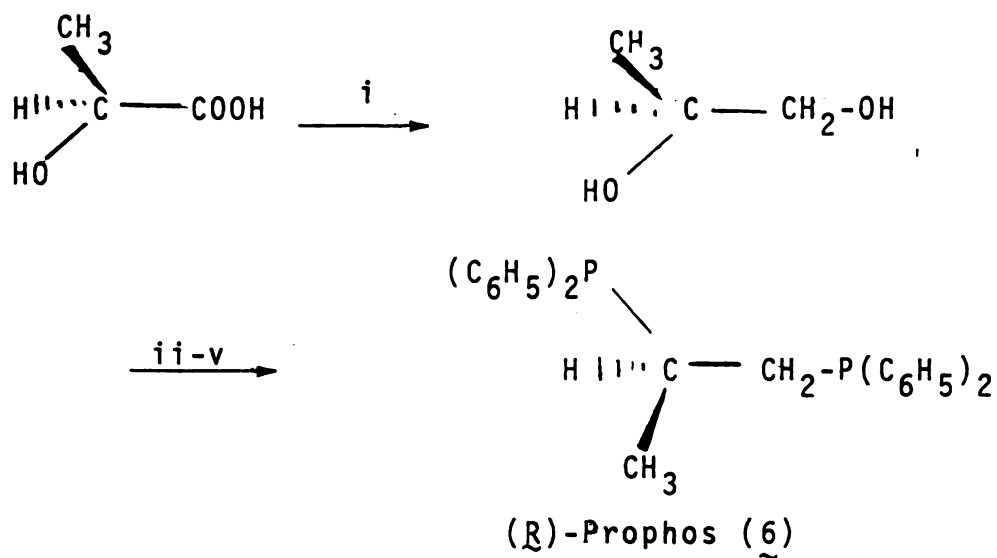
#### 1. Ligands Chiral at Carbon Backbone

The substituent at the carbon backbone of chiral diphosphine can restrain the chirality of the metal chelating ring and fix the orientation of the phenyl rings on the phosphorous atoms. High stereoselection can be achieved. The first highly effective ligand in this category, (S,S)-Chiraphos (5), was initially developed by Bosnich.<sup>9</sup> The ligand was prepared from commercially available (R,R)-2,3-butanediol, by a simple synthetic process (Scheme 5). With (Z)-dehydroamino acids as substrates, the optical yields were exceptionally high and not very sensitive to the solvent. Leucine and phenylalanine were obtained in optically pure forms. Bosnich also developed (R)-Prophos<sup>10</sup> (6) which was prepared from (S)-lactic acid (Scheme 6). This ligand only has a single methyl group at a chiral center to constrain the chirality of the chelate ring. The Rh(I)-(R)-Prophos (6) complex is an efficient hydrogenation catalyst. High optical



Reagents: (i)  $\text{TsCl}/\text{PY}$  (ii)  $\text{LiPPh}_2$  (iii)  $\text{Ni}^{+2}/\text{NCS}^-$   
 (iv)  $\text{CN}^-$

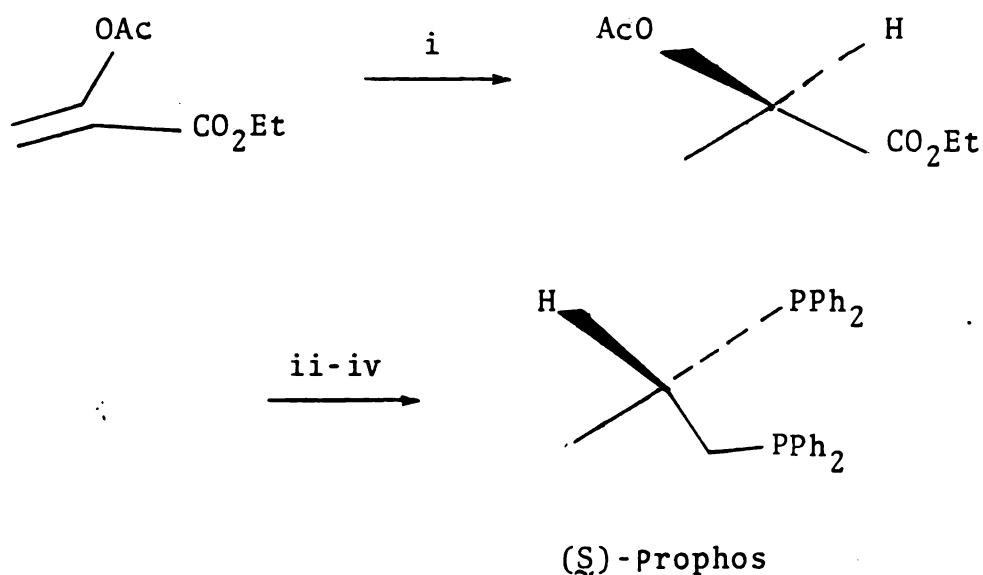
Scheme 5



Reagents: (i)  $\text{LiAlH}_4$  (ii)  $\text{TsCl}/\text{PY}$  (iii)  $\text{LiPPh}_2$   
 (iv)  $\text{Ni}^{+2}/\text{NCS}^-$  (v)  $\text{CN}^-$

Scheme 6

yields were achieved for a variety of (Z)-dehydroamino acids (around 90% e.e). With Rh(I)-(R)-Prophos catalyst the optical yields appear to be insensitive to the nature of the substituent on the substrate. In comparison with the Rh(I)-(S,S)-Chiraphos (5) catalyst, the optical yields are rather substituent dependent. Moreover, the catalyst is capable of breeding its own chirality, since a small amount of (R)-Prophos (6) can produce large quantities of itself (Scheme 7).



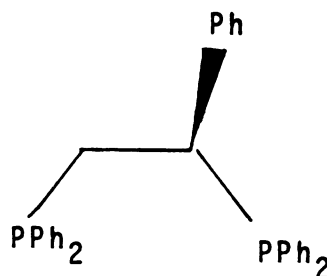
Reagents    (i) Rh(I)-(R)-Prophos/  $\text{H}_2$     (ii)  $\text{LiAlH}_4$   
                  (iii)  $\text{TsCl}$     (iv)  $\text{LiPPh}_2$

Scheme 7

The product, lactate, can be converted into (S)-Prophos easily by known procedures.

The (S,S)-Chiraphos (5) and (R)-Prophos (6) have proved to be highly effective rigid ligands. (R)-Prophos (6), which has nonequivalent phosphorous atoms, provides better structural information in the study of the reaction mechanism by  $^{31}\text{P}$  NMR. These advantages led the other investigators to develop the new analogue ligands.

(S)-Phenylbis(diphenylphosphineo)ethane<sup>11</sup> (7) was synthesized from (S)-mandelic acid by adopting the same process<sup>10</sup> which Bosnich used for the synthesis of (R)-Prophos.

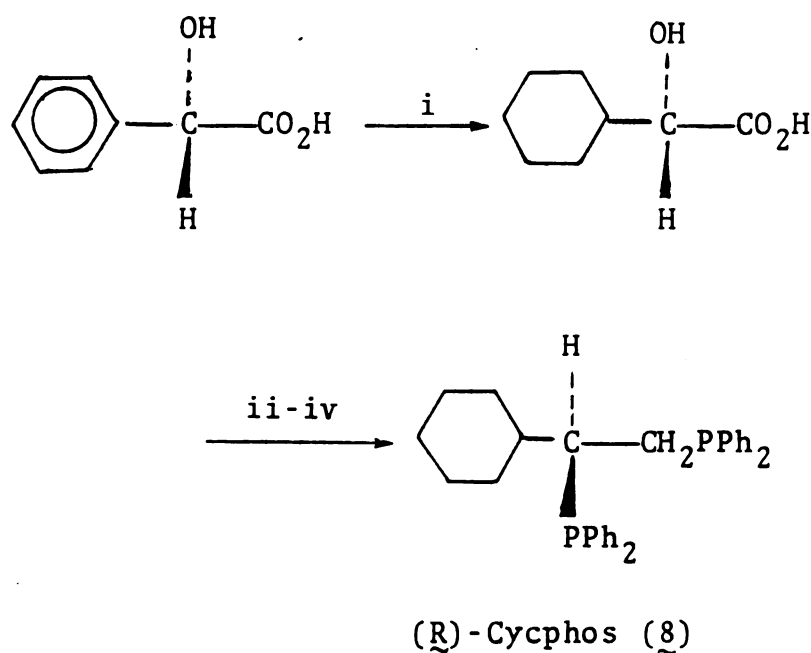


(7)

The higher boiling point of the ligand allows easy crystallization without tedious purification processing. The *in situ* Rh(I) catalyst was less active than the cationic Rh(I) catalyst and required high hydrogenation pressure for reaction. The ligand (7) is not as efficient as (R)-Prophos (6) for asymmetric hydrogenation. It has been successfully used for studying the reaction intermediates in asymmetric hydrogenation through  $^{31}\text{P}$  NMR by

Brown.<sup>12</sup>

(R)-Cycphos (8) was prepared from (S)-(+)-mandelic acid by Riley<sup>13</sup>. The optical yields of (S)- $\alpha$ -amino acid derivatives are generally above 90%. The synthetic scheme is shown here (Scheme 8).

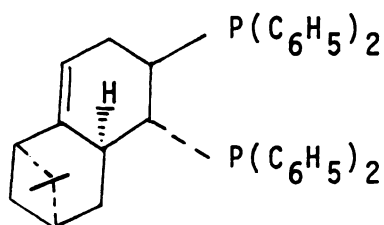
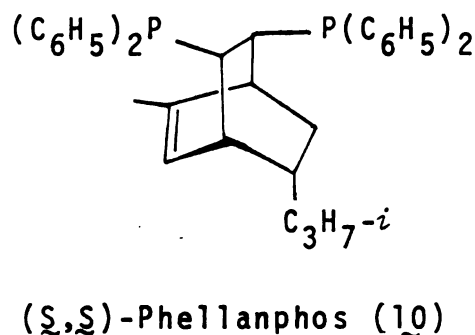
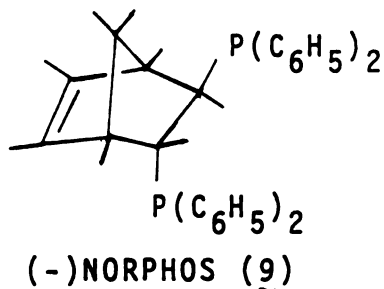


Reagents    (i)  $\text{H}_2/\text{Rh-Al}_2\text{O}_3$     (ii)  $\text{LiAlH}_4/\text{THF}$   
               (iii)  $\text{TsCl}/\text{PY}$     (iv) 10% Excess  $\text{LiPh}_2$

Scheme 8

The author rationalized that the high optical yields were associated with the bulky cyclohexyl substituent which could restrain the rigid chelate ring more effectively than other structurally analogous ligands.

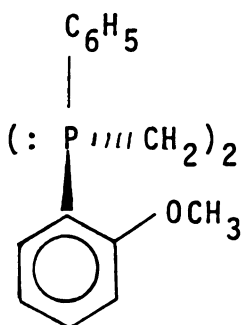
A series of new rigid ligands which have bulky chiral carbon skeletons were prepared by Diels-Alder reactions between the chiral dienes and P-C=C-P moieties such as (-)NORPHOS<sup>14</sup> (9), (S,S)-Phellaphos<sup>15</sup> (10) and (R,R)-Nopaphos<sup>15</sup> (11).



This is an alternative way of synthesizing the rigid type ligands instead of using conventional methods, such as the substitution of tosyl groups by diphenylphosphide. Best results were found in asymmetric synthesis of  $\alpha$ -amino acid derivatives (80-95% e.e.)<sup>14-15</sup>

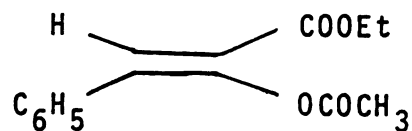
## 2. Ligand Chirality at Phosphorus

The highly efficient DIPAMP (12) was developed by Knowles and his co-workers.<sup>16</sup> Since the methoxy groups of ligand can partially bond with rhodium metal and fix the phenyl rings' chirality, excellent stereoselection can be achieved.



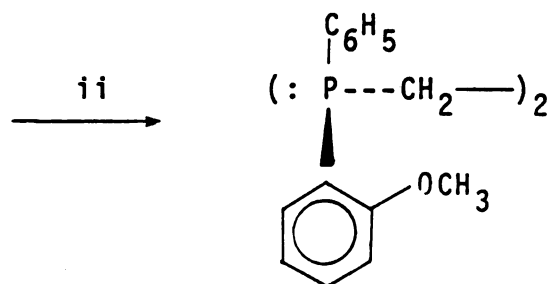
DIPAMP (12)

High optical yields of up to 96% were obtained in the hydrogenation of dehydroamino acids. These high optical yields were not markedly sensitive to temperature and pressure. Also, the ligand was effective for nonamide substrates. Excellent selectivity (approximately 90% e.e) was produced in reduction of the  $\alpha$ -enol ester, (Z)-ethyl-2-acetyloxy-3-phenyl-2-propenoate (13).



(13)

The ligand was synthesized by using a copper reagent to induce the coupling reaction of chiral monophosphine oxide, then it was reduced by  $\text{HSiCl}_3$  reagent (Scheme 9).



DIDAMP (12)

Reagents (i)  $(i\text{-C}_3\text{H}_7)_2\text{NLi}/\text{CuCl}_2$  (ii)  $\text{HSiCl}_3$

Scheme 9

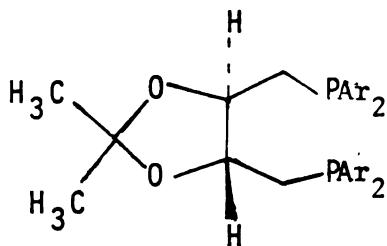
The drawback of the synthetic process is that it involves long synthetic processing and the overall yield is low.





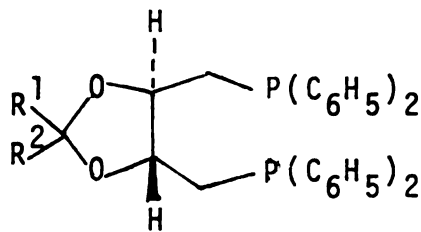
## B. DIOP and DIOP Analogues

The DIOP (3) which was first synthesized by Kagan<sup>7</sup> played a historically key role in the development of chiral diphosphines for asymmetric hydrogenation. Also, the DIOP (3) has proved to be useful for a variety of asymmetric catalytic reactions.<sup>2b</sup> Encouraging results obtained by using DIOP (3)/Rh(I) catalysts led to the development of a great number of new analogues, either for the elucidation of the mechanism or for the improvement of optical yields. The new DIOP analogues<sup>17,18</sup> (14-22) were synthesized either by varying the acetal substituents, replacing the acetonide ring by a carbocycle, or by changing the aromatic substituents. Modified acetal analogues (14,15) did not affect the optical yields, since these groups caused no perturbation on the chirality of the phenyl rings.



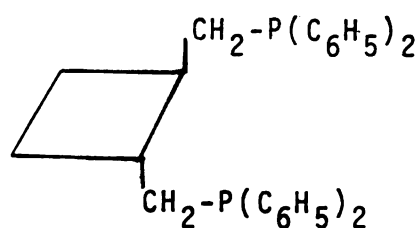
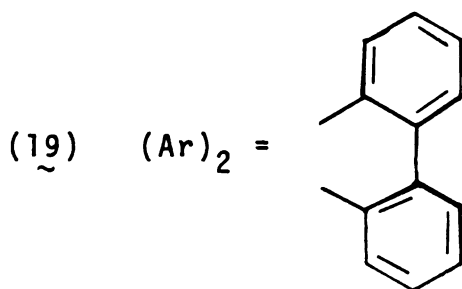
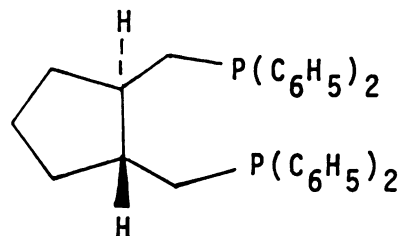
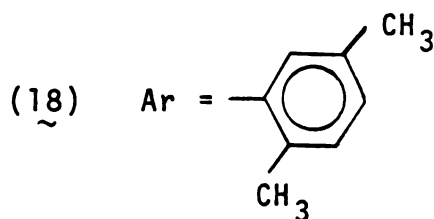
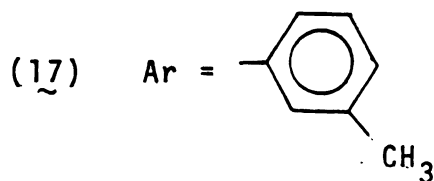
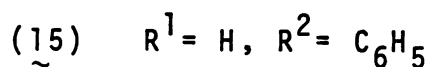
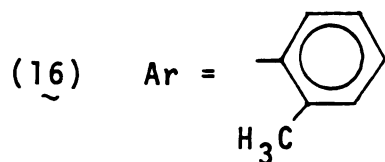
Ar = C<sub>6</sub>H<sub>5</sub> (DIOP)

(3)

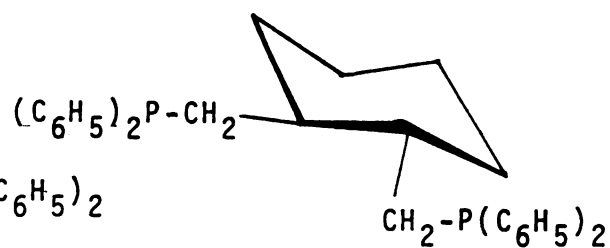


R<sup>1</sup> R<sup>2</sup> = -(CH<sub>2</sub>)<sub>5</sub>-

(14)



(20)



(22)

The DIOP analogues, (16, 18, 19) which have different substituents on the aromatic rings, generally give low optical yields. Only ligand (17) was exceptional. The optical yield of DOPA was enhanced (90% e.e). In comparison with DIOP (3) with carbocyclic analogues<sup>18</sup> (20, 21, 22), cyclobutane analogue (20) led to better

optical yields. Since the ligand (20) has a small *trans*-fused carbocyclic ring, it is more conformational rigid and results in better asymmetric induction (Table 4).

Table 4. Asymmetric Hydrogenation of Dehydroamino Acids Using DIOP (3) and Carbocyclic Analogues<sup>18</sup>

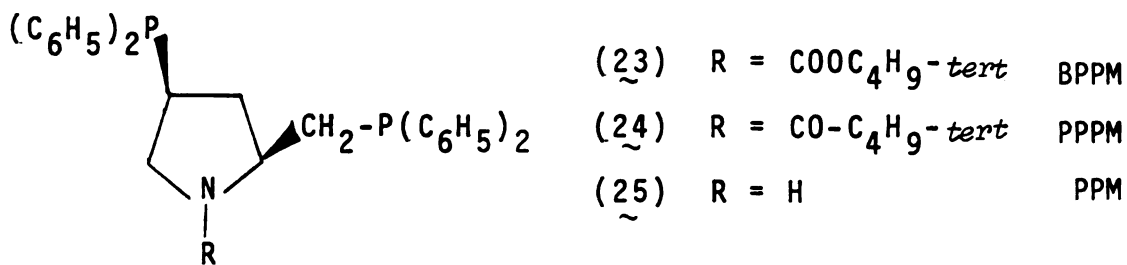
Substrate	Optical Yield (%)			
	(3)	(20)	(21)	(22)
	82(R)	86(R)	63(R)	35(S)
	73(R)	72(R)	72(R)	40(S)

### C. Pyrrolidinephosphines

The (2*S*, 4*S*)-*N*-butoxycarbonyl-4-diphenylphosphino-2-diphenylphosphinomethylpyrrolidine (BPPM)<sup>19</sup> (23) was first developed by K. Achiwa. The BPPM (23) has two kinds of function groups, two phosphines as ligand for metal complexion, and the amide group which is capable of being modified by different substituents in order to optimize optical yields. A series of pyrrolidinephosphines have been synthesized by variation of the amide substituents

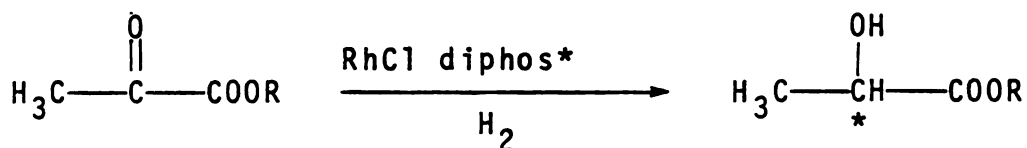


and have been successfully applied for a variety of catalytic asymmetric reactions.<sup>2b</sup> Interactions between the amide group and substrate were crucial for highly asymmetric inductions of some reactions.



The BPPM ligand (23) is effective for asymmetric hydrogenation.<sup>19</sup> High optical yields were obtained with (*Z*)-dehydroamino acids by adding triethylamine (Table 5).

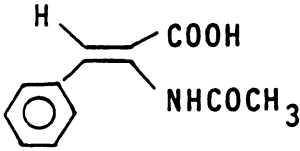
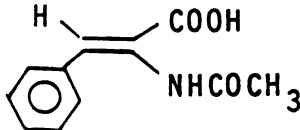
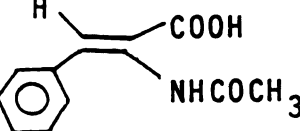
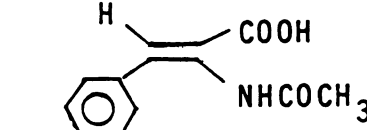
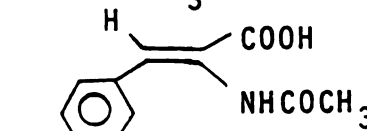
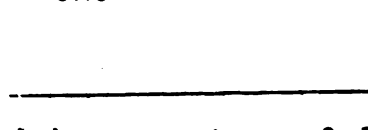
Rh(I)-BPPM catalyzed the hydrogenation of  $\alpha$ -keto-esters<sup>20</sup> in dry benzene or THF (Scheme 10). High optical yields of lactates were achieved in 65-75% enantiomeric excess. The catalyst was more stereoselective than Rh(I)-DIOP (3), which gave low optical yields (32-42%).



diphos\* = BPPM (23) or DIOP (3)

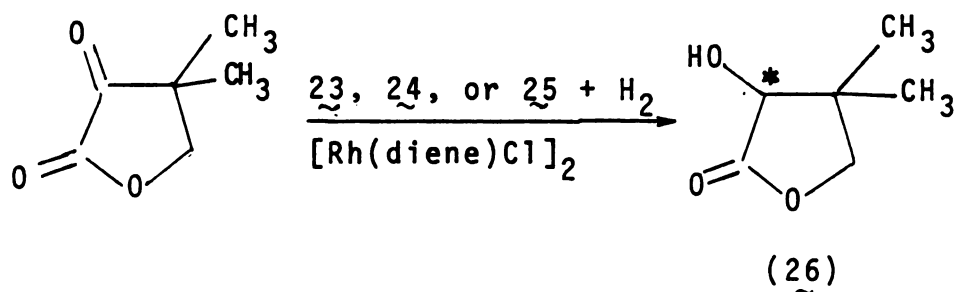
Scheme 10

Table 5. Asymmetric Hydrogenation of (Z)-Dehydroamino Acids with *In-situ* Rh(I)-BPPM (23) Complex<sup>a</sup> at 20°C and 50 atm.

Substrate	Solvent	Optical Yield (%)	
		without NEt <sub>3</sub>	with NEt <sub>3</sub>
	MeOH	30 (R)	83 (R)
	EtOH-H <sub>2</sub> O (2:1)	2 (R)	48 (R)
	EtOH	7 (S)	15 (R)
	EtOH	32 (R)	83 (R)
	EtOH	—	86 (R)
	EtOH	—	87 (R)

(a): *In-situ*: 0.5[Rh(1,5-hexadiene)Cl]<sub>2</sub> and BPPM (23) as catalyst precursor

The *In-Situ* Rh(I) catalysts which were prepared from  $[\text{Rh}(\text{diene})\text{Cl}]_2$  and PPM (25) or the analogues (23, 24) were used for asymmetric synthesis of (R)-(-)-pantolactone<sup>21</sup> (26) (Scheme 11).



Scheme 11

The hydrogenations were run at 30°-50°C and 50 atm hydrogen pressure. The best optical yield (87%) was obtained by using Rh(I)-BPPM (23) catalyst and was run under optimum conditions. (Table 6). When *N*-substituents of PPM (25) were varied, the optical yields were greatly reduced. In the case of ligand PPM (25), even the absolute configuration of pantolactone was reversed.

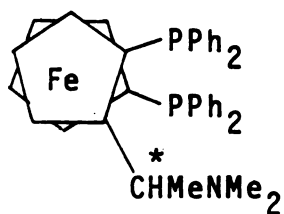


Table 6. Optical Yields of (R)-(-)-Pantolactone<sup>21</sup> (26)  
by Using PPM (25) and its Analogues

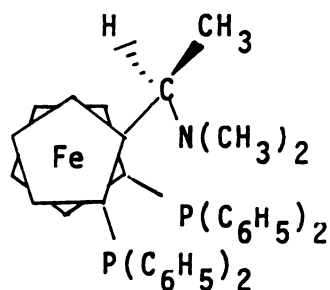
Solvent	Temperature	Optical Yields (%)		
		(23)	(24)	(25)
Benzene	30°C	86.7 (R)		
	50°C	84.8 (R)	59.2 (R)	15.4 (S)
Ethanol	50°C	32.1 (R)	35.9 (R)	8.5 (S)
THF	30°C	80.7 (R)		
Chlorobenzene	50°C	63.5 (R)		
Toluene	50°C	77.7 (R)		

#### D. Ferrocenylphosphines

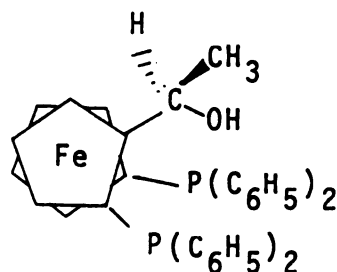
Ferrocenylphosphines which have planar chirality and various functional groups such as an amino or hydroxyl group have been demonstrated to be effective ligands (27-29) for catalytic asymmetric reactions.<sup>2b</sup>



(S)-(-)-BPPFA (27)



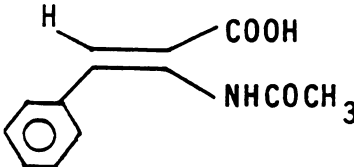
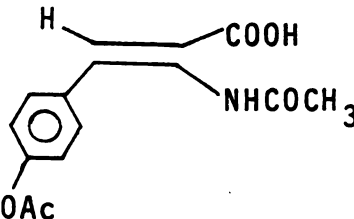
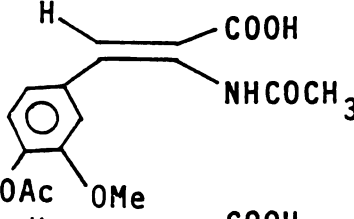

(R)-(S)-BPPFA (28)



(R)-(S)-BPPFOH (29)

The (S)-(R)-BPPFA ligand (27) is useful for asymmetric hydrogenation.<sup>22</sup> The catalyst, prepared *in situ* from  $[\text{Rh}(1,5\text{-hexadiene})\text{Cl}]_2$  and (S)-(R)-BPPFA (27), has been used to catalyze asymmetric hydrogenation of the (Z)-dehydroamino acids. The catalyst gave high optical yields in an aqueous solution (Table 7). Ammonium-carboxylate interactions between the amino group of (S)-(R)-BPPFA (27) and the carboxyl group of substrate are crucial for high asymmetric induction. By adding triethylamine the effect of the interactions will be reduced.

Table 7. Asymmetric Hydrogenation Catalyzed by Rh(I)-  
(S)-(R)-BPPFA (27) Complex

Substrate	Solvent	Optical Yield (%)
	MeOH	93 ( <u>S</u> )
	H <sub>2</sub> O/EtOH (1/1)	92 ( <u>S</u> )
	H <sub>2</sub> O/MeOH (1/1)	89 ( <u>S</u> )
	MeOH	8 ( <u>S</u> )
	EtOH	38 ( <u>S</u> )
	H <sub>2</sub> O/MeOH (1/3)	87 ( <u>S</u> )
	EtOH	36 ( <u>S</u> )
	H <sub>2</sub> O/MeOH (1/2)	86 ( <u>S</u> )
	H <sub>2</sub> O/MeOH (3/4)	52 ( <u>S</u> )

A series of ketones and  $\alpha$ -keto acids were reduced by Rh(I)-(R)-(S)-BPPFA (28) and Rh(I)-(R)-(S)-BPPFOH (29) catalysts<sup>23</sup> (Table 8). The high optical yields obtained with (R)-(S)-BPPFOH (29) can probably be ascribed to hydrogen bonding between the carbonyl of the substrate and the hydroxyl groups of the ligand, which may increase

Table 8. Asymmetric Hydrogenation of Carbonyl Compounds  $R^1-CO-R^2$  with (R)-(S)-BPPFOH (29) or (R)-(S)-BPPFA (28)

Substrate $R^1-CO-R^2$	Optical Yields (%)		
	Cationic Precursor <sup>a</sup>		<i>In Situ</i> Catalyst <sup>b</sup>
	(29)	(28)	(29)
$H_3C-CO-C_6H_5$	40 (R)	15 (S)	35 (R)
$C_2H_5-CO-C_6H_5$	31 (R)	—	—
$H_3C-CO-C_4H_9-t$	43 (R)	—	—
$H_3C-CO-COOH$	59 (R)	16 (S)	55 (R)
$H_3C-CO-COOH$	83 (R) <sup>c</sup>	—	—

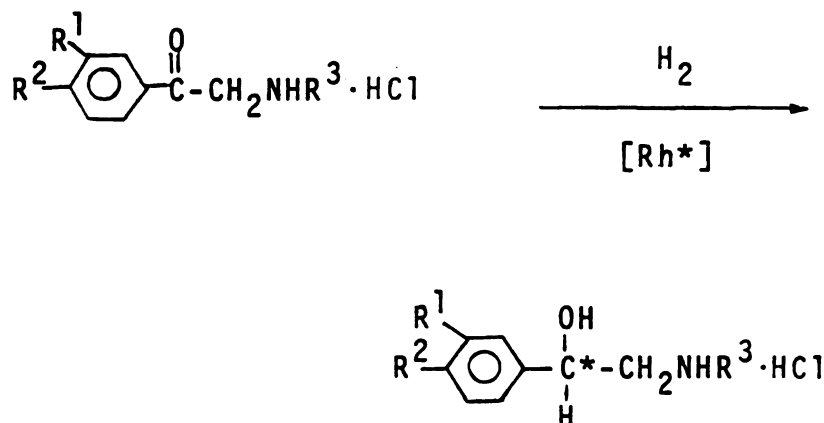
(a) Cationic precursor:  $[Rh(COD)(diphos^*)]ClO_4$   
 diphos\*: (R)-(S)-BPPFOH (29) or (R)-(S)-BPPFA (28)

(b) *In Situ* catalyst :  $0.5 [Rh(1,5-hexadiene)Cl]_2$  and (R)-(S)-BPPFOH (29)

(c) By adding 1 equivalent of triethylamine

conformational rigidity in diastomeric transitions resulting in high stereoselectivity.

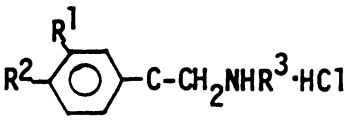
The (R)-(S)-BPPFOH-(29)-rhodium(I) complex also catalyzed hydrogenation of aminomethyl aryl ketones to give corresponding 2-amino-1-arylethanol (Scheme 12).



Scheme 12

High optical and chemical yields were obtained<sup>24</sup> (Table 9). Conventional chiral hydride agents are not very efficient with these prochiral carbonyl compounds because of the presence of active hydrogen on the starting ketones and the instability of the latter under base conditions. The highest optical yield (95%) was achieved with dihydroxyphenyl methylaminomethyl ketone in comparison with other prochiral carbonyl derivatives.<sup>1a, 25</sup>

Table 9. Asymmetric Hydrogenation of Aminomethyl Aryl Ketones with (R)-(S)-BPPFOH (29)

Substrate			Optical Yield (%)	
			Cationic precursor <sup>a</sup> ( <u>29</u> )	<i>In Situ</i> catalyst <sup>b</sup> ( <u>29</u> )
R <sup>1</sup>	R <sup>2</sup>	R <sup>3</sup>		
OMe	OMe	H	90 ( <u>R</u> )	92 ( <u>R</u> )
H	H	H	60 ( <u>R</u> )	57 <sup>c</sup> ( <u>S</u> )
H	OH	H	69 ( <u>R</u> )	—
OH	OH	CH <sub>3</sub>	95 ( <u>R</u> )	—

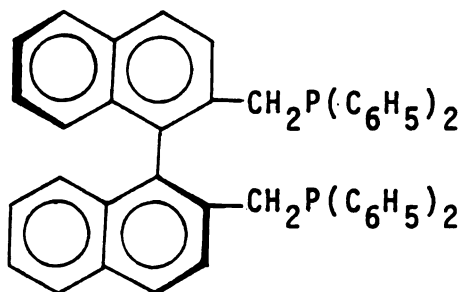
(a) Cationic precursor: [Rh(R)-(S)-BPPFOH-(29) (NBD)]ClO<sub>4</sub>

(b) *In situ* catalyst : (R)-(S)-BPPFOH (29) + 0.5 [Rh(1,5-hexadiene)Cl]<sub>2</sub>

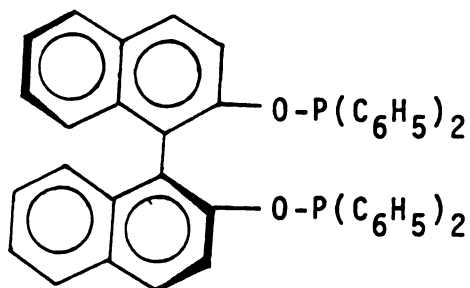
(c) Using enantiomeric (S)-(R)-BPPFOH

#### E. Atropisomeric Ligands

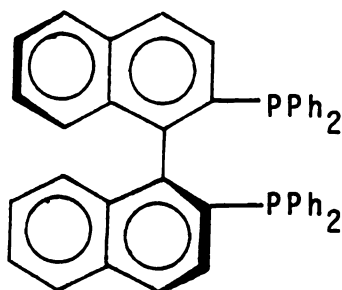
Recently, a series of atropisomeric ligands, (30, 31, 32), whose chirality was a result of atropisomerism due to the presence of a chiral axis and not to the asymmetric center on phosphorus or carbon, have been synthesized and used for asymmetric hydrogenation of dehydroamino acids. The (S)-(-)-NAPHOS<sup>26</sup> (30) and (S)-(-)-NAPHIN<sup>27</sup> (31), which were highly flexible ligands, generally gave low optical yields.



(S)-(-)-NAPHOS (30)



(S)-(-)-NAPHIN (31)



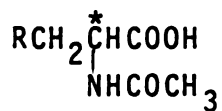
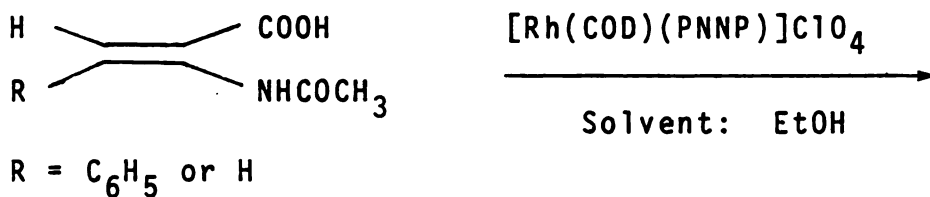
(S)-BINAP (32)

The ligand (S)-BINAP<sup>28</sup> (32) is more rigid than the two ligands (30,31) mentioned above. High optical yields were achieved under optimizing conditions (80-100% with low substrate concentrations and low pressure). The ligand also was very effective for hydrogenation of configurationally labile (E)- $\alpha$ -benzamidocinnamic acid. The optical yield (87% e.e.) was among the highest ever reported.

#### F. Bis-aminophosphines

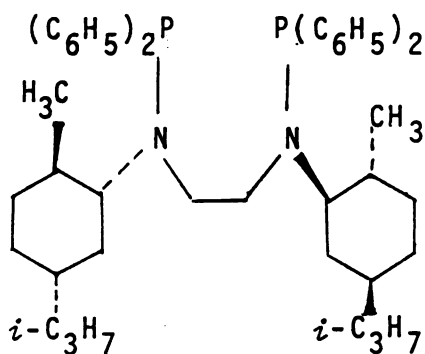
A series of bis-aminophosphines (33-39) were synthesized by Giongo.<sup>29</sup> Rhodium(I) complexes with the chiral

chelating bis-aminophosphines are efficient catalysts for the asymmetric hydrogenation of  $\alpha$ -acetamidoacrylic acid and (*Z*)- $\alpha$ -acetamidocinnamic acid (Scheme 13). The optical yields were around 70-94% with these bis-aminophosphines.

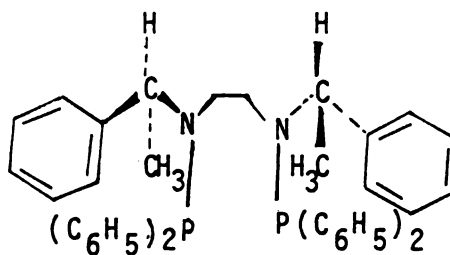


70-94% e.e

Scheme 13

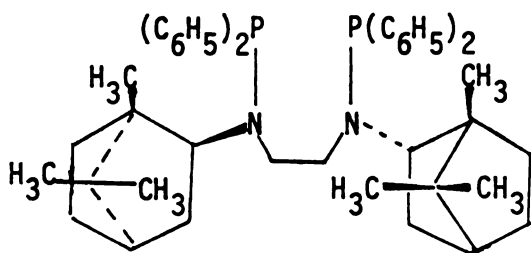


(33)

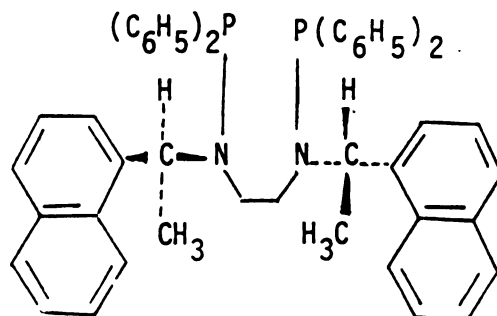


(34)

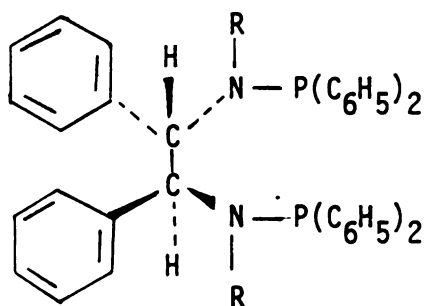




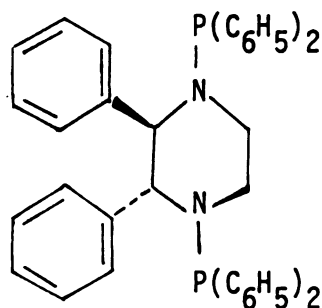
(35)



(36)

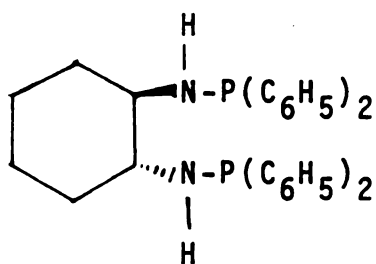


(37) R=H

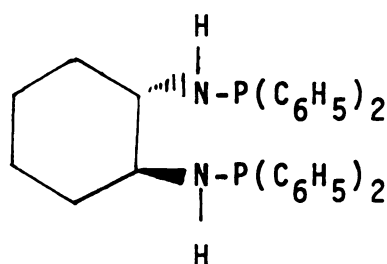
(38) R=CH<sub>3</sub>

(39)

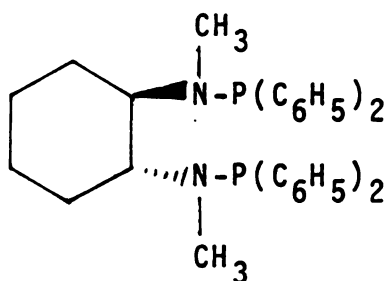
(1*R*, 2*R*)-Bis(diphenylphosphinamino)cyclohexane[(*R*,*R*)-40]<sup>30a</sup>, its enantiomer<sup>30a</sup> (*S*,*S*)-(41) and its *N,N'*dimethyl derivative ligand<sup>30b</sup> (*R*,*R*)-(42) were effective ligands for asymmetric hydrogenation of (*Z*)- $\alpha$ -dehydroamino acid derivatives<sup>30</sup> (Table 10).



(R,R)-(40)



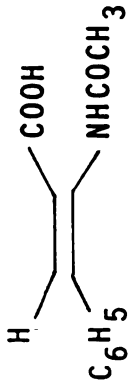
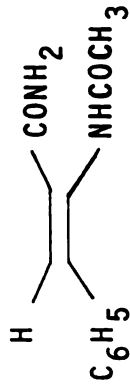
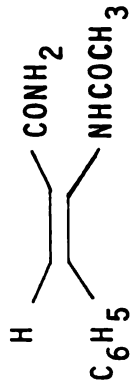
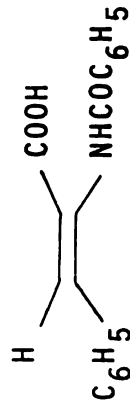

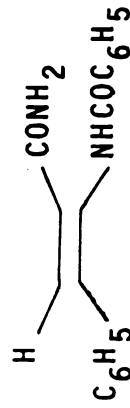
(S,S)-(41)



(R,R)-(42)

Inversion in the stereoselectivity of asymmetric hydrogenation of (Z)- $\alpha$ -acetamidocinnamic acid and (Z)- $\alpha$ -benzamido-cinnamic acid was found by using its *N,N*-dimethyl derivative ligand<sup>30b</sup>(R,R)-(42).

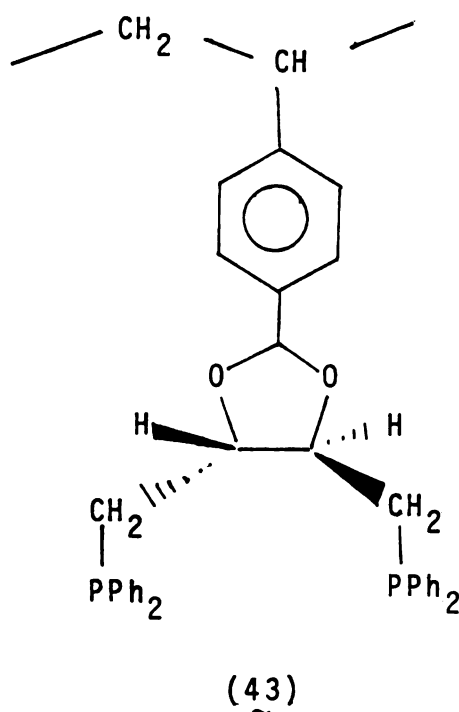
Table 10. Asymmetric Hydrogenation of ( $\tilde{Z}$ )-Dehydroamino Acid Derivatives

Substrate	Solvent	Optical Yield (%)		
		Cationic precursor <sup>a</sup> ( $\tilde{R}, \tilde{R}$ )-(40)	<i>In Situ</i> catalyst <sup>b</sup> ( $\tilde{S}, \tilde{S}$ )-(41)	( $\tilde{R}, \tilde{R}$ )-(42)
	EtOH	41 ( $\tilde{R}$ )	41 ( $\tilde{S}$ )	73 ( $\tilde{S}$ )
	EtOH-C <sub>6</sub> H <sub>6</sub> (1:1)	70 ( $\tilde{R}$ )	72 ( $\tilde{S}$ )	
	EtOH-C <sub>6</sub> H <sub>6</sub> (1:1)	92 ( $\tilde{R}$ )	92 ( $\tilde{S}$ )	
	EtOH	43 ( $\tilde{R}$ )	43 ( $\tilde{S}$ )	85 ( $\tilde{S}$ )
	EtOH-C <sub>6</sub> H <sub>6</sub> (1:1)	62 ( $\tilde{R}$ )	60 ( $\tilde{S}$ )	
	EtOH-C <sub>6</sub> H <sub>6</sub> (1:1)		70 ( $\tilde{S}$ )	

(a) Cationic precursor: [Rh(COD)diphos\*]ClO<sub>4</sub>; diphos\* = ( $\tilde{R}, \tilde{R}$ )-(40) or ( $\tilde{S}, \tilde{S}$ )-(41)  
 (b) *In Situ* catalyst : 0.5[Rh(CODCl)<sub>2</sub> and ( $\tilde{R}, \tilde{R}$ )-(42)]

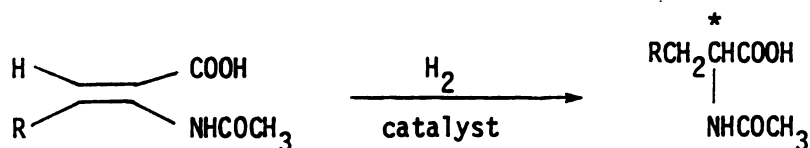
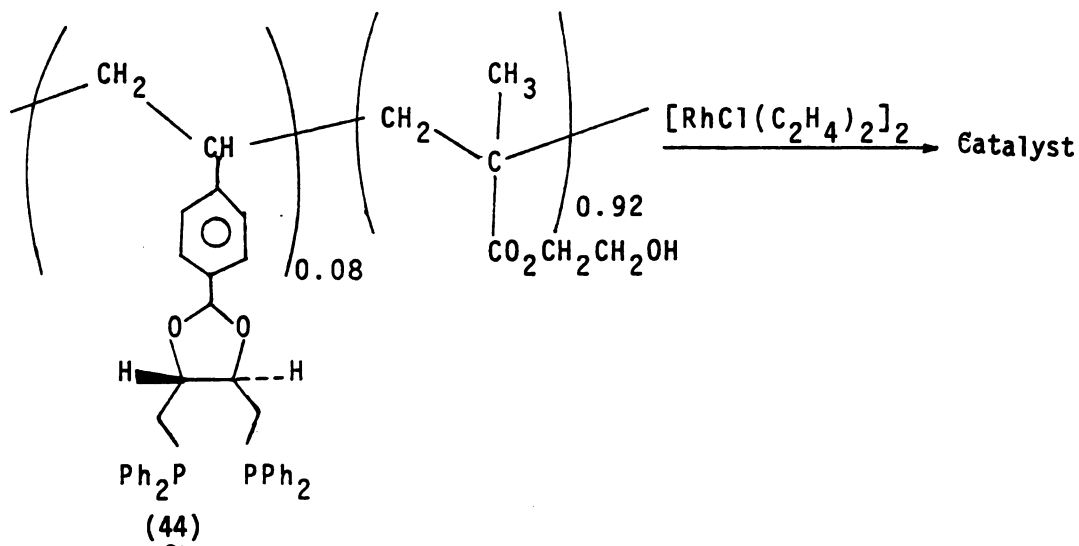
## G. Polymeric Chiral Diphosphines

Asymmetric hydrogenation with immobilized homogeneous catalysts have been studied for several years, but the optical yields achieved from the initial attempts were rather low.<sup>31, 32</sup> For example, in 1973, Kagan and his co-workers reported<sup>32</sup> that a DIOP type ligand, 2,3-*O*-isopropylidene-2,3-dihydroxy-1,4-bis(diphenylphosphino)butane (43), attached to cross-linked polystyrene, reacted with soluble rhodium(I) complexes to give asymmetric hydrogenation.



However, hydrogenation was possible only in benzene and the optical yields were only one-tenth of those found with the homogeneous catalyst. In polar solutions of the substrates, the beads collapsed and lost their catalytic

activity. To overcome this problem, Stille<sup>33</sup> and his co-workers successfully prepared a Rh(I)-DIOP (44) catalyst on a polar cross-linked copolymer of 2-hydroxyethyl-methacrylate and *p*-styryl (DIOP) with a 92:8 mole ratio. The preparation of this immobilized catalyst and asymmetric hydrogenation results are shown in Scheme 14.



R = Ph

86% e.e

R = H

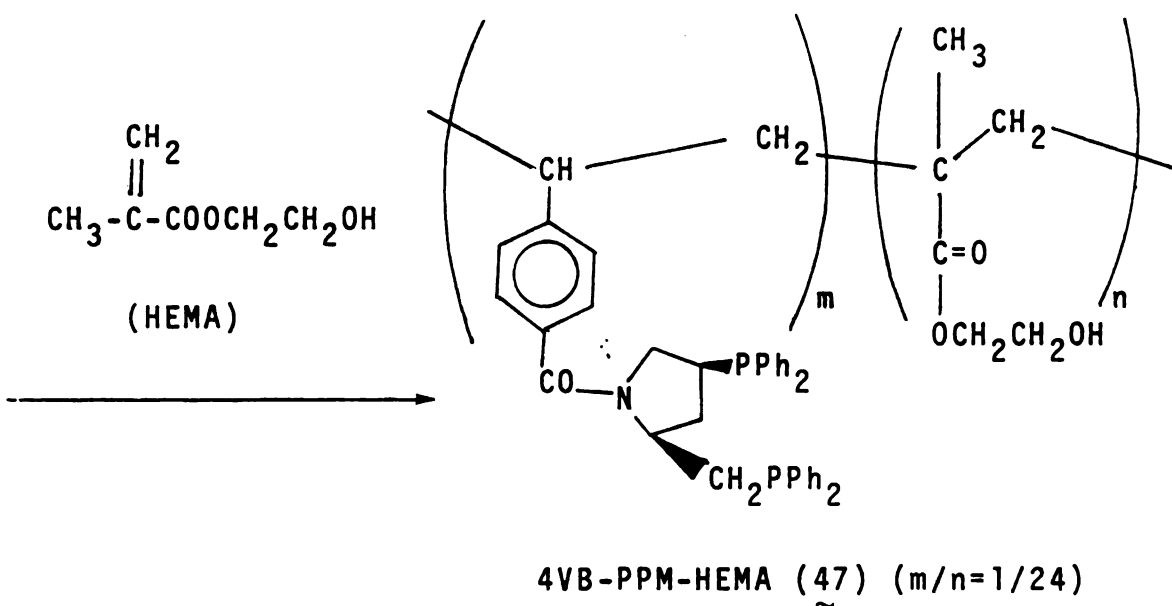
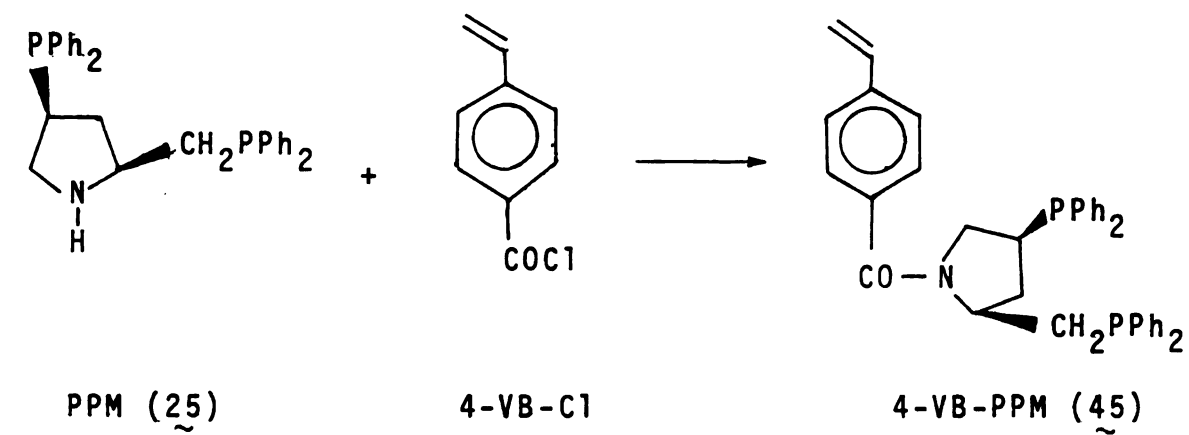
52-60% e.e.

Scheme 14

Since this copolymer was essentially a hydroxyethyl methacrylate gel, it could swell in polar solvents.  $\alpha$ -acetamidoacrylic acid and (*Z*)- $\alpha$ -acetamidocinnamic acid were hydrogenated in ethanol with this immobilized catalyst. The optical yields of both products were similar to those obtained in experiments with the homogeneous catalyst. The immobilized catalyst could be re-used, but repeated exposure to air during the filtering step led to low optical yields.

Achiwa used a similar method to prepare new polymer supported cationic and neutral chiral pyrrolidinephosphine rhodium complexes. 4VB-PPM-HEMA<sup>34</sup> (47), which was prepared by the copolymerization of 4-VB-PPM (45) with 2-hydroxy-ethyl methacrylate at a 1:24 mole ration, was allowed to react with rhodium(I) precursors to afford the new polymer supported catalysts (Scheme 15). Two substrates, itaconic acid and (*Z*)- $\alpha$ -acetamidocinnamic acid were hydrogenated with these supported Rh(I)-4-VB-PPM-HEMA (47) catalysts. The optical yields with polymer supported Rh(I)-4-VB-PPM-HEMA (47) catalysts depended on the conditions employed and whether triethylamine was added or not. The homogeneous analogous BZPPM (46) - rhodium (I) complexes gave almost the same optical yields (Table 11). Also, the polymer supported cationic catalyst was more effective than the supported neutral catalyst. In general, the supported Rh(I)-4-VB-PPM-HEMA (47) catalysts gave lower optical yields

than those of their homogeneous analogues.



Scheme 15

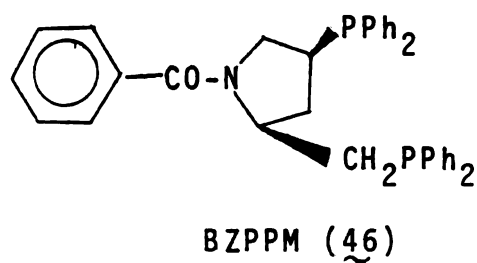
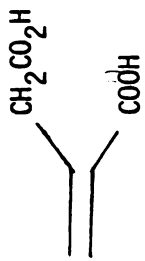
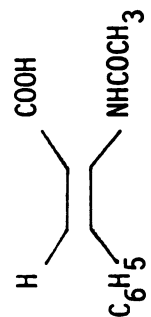


Table 11. Asymmetric Hydrogenation of Itaconic Acid and (Z)- $\alpha$ -Acetamidocinnamic Acid with Polymer Supported Rh(I)-4VB-PPM-HEMA (47) Catalysts and Homogeneous Analogues

Substrate	Solvent	Optical Yields (%)		
		Cationic Precursor <sup>a</sup> homogeneous (46)	<i>In Situ</i> Catalyst <sup>b</sup> homogeneous (46)	polymer (47)
	Methanol	82.3 (S)	83.5 (S)	—
	Methanol (NEt <sub>3</sub> )	88.9 (S)	80.6 (S)	—
	Ethanol	—	25.5 (S)	3.0 (R)
	Ethanol (NEt <sub>3</sub> )	—	82.3 (S)	40.3 (S)
	Recycled	—	77.6 (S)	—
	Ethanol (NEt <sub>3</sub> )	—	70.0 (R)	—
	Recycled	—	68.0 (R)	22.6 (R)

(a) Cationic precursor: [Rh(COD)(diphos\*)]ClO<sub>4</sub> diphos\* = BZPPM (46) or 4VB-PPM-HEMA(47)

(b) *In Situ* Catalyst : 0.5 [Rh(COD)Cl]<sub>2</sub> and BZPPM (46) or 4VB-PPM-HEMA (47)



Copolymer supported Rh(I)-PPM (25) catalysts also were synthesized by Stille and Baker.<sup>35</sup> The yields obtained from asymmetric hydrogenation of dehydroamino acids with copolymer supported catalysts were the same as those of the corresponding homogeneous results. The polymers containing optically active alcohols and chiral phosphines were also applied for asymmetric hydrogenation of dehydroamino acids. The results indicated that the solvent-polymer interactions dominated the effects of the additional chiral center.<sup>35</sup>

### III. Asymmetric Hydrogenation Mechanism Study

Asymmetric hydrogenation occurs as a result of the chiral rhodium complex reacting with the substrate to form diastereomeric transition states, which differ in energy.  $\Delta\Delta G^\ddagger$  determines the excess of one enantiomer over the other. The chiral diphosphine ligands play a key role in catalytic asymmetric hydrogenation with rhodium ions. The efficiency of the enantioselectivity is dependent upon on how well the chiral diphosphine ligand fits the substrate and how capably the substrate chelates the rhodium metal from a rigid complex in the transition states. Also, the solvation effect is very important since it can maximize the optical yields of the products.<sup>21,22</sup> In the polar solvent, solvent may form hydrogen bonds with functional groups of substrates and ligands.<sup>22</sup> The energy of such type bonding is comparatively small, (2-5kal/mol); but it is

enough to alter  $\Delta\Delta G^\ddagger$  and effect the optical yields.

#### A. Enamide Bonding Structure

Usually asymmetric hydrogenations of dehydroamino acids (enamides) with rhodium(I) chiral diphosphine complexes give high optical yields in comparison with other types of substrates. The enamides are capable of coordinating with rhodium via olefin and amide carbonyl residues to form rigid transition states, leading to higher asymmetric induction. The binding mode was first inferred from asymmetric hydrogenation data by Kagan.<sup>36</sup> The X-ray structure evidence was found by Halpern and co-workers.<sup>37</sup> The crystal structure of  $[\text{Rh}(\text{DIPHOS})(\text{methyl-(Z)}-\alpha\text{-acetamidocinnamate)}]^+$ <sup>37b</sup> showed bonding by the olefin and bonding by amide carbonyl in a square-planar complex (Figure 1). Also, Brown<sup>38</sup> and Chaloner have proved that the same structure was maintained in solution by the evidences of  $^{31}\text{P}$  and  $^{13}\text{C}$  NMR spectra.

#### B. Proposed Mechanisms and Asymmetric Induction Steps

Two kinds of mechanisms have been proposed for asymmetric hydrogenation.

1. Mechanism I "unsaturate route". In this mechanism, complexation of olefin proceeds the addition of hydrogen. Evidence was found by Halpern<sup>39</sup> and co-workers for support of the "unsaturate route" mechanism in the catalysis of hydrogenation by rhodium chelate diphosphine complexes. The catalytic cycle based upon his work is shown in Figure 2.

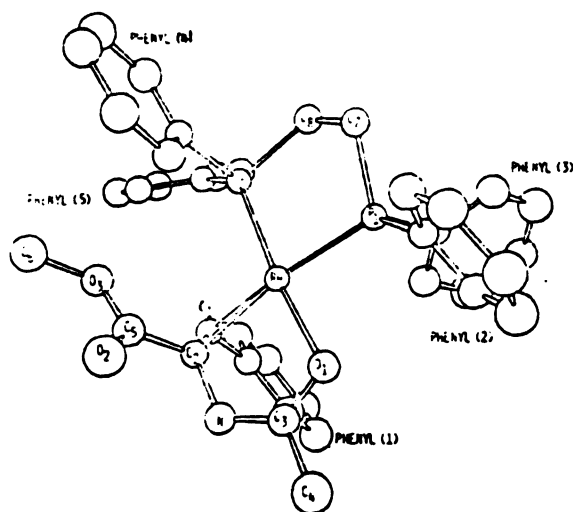
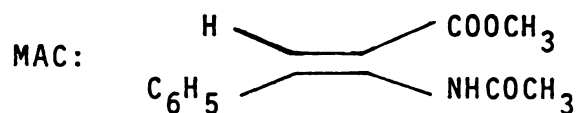


Figure 1. X-ray structure of  $[\text{Rh}(\text{DIPHOS})(\text{MAC})]^+$



DIPHOS: 1,2-Bis(diphenylphosphino)ethane

The catalyst precursor is usually a cationic  $[\text{Rh}(\text{diene})\text{diphos}^*]^+$  complex, where diphos\* is any chelating chiral or achiral diphosphine. The complex absorbs two moles of hydrogen to yield the highly active unsaturated complex,  $[\text{Rh}(\text{diphos}^*)]^+$ . The olefin will displace solvent from this complex to form a  $[\text{Rh}(\text{diphos}^*)\text{olefin}]^+$  complex then react with hydrogen, presumably to form the dihydride-olefin intermediate. Following the hydride transfer from the metal to coordinated face of the olefin it forms a rhodium alkyl hydride intermediate, which undergoes reductive elimination to produce the hydrogenated product (RH) and

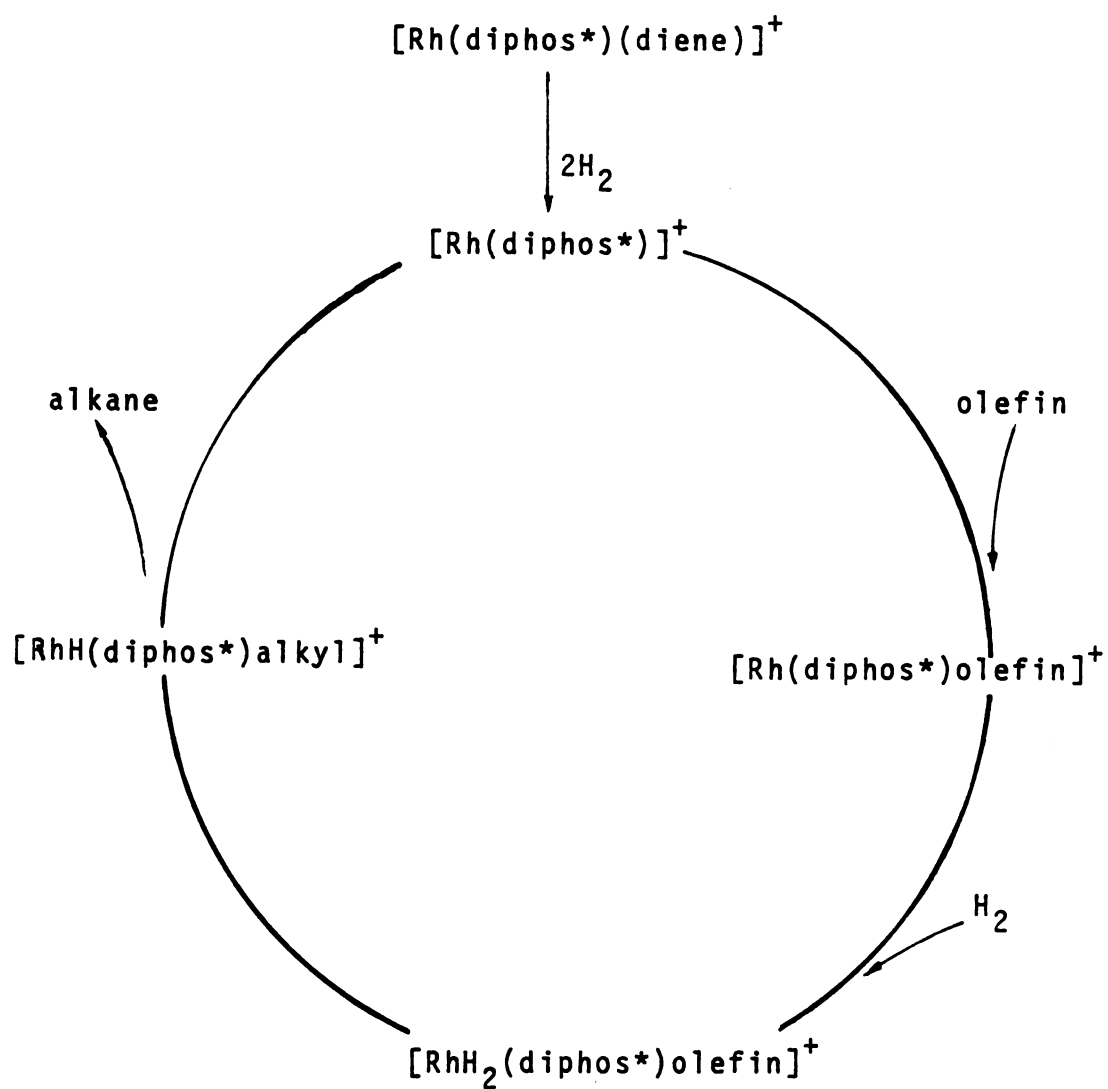


Figure 2. Hydrogenation catalytic cycle by unsaturated route

regenerates the catalyst.

Catalytic hydrogenation is normally conducted with 100-200 fold excess of enamide substrate over catalyst. The catalyst concentration is lower than  $10^{-3}$  M. Usually the rhodium(I) chiral diphosphine enamide complexes are present at steady-rate equilibrium. Two diastereomeric rhodium(I) enamide complexes can be observed with one predominating in most cases. Sometimes, however, the major diastereomeric Rh enamide complex does not correspond with the preferred final product.

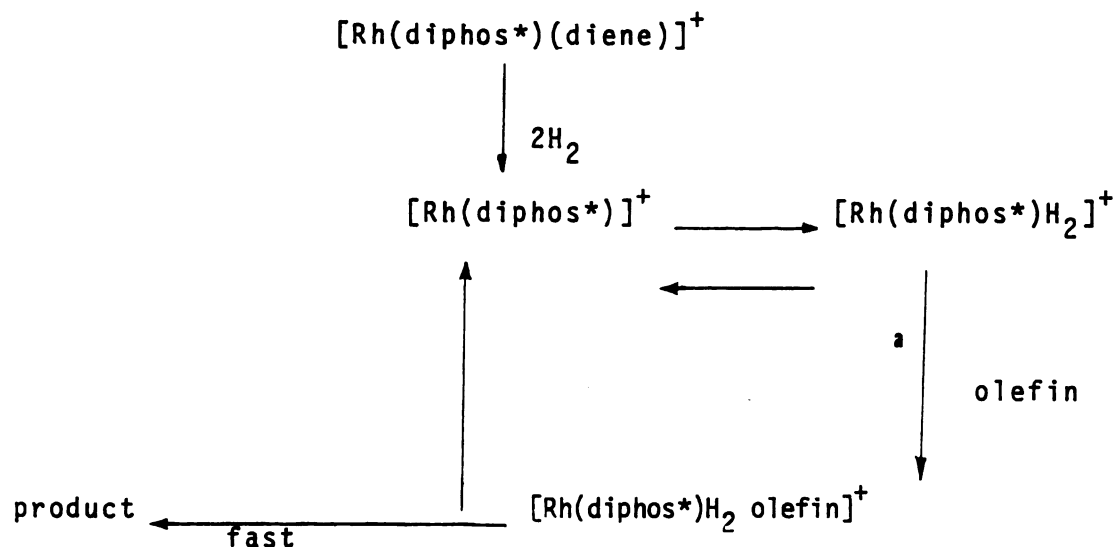
The asymmetric induction step can be either the displacement of the solvent by enamide, or the addition of hydrogen or *cis*-ligand migration, depending on the individual case. The type of chiral phosphine, temperature and pressure, are all factors which must be considered in the determination of the asymmetric induction step.

In the case of ( $\underline{S},\underline{S}$ )-Chirophos ( $\underline{5}$ ) system, Halpern, *et al.* reported that asymmetric induction occurred with the addition of the hydrogen step at low pressure.<sup>40</sup> The minor diastereomer Rh(I)-enamide complex (X-ray structure evidence) was the true intermediate which added hydrogen much faster than the major intermediate. With increasing pressure, the asymmetric induction step shifted to the initial catalyst-olefin adduct formation step. This led to lower enantioselectivity, even with the possibility to reverse the absolute configuration of the product.

With DIPAMP (12), Brown<sup>38</sup> reported that the optical yields observed by Knowles in hydrogenation of methyl-(Z)- $\alpha$ -acetamidocinnamate were higher than the diastereoselectivity in binding. This implies that the more stable rhodium(I) enamide complex was hydrogenated faster than the minor diastereomer. Moreover, the hydrogenation of methyl-(Z)- $\alpha$ -acetamidocinnamate was reported to be pressure dependent. At high pressure (27 atm) the optical yield was reduced to 78%, the enantiomer ratio of 89:19 corresponding closely with a diastereomer ratio of 91:9 which was observed by <sup>31</sup>P NMR. This may imply that at very high pressures the initial bonding of the prochiral olefinic substrate to the catalyst is the asymmetric induction step.

2. Mechanism II, "hydride route" (favorable under high hydrogen pressure). In this pathway, the dihydride Rh complex forms preceeding the olefin coordination with Rh metal.

This alternative mechanism was proposed by Ojima.<sup>41</sup> Mechanism II has been widely accepted for hydrogenation of olefins catalyzed with (Ph<sub>3</sub>P)<sub>3</sub>RhCl.<sup>42</sup> According to Ojima, Mechanism I favorably operated at low hydrogen pressure, whereas Mechanism II became predominant at higher pressures in the case of DIOP (3) and BPPM (23). In both Mechanism I and II, the formation of preferential Rh(I) enamide chiral diphosphine diastereomers are the asymmetric induction steps.<sup>41</sup> The stereochemistries of [Rh diphos\*]<sup>+</sup>



(a) rds = rate determining step

Figure 3. Hydrogenation catalytic cycle by the hydride route

and  $[\text{Rh H}_2\text{diphos}^*]^+$  dictate the orientation of prochiral olefin upon coordination, the latter leads to inversion in the configuration of the product. With the addition of triethylamine Mechanism II is greatly suppressed, i.e., triethylamine prevents pre-coordination of  $\text{H}_2$  at high pressures as well as improving optical yields. There needs to be more mechanistic work done to clarify the asymmetric induction steps in different chiral diphosphine systems.

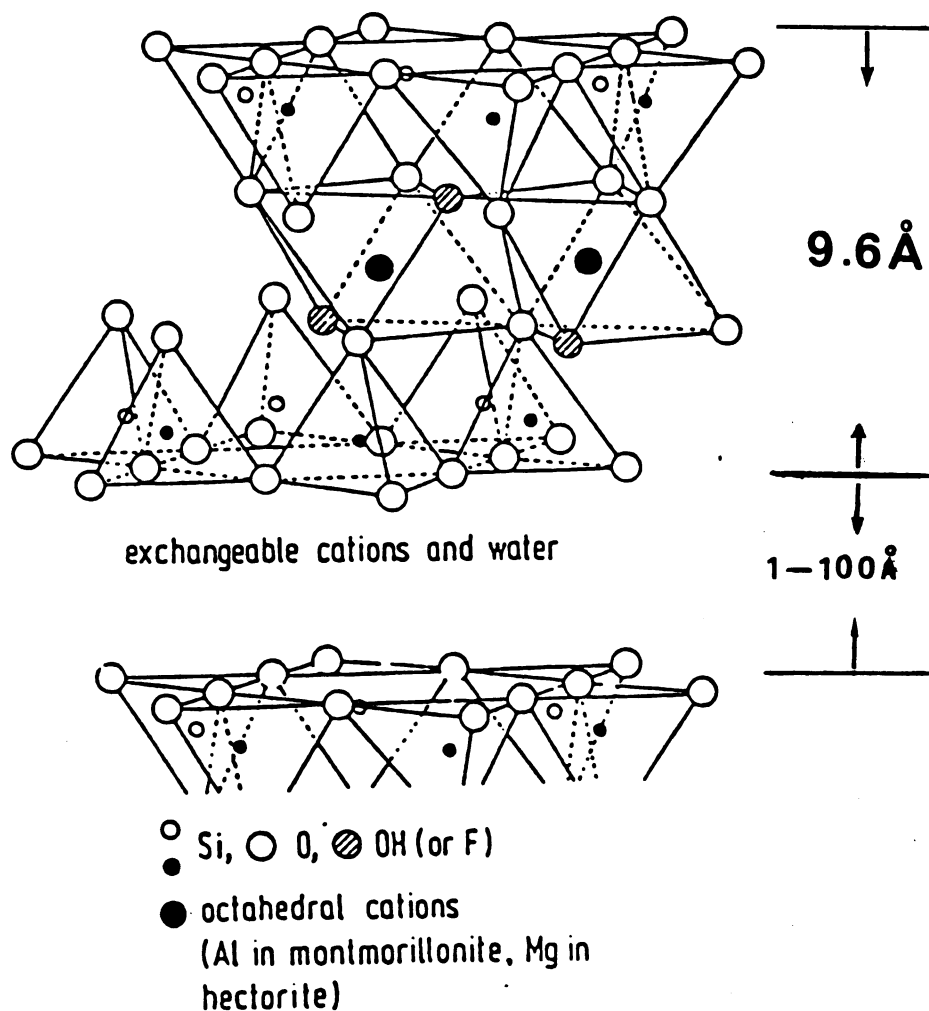
### C. $\underline{E}$ - $\underline{Z}$ Dehydroamino Acids Isomerization

The degree of  $\underline{E}$ - $\underline{Z}$  isomerization during hydrogenation of ( $\underline{E}$ )-dehydroamino acids with rhodium(I) chiral diphosphine complexes has been studied by NMR spectroscopy<sup>38,43</sup> and deuteration studies.<sup>44</sup> ( $\underline{E}$ )-dehydroamino acids do not bind strongly to rhodium(I) and convert into the corresponding ( $\underline{Z}$ )-enamide complexes, but stable complexes are formed in the presence of triethylamine.<sup>38</sup>

### IV. Catalyst Supports

The swelling mica-type silicates, better known as smectite clay minerals, have layer lattice structures, in which rigid two-dimensional silicate sheets approximately 9.6 Å thick are separated by interlayers of hydrated cations.<sup>45</sup> The structure of the oxygen framework of the silicate sheets and the position of interlayer cations are illustrated in Figure 4. The swelling layered silicates consist of one octahedral sheet sandwiched between two tetrahedral sheets. In the tetrahedral sheet, tetravalent Si is sometimes partly replaced by trivalent Al. In the octahedral sheet, Al<sup>III</sup> may also be replaced by Li<sup>I</sup>, Mg<sup>II</sup>, Fe<sup>II</sup>, and Fe<sup>III</sup>, etc. As a result of isomorphous substitution, the silicate sheet acquires a negative charge, and cations are incorporated in the spaces between the layers (interlayers) to preserve electroneutrality. In the presence of water, the cations on the layer surface may easily be exchanged by other





MONTMORILLONITE:  $\text{Na}_{0.66} \cdot \text{H}_2\text{O} [\text{Al}_{3.34}\text{Mg}_{0.66}] (\text{Si}_{8.0})_{20}(\text{OH})_4$

HECTORITE:  $\text{Na}_{0.66} \cdot \text{H}_2\text{O} [\text{Mg}_{5.34}\text{Li}_{0.66}] (\text{Si}_{8.0})_{20}(\text{OH, F})_4$

Figure 4. Structure of the mica-type swelling silicates such as montmorillonite or hectorite

cations when available in aqueous solution; hence they are called "exchangeable cations". The cation exchange sites in the layer silicates are found mainly in the interlamellar spaces (Figure 4). Additional exchange sites may exist at the edges and corners of silicate sheets, however, their contribution to the total cation exchange capacity is usually small.

Montmorillonite and hectorite are the two most important smectite minerals. In montmorillonite, which has an idealized anhydrous unit cell formula of  $\text{Na}_{0.66}[\text{Mg}_{0.66}\text{Al}_{3.34}](\text{Si}_{8.0})\text{O}_{20}(\text{OH})_4$ , two thirds of the octahedral positions are occupied by  $\text{Mg}^{+2}$  and  $\text{Al}^{+3}$  and the rest are vacant. In hectorite,  $\text{Na}_{0.66}[\text{Li}_{0.66}\text{Mg}_{5.34}](\text{Si}_{8.0})\text{O}_{20}(\text{OH}, \text{F})_4$ , the octahedral sites are filled by  $\text{Mg}^{+2}$  and  $\text{Li}^{+1}$ , and sometimes fluorine atoms are substituted for hydrogen atoms in the hydroxyl groups.

The properties of layered silicates are:

1. The internal surface area, which is calculated from the unit-cell weight, 769 g/mole, and unit-cell surface area,  $5.25 \times 9.18 \text{ \AA}^2$ , is about  $750 \text{ m}^2/\text{g}$ .
2. The cation exchange capacity is around 70 meq/100 g.
3. Interlayer swelling depends on the nature of the solvent and the interlayer cations and the charge density on the silicate framework.

The large internal surface area and the relatively high cation exchange capacity (70 meq/100 g, which compares favorably with the ion exchange capacities of resins), allow appreciable amounts of large catalytic cationic complexes to be intercalated. The cationic metal complexes can be electrostatically bonded between the silicate sheets. The intercalated catalysts can be sufficiently swollen in the polar solvents so that the active sites are accessible to the substrate. Also, the reaction products can easily diffuse through the layered silicates and out into the solution. In this manner they free a place for new portions of the substrate. Also, the intercalated catalysts are mechanically stable, and they cannot be crushed during the normal reaction process.

Studies of intercalates of the mica-type layered silicates, montmorillonite and hectorite are particularly appropriate at this time, since there has been a renewed interest in the use of such materials as catalysts or catalyst supports for highly specific chemical conversions. For example, highly thermally stable pillared interlayered clays (PILC) have been recently synthesized by the exchange of inorganic mono- and poly-nuclear cations.<sup>46</sup> {e.g.,  $\text{Al}_{13}\text{O}_4(\text{OH})_{24}^{+7}$ ,  $\text{Si}(\text{acac})_3^+$ ,  $[\text{Zr}_4(\text{OH})_{14}(\text{H}_2\text{O})_{10}]^{+2}$  and  $\text{Bi}_6(\text{OH})_{12}^{+6}$ } into the swelling layered silicates. These PILC clays offer interesting possibilities for industrial application

in cracking and hydro-cracking processes.<sup>47</sup> Also, Pinnavaia and his co-workers have proven that the swelling silicates are promising catalyst supports for the intercalation of a variety of cationic catalysts.<sup>48-51</sup> The intercalated catalysts could easily be isolated from reaction mixtures and reused. Several other advantages have also been reported for layered silicate systems. Among them are the enhancement of hydrogenation activity of the immobilized  $\text{Rh}(\text{PPh}_3)_n^+$  catalysts<sup>48</sup> and greater positional selectivity in both hydrogenation<sup>49,50</sup> and hydroformylation.<sup>51</sup>

## V. Research Objective

My research objective is asymmetric hydrogenation of prochiral olefins with rhodium(I) chiral diphosphine catalysts. This research can be divided into two parts.

I. Asymmetric hydrogenation of prochiral olefins with layered silicate intercalation catalysts.

II. Synthesis and characterization of new functionalized chiral diphosphine ligands for asymmetric hydrogenation.

In the first part of my research the focus was on the intercalation of different types of cationic chiral rhodium diphosphine complexes. Also, the effect of intercalation on the optical yields as a function

of substrate size, interlayer swelling and chelate ring size was studied. Optimization of enantioselectivity and a recycling of the catalysts were investigated.

In the second part of my research the emphasis was on the synthesis and characterization of new functionalized chiral diphosphine ligands; such as aminodiphos and hydroxydiphos ligands for asymmetric hydrogenation. The functionalized ligands were synthesized from natural occurring L-malic acid. The design of the new chiral diphosphine ligands was carried out keeping the following ideas in mind;

1. Ligands which are conformationally rigid are capable of producing high optical yields.
2. A third function group of the ligand can be modified in order to optimize the interactions between the third function group and substrate; resulting in enhanced asymmetric induction efficiency.
3. Ligands can be attached to polymeric, inorganic or organic carriers to recycle the precious catalysts and chiral ligands for practical use, and even improve optical yields.
4. Since chiral ligands have nonequivalent phosphorus, they can provide sensitive probes for elucidation

of the mechanism of asymmetric hydrogenation by  $^{31}\text{P}$  NMR.

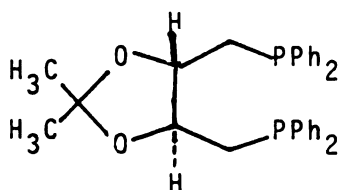
The results of the new ligands synthesis are encouraging, and these ligands are able to meet most of the requirements set forth above.

## RESULTS AND DISCUSSION

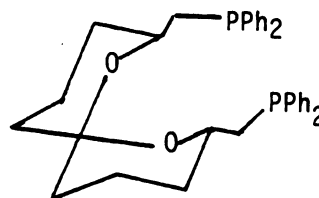
### I. Asymmetric Hydrogenation of Prochiral Olefins with Layered Silicate Intercalation Catalysts

#### A. Diphosphine Ligands

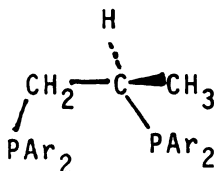
The diphosphine ligands, DIOP(+) (3), SPIPHOS (48), and (R)-Prophos (6) and its analogue, (R)-4-Me-Prophos (47), have been studied in this work.



DIOP(+) (3)



SPIPHOS (48)



(R)-Prophos Ar=C<sub>6</sub>H<sub>5</sub> (6)

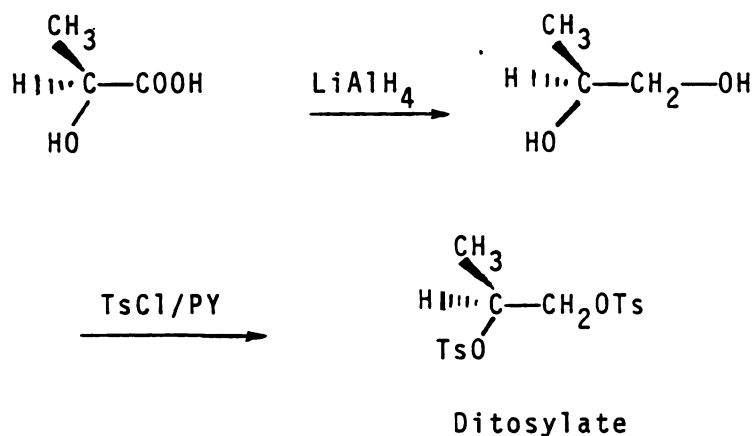
(R)-4-Me-Prophos Ar=4-CH<sub>3</sub>C<sub>6</sub>H<sub>4</sub>

(49)

DIOP (3) has proved to be a flexible ligand quite useful for asymmetric synthesis.<sup>1c,2b</sup> SPIPHOS (48) is also a highly flexible ligand;<sup>52</sup> it was obtained as a gift from Dr. DeVries. (R)-Prophos (6) and its analogues have been

shown to be rigid types of ligands. They are also effective for asymmetric hydrogenation of prochiral amino acids.<sup>9-15</sup>

(*R*)-Prophos (**6**) and new (*R*)-4-Me-Prophos (**49**) were prepared by modifying Bosnich's method.<sup>10</sup> The modified method differed from Bosnich's method in the final phosphination step. The purification of the ligands also was simplified. The synthetic precursor (*S*)-(+)-1,2-propanediol di-*p*-toluenesulfonate (ditosylate) was synthesized according to Bosnich's report<sup>10</sup> (Scheme 16).

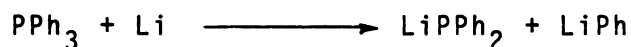


Scheme 16

The reduction of the L-lactic acid with lithium aluminum hydride in dry THF produced the (*S*)-(+)-1,2-propanediol in 85% yield. The (*S*)-(+)-1,2-propanediol was converted in ditosylate in 95% yield by reacting it with toluenesulfonyl chloride in pyridine. The phosphination of the ditosylate

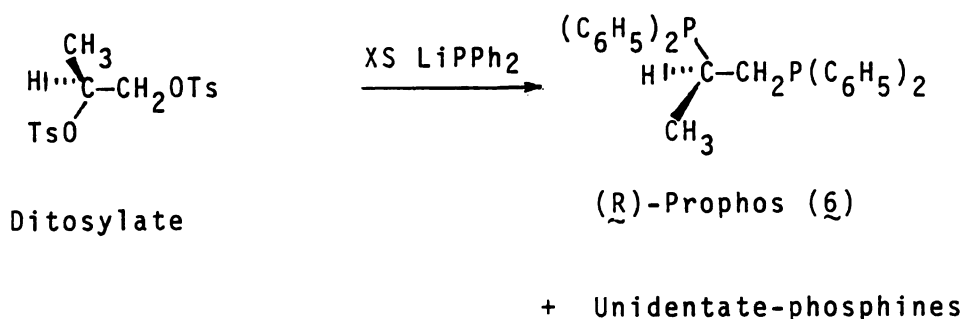


is the synthetic key step to form (R)-Prophos (6) and (R)-4-Me-Prophos (49). In Bosnich's method the phosphination reagent,  $\text{LiPPh}_2$ , was generated by cleavage of triphenylphosphine with a stoichiometric amount of lithium metal in THF (Scheme 17).



Scheme 17

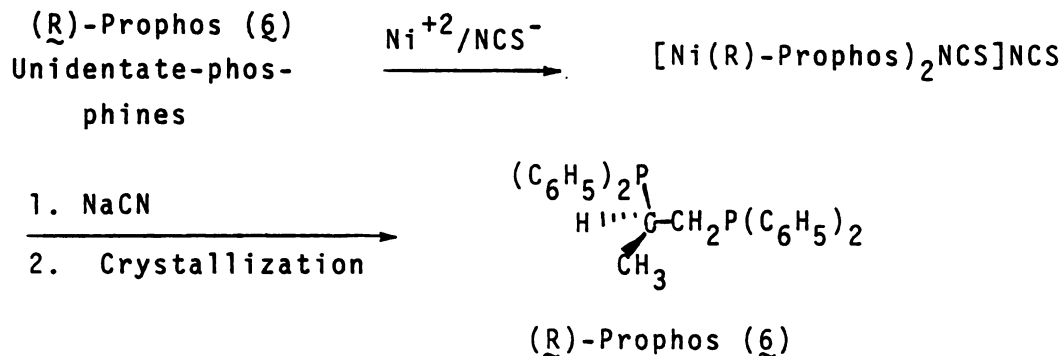
The by-product, phenyl lithium, was destroyed with a stoichiometric amount of *tert*-butyl chloride. 75% excess  $\text{LiPPh}_2$  was used for the phosphination reaction (assuming triphenylphosphine was converted quantitatively to  $\text{LiPPh}_2$ ). Phosphination of the ditosylate with excess  $\text{LiPPh}_2$  in THF afforded the crude oily product of (R)-Prophos (6) (Scheme 18).



Scheme 18

However, the crude product, (R)-Prophos (6), containing a large amount of unidentate phosphine by-products, caused a separation problem.

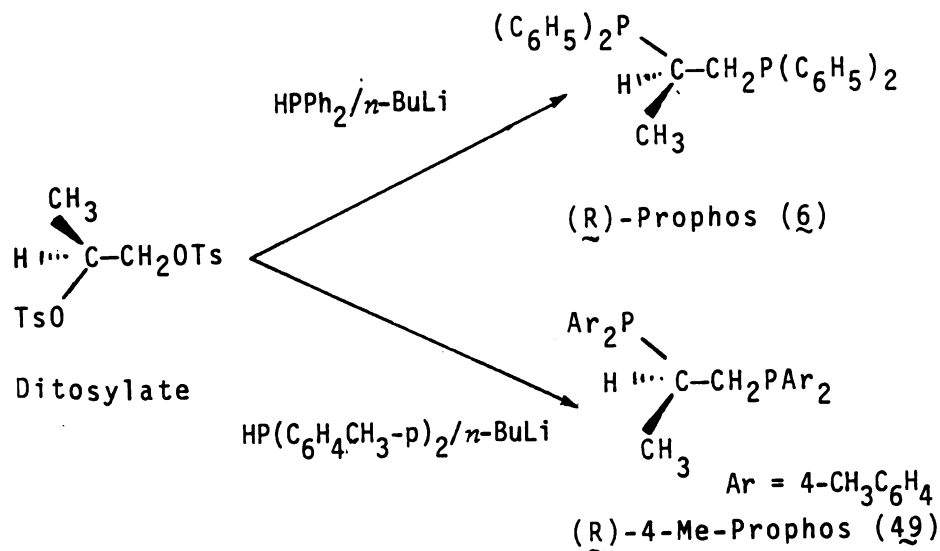
Bosnich used the following procedures to purify the crude product, (R)-Prophos (6) (Scheme 19).



Scheme 19

The addition of  $\text{Ni}(\text{ClO}_4)_2$  and  $\text{NaSCN}$  to the reaction mixture allowed the separation of the product as an insoluble  $\text{Ni}(\text{II})$  ( $\text{Prophos}$ )<sub>2</sub> thiocyanate complex. The pure (R)-Prophos (6) was obtained by treating  $\text{Ni}(\text{II})$  ( $\text{Prophos}$ )<sub>2</sub> thiocyanate complex with an excess of  $\text{NaCN}$  and crystallizing the ligand from absolute ethanol.

With the new, modified method, the phosphide reagents were generated from *n*-butyl lithium in hexane and diphenylphosphine or di-(4-methylphenyl)phosphine in THF. Only stoichiometric amounts of lithium phosphides were required for the phosphination reactions (Scheme 20). After the phosphination of the ditosylate with  $\text{LiPPh}_2$ , the crude (R)-Prophos (6) was separated from the oily reaction mixture by crystallization from absolute ethanol. A second



Scheme 20

crystallization from the same solvent gave (R)-Prophos (6) with the same specific rotation as Bosnich's product. Also, (R)-4-Me-Prophos (49) could be easily separated from the solid reaction mixture by crystallization from absolute ethanol/ $\text{CH}_2\text{Cl}_2$ . Further recrystallization did not change the optical rotation of (R)-4-Me-Prophos (49).

The advantages of the new, modified procedure lie in its simplicity and in the avoidance of the use of excess lithium-diphenylphosphide or lithium di-(4-methylphenyl) phosphide and highly toxic NaCN.

Table 12 shows the spectral parameters and physical properties of (6) and (49). In using the modified phosphination method the melting point and optical rotation of (R)-Prophos (6) were the same as Bosnich reported.<sup>10</sup> Since the four methyl groups of the 4-methylphenyl rings of (49)

Table 12. The Spectra Parameters and Their Physical Properties of (R)-Prophos (6) and (R)-4-Me-Prophos (49)

	(R)-Prophos (6)	(R)-4-Me-Prophos (49)
Melting point (C°)	67.5-68.5°C	129.5-130°C
Optical rotation	$[\alpha]_D^{26}$ 186.0° (c 1.0, acetone) <sup>a</sup>	$[\alpha]_D^{26}$ 172.6° (c 1.0, benzene)
<sup>31</sup> P NMR (85% H <sub>3</sub> PO <sub>4</sub> as external standard) (CDCl <sub>3</sub> , 25°C)	2.1 ppm, -20.2 ppm J <sub>P-P</sub> =21 Hz	0.3 ppm, -22.1 ppm J <sub>P-P</sub> =21 Hz
<sup>1</sup> H NMR (CDCl <sub>3</sub> , TMS) δ(ppm)	1.26 (dd, J <sub>1</sub> =15, J <sub>2</sub> = 6.5 Hz, 3H, CH <sub>3</sub> ) 1.84 (m, 1H, CH) 2.26 (m, 2H, CH <sub>2</sub> ) 7.25 (complex m, 20 H, 4 C <sub>6</sub> H <sub>5</sub> )	1.18 (dd, J <sub>1</sub> =15.8, J <sub>2</sub> = 6.7 Hz, 3H, CH <sub>3</sub> ) 1.78 (m, 1H, CH) 2.17, 2.21, 2.27 (3s, 4CH <sub>3</sub> , CH <sub>2</sub> ) 6.95 (complex m, 16H, 4 C <sub>6</sub> H <sub>4</sub> )
Mass spectra (m/e)	412 (M <sup>+</sup> ) 370 (M - CH <sub>2</sub> CHCH <sub>3</sub> ) <sup>+</sup> 303 (M - HPC <sub>6</sub> H <sub>5</sub> P) <sup>+</sup> 262, <sup>+</sup> P(C <sub>6</sub> H <sub>5</sub> ) <sub>3</sub> 185, <sup>+</sup> P(C <sub>6</sub> H <sub>5</sub> ) <sub>2</sub> 109, <sup>+</sup> HPC <sub>6</sub> H <sub>5</sub>	468 (M <sup>+</sup> ) 426 (M - CH <sub>3</sub> CHCH <sub>2</sub> ) <sup>+</sup> 345 (M - HPC <sub>6</sub> H <sub>4</sub> CH <sub>3</sub> ) <sup>+</sup> 304, <sup>+</sup> P(C <sub>6</sub> H <sub>4</sub> CH <sub>3</sub> ) <sub>3</sub> 213, <sup>+</sup> P(C <sub>6</sub> H <sub>4</sub> CH <sub>3</sub> ) <sub>2</sub> 123, <sup>+</sup> HPC <sub>6</sub> H <sub>4</sub> CH <sub>3</sub>
High resolution mass spectra (m/e)	_____	observed 468.21459 calcd (C <sub>31</sub> H <sub>34</sub> P <sub>2</sub> ) 468.21358
Chemical analysis	_____	found: C, 79.20; H, 7.36; P, 13.47 calcd: C, 79.46; H, 7.31; P, 13.22

<sup>a</sup> c = g/100 mL of solvent

are not identical, four methyl resonances are expected. However, the two methyl groups adjacent to the achiral carbon atom have the same chemical shifts, but the methyls near the chiral carbon atom are distinguishable. The  $^1\text{H}$  NMR spectrum of the four methyl groups (49) showed three distinguishable peaks in the region of 2.1-2.3 $\delta$  (Figure 5). Also, the  $\text{CH}_3$  at the carbon backbone showed a doublet of doublets due to coupling to the adjacent hydrogen and phosphorus atoms. The same characteristics are observed for (R)-Prophos (6). The  $^{31}\text{P}$  NMR spectrum of (49) showed two sets of doublets at -0.3, -22.1 ppm. The chemical shifts and the coupling constant are similar to those of (R)-Prophos (6) (see Table 12). (R)-4-Me-Prophos (49) has a high melting point (129.5-130°C) in comparison with that of (R)-Prophos (6) (68.9°C), and it is easily crystallized.

The mass spectrum of (R)-4-Me-Prophos (49) exhibits the fragmentation pattern similar to the pattern of (R)-Prophos (6). The high resolution mass spectrum and the chemical analysis of (R)-4-Me-Prophos (49) are in good agreement with the expected values.

#### B. General Method for the Preparation of Cationic Catalysts

$[\text{Rh}(\text{diene})\text{Cl}]_2$  was treated with silver perchlorate and then with diphos\* where diphos\* was DIOP(+) (3), SPIPHOS (48), (R)-Prophos (6) or (R)-4-Me-Prophos (49) to form the cationic precursor  $[\text{Rh}(\text{diene})\text{diphos}^*]\text{ClO}_4$  (Scheme 21).

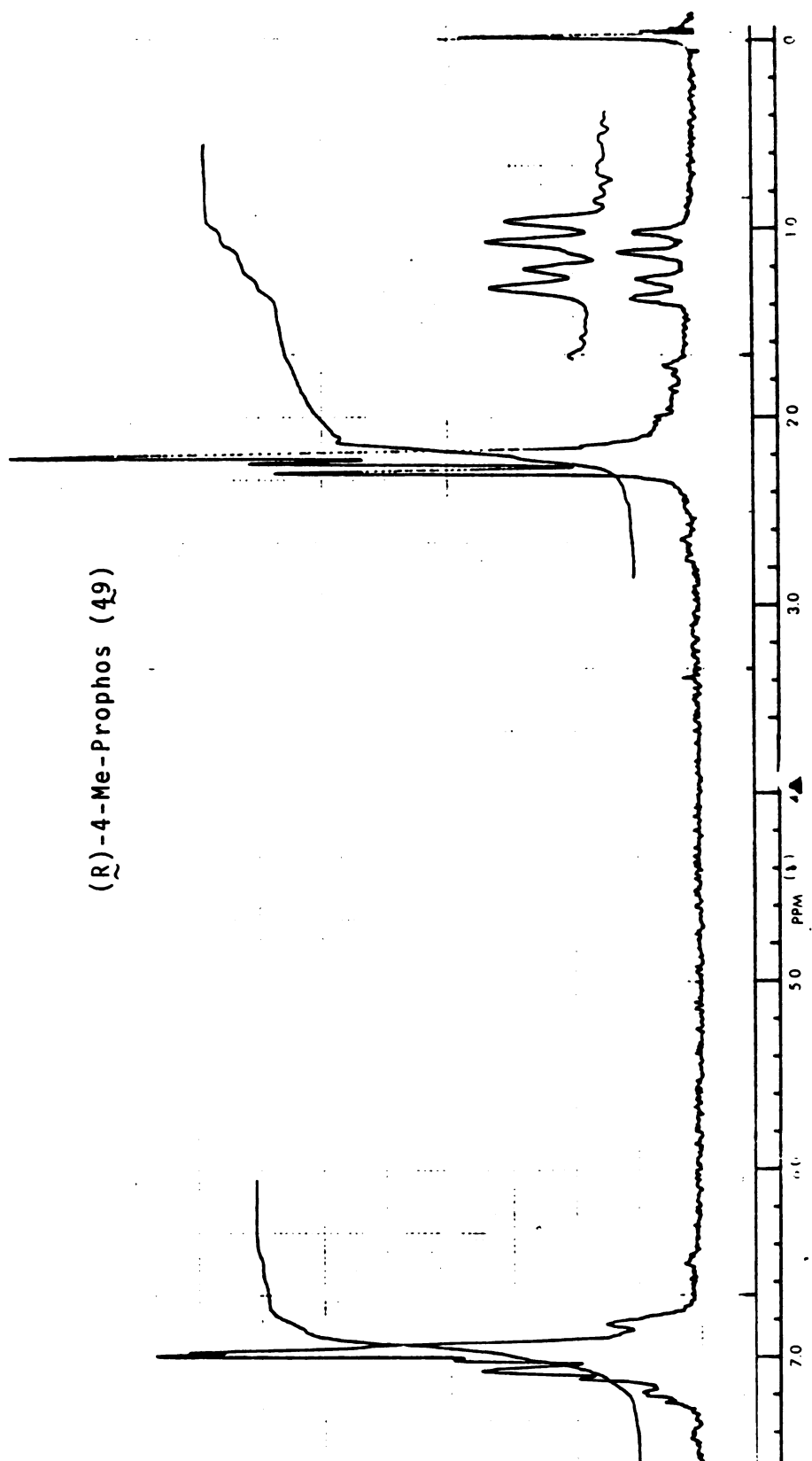
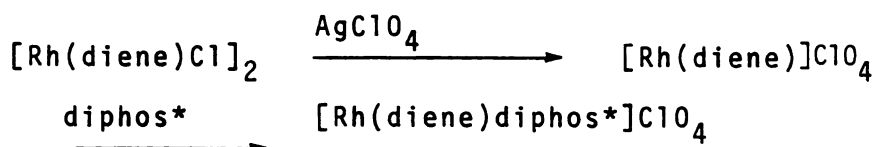


Figure 5.  $^1\text{H}$  NMR spectrum of (R)-4-Me-Propos (49) in  $\text{CDCl}_3$  at  $25^\circ\text{C}$  (60 MHz)



diene = NBD or COD

diphos\* = DIOP(+) (3), (R)-Prophos (6)  
 SPIPHOS (48) or (R)-4-Me-Prophos (49)

Scheme 21

The cationic precursor  $[\text{Rh(diene)diphos}^*]\text{ClO}_4$  can be used directly for homogeneous catalytic reactions, or it can be exchanged with Na-hectorite to form  $[\text{Rh(diene)diphos}^*]^+$ -hectorite for intercalated catalytic hydrogenation.

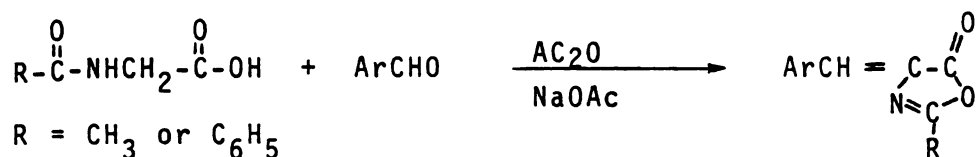
### C. Intercalation Catalysts and Interlayer Spacings

The cationic exchange of  $[\text{Rh(NBD)(diphos}^*)]^+$  complexes in MeOH or 95% EtOH with  $\text{Na}^+$ -hectorite led to the formation of intercalation complexes in which 15-20% of the  $\text{Na}^+$  ions have been replaced by the rhodium complex. The  $d(001)$  X-ray spacings for the unsolvated intercalation complexes were 16-18 Å. Typically, one order of 001 reflection was observed. The observed spacings agree with the expected values for monolayer coverage of the interlayer surfaces. Solvating the intercalation complexes with methanol or 95% ethanol causes the  $d(001)$  spacings to increase to 19-20 Å. Usually two orders of 001 reflection were observed.

Since the silicate sheets are  $9.6 \text{ \AA}$  thick, this means that interlayers occupied by the rhodium complexes are around  $9\text{-}10 \text{ \AA}$  thick.

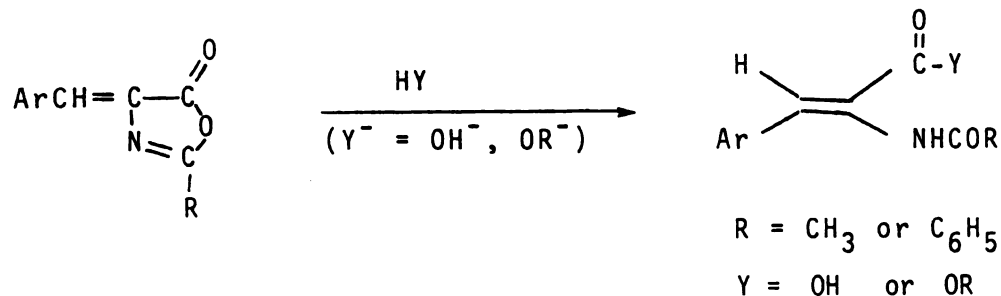
#### D. Preparation of Dehydroamino Acid Derivatives via Unsaturated Azlactones

The condensation of *N*-acetyl-glycines or *N*-benzoyl-glycines with aromatic aldehydes in the presence of acetic anhydride and sodium acetate is the commonly used method for the preparation of unsaturated azlactones<sup>53</sup> (Scheme 22).



Scheme 22

The carbonyl group of the azlactones can undergo nucleophilic attack by  $\text{OH}^-$  or  $\text{OR}^-$  to form dehydroamino acid derivatives (Scheme 23).



Scheme 23



The dehydroamino acid esters can be easily hydrolyzed to the corresponding carboxylic acids. Six dehydroamino acid derivatives used in this work were prepared by adopting the above procedures (Table 13).

#### E. Hydrogenation Conditions

In general, the concentration of the substrate used in the hydrogenation reactions were in the range of 0.13-0.27 M. The hydrogenation of the L- DOPA precursor, which has limited solubility, was carried out by utilizing 1.17 g of substrate in 30 mL of solvent. The molar ratio of substrate to rhodium under both homogeneous and intercalation catalyst conditions was 100 to 200. Methanol or 95% ethanol was used as the solvating medium. The hydrogenations were carried out at room temperature and 1 atmosphere pressure. The concentrations of Rh(I)(diphos\*) complexes were around  $10^{-3}$  M. The cationic rhodium(I)(diphos\*) catalysts formed under hydrogenation conditions are highly oxygen sensitive. Precautions were taken to exclude oxygen, since traces of oxygen will deactivate the catalysts easily and lead to low optical yields of the products.<sup>2c</sup> The hydrogenation rates were monitored by following hydrogen uptake as a function of time. The Rh(I)(diphos\*) enamide complexes, which formed as intermediates in the hydrogenation reactions, exhibited a characteristic orange-red color.

Table 13. The Preparation of (Z)-Dehydroamino Acids

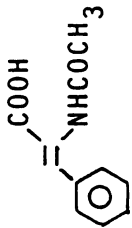
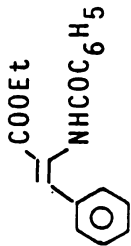
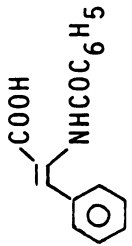
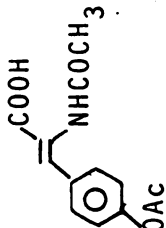
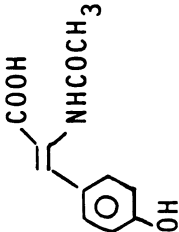
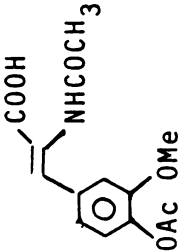
Substrate	Preparation Method
 <p>(Z)-g-Acetamidocinnamic Acid<sup>54</sup></p>	Hydrolysis of the corresponding azlactone in acetone/H <sub>2</sub> O
 <p>Ethyl (Z)-g-Benzamido-cinnamate<sup>55</sup></p>	Alcoholysis of the corresponding azlactone in NaOEt solution/toluene
 <p>(Z)-g-Benzamidocinnamic Acid<sup>55</sup></p>	Base hydrolysis of the corresponding ester in aqueous NaOH solution/EtOH
 <p>(Z)-α-Acetamido-4-acetoxycinnamic Acid<sup>56</sup></p>	Hydrolysis of the corresponding azlactone in H <sub>2</sub> O/acetone

Table 13. Continued

Substrate	Preparation Method
	Base hydrolysis of the corresponding azlactone in 0.5 N NaOH solution
	Hydrolysis of the corresponding azlactone <sup>a</sup> in H <sub>2</sub> O/acetone

<sup>a</sup>The azlactone was synthesized according to the method described for the azlactone of (Z)-α-benzamidocinnamic acid's derivative<sup>57</sup>

This color persisted throughout the hydrogenation periods. At the end of the reactions the color of the solutions instantly changed to straw-yellow. The same color changes were observed for the intercalated catalysts.

#### F. Characterization of Dehydroamino Acids and Their Corresponding $\alpha$ -Amino Acids

$^{13}\text{C}$  NMR provided distinguishable features for the dehydroamino acids and their corresponding hydrogenated products. Table 14, 15 and 16 show the  $^{13}\text{C}$  NMR chemical shifts of selected carbons of the dehydroamino acids and their corresponding  $\alpha$ -amino acids. The chemical shifts of the amide carbons ( $\text{NH}\text{C}\text{OR}$ ), carboxyl carbons ( $\text{COOH}$ ), and vinylic carbons ( $\alpha$  position) were significantly altered upon hydrogenation of the  $\text{C} = \text{C}$  bond. The chemical shifts of selected carbons were assigned based upon the literature<sup>38,58</sup>. The  $^1\text{H}$  NMR spectra of the dehydroamino acid substrates and the corresponding hydrogenated products also were different.

The chemical conversions were monitored by observing the disappearance of substrate and the appearance of product by  $^1\text{H}$  NMR. The differences in chemical shifts of the  $\alpha$  and  $\beta$  hydrogens in the corresponding  $\alpha$ -amino acid derivatives allowed accurate estimation of the percent chemical conversion in these systems. Chemical shift differences between the aromatic hydrogens of tyrosines and DOPA precursors and their corresponding hydrogenated products

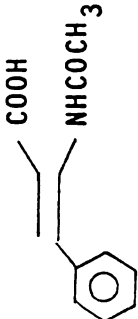
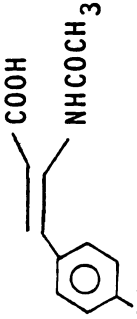
TABLE 14.  $^{13}\text{C}$  NMR Chemical Shifts of Dehydroamino Acids and Their Corresponding  $\alpha$ -Amino Acids in  $\text{D}_6$ -DMSO Solution at 20.03 MHz and 25°C<sup>a</sup>

	$\text{NHCOC}_6\text{H}_5$	COOH	$\text{ArCH}_2\text{CH}$	$\text{OCH}_2\text{CH}_3$	$\text{CH}_2\text{CH}_3$
	166.5	166.3	—	—	—
	173.3	166.5	54.3	—	—
	166.3	165.0	—	60.9	14.1
	171.7	166.5	54.4	60.5	14.0
	166.2	165.5	—	52.2 (OCH <sub>3</sub> )	—

<sup>a</sup> $^{13}\text{C}$  NMR are reported in parts per million (ppm) relative to TMS as an internal standard. All spectra were proton decoupled.

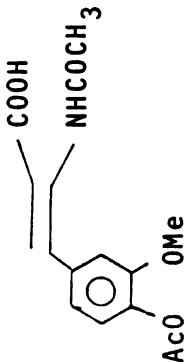
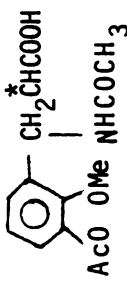


Table 15.  $^{13}\text{C}$  NMR Chemical Shifts of Dehydroamino Acids and Their Corresponding  $\alpha$ -Amino Acids in  $\text{D}_6$ -DMSO Solution at 20.03 MHz and 25°C<sup>a</sup>

	$\text{NHCOCH}_3$	$\text{COOH}$	$\text{NHCOCH}_3$	$\text{ArCH}_2\text{CH}$
	169.7	166.7	22.7	—
$\text{C}_6\text{H}_5\text{CH}_2\overset{*}{\text{CH}}\text{COOH}$ $\text{NHCOCH}_3$	173.3	169.9	22.5	53.7
	169.9	167.1	22.9	—
$4\text{-HOC}_6\text{H}_4\text{CH}_2\overset{*}{\text{CH}}\text{COOH}$ $\text{NHCOCH}_3$	173.4	169.5	22.5	54.0

<sup>a</sup>  $^{13}\text{C}$  NMR spectra are reported in parts per million (ppm) relative to TMS as an internal standard. All spectra were proton decoupled.

Table 16.  $^{13}\text{C}$  NMR Chemical Shifts of DOPA Precursor and L-DOPA in  $\text{D}_6\text{-DMSO}$  Solution at 20.05 MHz and  $25^\circ\text{C}$ <sup>a</sup>

	$\text{NHCOCH}_3$	COOH and $\text{CH}_3\text{COO}$	$\text{OCH}_3$	$\text{ArCH}_2\text{CH}$	$\text{NHCOCH}_3$	$\text{CH}_3\text{COO}$
	169.4	168.5, 166.5	55.8	—	22.5	20.4
	173.2	169.5 168.6	55.7	53.5	22.4	20.4

<sup>a</sup> $^{13}\text{C}$  NMR spectra are reported in parts per million (ppm) and relative to TMS as an internal standard. All spectra were proton decoupled.



provided additional information for estimating the chemical conversions of the products. Seven dehydroamino acids were used for this work. The percent chemical yields of the corresponding amino acids were larger than 97%, as evidenced by the  $^1\text{H}$  NMR spectra.

#### G. Optical Yields

The optical yields were determined by dividing the specific rotation of the product mixture by the absolute rotation of the pure enantiomer determined under identical conditions of temperature, concentration and wavelength. The method assumes a linear relationship between rotation and composition.<sup>1d</sup>

$$\% \text{optical yield} = \frac{[\alpha]}{[\alpha]_{\text{abs}}} \times 100\% = \% \text{enantiomeric excess}$$

It must be noted that the assumption is not always valid as in the case of  $\alpha$ -methyl- $\alpha$ -ethylsuccinic acid where the plot deviated appreciably from linearity.<sup>59</sup> The absolute rotations of the pure corresponding amino acid derivatives were taken from the literature<sup>9</sup>.

In this study optical rotations were recorded with a Perkin Elmer 141 automatic polarimeter. Two measurements were recorded for each sample by preparing two independent solutions. The optical rotation method is the commonly

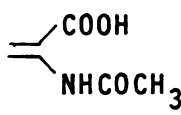
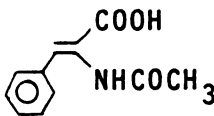
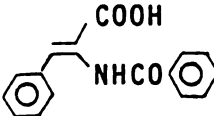
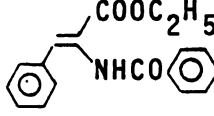
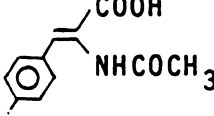
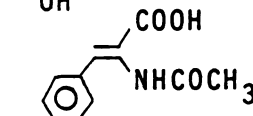
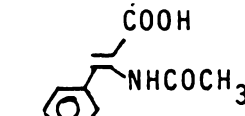
accepted method for estimating optical yields of asymmetric hydrogenation reactions. Other direct methods which are less sensitive to impurities are also possible such as NMR, GLC, or HPLC analysis of diastereomeric mixtures.<sup>1c</sup>

#### 1. (R)-Prophos (6) and (R)-4-Me-Prophos (49) Systems

The results of asymmetric hydrogenation of dehydro-amino acids with intercalated and homogeneous  $[\text{Rh}(\text{NBD})(\text{R})\text{-Prophos (6)}]^+$  catalysts are shown in Table 17. In the homogeneous system the optical yields of the different substrates were around 90%, in good agreement with the results of Bosnich<sup>10</sup>. The optical yields of the corresponding  $\alpha$ -amino acids with intercalation catalysts were generally lower than those obtained with the homogeneous catalyst, with one exception. The optical yield for N-acetyl tyrosine was slightly higher for the intercalated catalyst. In general, the deviations from solution yields were smallest for the acetyl derivatives of L-phenylalanine and DOPA (~5%). Larger deviations were observed for the remaining precursors (~15-30%).

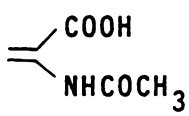
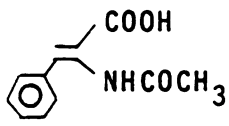
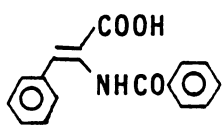
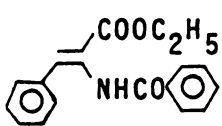
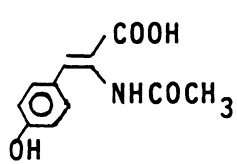
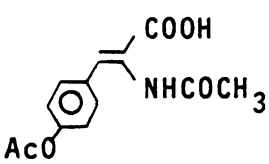
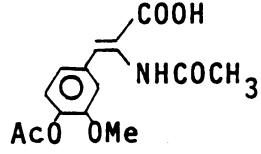
The results of asymmetric hydrogenation of dehydro-amino acids with intercalated and homogeneous  $[\text{Rh}(\text{NBD})(\text{R})\text{-4-Me-Prophos (49)}]^+$  catalysts are given in Table 18. In the (R)-4-Me-Prophos (49) system, the optical yields obtained with the homogeneous catalyst were similar to those obtained with the homogeneous Rh(I)-(R)-Prophos (6) catalyst.

Table 17. Asymmetric Hydrogenation of Dehydroamino Acids with Intercalated and Homogeneous  $[\text{Rh}(\text{NBD})(\text{R})\text{-Prophos (6)}]^+$  catalysts

<u>Substrate</u>	<u>Amino Acid</u>	<u>Optical Yield (%)</u>	
		<u>Intercal.</u>	<u>Homogen.</u>
	L-Alanine	73.3	93.7
	L-Phenylalanine	85.4	89.0
	L-Phenylalanine	70.0	92.0
	L-Phenylalanine	60.5	89.3
	L-Tyrosine	82.1	79.0
	L-Tyrosine	75.0	90.1
	L-DOPA	86.7	92.0

<sup>a</sup>The hydrogenations were carried out on 4-8 mmol of substrate in 30 mL 95% EtOH at 25°C and 740 torr. The amount of intercalated or homogeneous catalyst used for each reaction was 0.04 mmol. All the corresponding acids had (S)-configurations.

Table 18. Asymmetric Hydrogenation of Dehydroamino Acids with Intercalated and Homogeneous  $[\text{Rh}(\text{NBD})(\text{R})\text{-4-Me-Prophos (49)}]^+$  Catalysts

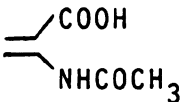
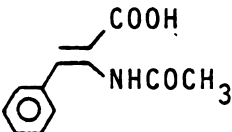
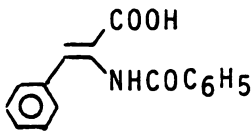
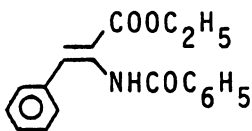
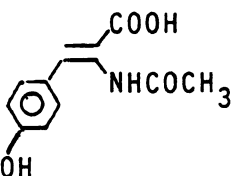
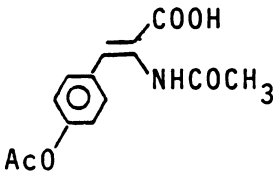
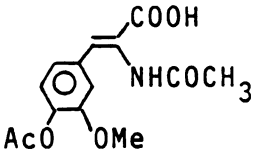
<u>Substrate</u>	<u>Amino acid</u>	<u>Optical Yield (%)<sup>a</sup></u>	
		<u>Intercal.</u>	<u>Homogen.</u>
	L-Alanine	76.5	88.0
	L-Phenylalanine	89.6	92.6
	L-Phenylalanine	75.7	94.5
	L-Phenylalanine	75.5	93.6
	L-Tyrosine	78.5	72.0
	L-Tyrosine	88.1	91.0
	L-DOPA	95.1	95.3

<sup>a</sup>The hydrogenations were carried out on 4-8 mmol of substrate in 30 mL 95% EtOH at 25°C and 740 torr. The amount of intercalated or homogeneous catalyst used for each reaction was 0.03 mmol. All the corresponding acids had (S)-configurations.

The optical yields of the corresponding  $\alpha$ -amino acids with the intercalated Rh(I)-(R)-4-Me-Prophos (49) catalyst precursor were lower than those obtained with the homogeneous catalyst. However, the deviations from homogeneous optical yields were less for the (R)-4-Me-Prophos (49) system than for the (R)-Prophos (6) system. This could be proven by comparing the difference in optical yields ( $Y_I - Y_H$ ) for the (R)-4-Me-Prophos (49) system with those of the (R)-Prophos (6) system; where  $Y_I$  = optical yield with intercalated  $[\text{Rh}(\text{NBD})\text{diphos*}]^+$  catalyst,  $Y_H$  = optical yield with homogeneous  $[\text{Rh}(\text{NBD})\text{diphos*}]^+$  catalyst (Table 19).

The methyl groups at the *para* positions of the phenyl rings of  $[\text{Rh}(\text{NBD})(\text{R})\text{-4-Me-Prophos (49)}]^+$  enhance the catalyst's size, relative to  $[\text{Rh}(\text{NBD})(\text{R})\text{-Prophos}]^+$ . The 4-Me-Prophos complex is intercalated into the layered silicates; the interlayers should be more solution-like than when the (R)-Prophos occupies the interlayers. Also, the optical yield (95%) of the most important amino acid derivative investigated, L-DOPA, was the same for intercalated and homogeneous  $[\text{Rh}(\text{NBD})(\text{R})\text{-4-Me-Prophos (49)}]^+$  catalyst precursors. Thus, there appears to be considerable potential for the practical application of layered silicate intercalation catalysts.

Table 19. Difference in Optical Yields ( $\gamma_I - \gamma_H$ ) for Intercalated and Homogeneous Cationic  $[\text{Rh}(\text{NBD})(\text{diphos}^*)]^+$  Precursors.

Substrate	$\gamma_I - \gamma_H^a$	
	(R)-Prophos (6)	4-Me-(R)-Prophos (49)
	-20.4	-11.5
	- 3.6	-3.0
	-22.0	-18.8
	-28.8	-18.1
	+3.1	+6.5
	-15.1	-2.9
	-5.3	-0.2

<sup>a</sup> $\gamma_I$  and  $\gamma_H$  are the optical yields for the products obtained with the intercalated catalyst and the homogeneous catalyst, respectively.

## 2. SPIPHOS (48) System

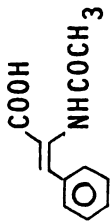
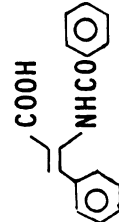
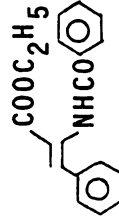
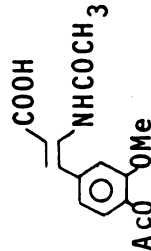
The SPIPHOS ligand (48), which had a high degree of conformational mobility, was prepared by DeVries.<sup>52</sup> The cationic  $[\text{Rh}(\text{COD})\text{SPIPHOS (48)}]^+$  precursor and *in situ* rhodium SPIPHOS (48) catalyst, which was prepared from  $[\text{Rh}(\text{cyclo-octene})_2\text{Cl}]_2$  and SPIPHOS (48), were used for the asymmetric hydrogenation of (*Z*)-dehydroamino acids and non-enamide type substrates. Both systems afforded moderate optical yields and showed a strong base effect with the addition of triethylamine.<sup>52</sup> In some cases, the absolute configuration of the products were reversed by the addition of triethylamine. Variations in temperature and pressure only slightly affected optical yields.

An inspection of molecular models suggests that when the ligand coordinates to rhodium, it is capable of forming a ten-membered chelate ring. The complex is highly flexible. Due to the large chelate ring size, the phosphorous atoms of the ligand could *trans*-coordinate to rhodium. A *trans* structure for the Rh(I)-SPIPHOS complex could lead to low asymmetric induction and thus low optical yields in the asymmetric hydrogenation of (*Z*)-dehydroamino acids.

In the layer silicate system, the flexibility of the Rh(I)-SPIPHOS (48) complex might be restricted by the silicate sheets. However, if the *trans*-coordinated structure of the complex dominated in the interlayer regions, the optical yields may not be improved by intercalation.

Table 20 shows the results of asymmetric hydrogenation of

Table 20. Asymmetric Hydrogenation of Dehydroamino Acids with Intercalated and Homogeneous  $[\text{Rh}(\text{NBD})\text{SPIPHOS} (48)]^{\dagger}$  Catalysts

Substrate	Amino Acid	Solvent	Optical yield <sup>a</sup> (%)	
			Intercal.	Homogen.
	Phenylalanine	95% EtOH Methanol	35 47	42 47
	Phenylalanine	95% EtOH Methanol	45 28	54 47
	Phenylalanine	95% EtOH Methanol	16 26	70 72
	DOPA	95% EtOH Methanol	44 44	56 62

<sup>a</sup>The hydrogenations were carried out on 4 or 5 mmol of substrate in 30 mL of MeOH or 95% EtOH at 25°C and 740 torr. The amount of intercalated or homogeneous catalysts used for each reaction was 0.03 mmol. All the corresponding acids had (*R*)-configurations.



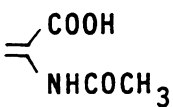
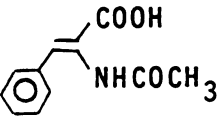
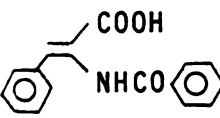
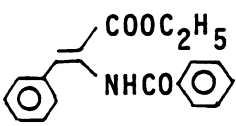
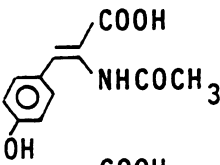
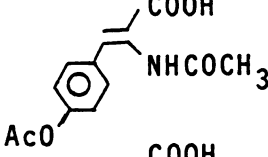
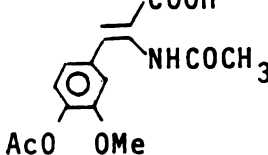
(2)-dehydroamino acids with intercalated and homogeneous  $[\text{Rh}(\text{NBD})\text{SPIPHOS } (48)]^+$  complexes. The lower optical yields obtained with the intercalated  $[\text{Rh}(\text{NBD})\text{SPIPHOS } (48)]^+$  catalyst appear to support this prediction.

### 3. DIOP(+) (3) System

As shown in Table 21, the optical yields obtained with  $[\text{Rh}(\text{NBD})\text{DIOP } (3)]^+$  intercalated in hectorite depend greatly on the nature of the substrate. With the intercalated  $[\text{Rh}(\text{NBD})\text{DIOP}(+) (3)]^+$  catalyst, the optical yields of *N*-acetyl amino acids of alanine, phenylalanine and DOPA deviate only slightly from those obtained with the homogeneous catalyst. The optical yields of *N*-acetyltyrosine and *N,O*-diacetyl-tyrosine were higher in comparison with the homogeneous results. The optical yield of the *N*-benzoylphenylalanine was lower than the homogeneous result, whereas the reduction of its corresponding ester gave zero optical yield with the intercalated catalyst. Since the recycled catalyst obtained from the reduction of the ester gave a 77% optical yield for *N,O*-diacetyl-tyrosine reduction, the zero optical yield obtained for the phenylalanine derivative was not due to the loss of the catalyst chirality.

The differences observed between the homogeneous and intercalated state are not surprising.  $\text{DIOP}(+) (3)$  forms a seven-membered chelate ring when complexed to rhodium. The optical yields obtained with such conformationally flexible ring systems are sensitive to solvation effects,<sup>36,60</sup>

Table 21. Asymmetric Hydrogenation of Dehydroamino Acids  
with Intercalated and Homogeneous  $[\text{Rh}(\text{NBD})\text{DIOP}(+)(3)]^+$  Catalysts

<u>Substrate</u>	<u>Amino acid</u>	<u>Optical Yield (%)<sup>a</sup></u>	
		<u>Intercal.</u>	<u>Homogen.</u>
	L-Alanine	74.0	76.0
	L-Phenylalanine	85.9	84.8
	L-Phenylalanine	46.0	58.0
	L-Phenylalanine	0	42.8
	L-Tyrosine	82.1	73.6
	L-Tyrosine	77.0	72.4
	L-DOPA	86.0	88.0

<sup>a</sup>The hydrogenations were carried out on 4-8 mmol of substrate in 30 mL 95% EtOH at 25°C and 740 torr. The amount of intercalated or homogeneous catalyst used for each reaction was 0.04 mmol. All the corresponding acids had (S)-configurations.

and, in some cases, the absolute configurations of the products can be reversed by changing solvent.<sup>36,60</sup> A strong solvent effect was observed in the asymmetric hydrogenation of 1-acetamido-1-phenylethene with cationic  $[\text{Rh}(\text{COD})\text{DIOP} (+) (\underline{3})]^+$  precursor and *in situ*  $\text{Rh}(\text{I})\text{-DIOP}(+) (\underline{3})$  catalyst in different solvents (Table 22).<sup>36,60</sup>

Table 22. Solvent Effect on the Optical Yields of Hydrogenation Product of 1-Acetamido-1-phenylethene with  $\text{DIOP}(+) (\underline{3})^a$

Substrate	Solvent	Optical Yield	
		Cation precursor <sup>b</sup>	<i>In situ</i> Catalyst <sup>c</sup>
$\begin{array}{c} \text{NHCOCH}_3 \\ \diagup \\ \text{C}_6\text{H}_5 \end{array}$	EtOH	38.5 ( <u>R</u> )	42.5 ( <u>R</u> )
	$\text{C}_6\text{H}_6$	68.0 ( <u>R</u> )	44.0 ( <u>S</u> )

<sup>a</sup>Data obtained from references 36 and 60.

<sup>b</sup>Cationic precursor:  $[\text{Rh}(\text{COD})\text{DIOP}(+) (\underline{3})]^+\text{ClO}_4$

<sup>c</sup>*In situ* catalyst:  $[\text{RhCl}(\text{C}_2\text{H}_4)_2]_2$  and  $\text{DIOP}(+) (\underline{3})$  with  $\text{DIOP}/\text{Rh}$  ratio of 1.1.

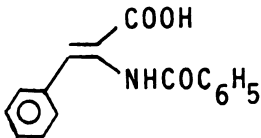
Even the absolute configuration of *N*-acetylphenylethylamine can be reversed by using *in situ*  $\text{Rh}(\text{I})\text{-DIOP}(+) (\underline{3})$  catalyst in benzene.<sup>36,60</sup> Also, in general, dehydroamino acids give higher optical yields than the corresponding esters.<sup>61</sup> With the *in situ*  $\text{Rh}(\text{I})\text{-DIOP}(+) (\underline{3})$  catalyst, *N*-acylamino-cinnamic acids were hydrogenated to phenylalanine derivatives with significantly higher optical yields (25-81%) than the corresponding esters (5-59%).<sup>61</sup> It is reasonable, therefore, to expect solvation differences also to exist between reaction

intermediates in the intercalated and homogeneous states. Of course, other factors such as specific interactions of the substrate with the silicate oxygens may also contribute to the observed differences.

#### 4. The Solvent Effect on the Optical Yields

(R)-Prophos (6) is a conformationally rigid type of ligand. With the homogeneous Rh(I)-(R)-Prophos (6) catalyst precursor the optical yields appear to be insensitive to the nature of the substituent on the substrate and solvent.<sup>10</sup> The solvent effect on the optical yields of one substrate obtained with intercalated [Rh(NBD)(R)-Prophos (6)]<sup>+</sup> is illustrated in Table 23.

Table 23. The Asymmetric Hydrogenation of (Z)- $\alpha$ -Benzamido-cinnamic Acid with Intercalated and Homogeneous [Rh(NBD)(R)-Prophos (6)]<sup>+</sup> Catalysts

<u>Substrate</u>	<u>Solvent</u>	<u>Optical Yield (%)</u> <sup>a</sup>	
		<u>Intercal.</u>	<u>Homogen.</u>
	H <sub>2</sub> O:EtOH (1:19)	70%	92%
	H <sub>2</sub> O:EtOH (1:3)	67%	—
	H <sub>2</sub> O:EtOH (1:2)	63%	—
	Methanol	71%	88%

<sup>a</sup>The hydrogenations were carried out on 4 mmol of substrate in 30 mL of solvent at 25°C and 740 torr. The amount of intercalated or homogeneous catalyst used for each reaction was 0.04 mmol. The corresponding  $\alpha$ -amino acid had an (S)-configuration.

In general, the intercalated catalyst afforded low optical yields relative to the homogeneous catalyst. The optical yields in EtOH/H<sub>2</sub>O decreased only slightly with increasing water content. It appears that the interactions between the layer silicates and the cationic Rh(I)-(R)-Prophos (6) enamide complex are dominant.

### 5. The Effect of Rhodium Complex Precursor on Optical Yields

With cationic Rh(diene)diphos\* catalysts, the rates of hydrogenation with six- or seven-membered chelate rings are somewhat faster than those observed for the five-membered chelate ring analogues. Either COD or NBD rhodium diphos\* precursors which form six- or seven-membered chelate rings can be used as effective asymmetric hydrogenation catalysts for reduction of dehydroamino acids at ambient conditions.<sup>60,62</sup> However, with five-membered chelate chiral diphosphine rhodium catalysts, COD precursors seemed to be less active than NBD precursors.<sup>9,15</sup> For some substrates, high hydrogenation pressure was required to observe reactions with COD derivatives.<sup>15</sup> Bosnich<sup>9</sup> observed that [Rh(NBD)Chiraphos (5)]<sup>+</sup> precursor was more active than cationic [Rh(COD)Chiraphos (5)]<sup>+</sup> for asymmetric hydrogenation of dehydroamino acids. The five-membered chelate [Rh(COD)(S,S)-Phellaphos (10)]<sup>+</sup>PF<sub>6</sub><sup>-</sup> and [Rh(COD)(R,R)-Nopaphos (11)]<sup>+</sup>PF<sub>6</sub><sup>-</sup> precursors were effective catalysts for asymmetric hydrogenation of dehydroamino acids and non-enamide type substrates in ethanol.<sup>15</sup> The best results were obtained in asymmetric

synthesis of  $\alpha$ -amino acid derivatives (80-95% e.e.).

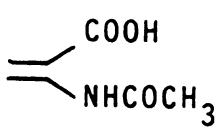
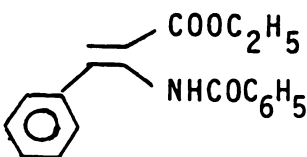
However, the (S,S)-Phellaphos (10) sometimes works under one atmosphere of hydrogen. The (R,R)-Nopaphos (11) gives a less active catalyst and high pressure (15 atm) is required for activating the catalyst.<sup>15</sup> Also, Schrock and Osborn<sup>63</sup> found that the cationic  $[\text{Rh}(\text{NBD})(\text{PPh}_3)_2]^+$  catalyst reacts with hydrogen approximately 100 times faster than the cationic  $[\text{Rh}(\text{COD})(\text{PPh}_3)_2]^+$  catalyst.

The intercalated  $[\text{Rh}(\text{NBD})(\text{R})\text{-Prophos (6)}]^+$  catalyst was found to be a more effective catalyst than intercalated  $[\text{Rh}(\text{COD})(\text{R})\text{-Prophos (6)}]^+$  for the asymmetric hydrogenation of the dehydroamino acids (Table 24). It is reasonable to assume that there is a reaction activity differentiation between the two cationic  $[\text{Rh}(\text{diene})(\text{R})\text{-Prophos (6)}]^+$  precursors (where diene is NBD or COD) in the layer silicate system. These results suggest that some decomposition of the  $[\text{Rh}(\text{diene})(\text{R})\text{-Prophos (6)}]^+$  species on the interlayer surfaces may contribute to lower optical yields. But the effect cannot be large with NBD precursor because of the high optical yields obtained with  $[\text{Rh}(\text{NBD})(\text{R})\text{-4-Me-Prophos (49)}]^+$ .

## 6. Asymmetric Hydrogenation with Recycled Catalysts

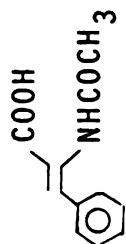
The results of asymmetric hydrogenation of  $\alpha$ -acetaminocinnamic acid with recycled  $[\text{Rh}(\text{NBD})\text{DIOP}(+) (3)]^+$  and  $[\text{Rh}(\text{NBD})(\text{R})\text{-Prophos (6)}]^+$  catalysts are shown in Table 25.

Table 24. Asymmetric Hydrogenation of Dehydroamino Acids with Intercalated and Homogeneous  $[\text{Rh}(\text{diene})(\text{R})\text{-Propos}(\text{S})]^+$  Catalysts

<u>Substrate</u>	<u>Diene</u>	<u>Amino Acid</u>	<u>Optical Yield (%)</u> <sup>a</sup>	
			<u>Intercal.</u>	<u>Homogen.</u>
	NBD	L-Alanine	73%	94%
	COD		50%	—
	NBD	L-Phenyl-Alanine	61%	89%
	COD		50%	—

<sup>a</sup>The hydrogenations were carried out on 8 mmol of  $\alpha$ -acetamidoacrylic acid or 4 mmol of ethyl (Z)- $\alpha$ -Benzamidocinnamate in 30 mL 95% EtOH. at 25°C and 740 torr. The amount of intercalated or homogeneous catalyst used for each reaction was 0.04 mmol. The corresponding  $\alpha$ -amino acid products had (S)-configurations.

Table 25. Asymmetric Hydrogenation of (Z)- $\alpha$ -Acetamidocinnamic Acid with Recycled Intercalated [Rh(NBD)(diphos\*)]<sup>+</sup> Catalysts

<u>Substrate</u>	<u>                    Diphos*</u>						
	<u>DIOP(+) (3)</u>		<u>(R)-prophos (6)</u>				
	<u>O.Y.<sup>a</sup></u>	<u>Rate<sup>b</sup></u>	<u>Time<sup>c</sup></u>	<u>O.Y.<sup>a</sup></u>	<u>Rate<sup>b</sup></u>	<u>Time<sup>c</sup></u>	
	1st cycle	86.2%	272	12 min.	85.4%	23.0	160 min.
	2nd cycle	84.2%	68	65 min.	81.0%	5.4	560 min.
	3rd cycle	81.2%	53	75 min.			

<sup>a</sup>The hydrogenations were carried out on 5 mmol of the substrate in 30 mL of 95% EtOH at 25°C and 740 torr. The concentrations of intercalated catalysts were around 1.33 X 10<sup>-3</sup> M. The *N*-acetyl-phenylalanine had an (*S*)-configuration

<sup>b</sup>Initial rates are reported as mL H<sub>2</sub>/min/mmol Rh

<sup>c</sup>Hydrogen uptake ceased



The rates of hydrogenation decreased by a factor of 4 with the reuse of the intercalated catalysts, but even after three cycles of the catalyst the optical yields of the product were not affected more than 5%. It is possible that the decrease in activity is due to loss of catalyst through oxidation by trace amounts of oxygen. Also, clogging the interlayers by adsorbed amino acid is possible.

#### H. The Observed Hydrogenation Rates

The hydrogen uptake plots for reduction of *N*-acetyl-dehydrophenylalanine with homogeneous and intercalated  $[\text{Rh}(\text{NBD})\text{diphos}^*]^+$  catalysts (where diphos\* is (R)-Prophos (6), (R)-4-Me-Prophos (49), SPIPHOS (48), or DIOP(+) (3) are shown in Figures 6 to 11.

The observed rates for hydrogenation of the dehydro-amino acids with homogeneous and intercalated  $[\text{Rh}(\text{NBD})(\text{R})\text{-Prophos}(\text{6})]^+$  catalysts are shown in Table 26. The homogeneous  $[\text{Rh}(\text{NBD})(\text{R})\text{-Prophos}(\text{6})]^+$  hydrogenation rates were in the range of 19 to 330 (mL  $\text{H}_2$ /min/mmol Rh). The observed hydrogen rates were similar to those Bosnich found.<sup>10</sup> In general, the rates of hydrogenation with intercalated  $[\text{Rh}(\text{NBD})(\text{R})\text{-Prophos}(\text{6})]^+$  catalyst were 0.13 - 0.45 as fast as those with the homogeneous catalyst.

The hydrogenation rates for reduction of dehydroamino acids with homogeneous and intercalated  $[\text{Rh}(\text{NBD})(\text{R})\text{-4-Me-Prophos}(\text{49})]^+$  catalysts are shown in Table 27. With

Figure 6. Hydrogen uptake plots for reduction of 5 mmol of *N*-acetyldehydrophenylalanine in 30 mL 95% ethanol at 25°C and 740 torr with  $[\text{Rh}(\text{NBD})(\text{R})\text{-Prophos (6)}]^+$  as the catalyst precursor. (A) Homogeneous catalyst (B) Intercalated catalyst. In each case the amount of rhodium complex used was 0.04 mmol.

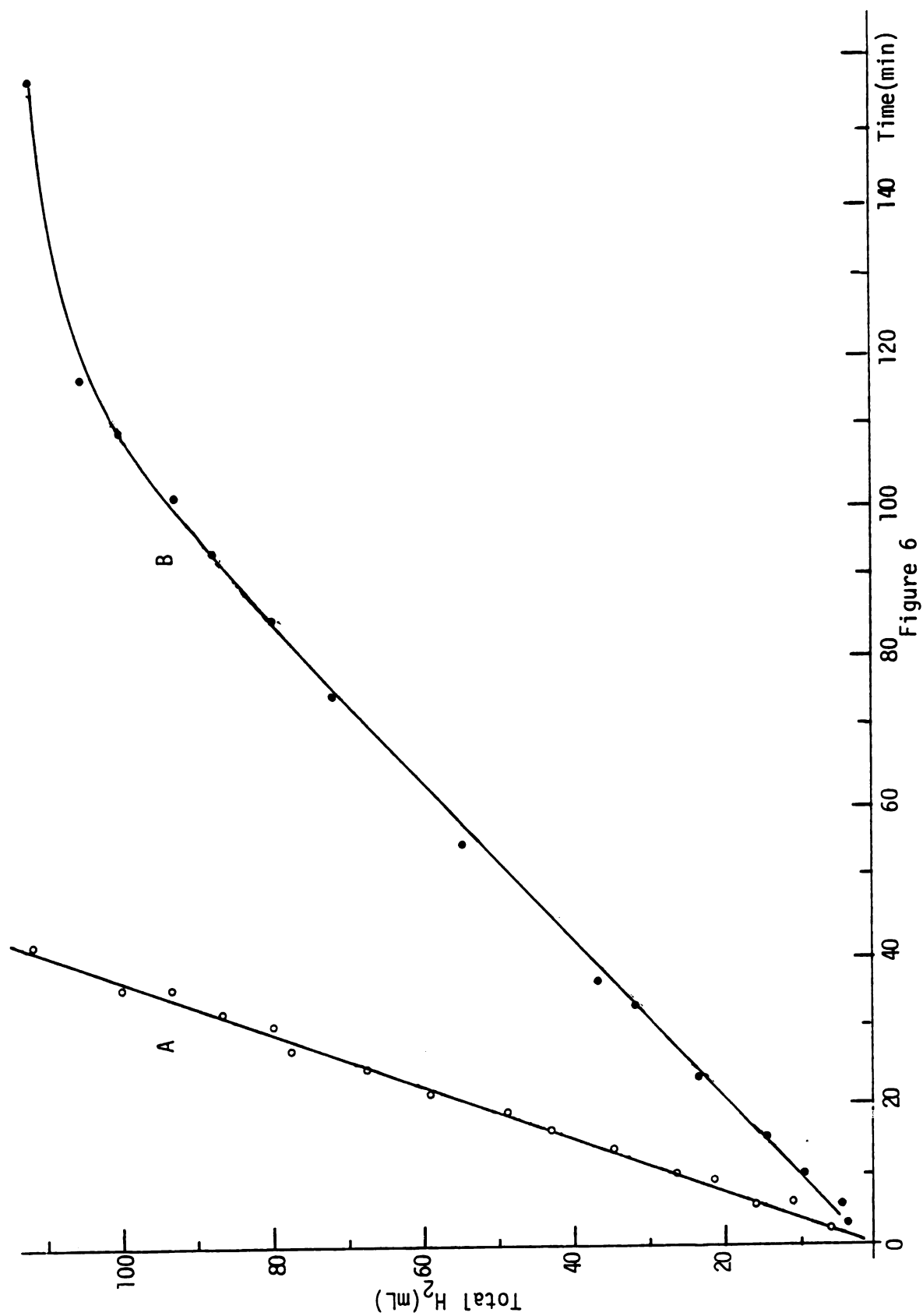


Figure 7. Hydrogen uptake plots for reduction of 5 mmol of *N*-acetyldehydrophenylalanine in 30 mL 95% ethanol at 25°C and 740 torr with intercalated  $[\text{Rh}(\text{NBD})(\text{R})\text{-Prophos}(\text{6})]^+$  catalyst. (A) First cycle (B) Second cycle. The amount of rhodium complex used was 0.04 mmol.

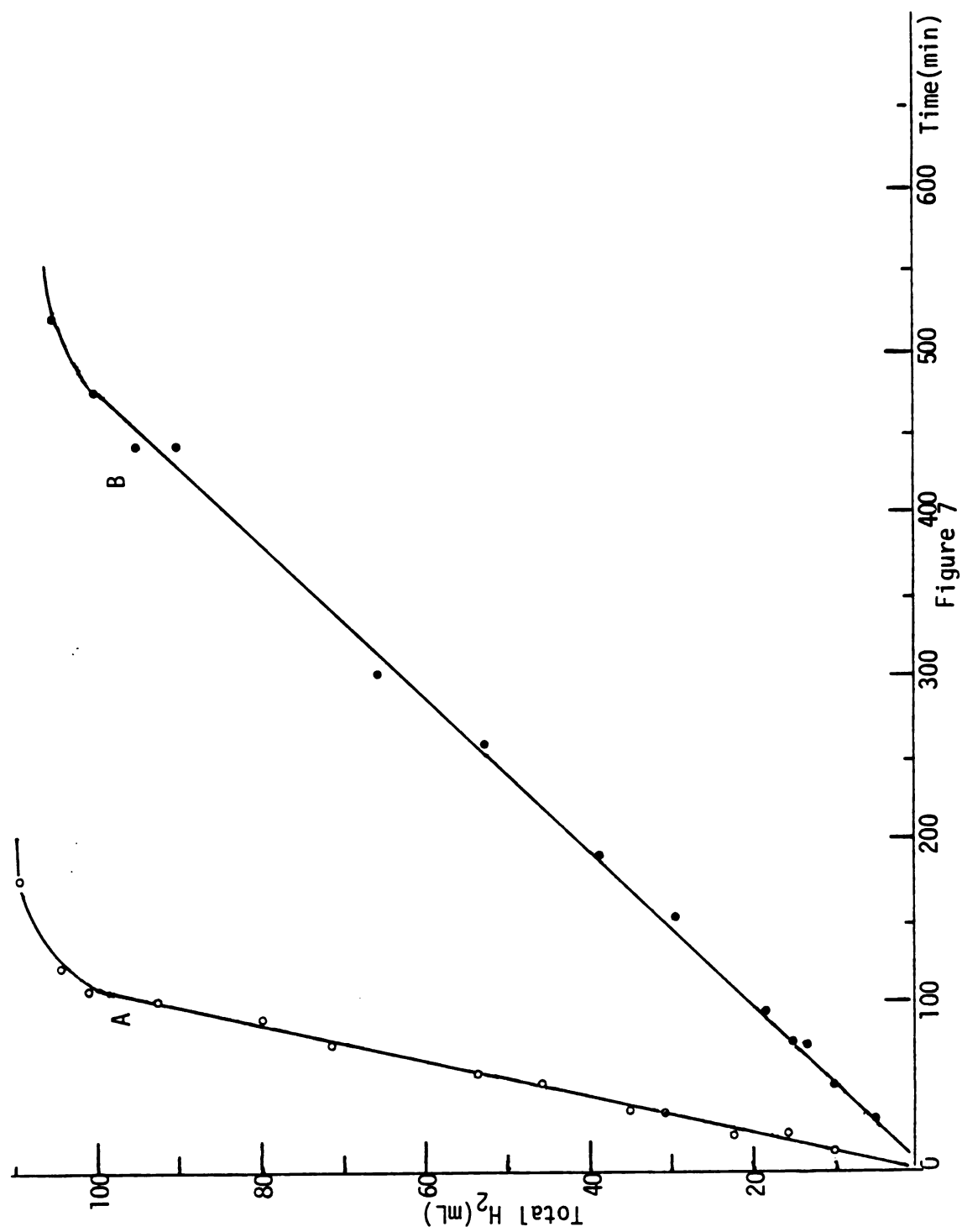


Figure 8. Hydrogen uptake plots for reduction of 5 mmol of *N*-acetyldehydrophenylalanine in 30 mL 95% ethanol at 25°C and 740 torr with  $[\text{Rh}(\text{NBD})(\text{R})\text{-4-Me-Propos (49)}]^+$  as the catalyst precursor. (A) Homogeneous catalyst (B) Intercalated catalyst. In each case the amount of rhodium complex used was 0.03 mmol.

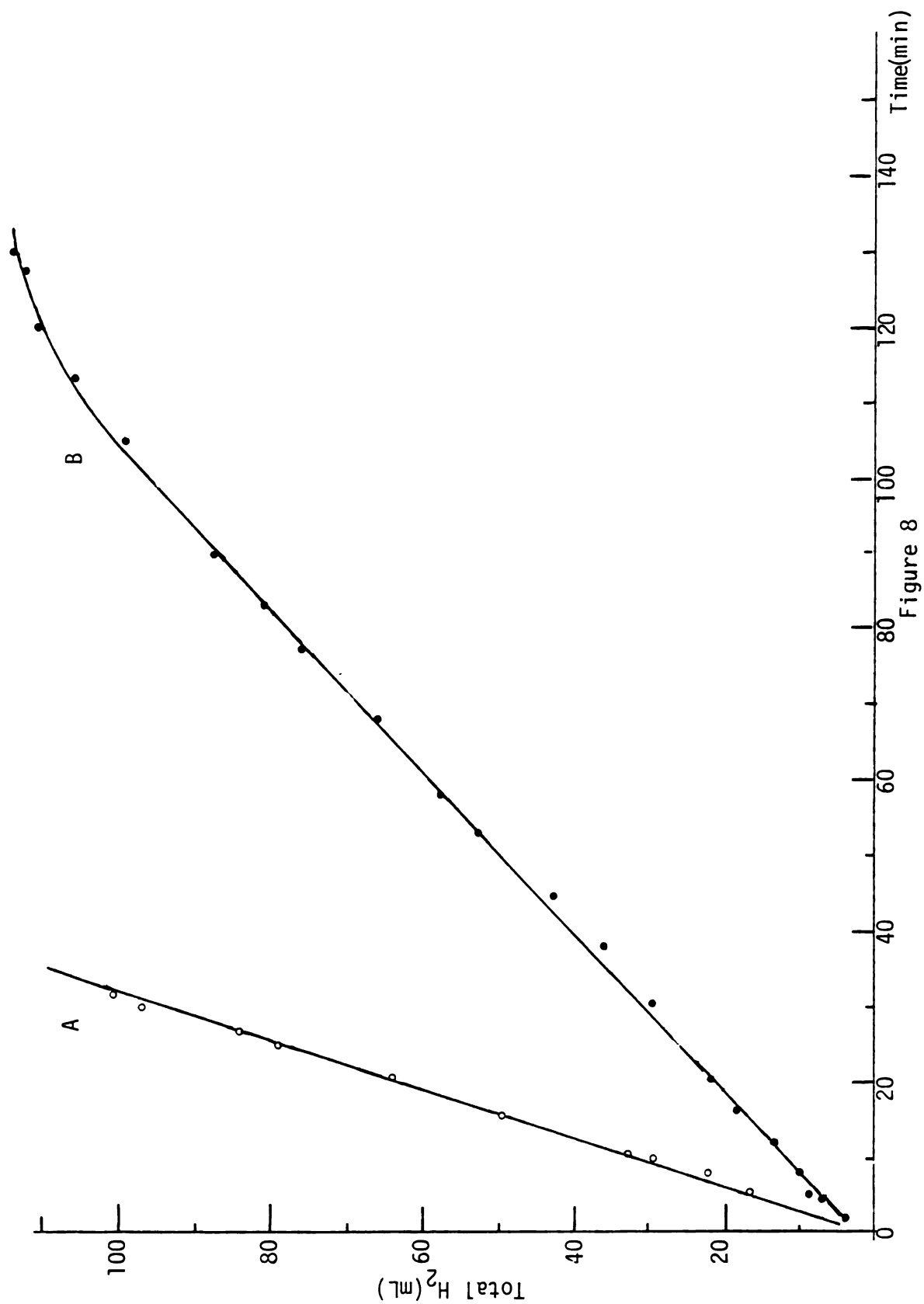


Figure 9. Hydrogen uptake plots for reduction of 5 mmol of *N*-acetyldehydrophenylalanine in 30 mL 95% ethanol at 25°C and 740 torr with  $[\text{Rh}(\text{NBD})\text{SPIPHOS (48)}]^+$  as the catalyst precursor. (A) Homogeneous catalyst (B) Intercalated catalyst. In each case the amount of rhodium complex used was 0.03 mmol.



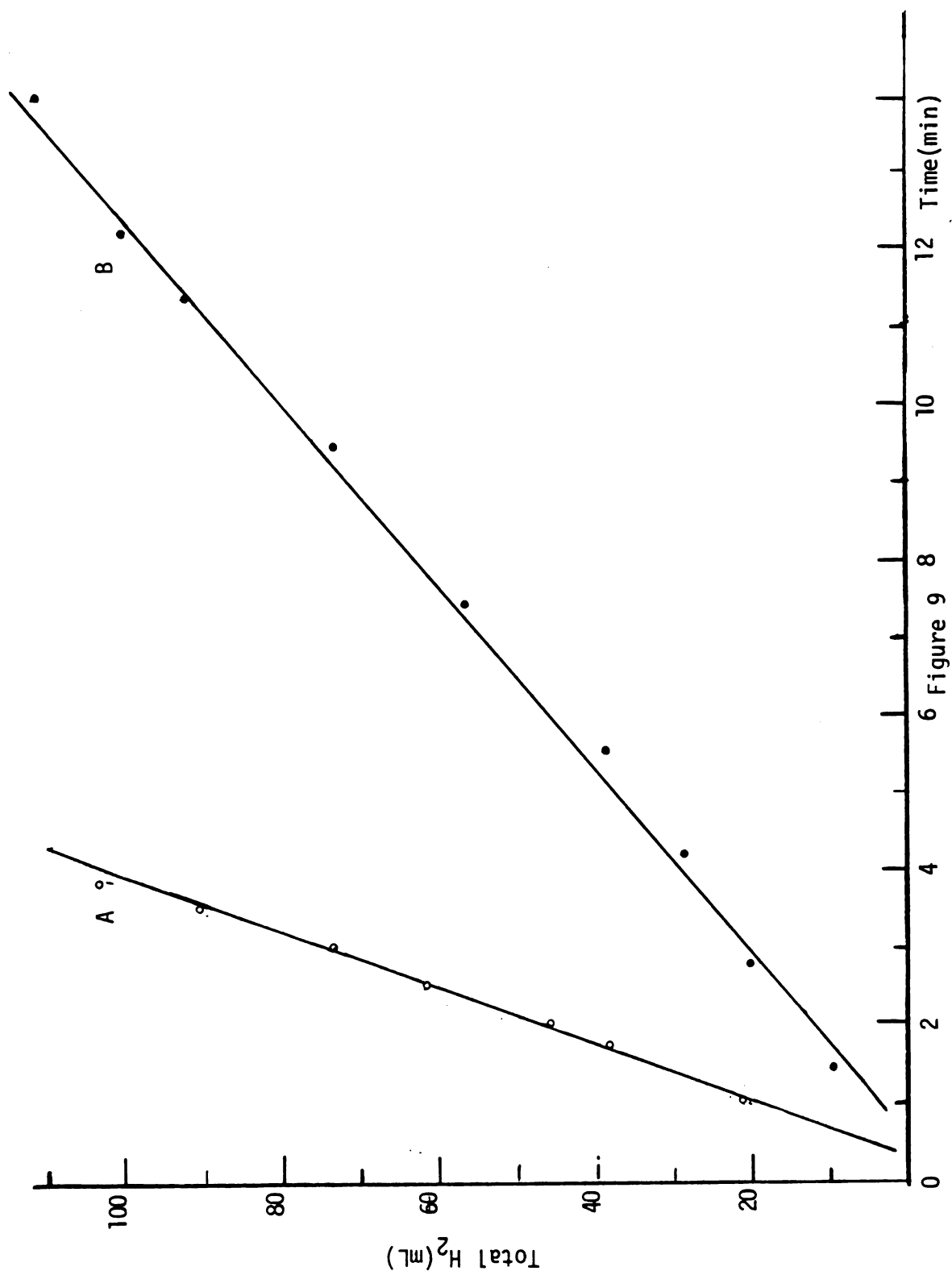


Figure 10. Hydrogen uptake plots for reduction of 5 mmol of *N*-acetyldehydrophenylalanine in 30 mL 95% ethanol at 25°C and 740 torr with  $[\text{Rh}(\text{NBD})\text{DIOP}(+) \text{ (3)}]^+$  as the catalyst precursor. (A) Homogeneous catalyst (B) Intercalated catalyst. In each case the amount of rhodium complex used was 0.04 mmol.

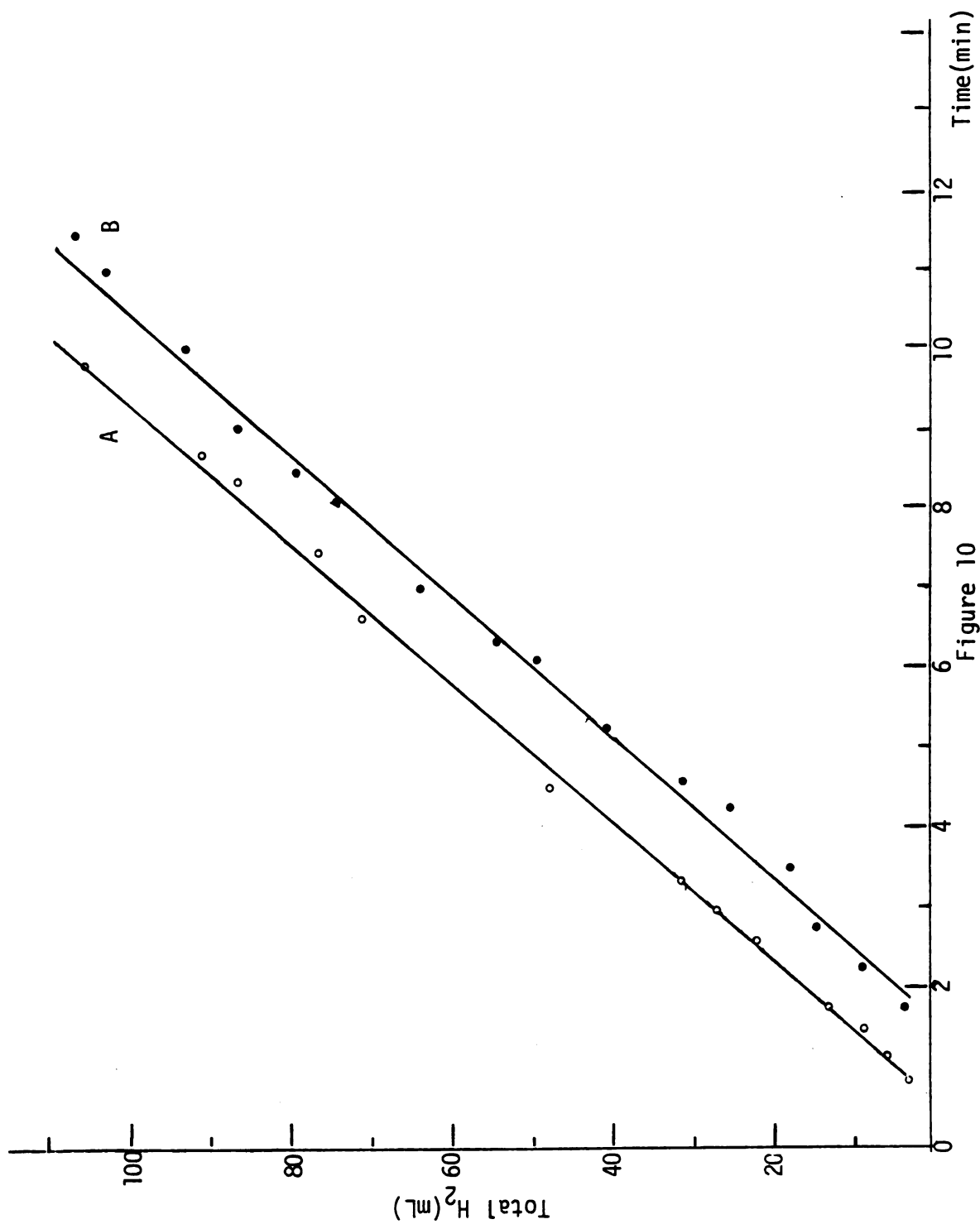


Figure 11. Hydrogen uptake plots for reduction of 5 mmol of *N*-acetyldehydrophenylalanine in 30 mL 95% ethanol at 25°C and 740 torr with intercalated  $[\text{Rh}(\text{NBD})\text{DIOP}(+) \text{ (3)}]^+$  catalyst. (A) First cycle (B) Second cycle. (C) Third cycle. The amount of rhodium complex used was 0.04 mmol.

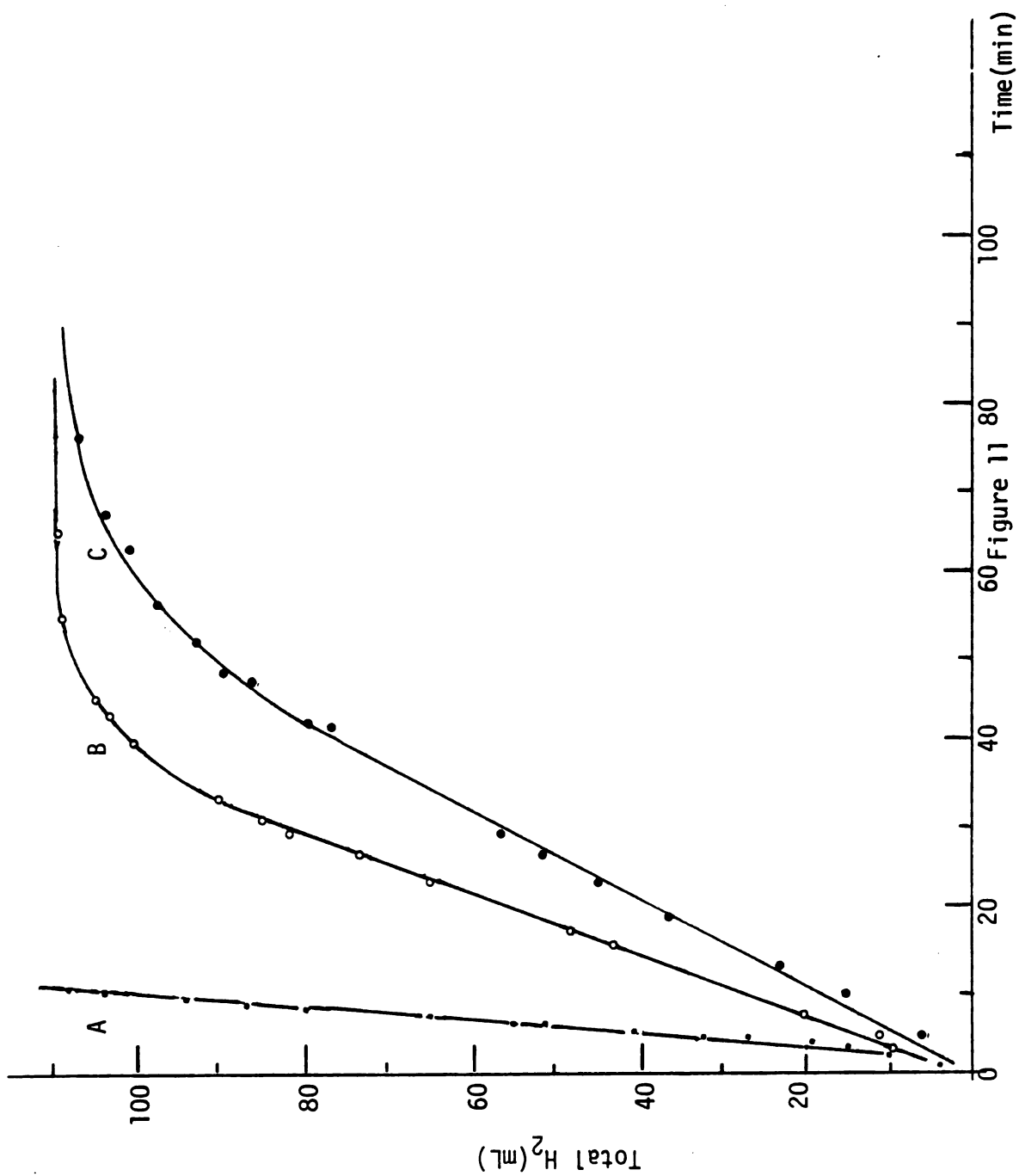
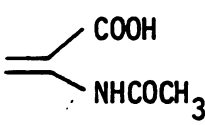
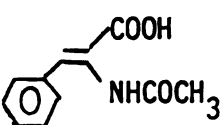
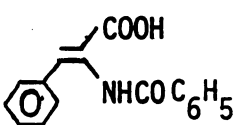
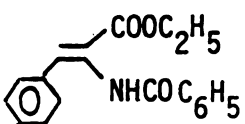
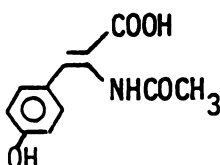
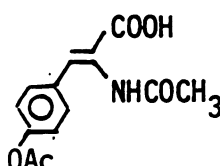
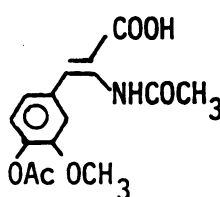


Figure 11

Table 26. Hydrogenation Rates for Intercalated  $[\text{Rh}(\text{NBD})(\text{R})\text{-prophos (6)}]^+$  Catalyst and Its Homogeneous Analogue

Substrate	Hydrogen Rates (ml $\text{H}_2$ /min/mmol Rh) <sup>a</sup>		
	Intercal.	Homogen.	Relative Rate
	128	328	0.39
	21.5	71	0.32
	16.3	50	0.33
	3.66	28.5	0.13
	8.60	19.1	0.45
	11.3	60.0	0.19
	13.3	51.3	0.26

<sup>a</sup> The reaction conditions are the same as those given in Table 17.

Table 27. Hydrogenation Rates for Intercalated  $[\text{Rh}(\text{NBD})(\text{R})\text{-4-Me-Prophos (49)}]^+$  Catalyst and Its Homogeneous Analogue

Substrate	Hydrogen Rates ( $\text{ml H}_2/\text{min}/\text{mmol Rh}$ ) <sup>a</sup>		
	Intercal.	Homogen.	Relative Rate
	333	537	0.62
	30.7	105	0.29
	45.6	80.0	0.57
	10.9	36.4	0.30
	11.7	22.2	0.53
	11.8	53.3	0.22
	30.7	46.0	0.67

<sup>a</sup> The reaction conditions are the same as those given in Table 18.

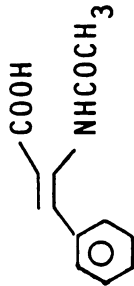
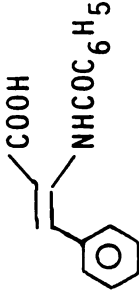
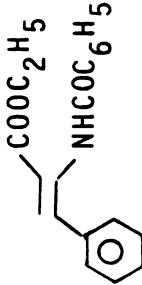
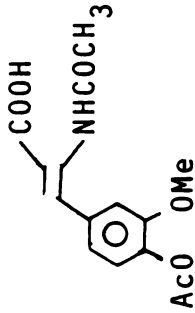
homogeneous  $[\text{Rh}(\text{NBD})(\text{R})\text{-4-Me-Prophos (49)}]^+$  catalyst, the hydrogenation rates for the reduction of dehydroamino acids were in the range of 22 to 540 ( $\text{mL H}_2/\text{min}/\text{mmol Rh}$ ). The observed hydrogenation rates with homogeneous  $[\text{Rh}(\text{NBD})(\text{R})\text{-4-Me-Prophos (49)}]^+$  catalyst were comparable to those with the homogeneous  $[\text{Rh}(\text{NBD})(\text{R})\text{-Prophos (6)}]^+$  catalyst. The observed rates with intercalated  $[\text{Rh}(\text{NBD})(\text{R})\text{-4-Me-Prophos (49)}]^+$  catalyst were 0.22 to 0.67 as fast as those with the homogeneous catalyst.

The *N*-acetyldehydroalanine and *N*-acetyldehydrotyrosine gave the highest and lowest rates, respectively, in the homogeneous  $(\text{R})\text{-Prophos (6)}$  and  $(\text{R})\text{-4-Me-Prophos (49)}$  systems. The same findings were observed by Bosnich with  $[\text{Rh}(\text{NBD})(\text{R})\text{-Prophos (6)}]^+$  catalyst.<sup>10</sup> In the layer silicate system, the ethyl *N*-benzoyldehydrophenylalanine ester gave the lowest rates in the intercalated  $(\text{R})\text{-Prophos (6)}$  and  $(\text{R})\text{-4-Me-Prophos (49)}$  systems.

The hydrogenation rates for reduction of dehydroamino acids with homogeneous and intercalated  $[\text{Rh}(\text{NBD})\text{SPIPHOS (48)}]^+$  catalysts are shown in Table 28. With homogeneous  $[\text{Rh}(\text{NBD})\text{SPIPHOS (48)}]^+$  catalyst, the hydrogenation rates for the reduction of dehydroamino acids were in the range of 500 to 1600 ( $\text{mL H}_2/\text{min}/\text{mmol Rh}$ ) in 95% ethanol and in the range of 1000 to 2500 in methanol. Hydrogenation rates are faster in methanol than in 95% ethanol. Ethyl *N*-benzoyldehydrophenylalanine ester gave the highest and lowest



Table 28. Hydrogenation Rates for Intercalated  $[\text{Rh}(\text{NBD})\text{SPIPHOS} (48)]^{\dagger}$  Catalyst and Its Homogeneous Analogue

Substrate	Hydrogen Rates (mL $\text{H}_2$ /min/mmol Rh) <sup>a</sup>			
	Solvent	Intercal.	Homogen.	Relative rate
	95% EtOH	283	987	0.29
	MeOH	575	2130	0.27
	95% EtOH	135	493	0.27
	MeOH	427	1290	0.33
	95% EtOH	72	1560	0.05
	MeOH	186	2460	0.08
	95% EtOH	156	540	0.29
	MeOH	390	977	0.40

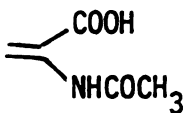
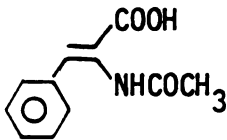
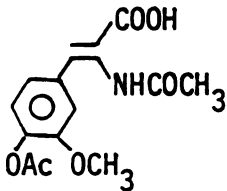
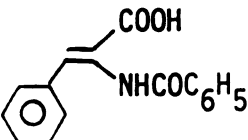
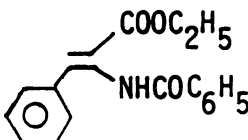
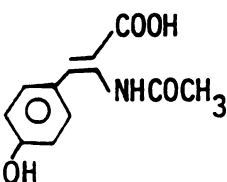
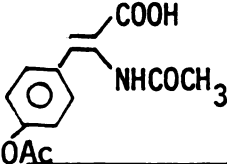
<sup>a</sup>The reaction conditions are the same as those given in Table 20.

rates in the homogeneous and intercalated system, respectively. The observed rates with intercalated  $[\text{Rh}(\text{NBD})\text{SPIPHOS}(\underline{48})]^+$  catalyst were 0.05 to 0.40 as fast as those with the homogeneous catalyst.

The hydrogenation rates for reduction of dehydroamino acids with homogeneous and intercalated  $[\text{Rh}(\text{NBD})\text{DIOP}(+) (\underline{3})]^+$  catalysts are shown in Table 29. The observed reaction rates for homogeneous  $[\text{Rh}(\text{NBD})\text{DIOP}(+) (\underline{3})]^+$  were in the range of 230 to 680 (mL  $\text{H}_2$ /min/mmol Rh). In the DIOP(+) (3) system, the *N*-acetyldehydroalanine and DOPA precursor gave the highest hydrogenation rates in the homogeneous and intercalated states. The *N*-benzoyldehydrophenylalanine and its ester gave the lowest hydrogenation rates in the homogeneous and intercalated states. The observed hydrogenation rates in the intercalated state were 0.43 to 0.94 as fast as those observed in the homogeneous state.

The hydrogenation rates of dehydroamino acids (enamides) with homogeneous  $[\text{Rh}(\text{diene})\text{diphos*}]^+$  catalysts are dependent on several factors, such as the type of the diene precursor, the steric and electronic effects of substrate, solvent, and the catalyst's chelate ring size. The hydrogenations of dehydroamino acids with NBD precursor are faster than the COD precursor in the five-membered chelate ring's cationic Rh diphos\* system. The steric and electronic effects of substrate are important. However, it is difficult to predict these two effects precisely in each substrate. The hydrogenation rates are faster in methanol

Table 29. Hydrogenation Rates for Intercalated  $[\text{Rh}(\text{NBD})\text{DIOP}(+) (3)]^+$  Catalyst and Its Homogeneous Analogue

Substrate	Hydrogen Rates (ml $\text{H}_2$ /min/mmol Rh) <sup>a</sup>		
	Intercal.	Homogen.	Relative Rate
	486	515	0.94
	272	291	0.93
	296	683	0.43
	191	234	0.82
	125	243	0.51
	237	375	0.63
	250	475	0.53

<sup>a</sup>The reaction conditions are the same as those given in Table 21.

than 95% ethanol for reduction of dehydroamino acid with Rh(NBD)diphos\* catalyst.

A series of homogeneous *in situ* rhodium diphosphine catalysts were prepared by Kagan<sup>64</sup> to study the effect of changing the catalyst's chelate ring size on the hydrogenation rates of  $\alpha$ -acetamidocinnamic acid. The results indicated that as the chelate ring size of the catalyst increased from 5 to 8, the reaction rates also increased (see Table 30). However, when the catalyst's chelate ring size increased to 9 the rate dropped again. DeVries<sup>52</sup> found that the homogeneous ten-membered chelate ring's rhodium SPIPHOS (48) catalyst, prepared from  $[\text{RhCl}(\text{cyclooctene})_2]_2$  and SPIPHOS (48), was inactive for asymmetric hydrogenation of *N*-acetyldehydrophenylalanine in ethanol/toluene at ambient conditions. High pressure was required for activating the catalyst. The finding was close to Kagan's prediction.<sup>64</sup>

With homogeneous cationic  $[\text{Rh}(\text{NBD})\text{diphos}^*]^+$  catalysts, the rates of hydrogenation of dehydroamino acids were dependent on the catalyst's chelate ring size.

SPIPHOS (48) > DIOP(+) (3) > (R)-4-Me-Propfos (49)  $\geq$  (R)-Propfos (6)

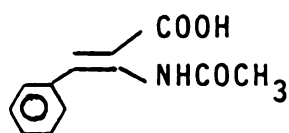
The hydrogenation rates of dehydroamino acids with the ten-membered chelate ring's cationic  $[\text{Rh}(\text{NBD})\text{SPIPHOS (48)}]^+$

Table 30 .<sup>a</sup> Hydrogenation Rates of (Z)- $\alpha$ -Acetamidocinnamic Acid<sup>b</sup> with *In situ* Rhodium Diphosphine Catalysts<sup>c</sup>

Diphosphine	Hydrogenation Rate <sup>d</sup> (mLH <sub>2</sub> /min)	Relative Rate
PPh <sub>2</sub> (CH <sub>2</sub> )PPh <sub>2</sub>	0	0
PPh <sub>2</sub> (CH <sub>2</sub> ) <sub>2</sub> PPh <sub>2</sub>	1.1	70
PPh <sub>2</sub> (CH <sub>2</sub> ) <sub>3</sub> PPh <sub>2</sub>	1.7	100
PPh <sub>2</sub> CH <sub>2</sub> OCH <sub>2</sub> PPh <sub>2</sub>	3.7	220
DIOP(+) (3)	12.5	740
PPh <sub>2</sub> (CH <sub>2</sub> ) <sub>4</sub> PPh <sub>2</sub>	17.0	1000
PPh <sub>2</sub> (CH <sub>2</sub> ) <sub>5</sub> PPh <sub>2</sub>	17.0	1000
PPh <sub>2</sub> (CH <sub>2</sub> ) <sub>6</sub> PPh <sub>2</sub>	1.5	90

<sup>a</sup>Data obtained from reference 64.

<sup>b</sup>(Z)- $\alpha$ -Acetamidocinnamic acid



<sup>c</sup>*In situ* Catalyst: [RhCl(C<sub>2</sub>H<sub>4</sub>)<sub>2</sub>]<sub>2</sub> and diphosphine with P/Rh ratio of 2.10; [Rh] = 5.0 X 10<sup>-3</sup>M; substrate/Rh = 100; P(H<sub>2</sub>) = 1.1 atm; Solvent: C<sub>6</sub>H<sub>6</sub>/EtOH (1:2)

<sup>d</sup>Maximum initial rate.

catalyst are faster than those with the seven-membered chelate cationic  $[\text{Rh}(\text{NBD})\text{DIOP}(+) \text{ (3)}]^+$  catalyst in the homogeneous state at ambient conditions.

The results seem to contradict Kagan's prediction<sup>64</sup>.

However, the  $\text{Rh(I)}\text{-SPIPHOS (48)}$  precursor was in cationic form instead of *in situ* form. The catalytic reaction path may be different with the cationic precursor, resulting in a dramatic change in the catalyst's activity at ambient conditions.

In the layer silicate system, the factors mentioned in the homogeneous system are crucial in determining the hydrogenation rates of dehydroamino acids with  $[\text{Rh}(\text{diene})\text{diphos*}]^+$  catalysts. Additional factors, viz., the diffusion channel (depending on the polarity of solvent and the size of the cationic rhodium diphos\* catalyst) and the substrate size.

The observed hydrogenation rates of dehydroamino acids in the intercalated state were slower than those obtained in the homogeneous state. The rates of the reactions might be controlled by the rates of diffusion of substrates to catalytically active sites. The polar solvents are suitable for highly swelling and desolving the dehydroamino acids. The interlayer spacing (001 spacing) is dependent on the interlayer swelling and the size of the rhodium diphos\* complex. With the large size of the catalysts, polar solvent

and appropriate rhodium loading (15-20%) the exchanged rhodium layer silicate sheets can be highly swollen and provide appropriate diffusion channels. The substrates are easily accessible to the active sites and the differentiation of the hydrogenation rates in the homogeneous and intercalated states can be reduced.

The effect of the catalyst and substrate size on the hydrogenation rates were observed in the layer silicate system. The largest size ethyl *N*-benzoyldehydrophenylalanine ester gave lower hydrogenation rates with all the intercalated  $[\text{Rh}(\text{NBD})\text{diphos}^*]^+$  catalysts. The smallest size  $[\text{Rh}(\text{NBD})(\text{R})\text{-Prophos (6)}]^+$  catalyst resulted in lower interlayer spacing. The relative ratios of intercalated to homogeneous rates with  $[\text{Rh}(\text{NBD})(\text{R})\text{-Prophos (6)}]^+$  were lower than those of the DIOP(+) (3) and (R)-4-Me-Prophos (49) systems.

The hydrogenation rates are faster in methanol than in 95% ethanol in layer silicates. However, the catalysts seem to be more stereoselective in 95% ethanol than in methanol in the DIOP(+) (3), (R)-Prophos (6) and (R)-4-Me-Prophos (49) systems.

The hydrogenation rates are dependent on the chelate ring size of the catalyst in the layer silicate system.

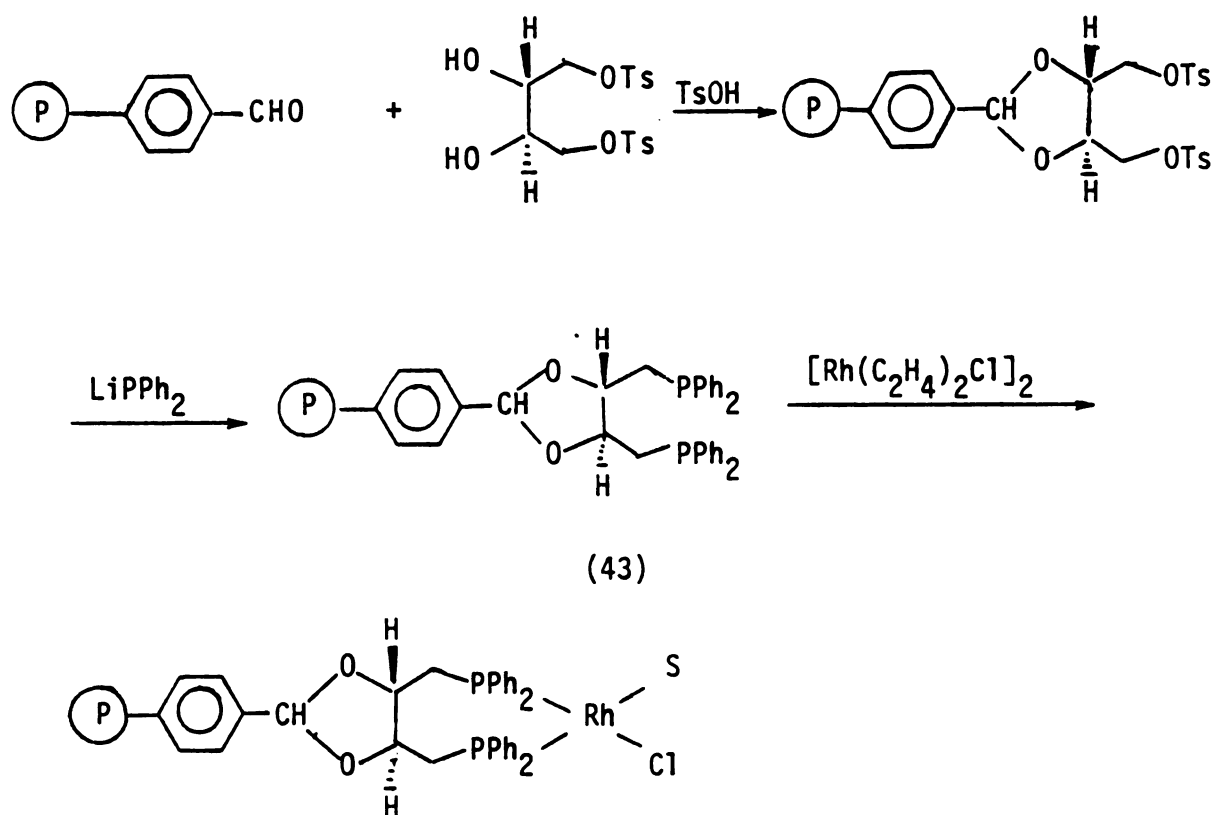
DIOP(+) (3) > SPIPHOS (48) > (R)-4-Me-Prophos (49) > (R)-Prophos (6)

The rate order is different than that of the homogeneous system. The rate order of SPIPHOS (48) and DIOP(+) (3) is reversed. The hydrogenation rates with intercalated  $[\text{Rh}(\text{NBD})\text{SPIPHOS (48)}]^+$  catalyst are lower than those observed with intercalated  $[\text{Rh}(\text{NBD})\text{DIOP(+) (3)}]^+$  catalyst.  $[\text{Rh}(\text{NBD})\text{SPIPHOS (48)}]^+$  is highly flexible due to the large ten-membered chelate ring. The phosphorus atoms of the ligand could possibly *trans*-coordinate with rhodium. In the layer silicates, the flexibility of the  $\text{Rh(I)}\text{-SPIPHOS (48)}$  complex may be restricted by the silicate sheets. The *trans*-coordinated structure of the complex could dominate in the interlayer region. However, the *trans*-coordination structure is unfavorable to asymmetric hydrogenation and the bonding structure may need rearranging in the asymmetric hydrogenation transition states. This may lead to low hydrogenation rates and even reverse the rate order of the catalyst's ring size effect.



# I. A Comparison of Intercalated Rh(I)-DIOP (3) System with Other Rh(I)-DIOP Systems

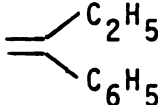
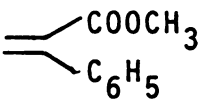
Kagan<sup>32</sup> and his coworkers were the first to synthesize the polymer attached Rh-DIOP catalyst for asymmetric hydrogenation. The chiral DIOP ligand (43) was attached to a cross-linked polystyrene (Merrifield resin).<sup>32</sup> The synthetic methods for the polymer supported Rh DIOP catalyst are shown in Scheme 24.



Scheme 24

The supported Rh-DIOP catalyst was used as an asymmetric hydrogenation catalyst to hydrogenate  $\alpha$ -ethylstyrene and  $\alpha$ -phenylacrylic acid to (R)-(-)-2-phenylbutane and (S)-(+)-methylhydratropate in benzene at 25°C and 1 atm H<sub>2</sub>. The optical yields of (R)-(-)-2-phenylbutane and (S)-(+)-methyl hydratropate with polymer supported catalyst were rather low compared with the homogeneous results<sup>32</sup> (Table 31).

Table 31. Asymmetric Hydrogenation of Prochiral Olefins with Polymer Supported Rh DIOP Catalyst and Homogeneous Analogue

Substrate	Optical Yield (%) <sup>a</sup>	
	[Rh(C <sub>2</sub> H <sub>4</sub> ) <sub>2</sub> Cl] <sub>2</sub> + DIOP	
	Homogeneous	Polymer Attached
	15 (R)	1.5 (R)
	7 (R)	2.5 (S) <sup>b</sup>

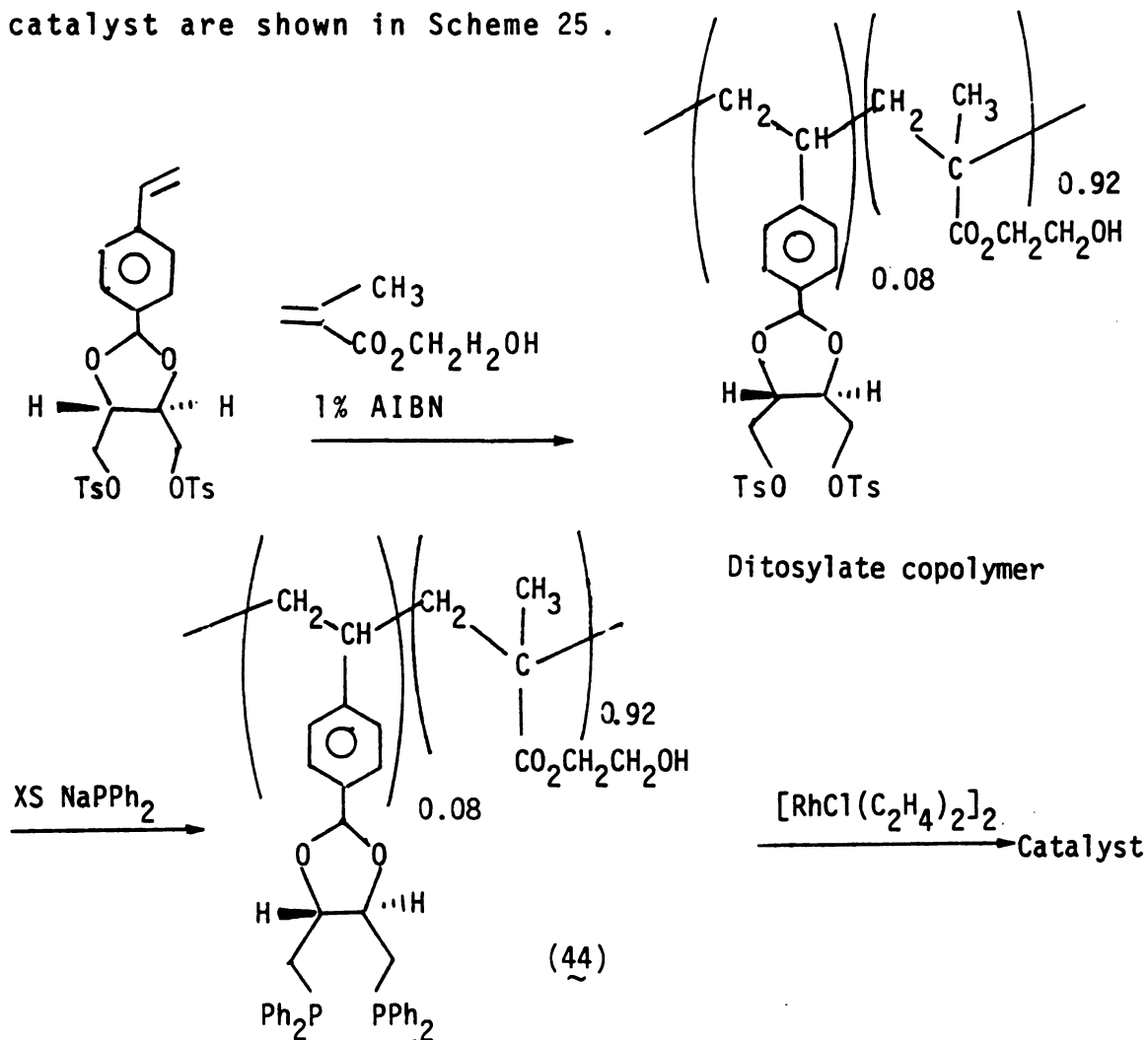
a Data were obtained from reference 32.

b 27% Chemical conversion

The polymer supported catalyst only swells in nonpolar solvents and is active for hydrogenation of nonpolar olefins. However, in benzene-ethanol, the catalyst is inactive toward the hydrogenation of  $\alpha$ -acetaminocinnamic

acid. The ethanol cosolvent is required to dissolve the polar substrates. However, the beads collapsed in the polar solvents, thus preventing the access of the substrates to the catalyst sites.

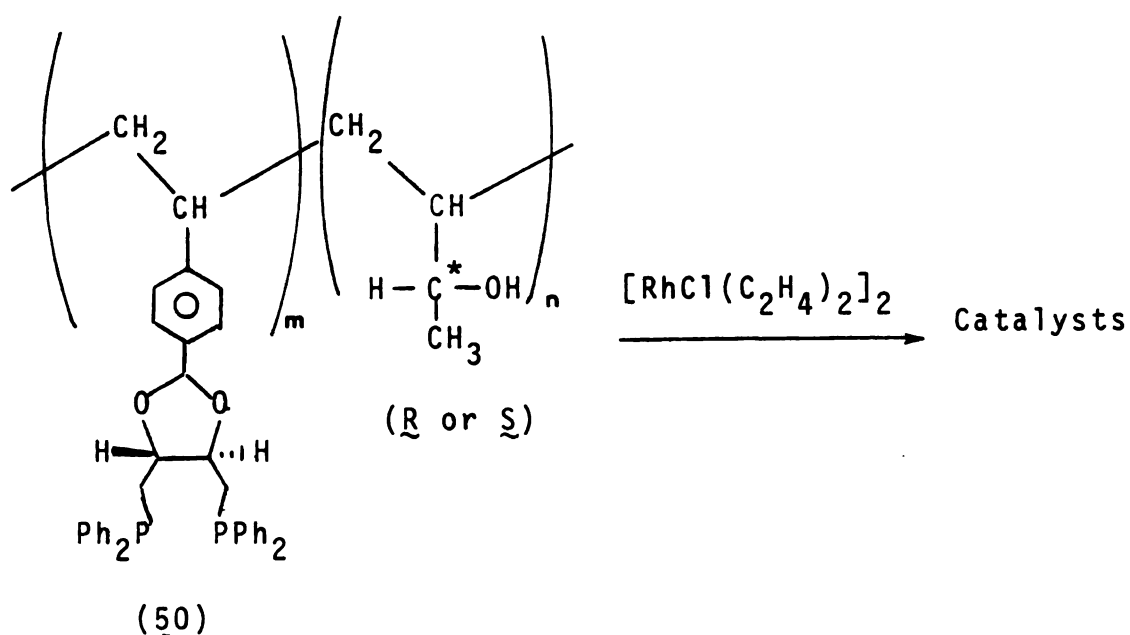
To overcome this polymer swelling problem, Stille<sup>33</sup> and his co-workers successfully prepared a Rh(I)-DIOP(-) (44) catalyst on a polar cross-linked copolymer of 2-hydroxyethylmethacrylate and *p*-styryl (DIOP). The synthetic processes of gel type copolymer supported Rh-DIOP(-) (44) catalyst are shown in Scheme 25.



Scheme 25

The ditosylate monomer was copolymerized with hydroxyethyl methacrylate (HEMA) to form the ditosylate copolymer. The ditosylate copolymer was phosphinated with excess  $\text{NaPPh}_2$  in a THF-dioxane mixture to afford phosphinated copolymer (44). Since the chemical conversion of the phosphination step was around 50% the final phosphinated copolymer contained bidentate phosphine and monodentate phosphine. Monodentate phosphine could coordinate to rhodium and lead to low optical yields for asymmetric hydrogenation of dehydroamino acids. A high phosphorus to rhodium ratio (4:1) was required so that rhodium would be complexed mainly by bidentate phosphine.<sup>33</sup> However, the complexation of rhodium by monophosphine was still possible.

Stille and Masuda adopted a similar method to synthesize gel type chiral copolymer supported Rh-DIOP(-) (50) catalyst containing chiral alcohol sites.<sup>65</sup> (Scheme 26)



Scheme 26

The ancillary asymmetric center was either the (R) or (S) secondary alcohol. These catalysts were used to hydrogenate  $\alpha$ -acetamidoacrylic acid,  $\alpha$ -acetamidocinnamic acid, DOPA precursor and atropic acid in benzene/EtOH to the corresponding (R)-amino acids or hydratropic acid.

The asymmetric hydrogenation products had the same configurations and comparable optical yields with those which were obtained with the homogeneous Rh-DIOP(-) (3) complex.<sup>65</sup> The ancillary center had little effect in benzene/EtOH. Hydrogenation of  $\alpha$ -acetamidoacrylic acid in THF gave varied optical yields (24-40%) of the corresponding amino acid depending on the configuration of the pendent alcohol group. The results indicated that the solvent-polymer interactions dominated the effects of the additional chiral center.<sup>65</sup>

Table 32 shows a comparison of the results of Rh(I)-DIOP in the gel type copolymers, hectorite and homogeneous systems. Stille and his co-workers developed two gel type copolymer systems (44, 50)<sup>33,65</sup> which proved to be better polymer support systems for asymmetric hydrogenation of dehydroamino acids than the cross-linked polystyrene support system developed earlier by Kagan and co-workers.<sup>32</sup> With the first copolymer supported catalyst (44)<sup>33</sup> (without chiral alcohol sites), only two prochiral amino acids were used in the study. The optical yield of alanine was around 52-60%, less than the homogeneous result. The optical yield of phenylalanine was better than the homogeneous yield. In the second type of copolymer system,<sup>65</sup> the

Table 32. Optical Yields for the Intercalated  $[\text{Rh}(\text{NBD})\text{DIOP}(+) (3)]^+ \text{ a}$  System Compared with Other  $\text{Rh}(\text{I})$ -DIOP Systems

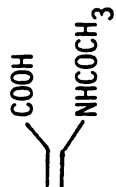
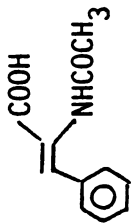
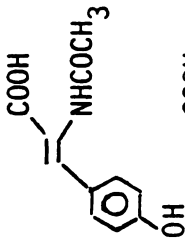
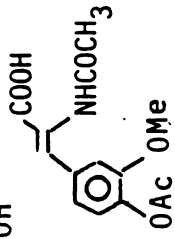
Substrate	$-\text{[Rh(NBD)DIOP}(+) (3)]^+ \text{ a}-$		$-\text{[RhCl(C}_2\text{H}_4)_2\text{]}_2 + \text{DIOP}(-) \text{ b}-$		
	Homogeneous	Intercalated	Homogeneous	Copolymer Attached DIOP(-) (44)	Chiral Copolymer Attached DIOP(-) (50)
	76	74	73	52-60	74-78
	85	86	81	86	83 <sup>c</sup>
	74	82	80	—	70
	88	86	83	—	78.5

Table 32 . Continued.

<sup>a</sup> Solvating medium for this precursor was 95% EtOH. The molar ratio of substrate to rhodium was around 100-200. All the products are (S)-configurations.

<sup>b</sup> These catalyst systems were formed *in situ* with C<sub>6</sub>H<sub>6</sub>/EtOH as the solvating medium. The substrate to rhodium ratio was around 50-100. The optical yields are literature values<sup>33,65</sup>. All the products had (R)-configurations.

<sup>c</sup> 70% chemical conversion.

copolymer supported catalysts (50) contained chiral alcohol sites. With the catalysts supported on the chiral copolymers the optical yields of analine and phenylalanine were slightly better than those obtained with the homogeneous analogue in benzene and ethanol mixture solvent.

The optical yields of tyrosine and DOPA were lower than those obtained with the homogeneous analogue. The chiral sites copolymer supported catalysts (50) were sensitive to solvent, in some cases leading to low conversions.<sup>65</sup> In the Rh(I)-DIOP(+) (3)-hectortie system, the optical yields of four substrates deviated only slightly from those obtained with the homogeneous analogue. Moreover, immobilization of the asymmetric hydrogenation catalyst was easily achieved by a simple cationic exchange process.

In general, the hydrogenation rates of dehydroamino acids with gel type copolymer supported Rh(I)-DIOP(-) catalysts (44, 50) were slower than those observed with the homogeneous analogue.<sup>33,65</sup> It took 2-24 hours to complete the reactions with the substrate to rhodium ratio around 50-100.<sup>33,65</sup> In the layer silicate system hydrogenation rates of dehydroamino acids with the intercalated [Rh(NBD) DIOP(+) (3)]<sup>+</sup> catalyst were 0.40 to 0.90 as fast as those observed with the homogeneous analogue. Most of the reactions could be completed in 1 hr with the substrate to rhodium ratio around 100-200.



From the discussion of the previous results it can be concluded that the choice of the polymer matrix and the synthesis of the catalyst site in the matrix are crucial for the successful use of the polymer supported rhodium complexes as efficient asymmetric hydrogenation catalysts.<sup>33,65</sup> However, through simple cationic exchange, the preparation of intercalation catalysts can be achieved easily without long synthetic processing. Also, intercalation catalysts are highly swollen in polar solvents, and substrates readily are accessible to the catalytic sites. By using intercalated  $[\text{Rh}(\text{NBD})\text{DIOP}(+) (\underline{3})]^+$  catalyst, one can obtain optical yields of asymmetric hydrogenated products that are comparable to the homogeneous results or even better. The hydrogenation rates of dehydroamino acids with intercalated  $[\text{Rh}(\text{NBD})\text{DIOP}(+) (\underline{3})]^+$  catalyst were faster than those observed with gel type copolymer supported  $\text{Rh}(\text{I})\text{-DIOP}(-)$  catalysts.

J. The Probable Asymmetric Hydrogenation Mechanism  
<sup>31</sup>P NMR Spectra of the Solution Structures of (R)-  
 4-Me-Propos (49) and its Rhodium Complexes

There have been great advances in the elucidation of asymmetric hydrogenation mechanism through the use of NMR and X-ray structure studies. A knowledge of the structures of the reaction intermediates is essential for the elucidation of asymmetric hydrogenation mechanism and for the improvement of catalytic systems for asymmetric hydrogenation.

Comprehensive studies on the mechanism of asymmetric hydrogenation of dehydroamino acids with cationic rhodium diphosphine catalysts have focused on the steps<sup>38, 40, 66</sup> in the catalytic cycle and the origins of chiral discrimination.<sup>62</sup> The "unsaturate route" which was proposed by Halpern<sup>39</sup> and co-workers is the most common asymmetric hydrogenation mechanism for most cationic Rh(I)-chiral diphosphine complex systems at low hydrogenation pressure. The catalytic cycle of asymmetric hydrogenation by the unsaturate route is shown in Figure 12. In this mechanism, the complexation of olefin proceeds the addition of hydrogen. Halpern and co-workers found definite evidence to support it.<sup>39</sup> The cationic  $[\text{Rh}(\text{NBD})\text{diphos*}]^+$  complex was hydrogenated in methanol to give a complex containing chelate diphosphine and solvent but no hydrogen.<sup>39</sup> Similar evidence was found by Slack<sup>67</sup> and Baird using a variety of chelating diphosphines. All the rhodium diphosphine complexes formed solvent adducts rather than hydride complexes on hydrogenation in polar solvents.<sup>67</sup> The solvent adducts of rhodium diphos\* complexes react with dehydroamino acid (enamide) to form cationic  $[\text{Rh}\text{diphos*}\text{enamide}]^+$  complexes. The enamides are capable of coordinating with rhodium via olefin and amide carbonyl residues to form a rigid chelate, square-planar complex. The binding mode was first inferred from asymmetric hydrogenation data by Kagan.<sup>36</sup> The X-ray crystal structure evidence was found by Halpern<sup>37</sup> and

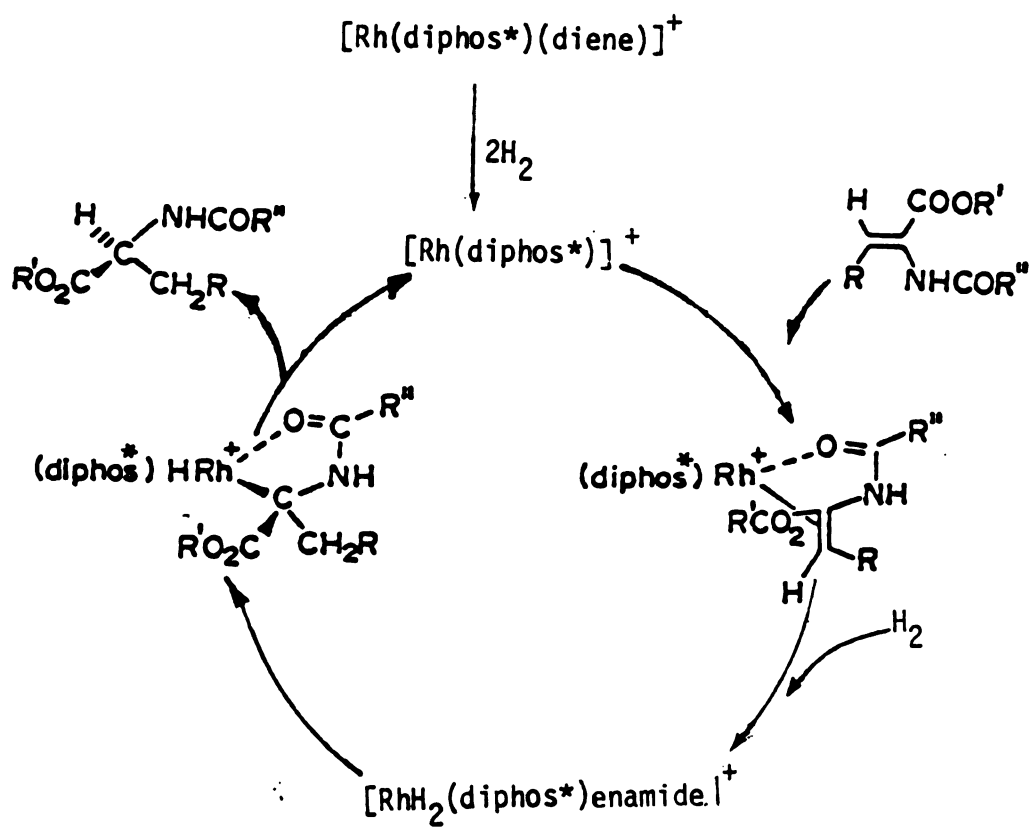


Figure 12. Asymmetric hydrogenation catalytic cycle using the unsaturated route

co-workers. Also, Brown and Chaloner have proved that the same structure was maintained in solution by  $^{31}\text{P}$  and  $^{13}\text{C}$  NMR spectroscopy<sup>38</sup>. The cationic  $[\text{Rh}(\text{diphos}^*)\text{enamide}]^+$  complex reacts further with  $\text{H}_2$ , presumably to form the dihydride-enamide intermediate. The hydride transfers from the rhodium to the coordinated face of the olefin, forming a monohydrido- $\sigma$ -alkyl intermediate, which undergoes reductive elimination to produce the corresponding amino acid and regenerate the catalyst. The monohydrido- $\sigma$ -alkyl intermediate has been detected and its structure has been deduced by NMR

The asymmetric induction step can be either the displacement of the solvent by enamide, or the addition of hydrogen or hydride insertion, depending on the individual case. Thermodynamic and kinetic factors of asymmetric hydrogenation are important for determining the asymmetric induction step.<sup>62</sup> The probable mechanism of asymmetric hydrogenation of dehydroamino acids using cationic rhodium (I) chiral diphosphine catalysts is shown in Figure 13. Usually two diastereomeric rhodium(I) enamide complexes can be observed, with one predominating in most instances. The attainment of the  $K_d$ <sup>40, 66, 68</sup> equilibrium of two diastereomers in most chiral diphosphine systems is rapid at ambient conditions (Figure 13). However,  $K_d$  is kinetically irrelevant in deciding the optical yield. The optical yield is decided by the different reaction rates of two diastereomeric

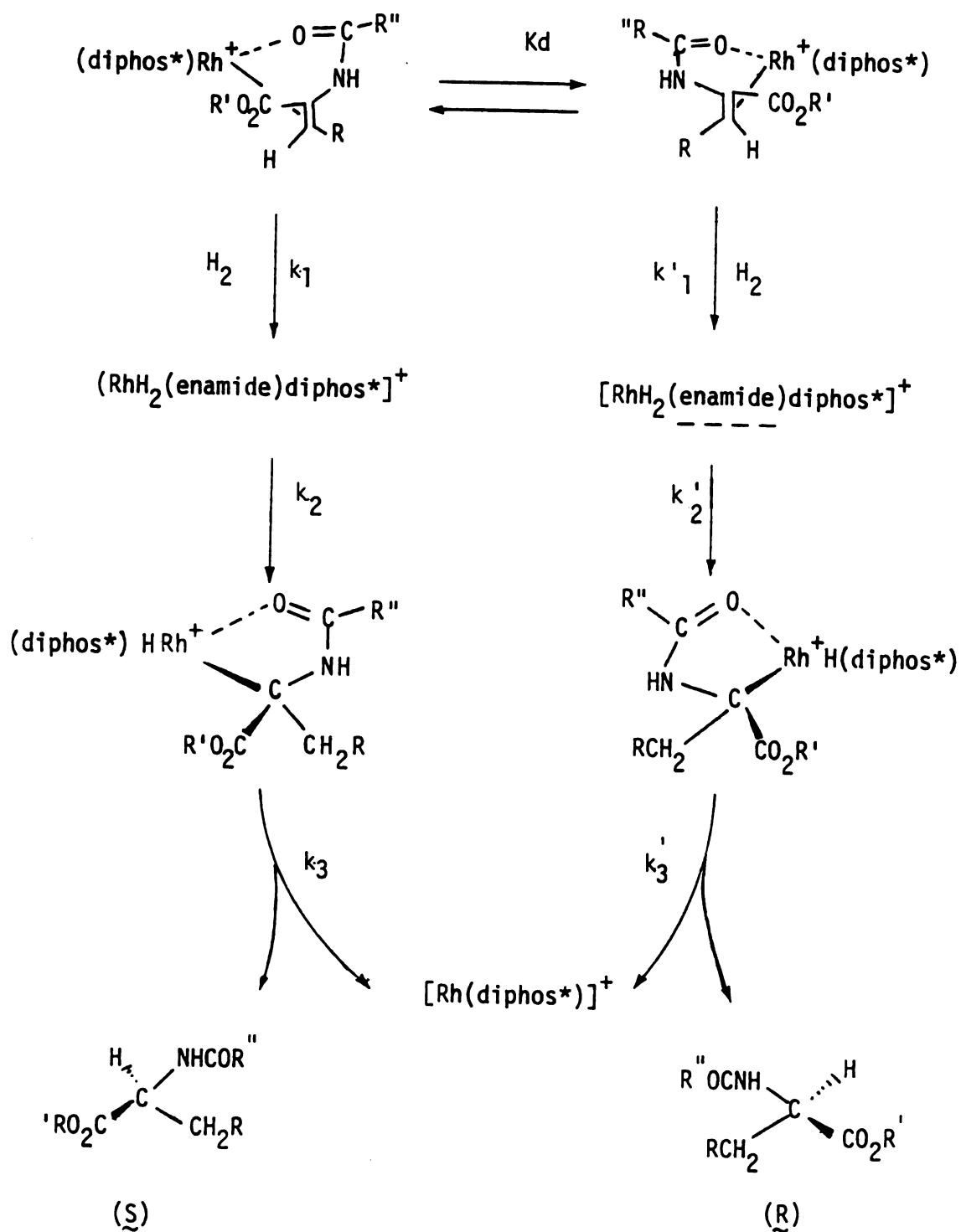


Figure 13. The probable mechanism of asymmetric hydrogenation of dehydroamino acids (enamides) using cationic rhodium(I) chiral diphosphine catalysts

rhodium enamide intermediates. These rates are determined by the relative energies of two diastereomeric transition states and are not reliant on the initial reactant energies<sup>69</sup> (Curtin-Hammett Principle). Also, Bosnich<sup>62</sup> believes that the origins of the dissymmetric rate differentiation must reside in the different dissymmetric interactions of the chiral diphosphine ligand and the prochiral substrate in the diastereomeric transition states of the reaction.

In the rigid-type diphosphine systems at ambient temperature and pressure, the rate determining step is presumably the oxidative addition of hydrogen ( $k_1$ ,  $k_1'$ ). The hydride insertion step ( $k_2$ ,  $k_2'$ ) is assumed to be faster. At low temperature (below  $-40^\circ\text{C}$ ) and ambient pressure, the rate determining step would shift to reductive elimination ( $k_3$ ,  $k_3'$ ). The evidence for the monohydrido- $\sigma$ -alkyl intermediate has been obtained by Halpern<sup>66a</sup> and Brown.<sup>66b</sup> In the case of ( $\underline{S},\underline{S}$ )-Chiraphos (5), Halpern<sup>40</sup> reported that the minor diastereomeric Rh(I)-enamide ( $\underline{S},\underline{S}$ )-Chiraphos (5) complex is the true intermediate which added hydrogen much faster than the major intermediate at ambient conditions. The result indicates that the rate constant ( $k_1'$ ) for hydrogenation of the minor diastereomer is more than 3 orders of magnitude faster than the rate constant ( $k_1$ ) for the major diastereomer.

In the layer silicate system, at ambient conditions, the rate determining step is expected to be the same as that of the homogeneous state. This means that the oxidative

addition of hydrogen ( $k_1, k_1'$ ) is the rate determining step. Since the interactions between the silicate sheets and diastereomeric  $[\text{Rh}(\text{diphos}^*)\text{enamide}]^+$  complexes take place, the relative energies of two diastereomeric transition states in the intercalation state may vary from those of the homogeneous state, resulting in differentiation in the hydrogenation rates of the two diastereomers. Also, changing the ratio of two diastereomers is possible in the intercalation state. However, changing the ratio of two diastereomers may not necessarily alter the optical yield. The effect on the optical yield in changing the rates of two diastereomers may be the most important consideration in the intercalation state. Optical yield variation of the corresponding amino acids obtained with  $\text{Rh}(\text{diphos}^*)$  complex in the homogeneous and intercalation states should be expected.

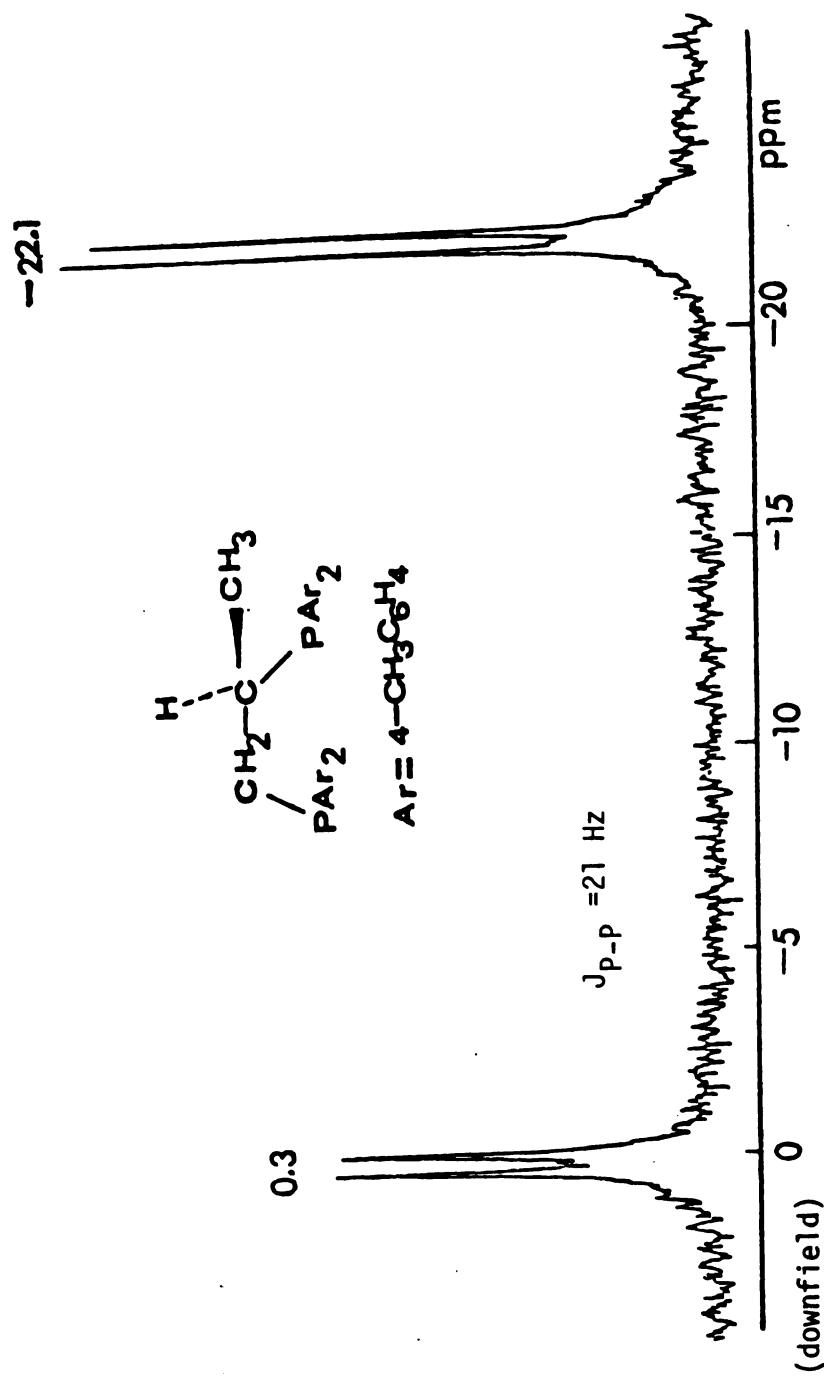
There is still a lack of sufficient evidence to determine the cause of the asymmetric induction step in most diphosphine systems, however. Along with a consideration of optical yields of the products and X-ray structures of intermediates,  $^{31}\text{P}$  NMR spectroscopy of the solution structures of asymmetric hydrogenation intermediates in each chiral diphosphine system can provide crucial evidence for elucidating the induction step.

(*R*)-4-Me-Propfos (*49*) is a new ligand. Studies of  $^{31}\text{P}$  NMR spectra of (*R*)-4-Me-Propfos (*49*) may provide useful information to clarify the reaction mechanism and elucidate the asymmetric induction step. The free ligand

has two nonequivalent phosphorous atoms, and they are coupled with each other. The  $^{31}\text{P}$  NMR spectrum shows two sets of doublets (Figure 14). The  $^{31}\text{P}$  NMR spectrum of a 0.01 M solution of  $[\text{Rh}(\text{NBD})(\text{R})\text{-4-Me-Prophos (49)}]^+\text{ClO}_4$  in  $\text{CDCl}_3$  at  $-16^\circ\text{C}$  is shown in Figure 15. Norboradiene (NBD) is a symmetrical molecule, and two nonequivalent phosphorous atoms couple with each other and with  $^{103}\text{Rh}$  nucleus ( $I = \frac{1}{2}$ , natural abundance = 100%). The spectrum shows two sets of four lines. It is an ABX type spectrum. The  $^{31}\text{P}$  NMR spectrum of  $[\text{Rh}(\text{NBD})(\text{R})\text{-4-Me-Prophos (49)}]^+\text{ClO}_4$  has the same features as the  $^{31}\text{P}$  NMR spectrum of  $[\text{Rh}(\text{NBD})(\text{R})\text{-Prophos (6)}]^+\text{ClO}_4$  (Table 33).

The  $^{31}\text{P}$  NMR spectrum of 0.01 M  $[\text{Rh}(\text{I})(\text{Z-ester})(\text{R})\text{-4-Me-Prophos (49)}]^+$  in EtOD in the presence of an 8 molar excess of ethyl (Z)- $\alpha$ -benzamodocinnamate (Z-ester) is shown in Figure 16. The chemical shifts and coupling constants of  $[\text{Rh}(\text{Z-ester})(\text{R})\text{-4-Me-Prophos (49)}]^+$  are shown in Table 33. Since the (R)-4-Me-Prophos (49) and (S)-Phenphos (7) are analogues, both ligands are chiral. There are four possible Rh enamide complexes for each ligand. Either face of the enamide may be cis or trans to  $\text{P}_1(\text{Ar}_2\text{PCH}_2)$ . Brown and Chaloner have used  $^{13}\text{C}$  enriched methyl (Z)- $\alpha$ -acetamidocinnamate (enriched amide carbon) and dideuterated (S)-Phenphos ( $-\text{CD}_2\text{-PAr}_2$ ) to study the solution structures of  $[\text{Rh}(\text{Z-ester})(\text{S})\text{-phenylphos (7)}]^+$  complexes by  $^{31}\text{P}$  NMR spectroscopy.<sup>12</sup> The



$(\tilde{R})$ -4-Me-Prophos (49)Figure 14. The  $^{31}\text{P}$  NMR spectrum of  $(\tilde{R})$ -4-Me-Prophos (49) in  $\text{CDCl}_3$  at  $25^\circ\text{C}$

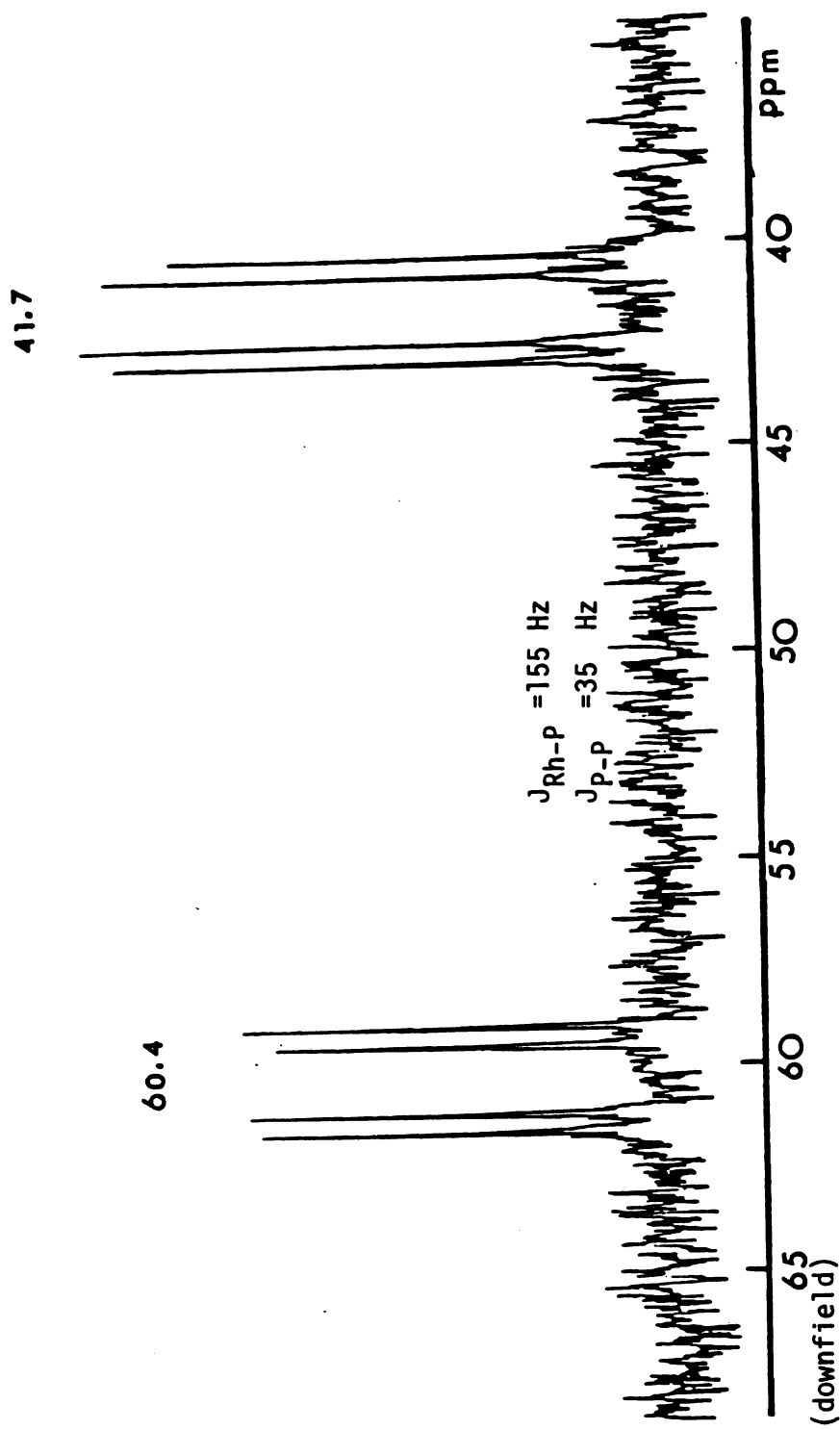
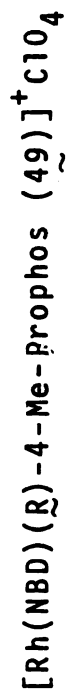


Figure 15. The  $^{31}\text{P}$  NMR spectrum of 0.01 M solution of  $[\text{Rh}(\text{NBD})(\text{R})-4\text{-Me-Prophos}(\text{R})]^+\text{ClO}_4^-$  in  $\text{CDCl}_3$  at  $-16^\circ\text{C}$

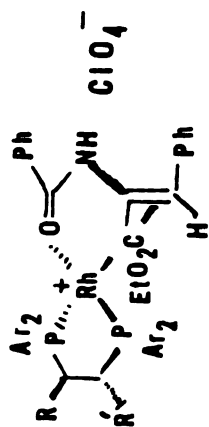
Table 33.  $^{31}\text{P}$  NMR Parameters of Chiral Diphosphines (L) and Their Rhodium(I) Complexes<sup>a</sup>

Chemical Shifts and Coupling Constants		
	( <u>R</u> )-Prophos ( <u>6</u> )	( <u>R</u> )-4-Me-Prophos ( <u>49</u> )
free ligand	2.1 ppm, -20.2 ppm, $J_{\text{P-P}}=21$ Hz ( $\text{CDCl}_3$ , 25°C)	0.3 ppm, -22.1 ppm $J_{\text{P-P}}=21$ Hz ( $\text{CDCl}_3$ , 25°C)
$[(\text{NBD})\text{Rh L}]^+$	61.6 ppm (dd, $J_{\text{Rh-P}}=155$ Hz), 42.9 ppm (dd, $J_{\text{Rh-P}}=155$ Hz), $J_{\text{P-P}}=34$ Hz; ( $\text{CDCl}_3$ , -20°C)	60.4 ppm (dd, $J_{\text{Rh-P}}=155$ Hz), 41.7 ppm (dd, $J_{\text{Rh-P}}=155$ Hz), $J_{\text{P-P}}=35$ Hz; ( $\text{CDCl}_3$ , -16°C)
$[\text{Z-ester Rh L}]^{+b}$	_____	74.9 ppm (dd, $J_{\text{Rh-P}}=162$ Hz), 46.7 ppm (dd, $J_{\text{Rh-P}}=155$ Hz), $J_{\text{P-P}}=46$ Hz; 64.9 ppm (dd, $J_{\text{Rh-P}}=155$ Hz), 59.7 ppm (dd, $J_{\text{Rh-P}}=158$ Hz), $J_{\text{P-P}}=46$ Hz; ( $\text{CH}_3\text{OD}$ , -30°C)

<sup>a</sup> 72.88 MHz, 85%  $\text{H}_3\text{PO}_4$  as external reference; downfield shifts positive.

<sup>b</sup> Z-ester = Etethyl-(Z)- $\alpha$ -benzamidocinnamate

$[\text{Rh}(\underline{\text{Z}}\text{-ester})(\text{R})\text{-4-Me-Prophos (49)}]^+ \text{ClO}_4^-$



- a)  $\text{R} = \text{CH}_3$   $\text{R}' = \text{H}$   
 b)  $\text{R} = \text{H}$   $\text{R}' = \text{CH}_3$

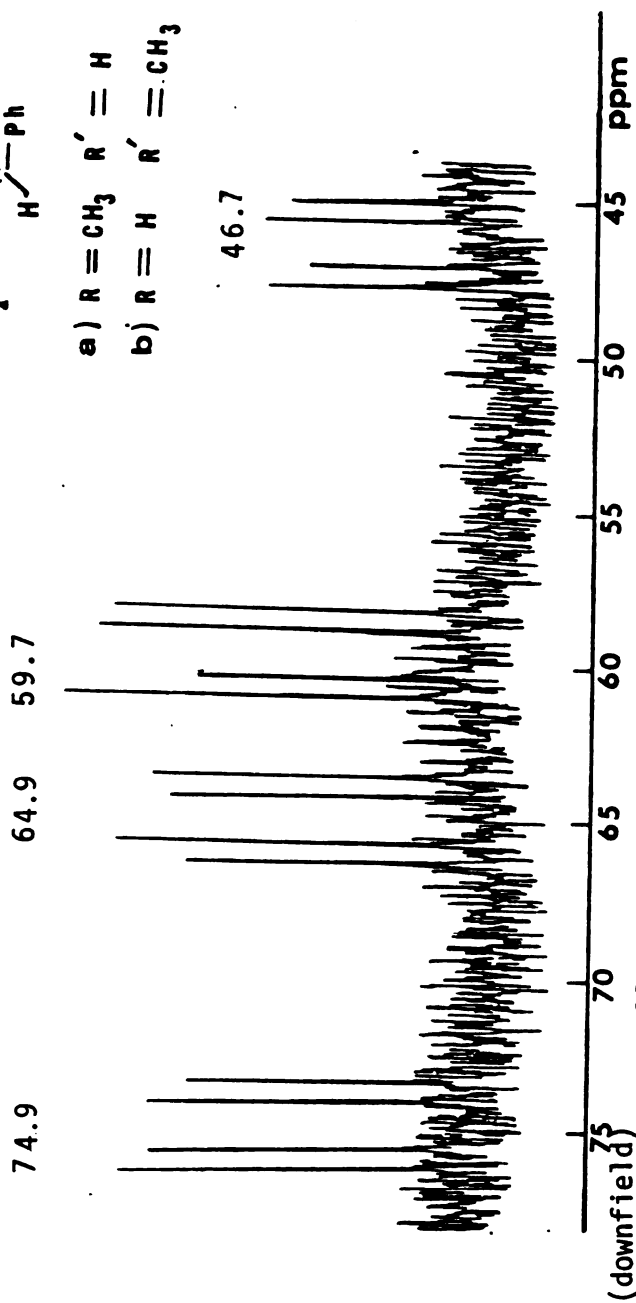


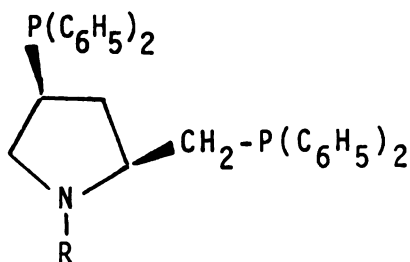
Figure 16. The  $^{31}\text{P}$  NMR of 0.01 M of  $[\text{Rh}(\text{Z-ester})(\text{R})\text{-4-Me-Prophos (49)}]^+ \text{ClO}_4^-$  in  $\text{CH}_3\text{OD}$  at  $-30^\circ\text{C}$

spectrum pattern is the same as that of  $[\text{Rh}(\text{Z-ester})(\text{S})\text{-Phenphos}(\text{Z})]^+$  complex<sup>12</sup>. It demonstrated that the  $[\text{Rh}(\text{Z-ester})(\text{R})\text{-4-Me-Prophos}(\text{49})]^+$  complex only has two geometric isomers in the solution and that they are not diastereomers. The result implies that  $[\text{Rh}(\text{I})(\text{R})\text{-4-Me-propbos}(\text{49})]^+$  complex is capable of enantioface differentiation of enamide to form preferential  $\text{Rh}(\text{I})\text{-enamide}(\text{R})\text{-4-Me-Prophos}(\text{49})$  diastereomer. The major diastereomer is possibly the true intermediate. However, further X-ray structure evidence of  $[\text{Rh}(\text{I})\text{-(R)-4-Me-Prophos}(\text{49})\text{enamide}]^+$  complex is needed to clarify this point.

## II. Synthesis and Characterization of New Functionalized Chiral Diphosphine Ligands

There have been significant advances in asymmetric hydrogenation of prochiral olefins with chiral rhodium phosphine catalysts<sup>1,2</sup> since its original development in 1968.<sup>3-5</sup>

Optical yields over 90% are possible with certain prochiral substrates.<sup>2b</sup> Chiral chelating phosphines play a key role in asymmetric induction of the rhodium asymmetric hydrogenation systems. The chiral diphosphine ligands (5-12) which can coordinate with rhodium and form rigid five-membered chelating ring complexes, usually give high optical yields with (Z)-dehydroamino acids.<sup>9-15</sup> The chiral diphosphine ligands which had the third functional groups were more useful for asymmetric synthesis,<sup>2b,22-24</sup> A series of pyrrolidinephosphines such as BPPM (23), PPPM (24), PPM (25) and their analogues which have third functional groups (the amide substituents) have been successfully used as ligands for a variety of rhodium catalyzed reactions<sup>2b</sup>.

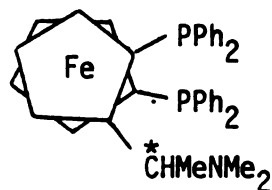


(23) R = COOC<sub>4</sub>H<sub>9</sub>-*tert* BPPM

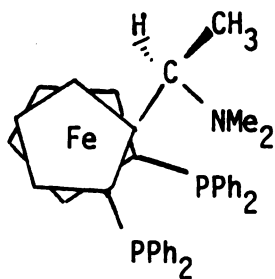
(24) R = CO-C<sub>4</sub>H<sub>9</sub>-*tert* PPPM

(25) R = H PPM

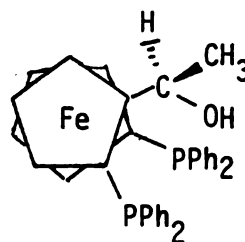
The amide group of ligand (23) was modified by different substituents in order to optimize the optical yields<sup>2b</sup> (see pages 20 to 24) to chemically clarify the reaction intermediates,<sup>70</sup> or to attach to the polymer<sup>34</sup>. Ferrocenyl-phosphines (27-29) which have planar chirality and various functional groups such as amino or hydroxyl groups have been demonstrated to be effective ligands for rhodium catalyzed asymmetric hydrogenation of dehydroamino acids,<sup>22</sup> ketones<sup>23</sup> and imines<sup>24</sup> (see pages 24 to 29). The interactions between the substrates and the third functional groups of the ligands in transition states are crucial for highly asymmetric inductions of these catalytic reactions.<sup>22-24</sup>



(S)-(R)-BPPFA (27)

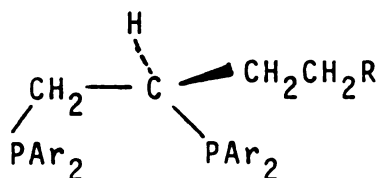


(R)-(S)-BPPFA (28)



(R)-(S)-BPPFOH (29)

The design of new rigid functionalized chiral diphosphines may provide the following advantages. The ligands, being rigid, can be highly effective for asymmetric hydrogenation of dehydroamino acids. The third functional group can be modified to optimize the optical yields and can be attached to the polymeric, organic or inorganic carriers. Also, the ligands have nonequivalent phosphorus. They can be used as spectroscopic probes for studying the reaction mechanism. The new THP-butaphos (51) (R)-hydroxylbutaphos (52) and *N*-BOC-butaphos (53) which were synthesized from natural occurring L-malic acid are in this category.



R = OTHP, Ar = C<sub>6</sub>H<sub>5</sub>, THP-butaphos (51)

R = OH, Ar = C<sub>6</sub>H<sub>5</sub>, (R)-hydroxylbutaphos (52)

R = NCH<sub>2</sub>CH(CH<sub>3</sub>)<sub>2</sub>, Ar = 4-CH<sub>3</sub>-C<sub>6</sub>H<sub>4</sub>

COO-C<sub>4</sub>H<sub>9</sub>-*tert* *N*-BOC-butaphos (53)

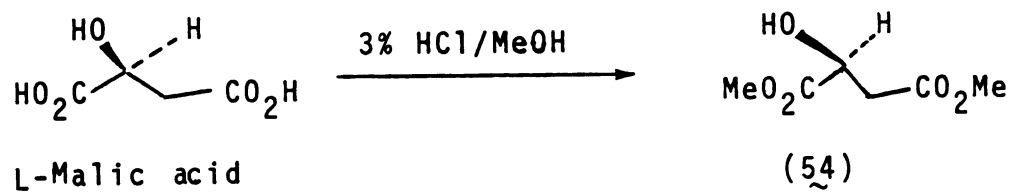
In this part the focus was on the synthesis and characterization of new functionalized chiral diphosphine ligands (51, 52, 53), and the application of the new, *N*-BOC-butaphos (52) ligand for asymmetric hydrogenation of (Z)-dehydroamino acids in homogeneous and intercalated systems.



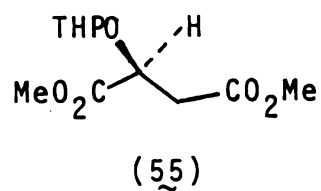
### A. Synthesis of the Key Synthetic Precursor

The key synthetic precursor, 1,2-*O*-isopropylidene-1,2,4-butanetriol [acetonide-triol (58)] was prepared in 60% overall yield from L-malic acid.<sup>71</sup> The synthetic route is shown in Scheme 27. Esterification of L-malic acid by stirring in 3% HCl-MeOH solution overnight gave (*S*)-di-methyl malate (54) in 94% yield. Reaction of (*S*)-di-methyl malate (54) with 1.1 equivalent of dihydropyran (DHP) and a catalytic amount of *p*-toluenesulfonic acid in ether at room temperature for 16 hours formed the corresponding THP ether (55) in 91% yield. Reducing the corresponding THP-ether (55) with excess lithium aluminum hydride in dry ether produced the diol THP ether (56) in 93% yield. Removal of the THP protecting group by stirring with a catalytic amount of *p*-toluenesulfonic acid in methanol for 16 hours afforded the triol (57) in 97% yield. Triol (57) was converted to acetonide-triol (58) in 78% yield by treatment with a catalytic amount of *p*-toluenesulfonic acid in dry acetone for two days.

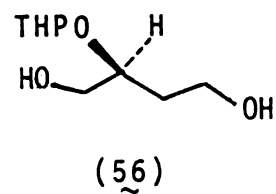
The synthetic precursor, acetonide-triol (58) had three hydroxyl groups. The two hydroxyl groups at the 1,2 positions of acetonide-triol (58) which were protected by isopropylidene group could be transformed into diphosphine. The third hydroxyl group could be functionalized. However, due to the limitation of the synthetic method, it is crucial to follow closely the proposed reaction



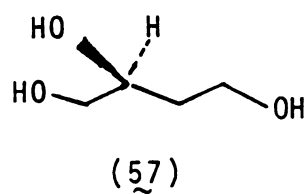
DHP /ether



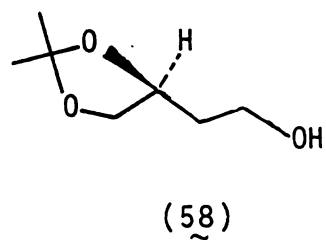
LiAlH<sub>4</sub>/ether



MeOH/TsOH



Acetone/TsOH

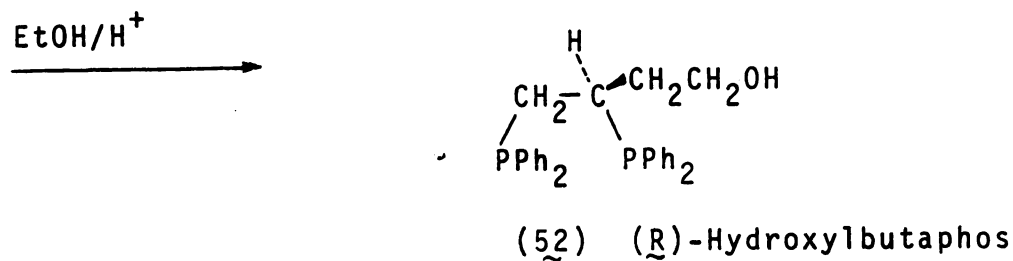
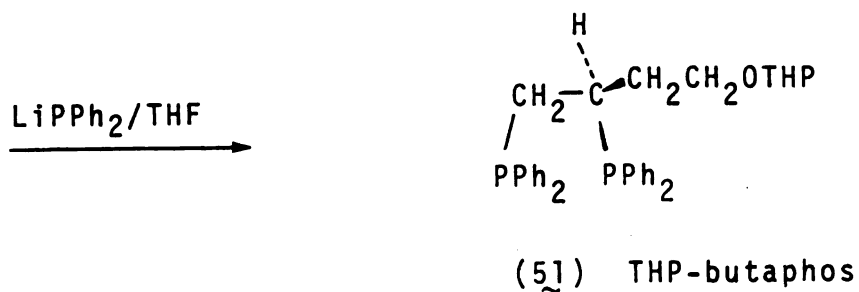
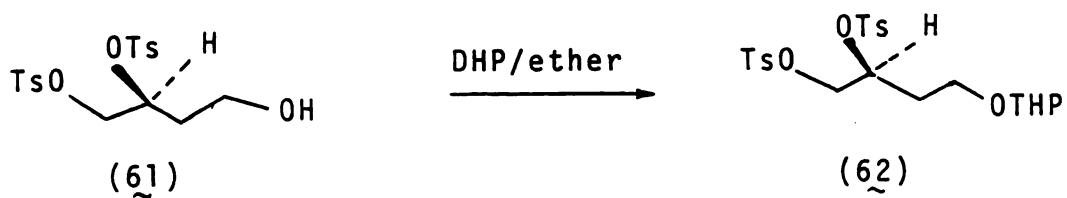
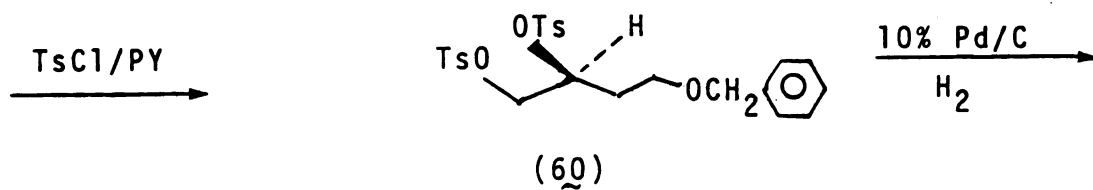
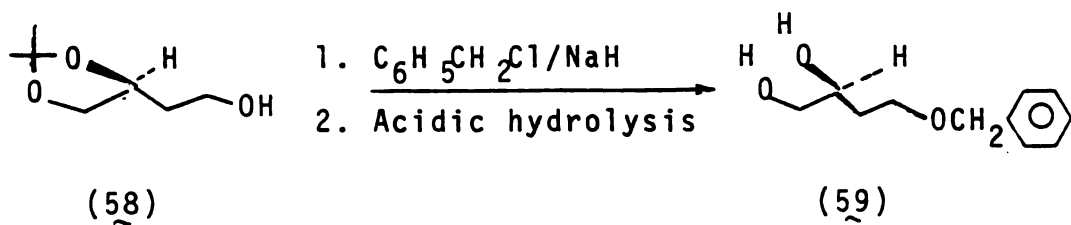


Scheme 27

sequences to achieve the synthetic goals.

B. Synthesis of 4-(1'-Tetrahydropyranloxy)-1,2-(R)-bis(diphenylphosphino)butane, [THP-butaphos (51)] and 4-Hydroxy-1,2-(R)-bis(diphenylphosphino)butane[(R)-Hydroxylbutaphos (52)]

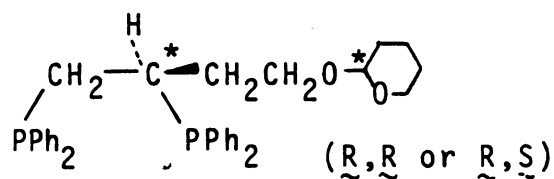
The 1,2-*O*-isopropylidene-1,2-(S)-4-butanetriol [acetone-triol (58)] is a key synthetic precursor for synthesis of THP-butaphos (51) and (R)-Hydroxylbutaphos (52). The synthetic route is shown in Scheme 28. The acetone-triol (58) was reacted with NaH and benzyl chloride in toluene at 70°C and followed by acidic hydrolysis in the mixed solvent (HAc:THF:H<sub>2</sub>O) at 45°C to give benzyl-diol (59) in 84% yield. The benzyl-diol (59) was converted into benzylether ditosylate (60) in 91% yield by reaction with toluenesulfonyl chloride in pyridine. The benzylether ditosylate (60) was hydrogenolized over 10% Pd/C to give hydroxylditosylate (61) in 98% yield. The hydroxylditosylate (61) was converted quantitatively into THP-ether-ditosylate (62) by treatment with dihydropyran and a catalytic amount of toluenesulfonic acid in ether. The THP-ether-ditosylate (62) was treated with a stoichiometric amount of LiP(C<sub>6</sub>H<sub>5</sub>)<sub>2</sub> to afford the crude product of THP-butaphos (51). The final product was difficult to crystallize. The purity of the product, which was determined by <sup>31</sup>P NMR, was larger than 90%. The (R)-Hydroxylbutaphos (52) was obtained by acidic hydrolysis of THP-butaphos (51) with a catalytic amount of toluenesulfonyl acid in ethanol.



The third hydroxyl group of the acetone-triol (58) was protected by benzylation. It was necessary to replace the benzyl protecting group by the THP group before phosphination. If phosphination were to precede debenylation, the final debenylation reaction, which requires the use of Pd/C as a catalyst, could permit reaction of the ligand with palladium and form a palladium complex. This undesirable side reaction could cause stoppage of the reaction or purification problems. However, the THP protecting group is unaffected by the phosphide reagent and can be removed easily by hydrolysis.

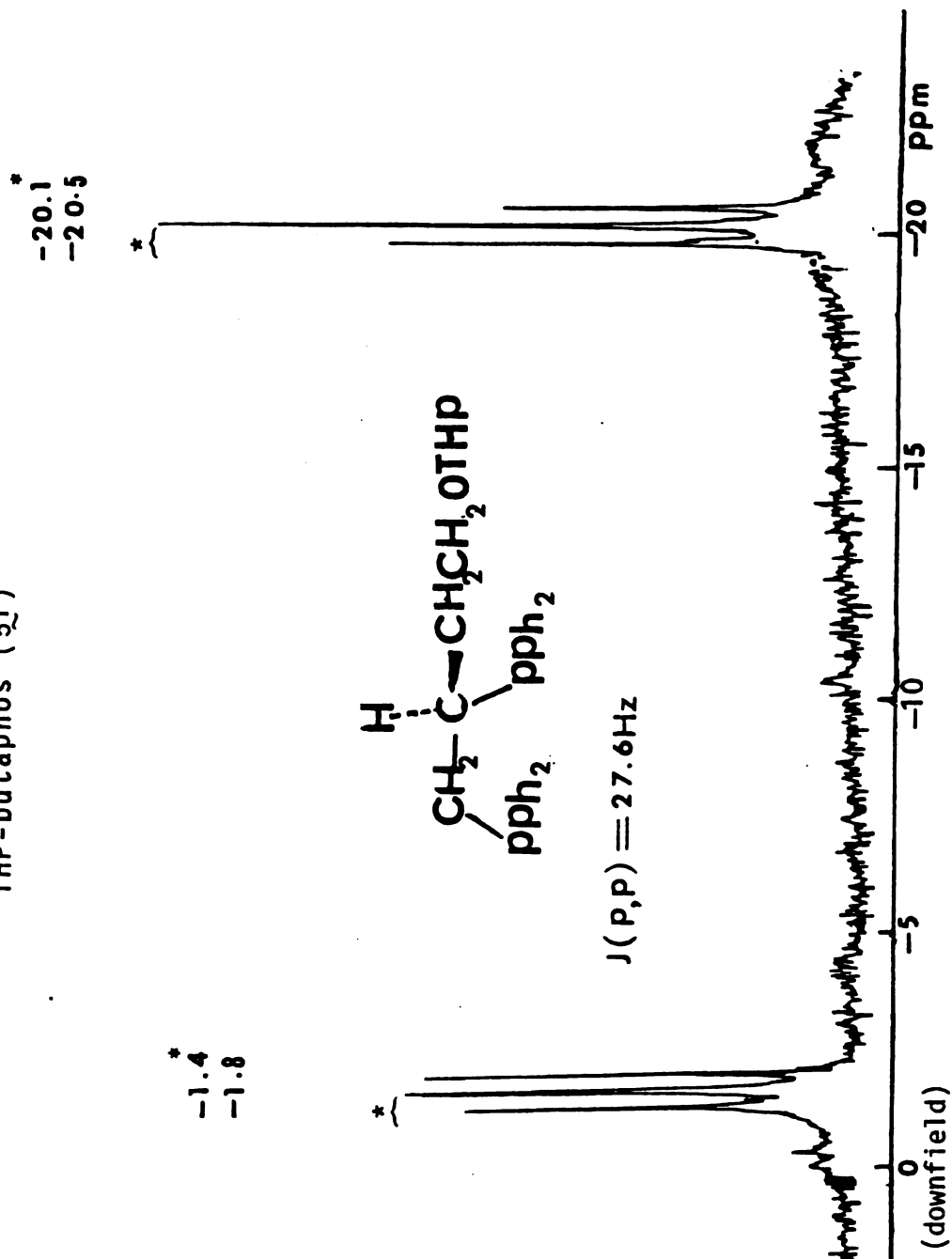
C. Characterization of THP-butaphos (51) and (R)-Hydroxyl-butaphos (52)

Figure 17 shows the  $^{31}\text{P}$  NMR spectrum of the THP-butaphos (51) ligand. The ligand (51) has two diastereomers and the nonequivalent phosphorous atoms are spin-coupled. The spectrum is supposed to show four sets of doublets, but two sets of resonances overlap each other. Therefore, the spectrum appears as two sets of triplets.



THP-butaphos (51)

## THP-butaphos (51)

Figure 17. The  $^{31}\text{P}$  NMR spectrum of THP-butaphos (51) in  $\text{CDCl}_3$ , at  $25^\circ\text{C}$

Upon acidic hydrolysis, the THP protecting group was removed, resulting in the destruction of two diastereomers, and the conversion of the ligand (51) into (R)-Hydroxylbutaphos (52). This was confirmed by  $^{31}\text{P}$  NMR spectra. (R)-Hydroxylbutaphos (52) only had one isomer. The  $^{31}\text{P}$  NMR of (R)-Hydroxylbutaphos (52) only showed two sets of doublets (Figure 18). The results confirmed the predictions. The chemical shifts of (R)-Hydroxylbutaphos (52) were similar to those of THP-butaphos (51). The spectroscopic evidence of (R)-Hydroxylbutaphos (52) proved that the THP-butaphos (51) had two diastereomers and no impurities.

D. Synthesis of 4-(((*tert*-Butyloxy)carbonyl)-isobutylamino)-1,2-(R)-bis(di-4-methylphenylphosphino)butane [*N*-BOC-butaphos (53)]

1,2-*O*-Isopropylidene-1,2-(S)-4-butanetriol [acetone-triol (58)] is the key synthetic precursor for the synthesis of *N*-BOC-butaphos (53). The synthetic route is shown in Scheme 29.

The acetone-triol (58) was converted into (S)-tosylate (63) with *p*-toluenesulfonic chloride in pyridine in 81% yields. The displacement of the (S)-tosylate (63) in excess isobutylamine produced the corresponding amine (64) in 93% yield. Acidic hydrolysis of the corresponding amine furnished the aminodiol (65) in 78% yield. The aminodiol (65) was treated with di-*tert*-butyl dicarbonate to form the *N*-BOC-aminodiol (66) in quantitative yield.

( $\tilde{R}$ )-Hydroxybutaphos (52)

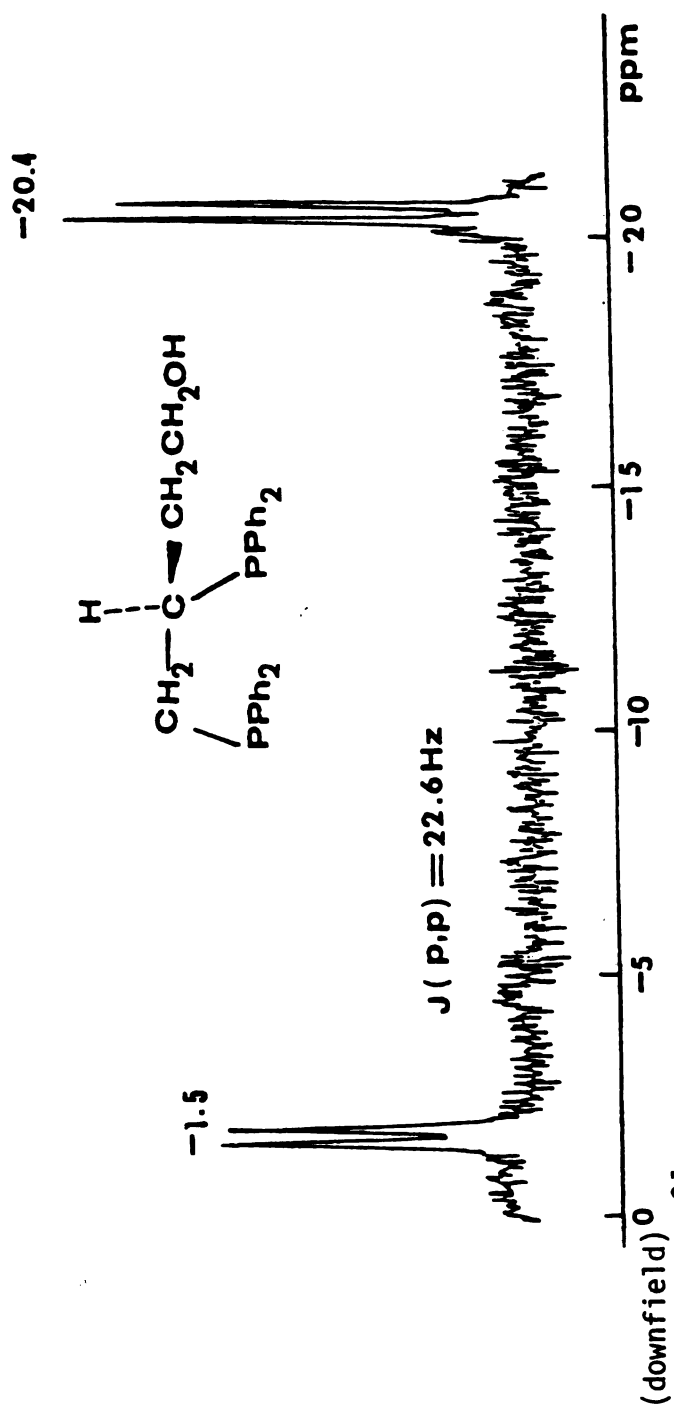
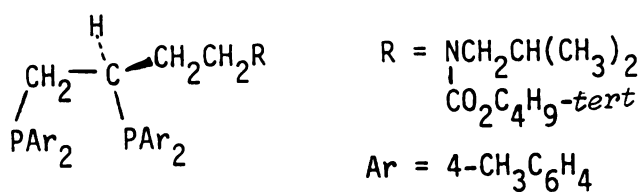
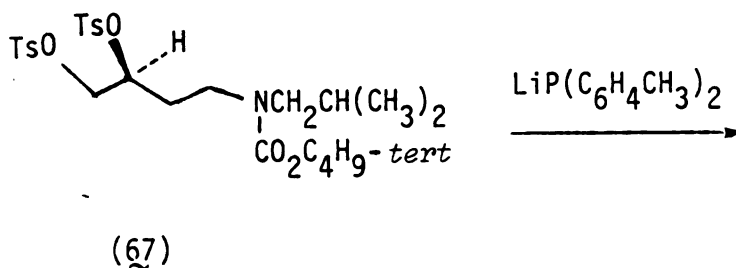
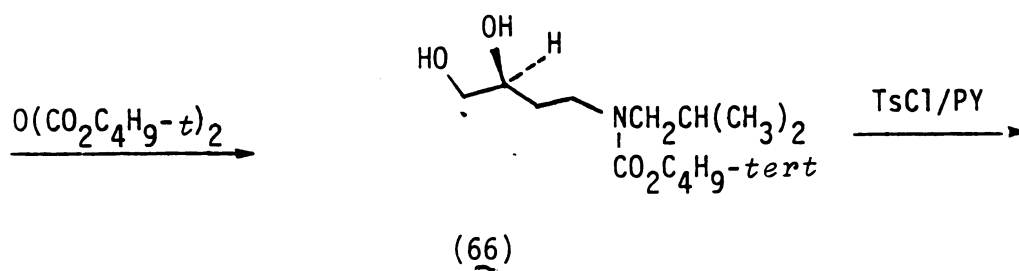
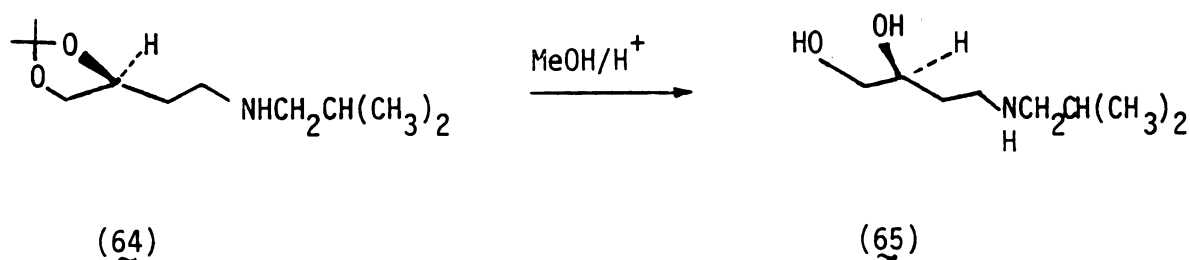
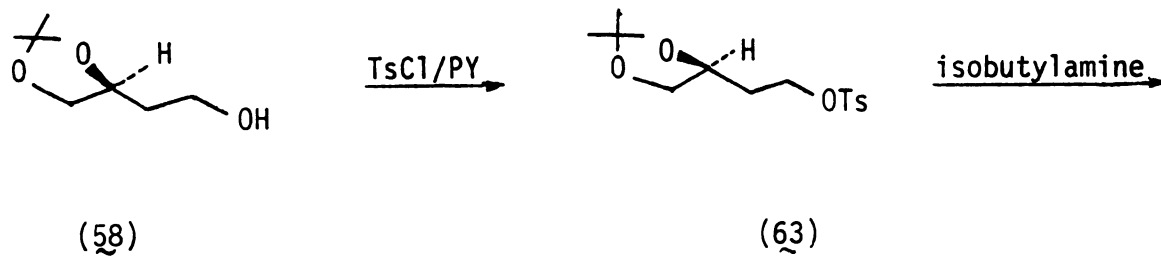


Figure 18.  $^{31}\text{P}$  NMR spectrum of ( $\tilde{R}$ )-Hydroxybutaphos (52) in EtOD, at 25°C





N-BOC-butaphos (53)

*N*-BOC-aminodiol (66) was converted into *N*-BOC-amino-ditosylate (67) with *p*-toluenesulfonic chloride in pyridine in 89% yield. Finally, phosphination of the *N*-BOC-amino-ditosylate (67) with a stoichiometric amount of lithium bis(4-methylphenyl)phosphide in THF afforded the crude oily product. Crystallization of the crude product from 95% EtOH produced pure *N*-BOC-butaphos (53).

The third unprotected hydroxyl group of acetonide-triol (58) was first transformed into isobutylamino group. After acidic hydrolysis of the acetonide group, the isobutylamino group was protected by the BOC group to prevent tosylation and phosphination in the following reaction sequences.

Also, BOC protecting group can be removed rapidly by mild acid. Variation of amide substituent may alter optical yields. The BOC functionality may also be useful for attachment of the ligand to organic or inorganic carriers.

E. Characterization of 4-{\{(*tert*-Butyloxy)carbonyl}-isobutylamino}-1,2-(*R*)-bis(di-4-methylphenylphosphino)butane [*N*-BOC-butaphos (53)]

The four methyl groups of 4-methylphenyl rings of *N*-BOC-butaphos (53) are not in identical environments. Two methyl groups, however, have the same <sup>1</sup>H NMR chemical shifts. The other two methyls gave different chemical shifts. Thus, the <sup>1</sup>H NMR spectrum (Figure 19) exhibits three

*N*-BOC-butaphos (53)  
(diluted solution)

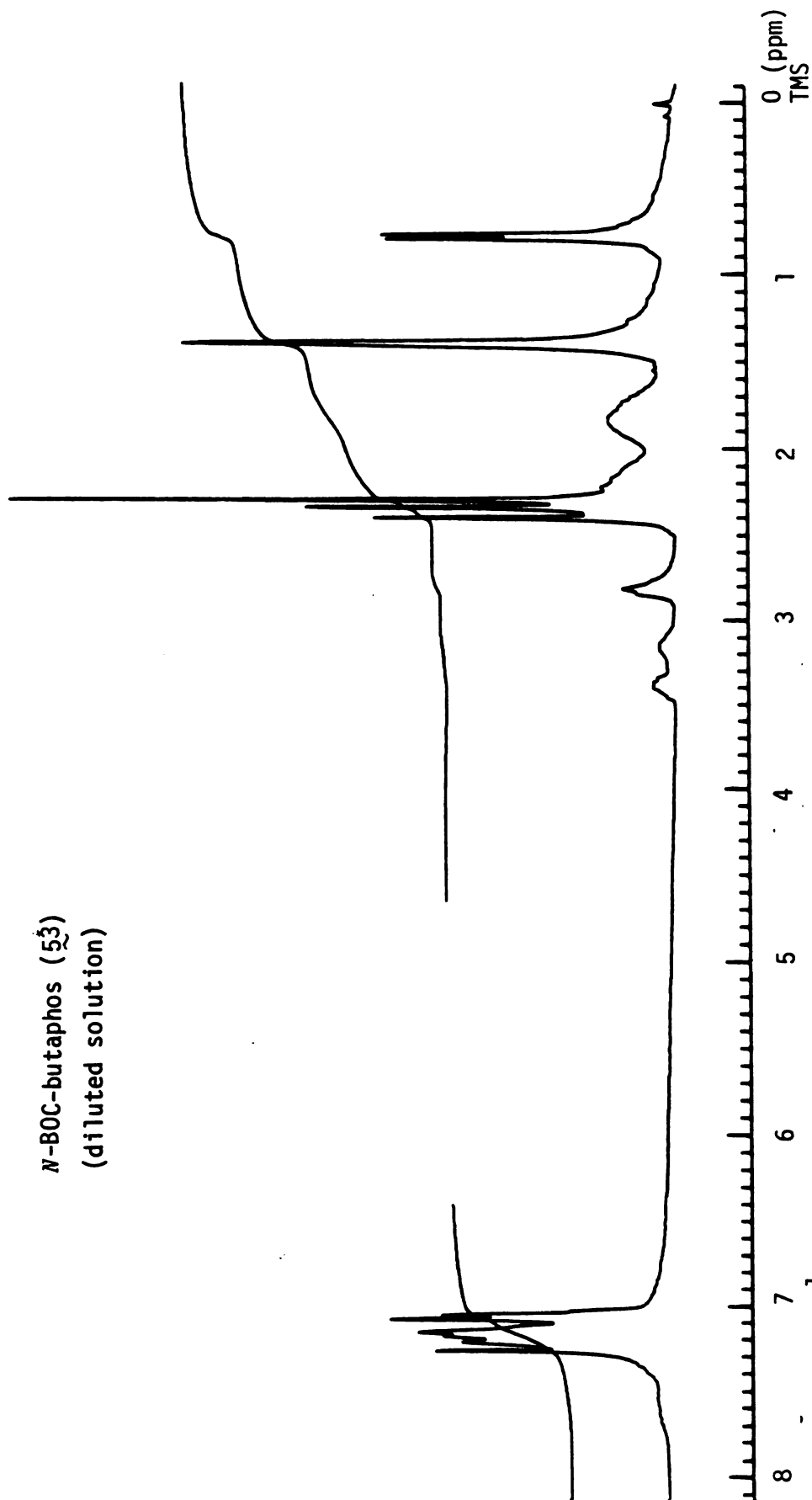


Figure 19.  $^1\text{H}$  NMR spectrum of *N*-BOC-butaphos (53) in  $\text{CDCl}_3$ , at  $25^\circ\text{C}$  (250 MHz).

distinguishable singlet peaks in the range of 2.1 - 2.5 ppm. The spectrum of the methyl groups on the 4-methyl-phenyl rings show the same characteristics as (*R*)-4-Me-Propios (49). The amide groups (*N*-BOC) of the ligand (53) may not rotate freely, resulting in conformational isomers. This could be confirmed by  $^1\text{H}$  and  $^{31}\text{P}$  NMR. When the concentration of *N*-BOC-butaphos (53) is increased, the three distinguishable methyl lines at 2.2 - 2.5 ppm split into three sets of doublets (Figure 20). The  $^{31}\text{P}$  NMR spectrum shows two small shoulders at the low-field side of each major doublet peak (-4.4 and -22.6 ppm) (Figure 21). The compound is difficult to crystallize from solvents other than 95% ethanol. The compound was isolated as the monohydrate. The mass spectrum and high resolution mass spectrum gave the expected parent peak. The  $^1\text{H}$  and  $^{31}\text{P}$  NMR spectra proved that the compound was not contaminated by phosphine oxide. If the compound was oxidized to phosphine oxide, the  $^1\text{H}$  NMR spectra of the ortho and meta hydrogen peaks of the phenyl groups of the ligand would split into two sets of complex peaks (Figure 20).

*N*-BOC-butaphos (53)  
(concentrated solution)

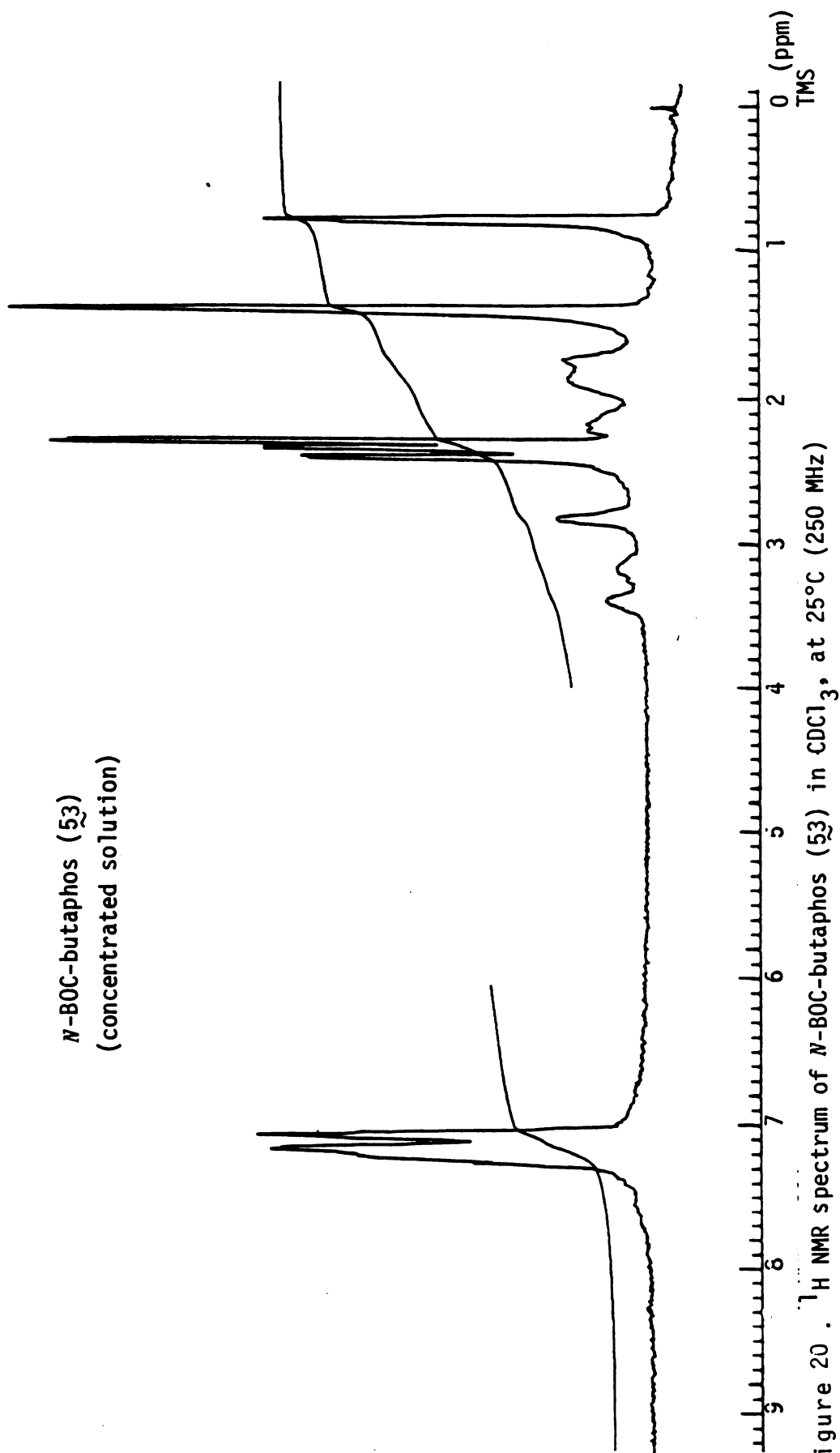


Figure 20.  $^1\text{H}$  NMR spectrum of *N*-BOC-butaphos (53) in  $\text{CDCl}_3$ , at  $25^\circ\text{C}$  (250 MHz)

*N*-BOC-butaphos (53)

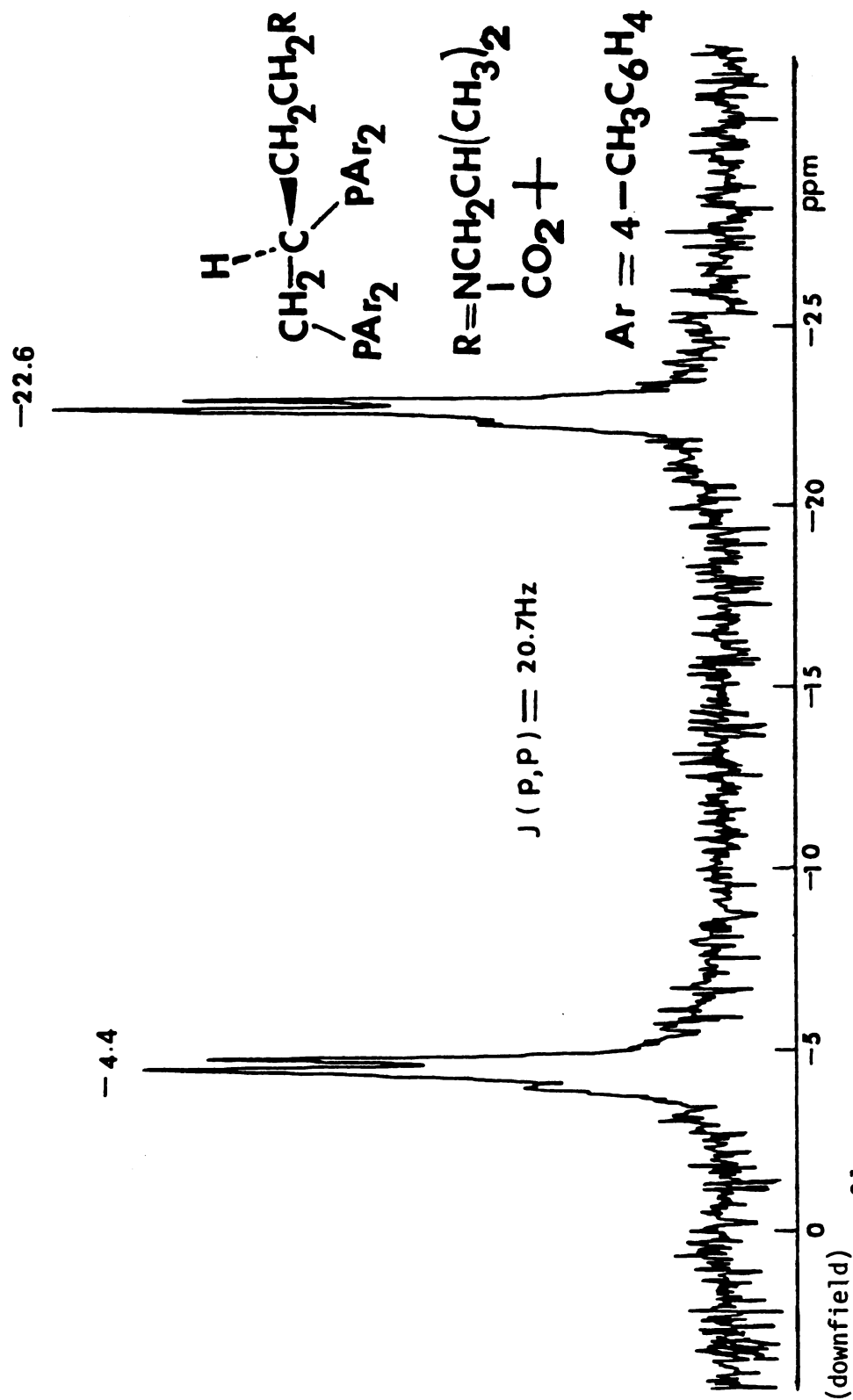


Figure 21. <sup>31</sup>P NMR spectrum of *N*-BOC-butaphos (53) in CDCl<sub>3</sub>, at 0°C

F. The Observed Hydrogenation Rates and Optical Yields in the *N*-BOC-butaphos (53) System

The hydrogenation uptake plots for reduction of *N*-acetyldehydrophenylalanine with homogeneous and intercalated  $[\text{Rh}(\text{NBD})\text{-}i\text{N}\text{-BOC-butaphos (53)}]^+$  catalysts are shown in figure 22 . The observed rates for hydrogenation of dehydroamino acids with homogeneous and intercalated  $[\text{Rh}(\text{NBD})\text{-}i\text{N}\text{-BOC-butaphos (53)}]^+$  catalysts are shown in Table 34 . The hydrogenation rates with homogeneous catalyst in THF were 2 - 3.6 as fast as those observed in 95% ethanol. The hydrogenation rates with intercalated catalyst were 0.09 to 0.55 as fast as those with the homogeneous analogue in 95% EtOH.

The results of asymmetric hydrogenation of (*Z*)-dehydroamino acids with homogeneous  $[\text{Rh}(\text{NBD})\text{-}i\text{N}\text{-BOC-butaphos (53)}]^+$  catalyst in different solvents at ambient temperature and pressure are shown in Table 35. In the 95% EtOH solvent system, the optical yields of the corresponding (*S*)- $\alpha$ -amino acids obtained with this catalyst were around 85 - 96%. The optical yields of *N*-acetylphenylalanine, *N*-benzoylphenylalanine and *N,O*-diacetyltyrosine and DOPA were around 85%. The optical yield of *N*-benzoylphenylalanine ethyl ester was 96%. In the dry THF solvent system the optical yields of the corresponding (*S*)- $\alpha$ -amino acids were around 90-96%. The optical yields of *N*-acetylphenylalanine and *N*-benzoylphenylalanine ethyl ester were around 96%. The optical yields of *N,O*-diacetyltyrosine and DOPA were

Figure 22. Hydrogen uptake plots for reduction of 5 mmol of *N*-acetyldehydrophenylalanine in 30 mL solvent at 25°C and 740 torr with  $[\text{Rh}(\text{NBD}) \text{ } N\text{-BOC-butaphos (53)}]^+$  as the catalyst precursor. (A) Homogeneous catalyst in THF (B) Homogeneous catalyst in 95% ethanol (C) Intercalated catalyst in 95% ethanol. In each case, the amount of rhodium complex used was 0.03 mmol.



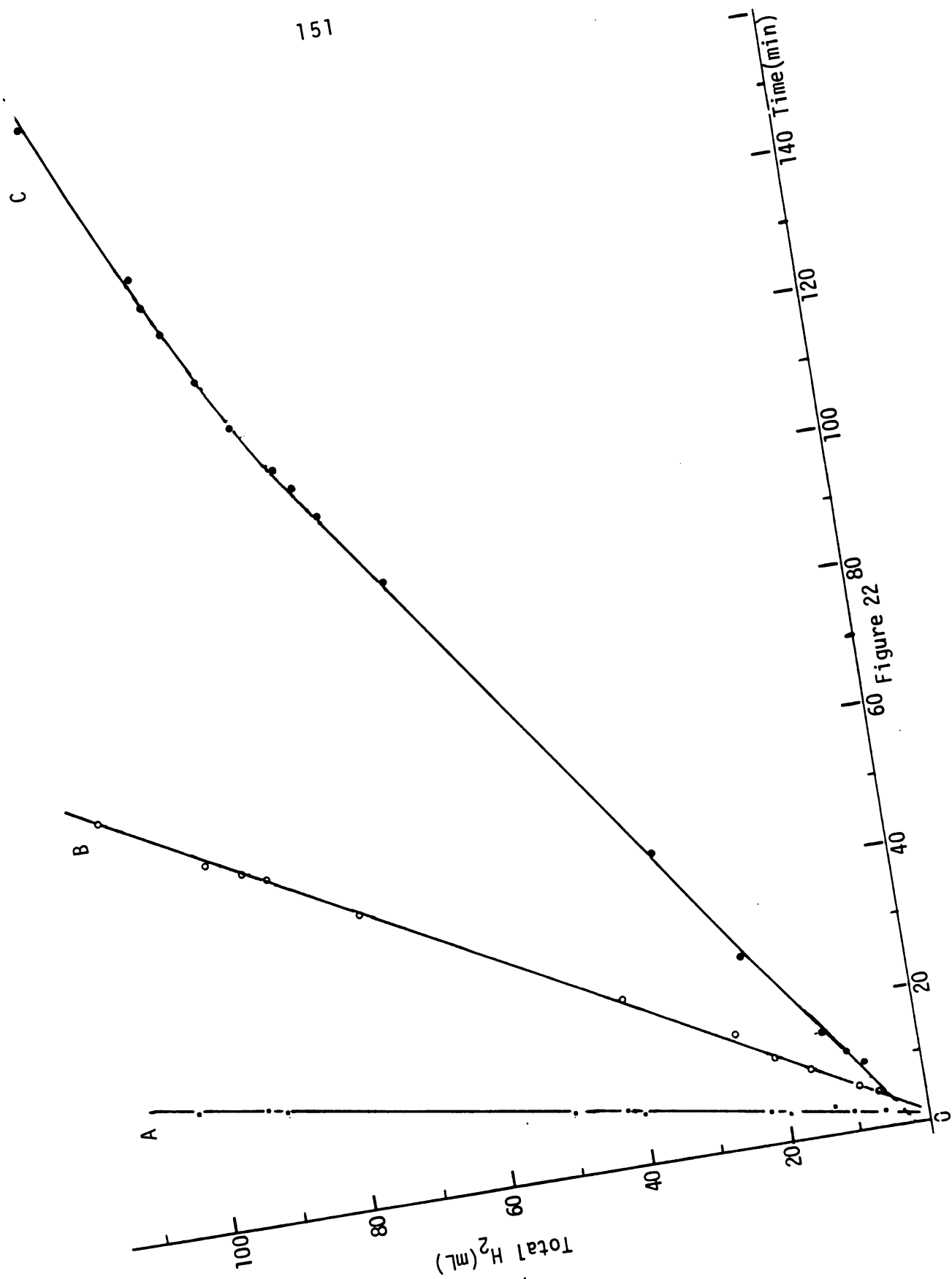
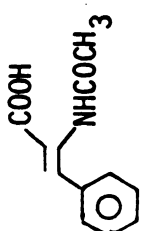
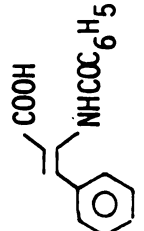
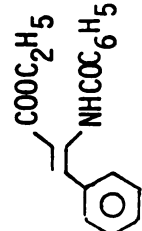
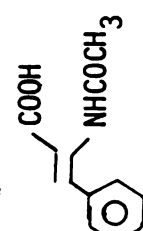
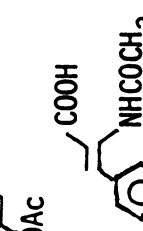
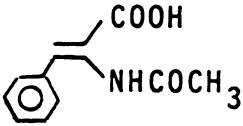
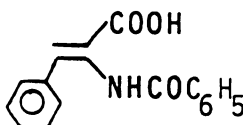
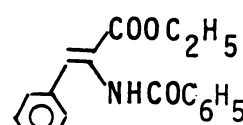
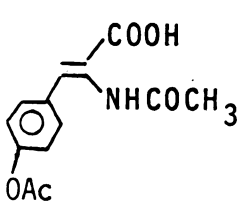
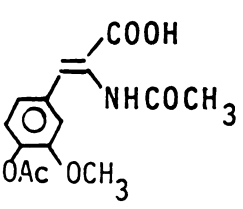


Table 34. Hydrogenation Rates for Intercalated  $[\text{Rh}(\text{NBD}) \text{N}-\text{R}(\text{OC}-\text{butaphos} (53)]^+$  Catalyst and Its Homogeneous Analogue

Substrate	THF Homogen.	Hydrogen Rates (ml $\text{H}_2$ /min/mmol Rh) <sup>a</sup>		
		Intercal.	Homogen.	Relative Rate
	188	23.0	63.0	0.37
	—	14.8	36.0	0.41
	38.1	10.3	18.6	0.55
	133	—	36.5	—
	103	3.0	32.2	0.09

<sup>a</sup> The reaction conditions are the same as those given in Tables 35 and 36.

Table 35 . Asymmetric Hydrogenation of Dehydroamino Acids with Homogeneous  $[\text{Rh}(\text{NBD})\text{N-BOC-butaphos} (53)]^+$  Catalyst

<u>Substrate</u>	<u>Amino acid</u>	<u>— Optical Yield (%)<sup>a</sup> —</u>	
		<u>95% EtOH</u>	<u>THF</u>
	L-Phenylalanine	86	95
	L-Phenylalanine	86	—
	L-Phenylalanine	94	96
	L-Tyrosine	85	90
	L- DOPA	86	91

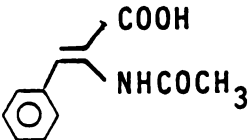
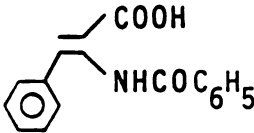
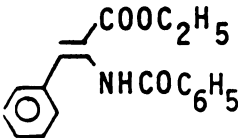
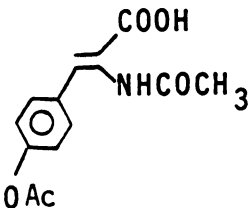
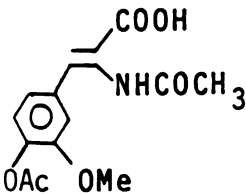
<sup>a</sup>The hydrogenations were carried out in 30 mL of 95% EtOH or THF on 4-5 mmol of substrates at 25°C and 740 torr. The concentrations of the homogeneous catalyst were  $1.0 \times 10^{-3}$  M. All the corresponding amino acids had (S)-configurations.

90%. The catalyst was more efficient and gave better optical yields in THF than in 95% EtOH.

The results of asymmetric hydrogenation of (Z)-dehydro-amino acids with intercalated and homogeneous  $[\text{Rh}(\text{NBD})\text{-}N\text{-BOC-butaphos (53)}]^+$  catalysts in 95% EtOH are shown in Table 36. The optical yields obtained with intercalated catalyst were comparable to or even better than those obtained with the homogeneous catalyst. With the intercalated  $[\text{Rh}(\text{NBD})\text{-}N\text{-BOC-butaphos (53)}]^+$  catalyst the optical yields of *N*-acetylphenylalanine and L-DOPA were better than the homogeneous results. The optical yields of *N*-benzoylphenylalanine and *N*-benzoylphenylalanine ethyl ester were the same as the homogeneous results.

(R)-Prophos (6) has proved to be a highly effective ligand for asymmetric hydrogenation of dehydroamino acids.<sup>10</sup> The optical yields of the corresponding amino acids obtained with homogeneous  $[\text{Rh}(\text{NBD})(\text{R})\text{-Prophos (6)}]^+$  catalyst were around  $90 \pm 3\%$  in THF and 95% EtOH.<sup>10</sup> The optical yields appear to be less sensitive to the nature of the substituent on the substrate and the solvent.<sup>10</sup> *N*-BOC-butaphos (53) and (R)-Prophos (6) are analogues. As with R-Prophos (6), *N*-BOC-butaphos (53) is an effective ligand, giving high optical yields (85-96%). However, the optical yields obtained with  $[\text{Rh}(\text{NBD})\text{-}N\text{-BOC-butaphos (53)}]^+$  catalyst are varied by changing the solvent. In the protic solvent (95% ethanol) the amide carbonyl group of the ligand

Table 36 . Asymmetric Hydrogenation of Dehydroamino Acids with Intercalated and Homogeneous  $[\text{Rh}(\text{NBD})N\text{-BOC-butaphos} (53)]^+$  Catalysts

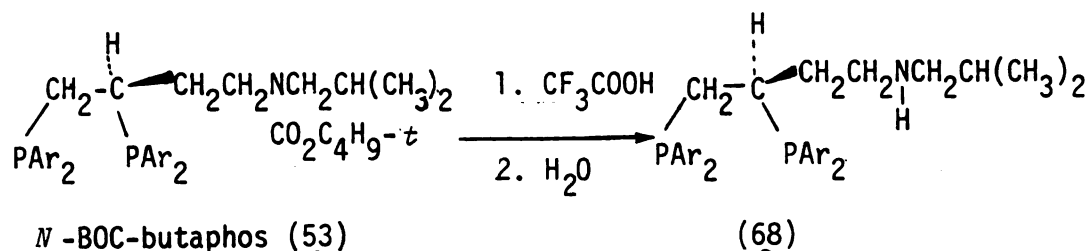
<u>Substrate</u>	<u>Amino acid</u>	<u>Optical Yield(%)<sup>a</sup></u>	
		<u>Intercal.</u>	<u>Homogen.</u>
	L-Phenylalanine	93	86
	L-Phenylalanine	86	86
	L-Phenylalanine	94	94
	L-Tyrosine	—	85
	L-DOPA	89	86

<sup>a</sup>The hydrogenations were carried out in 30 mL of 95% EtOH on 4-5 mmol of substrates at 25°C and 740 torr. The concentrations of intercalated and homogeneous catalysts were around  $1.0 \times 10^{-3}$  M. All the corresponding amino acids had (S)-configurations.

may form intermolecular hydrogen bonds with the solvent or intramolecular hydrogen bonds with the rhodium enamide complex during the asymmetric hydrogenation cycle. The intramolecular hydrogen bonding interactions may lead to low stereoselection of dehydroamino acids and reduce optical yields. However, the possibilities of forming intramolecular hydrogen bonding was low. The optical yields of the corresponding amino acids were only 3 - 6% lower than those obtained with homogeneous  $[\text{Rh}(\text{NBD})(\text{R})\text{-Propphos (6)}]^+$  catalyst in 95% EtOH. With *N*-benzoyldehydrophenylalanine ethyl ester intramolecular hydrogen bonding between the ligand amide carbonyl and the substrate is not possible. A high optical yield was obtained (96%). With the aprotic solvent THF, intra- and inter-molecular hydrogen bonding are not possible. The possibility of intramolecular interactions between amide carbonyl and rhodium intermediates could be eliminated and high optical yields could be achieved.

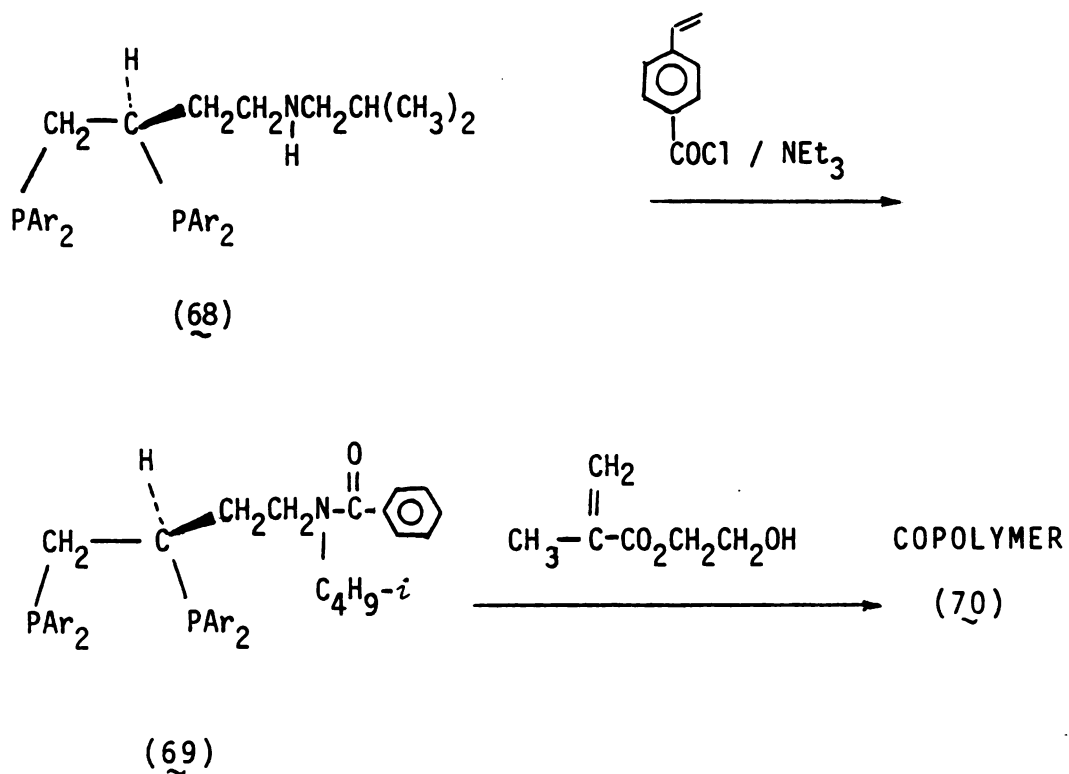
### Suggested Future Work

Two flexible type chiral diphosphine ligands, DIOP (3) and BPPM (23) have been attached to gel type copolymers.<sup>33,34</sup> In general, the optical yields afforded by the supported catalysts were lower than their homogeneous analogues. DIOP (3) and BPPM (23) were also attached to modified gel type copolymers containing chiral alcohol sites.<sup>35,65</sup> The findings indicated that the solvent-polymer interactions dominated the effects of the additional chiral centers.<sup>35,65</sup> The *N*-BOC-butaphos (53) is a rigid type ligand and provides high optical yields for asymmetric homogeneous hydrogenation of (*Z*)-dehydroamino acids. The ligand is less sensitive to the solvent. In the light of these advantages, *N*-BOC-butaphos (52) may provide superior immobilization systems for attaching the ligand to polymeric, inorganic or organic carriers. Below are two possible routes for attachment of the *N*-BOC-butaphos (53) to polymer and glass. First, removal of the protecting BOC group of *N*-BOC-butaphos (52) by treatment with CF<sub>3</sub>COOH should produce the 4-isobutyl-1,2-bis(di-4-methylphenylphosphino)butane [ aminobutaphos (68)] Scheme 30 .



(Scheme 30 )

Scheme 31 proposes a route to attach the ligand to a polymer support. The aminobutaphos (68) is treated with 4-vinylbenzoyl chloride to produce the monomer (69). The monomer (69) is copolymerized with 2-hydroxyethyl methacrylate to form the gel type copolymerized ligand (70). The copolymerized ligand (70) is allowed to react with rhodium precursor to form the supported catalyst precursor.

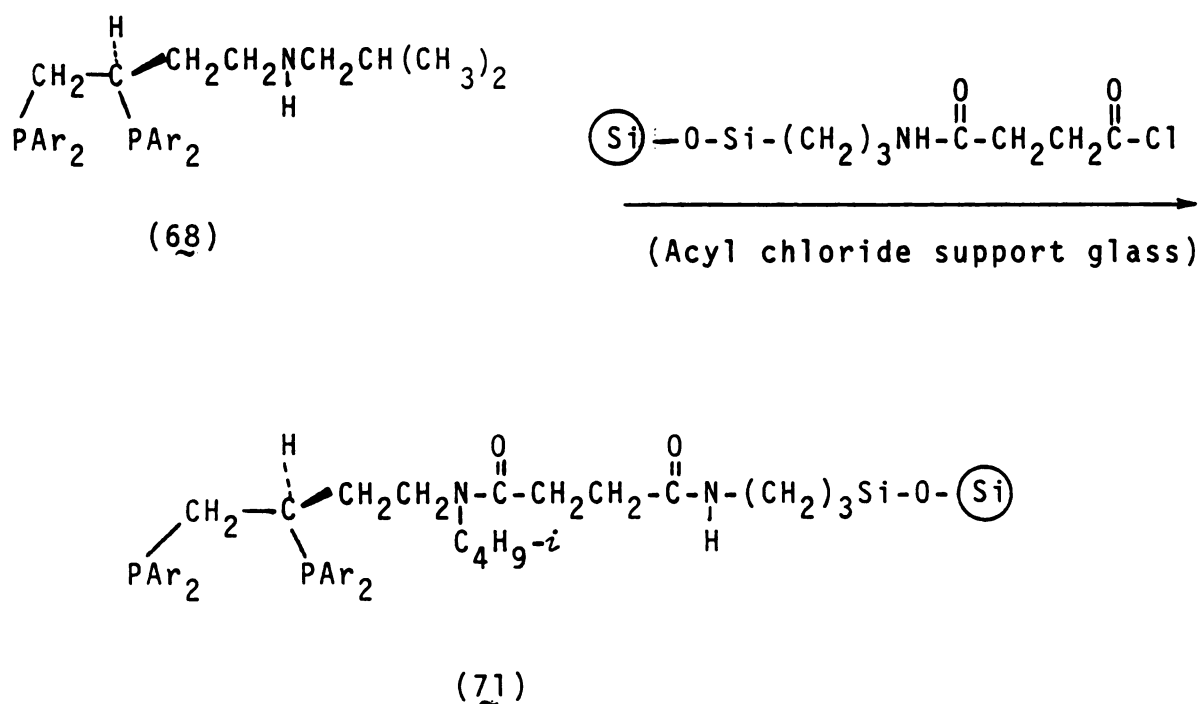


Scheme 31

Scheme 32 shows the route for the attachment of the *N*-BOC-butaphos (53) to glass. The aminobutaphos (68) is coupled with an acyl chloride functionalized glass to form glass



supported aminobutaphos (71). The glass supported aminobutaphos (71) is allowed to react with rhodium precursor to form the supported catalyst precursor. The glass support has a covalently attached aliphatic group terminating in an active carboxyl group. The 10 Å length of the extension arm should be long enough to permit immobilization of bulky aminobutaphos (68).



Scheme 32

## EXPERIMENTAL

### A. General

Manipulations involving air-sensitive materials were performed either under argon by Schlenk techniques or in a nitrogen filled glove box. Melting points were determined in capillary tubes and were uncorrected. Optical rotations were recorded with a Perkin-Elmer 141 automatic polarimeter and a 10-cm path length micro-cell.  $^1\text{H}$  NMR spectra were obtained with a Varian T60 or Bruker WH-250 spectrometer.  $^{31}\text{P}$  NMR measurements were obtained with a Bruker WH-180 spectrometer operating at a field of 4.23 Tesla and a frequency of 72.88 MHz in the pulsed Fourier Transform mode. The  $^{31}\text{P}$  NMR spectra were calibrated in parts per million ( $\delta$ ) downfield from 85%  $\text{H}_3\text{PO}_4$  as an external standard. All spectra were proton decoupled.  $^{13}\text{C}$  NMR spectra were performed with a Varian CFT-20 spectrometer operating at a field of 1.868 Tesla and a frequency of 20 MHz. The  $^{13}\text{C}$  NMR spectra were calibrated in parts per million ( $\delta$ ) downfield from tetramethylsilane as an internal standard. All spectra were proton decoupled. Infrared spectra were obtained with a Perkin-Elmer 237B spectrometer. The infrared spectrometer was calibrated with polystyrene. Mass spectra (MS) were obtained with a Finnigan 4000 GC/MS spectrometer.

High resolution mass spectra were obtained with a Varian CH5 double focusing mass spectrometer; NIH/M.S.U. mass spectra facilities. Elemental analyses were done by the Galbraith Laboratories Inc., Knoxville, Tennessee. All solvents used were A.C.S. reagent grade. THF and ether were purified by distillation from lithium aluminum hydride under argon. Cyclohexane was distilled from sodium metal under argon. Pyridine was distilled from barium oxide under argon. Chlorodiphenylphosphine, 1,5-cyclooctadiene, 2,5-norboradiene, 4-hydroxybenzaldehyde, vanillin, dihydropyran, benzylchloride, isobutylamine, di-*tert*-butyl dicarbonate, Pd on activated carbon 10% and *n*-butyl lithium were obtained from Aldrich Chemical Company. (S)-Lactic acid, and L-malic acid were purchased from Sigma Chemical Company. *Text*-butyl alcohol was obtained from Mallinckrodt, Inc. Lithium metal wire 1/8" diameter was purchased from Matheson, Coleman & Bell. Sodium hydride (56.2% dispersion in mineral oil) was obtained from Metal Hydrides Inc. Tris(4-methylphenyl) phosphine was purchased from Strem Chemicals, Inc. Rhodium trichloride hydrate was obtained from Engelhard Minerals & Corporation. Hydrogen (99.999% purity) was purchased from Matheson. SPIPHOS<sup>52</sup> was a gift from Dr. R. A. DeVries. (+)-2,3-*O*-Isopropylidene-2,3-dihydroxy-1,4-bis(diphenylphosphino)butane [DIOP(+)] was purchased from Sigma Chemical Company.

## B. Substrates

1. 2-Acetamido-2-propenoic Acid ( $\alpha$ -Acetamidoacrylic Acid)

This compound was purchased from Aldrich, and the purity was checked by  $^1\text{H}$  NMR, MS and melting point. mp 185-186°C; MS m/e 129 ( $\text{M}^+$ );  $^1\text{H}$  NMR (60 MHz, TMS,  $\text{D}_6$ -DMSO)  $\delta$  = 8.86 (brs, 1H, COOH) 6.17 (s, 1H, olefinic H), 5.63 (s, 1H, olefinic H), 2.0 (s, 1H,  $\text{CH}_3$ ).

2. (Z)-2-Acetamido-3-phenyl-2-propenoic Acid [(Z)- $\alpha$ -Acetamidocinnamic Acid]

This compound was prepared according to the procedure of Herbst and Shemin.<sup>54</sup> mp 192-193°C, MS m/e 205 ( $\text{M}^+$ );  $^1\text{H}$  NMR (60 MHz, TMS,  $\text{D}_6$ -DMSO)  $\delta$  = 9.26 (s, 1H, COOH) 7.7-6.9 (complex m, 6H,  $\text{C}_6\text{H}_5$  and olefinic H), 2.0 (s, 3H,  $\text{CH}_3$ );  $^{13}\text{C}$  NMR (20 MHz, TMS,  $\text{D}_6$ -DMSO)  $\delta$  = 169.7 ( $\text{NHCOCH}_3$ ) 166.7 (COOH), 133.9, 131.6, 129.9, 129.4, 128.8, 127.5, 22.7 ( $\text{NHCOCH}_3$ ).

3. (Z)-2-Benzamido-3-phenyl-2-propenoic Acid [(Z)- $\alpha$ -Benzamidocinnamic Acid]

This compound was prepared by base hydrolysis of the ethyl (Z)- $\alpha$ -benzamidocinnamate according to the procedure of Carter, et al.<sup>55</sup> mp 224-226°C;  $^1\text{H}$  NMR (60 MHz, TMS,  $\text{D}_6$ -DMSO)  $\delta$  = 9.92 (s, 1H, COOH) 8.15-7.8, 7.8-7.05 (complex m, 12 H);  $^{13}\text{C}$  NMR (20 MHz, TMS,  $\text{D}_6$ -DMSO)  $\delta$  = 166.5 ( $\text{NHCOCH}_2\text{C}_6\text{H}_5$ ), 166.3 (COOH), 133.9, 133.8, 133.2, 131.9, 129.9, 129.4, 128.6, 127.8, 127.6.

4. Ethyl (Z)-2-Benzamido-3-phenyl-2-propenoate [Ethyl(Z)- $\alpha$ -Benzamidocinnamate]

This compound was prepared by a slight modification of the procedure described by Carter et al.<sup>55</sup> Azlactone (15 g) was suspended in 80 mL toluene and 10 mL of 1 N sodium ethoxide solution was added in one portion. The azlactone rapidly dissolved and ethyl (Z)- $\alpha$ -benzamido-cinnamate began to separate almost immediately. After 5 minutes an excess of dilute hydrochloric acid was added and the mixture was vigorously shaken. The white solid was collected by filtration, washed with water and petroleum ether and then dried. The crude product was recrystallized from EtOH/H<sub>2</sub>O to give a pure needle-like crystalline product (16.6 g, 94%). mp 148.5-149°C; MS m/e 295 (M<sup>+</sup>); <sup>1</sup>H NMR (60 MHz, TMS, CDCl<sub>3</sub>)  $\delta$  = 7.9 (s, 1H), 7.8-6.9 (complex m, 11H), 4.13 (q, J = 7Hz, 2H, CH<sub>2</sub>), 1.23 (t, J=6Hz, 3H, CH<sub>3</sub>); <sup>13</sup>C NMR (20 MHz, TMS, CDCl<sub>3</sub>)  $\delta$  = 166.3 (NHCO<sub>2</sub>C<sub>6</sub>H<sub>5</sub>), 165.0 (COOH), 133.6, 132.9, 132.4, 132.2, 131.9, 129.9, 129.6, 128.6, 127.8, 127.1, 60.9, (OCH<sub>2</sub>CH<sub>3</sub>), 14.1 (CH<sub>2</sub>CH<sub>3</sub>).

5. (Z)-2-Acetamido-3-(4'-hydroxyphenyl)-2-propenoic Acid [(Z)-Acetamido-4-hydroxycinnamic Acid]

This compound was prepared according to the procedure of Dakin<sup>56</sup>. mp 203-205°C; MS m/e 221 (M<sup>+</sup>); <sup>1</sup>H NMR (60 MHz, TMS, D<sub>6</sub>-DMSO)  $\delta$  = 9.13 (s, 1H, COOH) 7.28 and 6.67 (2d, J=8 Hz, 4H, arom. H), 7.1 (s, 1H, olefinic H), 1.96 (s, 3H, CH<sub>3</sub>). <sup>13</sup>C NMR (20 MHz, TMS, D<sub>6</sub>-DMSO)  $\delta$  = 169.9 (NHCOCH<sub>3</sub>), 167.1 (COOH), 159.0, 133.1, 132.2, 124.9,

124.2, 115.9, 22.9 ( $\text{NHCOCH}_3$ ).

6. (Z)-2-Acetamido-3-(4'-acetoxyphenyl)-2-propenoic Acid  
[(Z)- $\alpha$ -Acetamido-4-acetoxycinnamic Acid]

The azlactone of (Z)- $\alpha$ -acetamido-4-acetoxycinnamic acid was prepared according to the procedure of Dakin.<sup>56</sup> The compound was obtained by hydrolysis of the azlactone in boiling acetone/ $\text{H}_2\text{O}$ , according to the procedure of Herbst and Shemin.<sup>54</sup> mp 224-225°C;  $^1\text{H}$  NMR (60 MHz, TMS,  $\text{D}_6$ -DMSO);  $\delta$  = 9.3 (s, H, COOH) 7.5 and 7.0 (2d, J=8 Hz, 4H, arom. H), 7.06 (s, 1H, olefinic H), 2.13 (s, 3H,  $\text{CH}_3\text{COO}$ ), 1.96 (s, 3H,  $\text{NHCOCH}_3$ ).

7. (Z)-2-Acetamido-3-(3'-methoxy-4'-acetoxyphenyl)-2-propenoic Acid  
[(Z)- $\alpha$ -Acetamido-3-methoxy-4-acetoxycinnamic Acid]

The azlactone of (Z)- $\alpha$ -acetamido-3-methoxy-4-acetoxycinnamic acid was synthesized according to the method described for the azlactone of (Z)- $\alpha$ -benzamidocinnamic acid's derivative<sup>57</sup>. The compound was obtained by hydrolysis of the azlactone in boiling acetone/ $\text{H}_2\text{O}$ , according to the procedure of Herbst and Shemin.<sup>54</sup> mp 206-207°C; MS m/e 294 ( $\text{M}+1$ ), 293 ( $\text{M}^+$ );  $^1\text{H}$  NMR (60 MHz, TMS,  $\text{D}_6$ -DMSO),  $\delta$  = 9.3 (s, 1H, COOH) 7.3-6.9 (complex m, 4H, arom. H and olefinic H), 3.7 (s, 3H,  $\text{OCH}_3$ ), 2.2 (s, 3H,  $\text{CH}_3\text{COO}$ ) 1.93 (s, 3H,  $\text{NHCOCH}_3$ );  $^{13}\text{C}$  NMR (20 MHz, TMS,  $\text{D}_6$ -DMSO)  $\delta$  = 169.4 ( $\text{NHCOCH}_3$ ) 168.5, 166.5 (COOH and  $\text{CH}_3\text{COO}$ ), 150.7, 140.0, 132.6, 130.6, 127.5, 123.0, 122.7, 113.9, 55.8 ( $\text{OCH}_3$ ), 22.5 ( $\text{NHCOCH}_3$ ), 20.4 ( $\text{CH}_3\text{COO}$ ).

### C. Identification of $\alpha$ -Amino Acid Derivatives (Hydrogenated Products)

The products obtained from the hydrogenation reactions were identified by mass spectroscopy and  $^1\text{H}$  and  $^{13}\text{C}$  NMR spectroscopy:

#### 1. N-Acetyl-(S)-phenylalanine

MS m/e 207 ( $\text{M}^+$ );  $^{13}\text{C}$  NMR (20 MHz, TMS,  $\text{D}_6$ -DMSO)  $\delta$  = 173.3 ( $\text{NHCOCH}_3$ ), 169.9 ( $\text{COOH}$ ), 137.9, 129.2, 128.4, 126.6, 53.7 ( $\text{ArCH}_2\text{CH}$ ), 37.1, 22.5 ( $\text{NHCOCH}_3$ ).

#### 2. N-Benzoyl-(S)-phenylalanine

MS m/e 225 ( $\text{M} - 44$ ) $^+$ ;  $^{13}\text{C}$  NMR (20 MHz, TMS,  $\text{D}_6$ -DMSO)  $\delta$  = 173.3 ( $\text{NHCOCH}_2\text{C}_6\text{H}_5$ ), 166.5 ( $\text{COOH}$ ), 138.3, 134.1, 131.4, 129.1, 128.3, 127.4, 126.4, 54.3 ( $\text{ArCH}_2\text{CH}$ ), 36.5

#### 3. N-Benzoyl-(S)-phenylalanine ethyl ester

MS m/e 297 ( $\text{M}^+$ );  $^{13}\text{C}$  NMR (20 MHz, TMS,  $\text{D}_6$ -DMSO)  $\delta$  = 171.7 ( $\text{NHCOCH}_2\text{C}_6\text{H}_5$ ), 166.5 ( $\text{COOH}$ ), 137.7, 133.8, 131.4, 129.1, 128.2, 127.4, 126.4, 60.5 ( $\text{OCH}_2\text{CH}_3$ ), 54.4 ( $\text{ArCH}_2\text{CH}$ ), 36.4, 14.0 ( $\text{CH}_2\text{CH}_3$ ).

#### 4. N-Acetyl-(S)-tyrosine

$^{13}\text{C}$  NMR (20 MHz, TMS,  $\text{D}_6$ -DMSO)  $\delta$  = 173.4 ( $\text{NHCOCH}_3$ ), 169.5 ( $\text{COOH}$ ), 156.1, 130.1, 127.9, 115.2, 54.0 ( $\text{ArCH}_2\text{CH}$ ), 36.3, 22.5 ( $\text{NHCOCH}_3$ ).

#### 5. N-Acetyl-3-(4-acetoxy-3-methoxyphenyl)-(S)-alanine

$^{13}\text{C}$  NMR (20 MHz, TMS,  $\text{D}_6$ -DMSO)  $\delta$  = 173.2 ( $\text{NHCOCH}_3$ ), 169.5, 168.6 ( $\text{COOH}$  and  $\text{CH}_3\text{COO}$ ), 150.5, 138.0, 136.7, 122.4, 121.1, 113.8, 55.7 ( $\text{OCH}_3$ ), 53.5 ( $\text{ArCH}_2\text{CH}$ ), 36.6,

22.4 ( $\text{NHCOCH}_3$ ), 20.4 ( $\text{CH}_3\text{COO}$ ).

D. Preparation of (R)-Prophos (6) and (R)-4-Me-Prophos (49)

1. Preparation of (S)-(-)-1,2-Propenediol Di-*p*-toluene-sulfonate

(S)-Lactic acid (Sigma) was converted to the ditosylate derivative in 93% yield by the procedure previously described.<sup>10</sup> mp 68-69°C; (lit.<sup>10</sup> mp 62°C)  $[\alpha]_{\text{D}}^{26}$  -20.6° (c 1.15,  $\text{CHCl}_3$ ); MS m/e 384 ( $\text{M}^+$ );  $^1\text{H}$  NMR (60 MHz, TMS,  $\text{CDCl}_3$ )  $\delta$  = 7.60 (dd,  $J_1=8$ ,  $J_2=2$  Hz, 4H, *p*- $\text{C}_6\text{H}_4$ ), 7.17 (d,  $J=9$  Hz, 4H, *p*- $\text{C}_6\text{H}_4$ ), 4.63 (m, 1H, CH), 3.90 (d,  $J=6$  Hz, 2H,  $\text{CH}_2$ ), 2.43 (s, 6H, 2 $\text{CH}_3$ ), 1.23 (d,  $J=7$  Hz, 3H,  $\text{CH}_3$ ).

2. Preparation of (R)-(+)-1,2-Bis(diphenylphosphino)propane [(R)-Prophos (6)]

The  $\text{HP}(\text{C}_6\text{H}_5)_2$  could be prepared by reducing<sup>72</sup>  $\text{ClP}(\text{C}_6\text{H}_5)_2$  with  $\text{LiAlH}_4$  in ether or cleaving<sup>73</sup> triphenylphosphine with lithium metal in THF. This modified method for synthesis of (R)-Prophos (6) was different from Bosnich's report.<sup>10</sup> Only a stoichiometric amount of  $\text{LiP}(\text{C}_6\text{H}_5)_2$  was used and the pure product could be easily separated by crystallization from absolute ethanol.

Into a flame-dried, argon-flushed, three-necked, 250-mL flask equipped with a teflon-coated stirring bar, a 50-mL addition funnel and a reflux condenser, and capped with rubber septums was placed dry THF (50 mL) followed by  $(\text{C}_6\text{H}_5)_2\text{PH}^{72}$  (9.33 mL, 53.6 mmol). The mixture was cooled to -5°C and 34.7 mL of 1.6 M *n*-butyllithium (55.52 mmol) in hexane was added by syringe. The resulting orange-red



solution was held at  $-5^{\circ}\text{C}$  for 15 minutes, warmed to room temperature for 1.5 hours, and cooled to  $-5^{\circ}\text{C}$  again.

A solution of (*S*)-(-)-1,2-propanediol-di-*p*-toluene-sulfonate (10.38 g, 26.8 mmol) in 15 mL of dry THF was added dropwise over a 45 minute period to the stirred phosphide solution. The resulting light yellow solution was allowed to stir for 1 hr at room temperature. Deoxygenated water (50 mL) was then added and most of the THF was removed under reduced pressure with a vacuum pump. The aqueous mixture was extracted three times with 40-mL portions of ether. The combined ether extracts were washed with 30 mL water and filtered. Ether was removed from the filtrate under reduced pressure to give an oily residue. The oily residue was taken up in absolute ethanol under argon at  $50^{\circ}\text{C}$ . The solution was allowed to slowly cool to  $25^{\circ}\text{C}$  and then was held at  $5^{\circ}\text{C}$  for 2 days. The crude product (5.7 g) was collected and recrystallized from absolute ethanol to give 4.3 g of pure (*R*)-Prophos (*6*) as small colorless prismatic crystals. mp  $67.5 - 68.5^{\circ}\text{C}$ ,  $[\alpha]_{\text{D}}^{26} 186.0^{\circ}$  (c 1.0, acetone); MS m/e (relative intensity) 412 ( $\text{M}^{+}$ , 3.51), 370 (7.96), 303 (7.19), 262 (16.8), 185 (59.6), 183 (100), 109 (16.5), 108 (23.3).  $^1\text{H}$  NMR (60 MHz, TMS,  $\text{CDCl}_3$ )  $\delta$  = 1.26 (dd,  $J_1=15$ ,  $J_2=6.5$  Hz, 3H,  $\text{CH}_3$ ), 1.84 (m, 1H, CH), 2.26 (m, 2H,  $\text{CH}_2$ ) 7.25 (complex m, 20 H,  $4\text{C}_6\text{H}_5$ ),  $^{31}\text{P}$  NMR ( $\text{CDCl}_3$ , 85%  $\text{H}_3\text{PO}_4$  as external standard, downfield shifts positive),  $\delta$ (ppm) 2.1, -20.2,  $J_{\text{P-P}}=21$  Hz.

### 3. Preparation of Bis(4-methylphenyl)phosphine

Bis(4-methylphenyl)phosphine was obtained from tris-(4-methylphenyl)phosphine by cleavage with lithium metal in tetrahydrofuran, followed by protonation with  $\text{NH}_4\text{Cl}$  and distillation.

A 250-mL, three-necked flask, containing a magnetic stirring bar and fitted with an argon inlet was charged with tris(4-methylphenyl)phosphine (9.34 g, 30.7 mmol) and 100 mL of dry tetrahydrofuran. To the stirred solution was added lithium (177.3 mmol, 36.1 cm of 1/8 inch diameter wire) which was washed with hexane and dried carefully with a paper towel. Lithium wire was added by cutting 3-5 mm segments directly into the center neck of the flask with scissors. A slow argon flow was maintained throughout the addition, which required about 5 minutes. The red solution was allowed to stir for 4 hours and then filtered. The filtrate was treated with 20 mL of deoxygenated water and 3.5 g of  $\text{NH}_4\text{Cl}$ . The mixture was allowed to stir for an additional hour. During this treatment the solution became clear and almost colorless. The solution was extracted with two 25-mL portions of ether and the combined ether layers were washed with two 15-mL portions of saturated aqueous sodium chloride. The ether solution was dried over magnesium sulfate for about 0.5 hours and filtered. The solvent was pumped off under vacuum. The residue was transferred under argon to a small flask for distillation under reduced pressure. The yield was 4.9 g

(74.6%) of bis(4-methylphenyl)phosphine. bp 100-105°C (0.3 torr). It was used within 24 hours without further characterization.

4. Preparation of (R)-(+)-1,2-Bis(di-4'-methyl-phenylphosphino)propane, [(R)-4-Me-Prophos (49)]

To a solution of freshly distilled  $\text{HP}(\text{C}_6\text{H}_4\text{CH}_3)_2$  (4.54 g, 21.2 mmol) dissolved in 35 mL dry THF and cooled to -5°C, a 1.6 M hexane solution of *n*-butyl lithium (13.8 mL, 22.1 mmol) was added dropwise. The resulting orange-red solution was allowed to stir at -5°C for 15 minutes. The solution was warmed to room temperature and then allowed to stir for another 1.0 hour. The mixture was cooled to -5°C again. A solution of (S)-(-)-1,2-propanediol di-*p*-toluenesulfonate (4.04 g, 10.5 mmol) in dry THF (7 mL) was added dropwise over a 30-minute period to the stirred phosphide solution. The resulting light yellow solution was allowed to stir for 1 hour at room temperature. Deoxygenated aqueous ammonium chloride (3.5 g  $\text{NH}_4\text{Cl}$  in 20 mL  $\text{H}_2\text{O}$ ) was then added and most of the THF was removed under reduced pressure. The aqueous mixture was extracted with two 30-mL portions of  $\text{CH}_2\text{Cl}_2$ . The combined  $\text{CH}_2\text{Cl}_2$  extracts were washed with water and dried over anhydrous  $\text{MgSO}_4$  and filtered. Upon concentration of the filtrate under vacuum a crude white precipitate was obtained (3.9 g). The product was crystallized from absolute ethanol/ $\text{CH}_2\text{Cl}_2$  to give (2.3 g, 45%) of pure (R)-4-Me-Prophos (49). mp 129.5-130°C;  $[\alpha]_D^{26}$  172.6° (c 1.0, benzene); MS m/e (relative intensity) 468 ( $\text{M}^+$ , 18.3) 426 (10.42), 345

(14.07), 304 (21.70), 213 (100), 123 (17.95);  $^1\text{H}$  NMR (60 MHz, TMS,  $\text{CDCl}_3$ )  $\delta$  = 1.18, (dd,  $J_1=15.8$ ,  $J_2=6.7$  Hz, 3H,  $\text{CH}_3$ ), 1.78 (m, 1H, CH) 2.17, 2.21, 2.27 (3s, 14H, 4 $\text{CH}_3$ ,  $\text{CH}_2$ ), 6.7-7.3 (complex m, 16H, 4 $\text{C}_6\text{H}_4$ );  $^{31}\text{P}$  NMR (72.88 MHz, 85%  $\text{H}_3\text{PO}_4$  as external standard, downfield shifts positive),  $\delta$ (ppm) 0.3, -22.1  $J_{\text{P-P}}=21$  Hz, ( $\text{CDCl}_3$ , 25°C);

High resolution MS m/e 468.21459

Calcd for  $\text{C}_{31}\text{H}_{34}\text{P}_2$ : 468.21358

Anal. Calcd for  $\text{C}_{31}\text{H}_{34}\text{P}_2$ : C, 79.46; H, 7.31; P, 13.22

Found: C, 79.20; H, 7.36; P, 13.47

#### E. Preparation of the Synthetic Precursor

##### Preparation of 1,2-O-Isopropylidene-1,2-(S)-4-butanetriol [Acetonide-triol (58)]

Acetonide-triol (58) was prepared in 60% overall yield from L-malic acid by known procedures.<sup>71</sup>  $\alpha_{\text{D}}^{25}$  0.600 (neat,  $l=1$  dm);  $^1\text{H}$  NMR (250 MHz, TMS,  $\text{CDCl}_3$ )  $\delta$  = 4.25 (m,  $J=6$  Hz, 1H,  $\text{CH}_2\text{CH-O}$ ), 4.09 (t,  $J=8$  Hz, 1H,  $\text{CHH-CHO}$ ), 3.74 (t,  $J=6$  Hz, 2H,  $\text{CH}_2\text{CH}_2\text{OH}$ ), 3.58 (t,  $J=8$  Hz, 1H,  $\text{CHH-CH-O}$ ), 3.37 (brs, 1H, OH), 2.80 (q, 2H,  $\text{CH}_2\text{OH}$ ), 1.41 and 1.36 (2s, 6H, 2 $\text{CH}_3$ ).

#### F. Synthesis of THP-butaphos (51) and (R)-Hydroxylbutaphos (52)

##### 1. Preparation of 4-O-Benzyl-1,2-(S)-4-butanetriol [Benzyl-diol (59)]

Sodium hydride (1.92 g, 45.0 mmol) as a 56.2 wt% mineral oil dispersion, was washed three time with *n*-pentane to

remove the mineral oil, and suspended in 30 mL of toluene. The mixture was allowed to stir under nitrogen while a toluene solution of acetonide-triol (58) (5.48 g, 37.5 mmol) was added dropwise. After the addition was complete (0.5 hours), the mixture was stirred at room temperature for 0.5 hours and benzyl chloride (5.7 g, 45 mmol) was added in one portion. The mixture was heated at reflux for 8 hours, allowed to cool to room temperature, and allowed to stir at room temperature overnight. The mixture was filtered through a bed of Celite which was then washed with ether, and the filtrate was evaporated *in vacuo*. The residue was dissolved in 80 mL of a mixed solution of HAC, THF and H<sub>2</sub>O, (1:1:1) and the solution was heated at 45°C for 2 hours. The solvent was removed *in vacuo* and the residue was coevaporated with ethanol (4 x 20 mL). Kugelrohr distillation (145°C, 0.017 torr) gave 6.18 g (84%) of benzyl-diol (59).  $[\alpha]_D^{25}$  20.0° (c 1.0, MeOH); MS m/e 196 (M<sup>+</sup>); <sup>1</sup>H NMR (250 MHz, TMS, CDCl<sub>3</sub>)  $\delta$  = 7.3 (s, 5H, C<sub>6</sub>H<sub>5</sub>), 4.47 (s, 2H, CH<sub>2</sub>Ar), 4.05-3.75, 3.35-3.57 (br, 5H, CHO, 2 OH, and CH<sub>2</sub>O), 3.6 (br, 2H, CH<sub>2</sub>CH<sub>2</sub>O), 3.42 (br, 2H, CH<sub>2</sub>O), 1.7 (q, J=6 Hz, 2H, CH<sub>2</sub>CH<sub>2</sub>O).

Anal. High resolution MS m/e 196.10965

Calcd for C<sub>11</sub>H<sub>16</sub>O<sub>3</sub>: 196.10995

2. Preparation of 4-*O*-Benzyl-1,2-di-*O*-(*p*-toluenesulfonyl)-1,2-(*S*)-4-butanetriol [Benzylother-ditosylate (60)]

A solution of benzyl-diol (59) (5.7 g, 29.1 mmol) in 5 mL pyridine was added dropwise to a stirred mixture of *p*-toluenesulfonyl chloride (11.4 g, 59.8 mmol) and

pyridine (25 mL) at 0°C over a period of 0.5 hours. The mixture was allowed to stir at 0°C for an additional hour and then was kept in a refrigerator for 48 hours, with occasional shaking. The reaction mixture was diluted with 100 mL ether and washed with cold 1 N HCl aqueous solution until the washings were acidic. It was then washed with saturated aqueous NaHCO<sub>3</sub> and H<sub>2</sub>O. The organic layer was dried over anhydrous MgSO<sub>4</sub>. The filtrate was concentrated to give 13.4 g (91%) of benzylether-ditosylate (60), which was used for further reactions without purification. <sup>1</sup>H NMR (60 MHz, TMS, CDCl<sub>3</sub>) δ = 7.7-6.9 (complex m, 13H, arom. H), 5.0-4.53 (m, 1H, CH), 4.24 (s, 2H, CH<sub>2</sub>Ar), 4.05 (d, J=4 Hz, 2H, CH<sub>2</sub>-OTs), 3.34 (t, J=5 Hz, 2H, CH<sub>2</sub>CH<sub>2</sub>O), 2.40 (s, 6H, 2CH<sub>3</sub>), 1.90 (q, J=6 Hz, 2H, CHCH<sub>2</sub>CH<sub>2</sub>).

3. Preparation of 1,2-Di-*o*-(*p*-toluenesulfonyl)-1,2-(*S*)-4-butanetriol [Hydroxylditosylate (61)]

Benzylether-ditosylate (60) (10.1 g, 20 mmol) was dissolved in dioxane (70 mL) containing a few drops of concentrated hydrochloric acid. 10% Pd (0.35 g) on charcoal was added, and the mixture was hydrogenated at 1 atmosphere pressure and 25°C until the hydrogen consumption had ceased (0.49 L). The catalyst was removed by filtration through a bed of Celite. The filtrate was concentrated *in vacuo* to give 8.1 g (98%) of hydroxylditosylate (61). The product was used in further experiments without purification.

<sup>1</sup>H NMR (250 MHz, TMS, CDCl<sub>3</sub>) δ = 7.74, 7.67 (2d, J=8 Hz, 4H, arom. H), 7.33 (d, J=8 Hz, 4H, arom. H), 4.89 (m, 1H,

CH-O), 4.04 (t, 2H,  $\text{CH}_2\text{CH}$ ), 3.65 (t, 2H,  $\text{CH}_2\text{CH}_2$ ), 2.45 (s, 6H, 2 $\text{CH}_3$ ), 1.84 (q, J = 6Hz,  $\text{CH}_2\text{CH}_2\text{OH}$ ).

4. Preparation of 4-O-(2'-Tetrahydropyranyl)-1,2-di-O-(p-toluenesulfonyl)-1,2-(S)-4-butanetriol [THP ether-ditosylate (62)]

Dihydropyran (1.52 g, 18 mmol) and a catalytic amount of p-TsOH (45 mg) were added to a stirred solution of hydroxylditosylate (61) (6.63 g, 16 mmol) in dry ether (100 mL). The reaction mixture was allowed to stir overnight at room temperature. Then it was washed with aqueous  $\text{Na}_2\text{CO}_3$  solution and water. The ether layer was dried over anhydrous  $\text{MgSO}_4$ , filtered and concentrated *in vacuo* at 40°C (0.1 torr) overnight. A product (7.73 g, 97%) of THP ether-ditosylate (62) was obtained and used for phosphination without further purification.  $^1\text{H}$  NMR (250 MHz, TMS,  $\text{CDCl}_3$ )  $\delta$  = 7.8-7.6, 7.4-7.2 (2 complex peaks) 4.87 (br, 1H,  $\text{CHOTs}$ ), 4.5 and 4.33 (2t, 1H,  $\text{CH}_2\text{CHOCH}_2$ ), 4.13 (m, 2H,  $\text{CH}_2\text{OTHP}$ ), 3.74 (m, 2H,  $\text{CH}_2\text{OTs}$ ), 3.6-3.2 (br, 2H,  $\text{OCHOCH}_2$ ) 2.45 (s, 6H, 2 $\text{CH}_3$ ), 1.93 (m, 2H,  $\text{CH}_2\text{CH}_2\text{OTHP}$ ), 1.82-1.23 (br, 6H,  $\text{CH}_2\text{CH}_2\text{CH}_2\text{CH}_2\text{-O}$ ).

5. Preparation of 4-(1'-Tetrahydropyranyloxy)-1,2-(R)-bis(diphenylphosphino)butane [THP-butaphos (51)]

To a solution of 2.79 g (15 mmol) of freshly distilled  $\text{HP}(\text{C}_6\text{H}_5)_2$  dissolved in 15 mL of dry THF and cooled to -5°C a 1.6 M hexane solution of *n*-butyl lithium (9.8 mL, 15.6 mmol) was added dropwise. The resulting orange-red solution was stirred at -5°C for 15 minutes and warmed to room temperature and stirred for another 1.0 hour. The mixture was cooled to -5°C again. A solution of THP ether-ditosylate (62) (3.74 g, 7.5 mmol) in 5 mL dry THF was added dropwise for

over 20 minutes to the stirred phosphide solution. The resulting light yellow solution was stirred for 1 hour at room temperature. Deoxygenated water (15 mL) was then added and most of the THF was removed under reduced pressure. The aqueous mixture was extracted with 2 x 5 mL ether. The combined ether extracts were washed with water and dried over anhydrous  $\text{MgSO}_4$  and filtered. Upon concentration under vacuum, a crude oil product of THP-butaphos (51) was obtained. The purity of the product was confirmed by  $^{31}\text{P}$  NMR and was larger than 90%.  $^{31}\text{P}$  NMR (72.88 MHz, 85%  $\text{H}_3\text{PO}_4$  as external standard, downfield shifts positive), two diastereomers  $\delta(\text{ppm})$  -1.4, -20.1,  $J_{\text{P-P}}=27.6$  Hz;  $\delta(\text{ppm})$  -1.8, -20.5,  $J_{\text{P-P}}=27.6$  Hz, ( $\text{CDCl}_3$ , 25°C).

6. Preparation of 4-Hydroxy-1,2-(R)-bis(diphenylphosphino)butane [(R)-Hydroxylbutaphos (52)]

(R)-Hydroxylbutaphos (52) was obtained by acid hydrolysis of THP-butaphos (51) with a catalytic amount of TsOH in ethanol. THP-butaphos (51) (1.25 g) was dissolved in 10 mL ethanol with a catalytic amount of TsOH (10 mg). The solution was allowed to stir overnight under  $\text{N}_2$  atmosphere. The solution was concentrated *in vacuo* to a small amount and then diluted with ether (10 mL). The solution was washed with aqueous  $\text{NaHCO}_3$  and  $\text{H}_2\text{O}$ . Upon concentration under vacuum, a crude, oily product (1.1 g) of (R)-hydroxylbutaphos (52) was obtained.  $^{31}\text{P}$  NMR (72.88 MHz, 85%  $\text{H}_3\text{PO}_4$  as external standard, downfield shifts positive)  $\delta(\text{ppm})$  -1.5, -20.4,  $J_{\text{P-P}}=22.6$  Hz, ( $\text{EtOD}$ , 25°C).



G. Synthesis of *N*-BOC-butaphos (53)1. Preparation of 4-*O*-(*p*-Toluenesulfonyl)-1,2-*O*-isopropylidene-1,2-(*S*)-4-butanetriol [Acetonide-tosylate (63)]

A solution of 1,2-*O*-isopropylidene-1,2-(*S*)-4-butanetriol (58) (11.7 g, 80.0 mmol) in 5 mL pyridine was added dropwise to a stirred mixture of *p*-toluenesulfonyl chloride (15.9 g, 83.2 mmol) and pyridine (50 mL) at 0°C over a period of 0.5 hours. The mixture was allowed to stir at 0°C for 1 additional hour, and then it was kept in a refrigerator for 24 hours. The reaction mixture was diluted with 100 mL ether and washed with cold 0.5 N aqueous HCl until the aqueous wash solutions were acidic. It was then washed with saturated aqueous NaHCO<sub>3</sub> and H<sub>2</sub>O. The organic layer was dried over anhydrous MgSO<sub>4</sub>. The filtrate was concentrated to give 19.5 g (81%) of 4-*O*-(*p*-toluenesulfonyl)-1,2-*O*-isopropylidene-1,2-(*S*)-4-butanetriol (63), which was used without further purification for further reaction.

<sup>1</sup>H NMR (60 MHz, TMS, CDCl<sub>3</sub>) δ = 7.70 and 7.25 (A, A', B, B', 4H, arom. H), 4.30-3.70 (m, 4H, 2H<sub>2</sub>C-O), 3.70-3.10 (m, 1H, HC-O), 2.42 (s, 3H, CH<sub>3</sub>), 1.92 (dt, 2H, CH<sub>2</sub>), 1.32 (s, 3H, CH<sub>3</sub>), 1.25 (s, 3H, CH<sub>3</sub>); <sup>1</sup>H NMR (250 MHz, TMS, CDCl<sub>3</sub>) δ = 7.80 and 7.35 (A, A', B, B', 4H, C<sub>6</sub>H<sub>4</sub>), 4.30-4.0 (m, 3H, CH-O, CH<sub>2</sub>OTs), 4.0 (t, J<sub>1,1'</sub>=J<sub>1,2</sub>=8 Hz, CHH'-O), 3.5 (t, J<sub>1,1'</sub>=J<sub>1,2</sub>=8 Hz, CHH'-O), 2.43 (s, 3H, CH<sub>3</sub>), 1.90 (brdt, 2H, CH<sub>2</sub>CH<sub>2</sub>OTs), 1.33 (s, 3H, CH<sub>3</sub>), 1.28 (s, 3H, CH<sub>3</sub>).

2. Preparation of 4-Isobutylamino-1,2-*o*-isopropylidene-1,2-(*S*)-butanediol (64)

4-*o*-(*p*-Toluenesulfonyl)-1,2-*o*-isopropylidene-1,2-(*S*)-4-butanetriol (63) (19.5 g, 64.9 mmol) was dissolved in 120 mL isobutylamine (freshly distilled from  $\text{CaH}_2$ ) and refluxed at 60-70°C for 10 hours. It was allowed to stir overnight at room temperature. The solvent was slowly evaporated under vacuum until crystals formed. Once the crystals formed, evaporation was discontinued. The solution was then diluted with dry ether (60 mL) and filtered. The filtrate was concentrated and distilled at 80°C/0.1 torr to yield 12.2 g (93%) of a light yellow oil.  $\alpha_D^{25}$  3.71 (neat,  $l = 1$  dm);  $^1\text{H}$  NMR (250 MHz, TMS,  $\text{CDCl}_3$ )  $\delta$  = 4.17 (m, 1H,  $\text{CH-O}$ ), 4.07 (t,  $J_{1,1'}=J_{1,2}=8$  Hz, 1H,  $\text{CHH'-O}$ ), 3.55 (t,  $J_{1,1'}=J_{1,2}=8$  Hz, 1H,  $\text{CHH'-O}$ ), 2.75 (m, 2H,  $\text{CH}_2\text{CH}_2\text{NH}$ ), 2.45 (d,  $J=\text{Hz}$ , 2H,  $\text{NHCH}_2\text{CH}$ ), 2.26 (s, 1H, NH), 1.6-1.9 (brm, 3H,  $\text{CH}_2\text{CH}_2\text{NH}$  and  $\text{CH}(\text{CH}_3)_2$ ), 1.42 (s, 3H,  $\text{CH}_3$ ), 1.35 (s, 3H,  $\text{CH}_3$ ), 0.09 (d,  $J=7$  Hz, 6H,  $2\text{CH}_3$ ).

Anal. High resolution MS  $m/e$  201.17156

Calcd for  $\text{C}_{11}\text{H}_{23}\text{NO}_2$ : 201.17288

3. Preparation of 4-Isobutylamino-1,2-(*S*)-butanediol [Aminodiol (65)]

4-Isobutylamino-1,2-*o*-isopropylidene-1,2-(*S*)-butanediol (64) (12.1 g, 60 mmol) was dissolved in 1 N HCl (80 mL) and 120 mL MeOH. The solution was refluxed at 50-70°C for 4-5 hours and stirred overnight at 25°C. The solution was made alkaline by the addition of NaOH (4 g, 100 mmol). After the methanol was removed under vacuum, the aqueous

solution was extracted with ether (3 x 200 mL). The combined ether extracts were dried over anhydrous  $\text{MgSO}_4$  and evaporated under reduced pressure to yield 7.55 g (78%) of a light yellow oil. MS  $m/e$  162 ( $M+1$ )<sup>+</sup>; IR (neat)  $3400\text{ cm}^{-1}$ ;  $^1\text{H}$  NMR (250 MHz, TMS,  $\text{CDCl}_3$ )  $\delta$ =3.8-4.0 (m, 2H, 2 OH), 3.65-3.90 (m, 1H, CH-O), 3.45-3.65 (m,  $J=5\text{ Hz}$ , 2H,  $\text{CH}_2\text{-O}$ ), 2.73-3.00 (m,  $J=7\text{ Hz}$ , 2H,  $\text{CH}_2\text{CH}_2\text{NH}$ ), 2.33-2.53 (m,  $J=7\text{ Hz}$ , 2H,  $\text{NHCH}_2\text{CH}$ ), 1.60-1.84 (m,  $J=7\text{ Hz}$ , 1H,  $\text{CH}(\text{CH}_3)_2$ ), 1.60-1.73 (m,  $J=6\text{ Hz}$ , 2H,  $\text{CH}_2\text{CH}_2\text{NH}$ ), 0.92 (d,  $J=7\text{ Hz}$ , 6H,  $2\text{CH}_3$ ).

4. Preparation of 4-[(*tert*-Butyloxy)carbonyl]-isobutylamino-1,2-(*S*)-butanediol [*N*-BOC-aminodiol (66)]

To a solution of 4-isobutylamino-1,2-(*S*)-butanediol (65) (6.65 g, 41.24 mmol) in 50 mL of *tert*-butyl alcohol at room temperature was added di-*tert*-butyldicarbonate (10.36 g, 47.44 mmol). After the reaction mixture was allowed to stir for 2 hours, excess di-*tert*-butyldicarbonate was quenched by adding in one portion 5 mL  $\text{H}_2\text{O}$  to the solution. After one additional hour, the solution was concentrated at  $40^\circ\text{C}$  and the residue was taken up in ether and re-concentrated to give a light yellow crude product. Kugelrohr distillation ( $145^\circ\text{C}$ , 0.035 torr) gave 10.46 (97%) of *N*-BOC-aminodiol (66);  $[\alpha]_D^{25} 13.5^\circ$  (c 2.0, MeOH); MS  $m/e$  261 ( $M^+$ ); IR (neat)  $3400, 1680\text{ cm}^{-1}$ ;

High resolution MS  $m/e$  261.19633

Calcd for  $\text{C}_{13}\text{H}_{27}\text{NO}_4$ : 261.19401

Anal. Calcd for  $\text{C}_{13}\text{H}_{27}\text{NO}_4$ : C, 59.74; H, 10.41; N, 5.36

Found: C, 59.84; H, 10.32; N, 5.29

5. Preparation of 4-[[(*tert*-Butyloxy)carbonyl]-isobutylamino]-1,2-di-*O*-(*p*-toluenesulfonyl)-1,2-(*S*)-butanediol [*N*-BOC-aminoditosylate (67)]

*N*-BOC-aminodiol (66) (5.33 g, 20.0 mmol) was dissolved in 7 mL of dry pyridine and this solution was then added dropwise over 0.5 hours to an ice cold solution containing *p*-toluenesulfonyl chloride (7.85 g, 41.2 mmol) in 25 mL of dry pyridine. The solution was allowed to stir at 0°C for 1 hour, and then stored in a refrigerator for 48 hours. At this point, the solvent of the mixture was pumped off. The residue was diluted with 100 mL of ether and washed with cold H<sub>2</sub>O (15 mL x 2). The organic layer was dried over MgSO<sub>4</sub>, and filtered. The filtrate was concentrated *in vacuo* to give a chromatographically pure product (10.16 g, 89.1%) of *N*-BOC-aminoditosylate (67) which was used in further experimentation without purification. <sup>1</sup>H NMR (60 MHz, TMS, CDCl<sub>3</sub>) δ = 7.55 and 7.17 (A, A', B, B', 8H, 2C<sub>6</sub>H<sub>4</sub>, 4.5 (m, J=5 Hz, 1H, CH-OTs), 4.0 (d, J=4 Hz, 2H, CH<sub>2</sub>-OTs), 3.0 (tr, J=6 Hz, 2H, CH<sub>2</sub>CH<sub>2</sub>N), 2.83 (d, J=8 Hz, 2H, NCH<sub>2</sub>CH), 2.37 (s, 6H, 2CH<sub>3</sub>), 1.6-2.01 (m, 3H, CH(CH<sub>3</sub>)<sub>2</sub> and CH<sub>2</sub>CH<sub>2</sub>N), 1.4 (s, 9H, 3CH<sub>3</sub>), 0.83 (d, 6H, 2CH<sub>3</sub>).

6. Preparation of 4-[[(*tert*-Butyloxy)carbonyl]-isobutylamino]-1,2-(*R*)-bis(di-4'-methylphenylphosphino)butane [*N*-BOC-butaphos (53)]

Lithium bis(4-methylphenyl)phosphide was generated from *n*-butyl lithium and bis(4-methylphenyl)phosphine. The latter compound was obtained from tris(4-methylphenyl)phosphine by cleavage with lithium metal in THF at room temperature, followed by protonation with NH<sub>4</sub>Cl and distillation.

The secondary phosphine had a boiling point of 100-105°C (0.3 torr). It was used directly without further characterization.

To a solution of freshly distilled bis(4-methylphenyl) phosphine (6.76 g, 31.57 mmol) in 30 mL dry THF and cooled to -5°C a 1.6 M hexane solution of *n*-butyl lithium (20.5 mL, 32.8 mmol) was added dropwise. The resulting orange-red solution was allowed to stir at -5°C for 15 minutes and then was warmed to room temperature for 1.0 hour. The mixture was cooled again to -5°C. A solution of *N*-BOC-amino-ditosylate (67) (8.99 g, 15.78 mmol) in dry THF (8 mL) was added dropwise over a period of 30 minutes to the stirred phosphide solution. The resulting light yellow solution was stirred for 1 hour at room temperature. Deoxygenated water (20 mL) then was added and most of the THF was removed under reduced pressure. The aqueous mixture was extracted with ether (2 x 50 mL). The combined ether extracts were washed with water and dried over anhydrous MgSO<sub>4</sub> and filtered. Upon concentration under vacuum, a crude oil product was obtained. The product was crystallized from 95% ethanol to give 3.92 g of *N*-BOC-butaphos (53) as a monohydrate; mp 89.5-90°C;  $[\alpha]_D^{25}$  56.0° (c 1.0, acetone); MS m/e (relative intensity) 653 (M<sup>+</sup>, 19.9), 426 (78.7), 304 (67.4), 213 (100), 122 (28.9) 57 (94.9); <sup>1</sup>H NMR (250 MHz, TMS, CDCl<sub>3</sub>) δ = 7.0-7.4 (complex m, 16H, 4C<sub>6</sub>H<sub>4</sub>), 3.4-3.15 (m, 2H), 2.8 (m, 2H, CH<sub>2</sub>), 2.25-2.50 (3s, 12H, 4 CH<sub>3</sub>Ar), 2.2 (m, 2H), 1.7-2.0 (m, 4H), 1.4 (s, 9H, C(CH<sub>3</sub>)<sub>3</sub>), 0.8 (d, 6H, 2CH<sub>3</sub>);

$^{31}\text{P}$  NMR (72.88 MHz, 85%  $\text{H}_3\text{PO}_4$  as external standard, down-field shifts positive)  $\delta(\text{ppm})$  -4.4, -22.6,  $J_{\text{P-P}}=20.7$  Hz, ( $\text{CDCl}_3$ ,  $0^\circ\text{C}$ );

High resolution MS  $m/e$  653.35352

Calcd for  $\text{C}_{41}\text{H}_{53}\text{O}_2\text{P}_2\text{N}$ : 653.35517

Anal. Calcd for  $\text{C}_{41}\text{H}_{53}\text{O}_2\text{P}_2\text{N} \cdot \text{H}_2\text{O}$ : C, 73.30; H, 8.25;  
N, 2.08; P, 9.22  
Found: C, 73.27; H, 8.40;  
N, 2.06; P, 8.83

#### H. Hectorite

Naturally occurring  $\text{Na}^+$ -hectorite (California) was obtained from the Baroid Division of National Lead Company. The hectorite was used in a freeze-dried form and with a particle size  $< 2\mu\text{m}$ . Chemical exchange of  $\text{Na}^+$  in the native mineral with 1.0  $\text{M}$   $\text{Cu}(\text{NO}_3)_2$  and subsequent chemical analysis of the mineral for  $\text{Cu}^{2+}$  indicated the cation exchange capacity was 70.0 meg/100 g.

#### I. Catalyst Precursors

##### 1. Preparation of Cationic $[\text{Rh}(\text{NBD})\text{diphos}^*]\text{ClO}_4$ Solution

[Diphos\* = DIOP(+) (3), (R)-Prophos (6), (R)-4-Me-Prophos (49), SPIPHOS (48) or *N*-B $\hat{\text{O}}$ C-butaphos (53)]

$[\text{Rh}(\text{NBD})\text{Cl}]_2^{74}$  (18.44 mg, 0.04 mmol) and  $\text{AgClO}_4$  (16.60 mg, 0.08 mmol) were allowed to react in a mixture of 4 mL  $\text{CH}_2\text{Cl}_2$  and 0.5 mL 95% EtOH or MeOH (0.1%  $\text{H}_2\text{O}$ ) for 15 minutes in a  $\text{N}_2$  glove box. The resulting pale-yellow solution was filtered through a fritted funnel. The funnel

was rinsed with 3 mL  $\text{CH}_2\text{Cl}_2$ . Then the filtrate was added to a solution of diphos\* (0.06 mmol) in 4 mL of 95% EtOH or MeOH (0.1%  $\text{H}_2\text{O}$ ). After 30 minutes, the orange-red solution was concentrated to a small amount (ca. 3 mL) and then diluted to 20 mL with 95% EtOH or MeOH (0.1%  $\text{H}_2\text{O}$ ). The solution was divided into two parts for homogeneous hydrogenation and for preparation of  $[\text{Rh}(\text{NBD})\text{diphos*}]^+-\text{hectorite}$ .

## 2. Preparation of Cationic $[\text{Rh}(\text{COD})(\text{R})\text{-Prophos (6)}]^+\text{ClO}_4$ Solution

The cationic  $[\text{Rh}(\text{COD})(\text{R})\text{-Prophos (6)}]$  solution was prepared by adopting the same method previously described. The precursor  $[\text{Rh}(\text{COD})\text{Cl}]_2^{75}$  was prepared according to the literature method.

## 3. Preparation of $[\text{Rh}(\text{diene})\text{diphos*}]^+-\text{hectorite}$

[Diene: COD or NBD; Diphos\* = DIOP(+) (3), (R)-Prophos (6), (R)-4-Me-Prophos (49), SPIPHOS (48) or *N*-BOC-butaphos (52)]

In a typical experiment, 0.3 g of freeze dried  $\text{Na}^+-\text{hectorite}$  was suspended for an hour in 10 mL 95% EtOH or MeOH (0.1%  $\text{H}_2\text{O}$ ) in a  $\text{N}_2$  glove box. To this slurry was added a 10 mL solution of  $[\text{Rh}(\text{diene})\text{diphos*}]^+\text{ClO}_4$  (0.04 mmol) prepared above. After 1 to 2 hours, the mixture was filtered and washed with the same solvent (3 mL x 4) to remove unexchanged rhodium complex. The  $[\text{Rh}(\text{NBD})\text{diphos*}]^+-\text{hectorite}$  was dried by suction.

Elemental analyses:

$[\text{Rh}(\text{NBD})\text{DIOP}(+) (3)]^+-\text{hectorite}$ , Rh 1.1 wt%;

$[\text{Rh}(\text{NBD})(\text{R})\text{-Prophos (6)}]^+-\text{hectorite}$ , Rh 0.91 wt%.

4. Preparation of Cationic  $[\text{Rh}(\text{NBD})\text{diphos}^*]\text{ClO}_4$  in Solid Form [Diphos\* = (R)-Prophos (6) or (R)-4-Me-Prophos(49)]

$[\text{Rh}(\text{NBD})\text{Cl}]_2$ <sup>74</sup> (13.83 mg, 0.03 mmol) and  $\text{AgClO}_4$  (12.45 mg, 0.06 mmol) were allowed to react in a mixture of 4 mL  $\text{CH}_2\text{Cl}_2$  and 0.5 mL 95% EtOH for 15 minutes in a  $\text{N}_2$  glove box. The resulting pale-yellow solution was filtered through a fritted funnel, and the funnel was rinsed with 3 mL  $\text{CH}_2\text{Cl}_2$ . Then the filtrate was added to a solution of diphos\* (0.06 mmol) in 4 mL of 95% EtOH. After 30 minutes, the solution was concentrated to a small amount under reduced pressure and 4 mL of 95% ethanol was added and the solution was filtered. The fine yellow-orange precipitate was formed by slow evaporation of the ethanol. The orange precipitate was filtered, washed with water and dried *in vacuo*. The yields of  $[\text{Rh}(\text{NBD})(\text{R})\text{-Prophos (6)}]\text{ClO}_4$  and  $[\text{Rh}(\text{NBD})(\text{R})\text{-4-Me-Prophos (49)}]\text{ClO}_4$  were around 90%.  $^{31}\text{P}$  NMR (72.88 MHz, 85%  $\text{H}_3\text{PO}_4$  as external reference; downfield shifts positive)  $\delta$ (ppm);  $[\text{Rh}(\text{NBD})(\text{R})\text{-Prophos (6)}]\text{ClO}_4$ :  $\delta$  = 61.6 (dd,  $J_{\text{Rh-P}}$ =155 Hz), 42.9 (dd,  $J_{\text{Rh-P}}$ =155 Hz,  $J_{\text{P-P}}$ =34 Hz, ( $\text{CDCl}_3$ ,  $-20^\circ\text{C}$ ).  $[\text{Rh}(\text{NBD})(\text{R})\text{-4-Me-Prophos(49)}]\text{ClO}_4$ :  $\delta$  = 60.4 (dd,  $J_{\text{Rh-P}}$ =155 Hz), 41.7 (dd,  $J_{\text{Rh-P}}$ =155 Hz,  $J_{\text{P-P}}$ =35 Hz, ( $\text{CDCl}_3$ ,  $-16^\circ\text{C}$ ).

5. Preparation of  $[\text{Z-ester Rh}(\text{R})\text{-4-Me-Prophos (49)}]^+$  Solution for  $^{31}\text{P}$  NMR

$[\text{Rh}(\text{NBD})(\text{R})\text{-4-Me-Prophos (49)}]\text{ClO}_4$  (31 mg, 0.04 mmol) and an excess of ethyl (Z)- $\alpha$ -benzamido cinnamate (Z-ester) (95 mg, 0.32 mmol) were dissolved in EtOD (4 mL) in a 10 mm NMR tube fitted with a silicon rubber septum. The solution was prepared under  $\text{N}_2$  atmosphere in a  $\text{N}_2$  glove box. The





tube was attached to a vacuum line, evacuated, and hydrogen was admitted at  $-20^{\circ}\text{C}$ . The tube was kept at positive  $\text{H}_2$  pressure until the solution became deep orange-red, then hydrogen was removed by two further freeze-pump-thaw cycles. Finally, the tube was filled with argon.  $^{31}\text{P}$  NMR (72.88 MHz, 85%  $\text{H}_3\text{PO}_4$  as external reference; downfield shifts positive)  $\delta(\text{ppm})$ , 74.9 (dd,  $J_{\text{Rh-P}}=162$  Hz), 46.7 (dd,  $J_{\text{Rh-P}}=155$  Hz),  $J_{\text{P-P}}=46$  Hz; 64.9 (dd,  $J_{\text{Rh-P}}=155$  Hz), 59.7 (dd,  $J_{\text{Rh-P}}=158$  Hz),  $J_{\text{P-P}}=46$  Hz, ( $\text{CH}_3\text{OD}$ ,  $-30^{\circ}\text{C}$ ).

#### J. X-ray Powder Diffraction Measurements

A Phillips X-ray diffractometer with Ni-filtered  $\text{Cu-K}\alpha$  radiation was used to determine  $d(001)$  basal spacing. Film samples of the  $[\text{Rh}(\text{NBD})\text{diphos*}]^+$ -hectorite were prepared by placing solvent suspensions onto glass slides and drying them at room temperature. Diffraction patterns under different conditions of solvation were obtained by allowing the film to equilibrate under the solvent for 30 minutes and then keeping the film wetted while under the X-ray beam. The basal spacings of  $[\text{Rh}(\text{NBD})\text{diphos*}]$ -hectorite complexes [where diphos\* is DIOP(+) (3), (R)-Prophos (6) or (R)-4-Me-Prophos (49)] are shown in Table 37.

Table 37. Basal Spacings of  $[\text{Rh}(\text{NBD})\text{diphos}^*]^+$ -hectorite

Solvent	D(001) ( $\text{\AA}$ )		
	DIOP(+) (3)	(R)-Prophos (6)	(R)-4-Me-Prophos (49)
Air dry	18.3 $\text{\AA}$	17.0 $\text{\AA}$	16.1 $\text{\AA}$
MeOH (0.1% $\text{H}_2\text{O}$ )	19.2 $\text{\AA}^*$	19.6 $\text{\AA}^*$	19.2 $\text{\AA}$
95% EtOH	19.2 $\text{\AA}^*$	19.6 $\text{\AA}^*$	19.2 $\text{\AA}^*$

\*Two orders of reflection were observed.

#### K. Hydrogenation Procedure

The prochiral substrate (4-8 mmol) was weighed into the hydrogenation vessel. The catalyst solution or  $[\text{Rh}(\text{NBD})\text{diphos}^*]^+$ -hectorite and the required 20-30 mL of oxygen-free MeOH (0.1%  $\text{H}_2\text{O}$ ) or 95% EtOH were added to the hydrogenation vessel in a  $\text{N}_2$  glove box. The vessel was attached to a glass vacuum manifold with gas inlets, gas burette, mercury leveling bulb, and mercury manometer. The vessel then was purged by filling and evacuating with purified hydrogen. The hydrogen uptakes were monitored at  $25^\circ\text{C}$  and a total pressure of 740 torr. The hydrogenation rates for rhodium(I) (diphos\*) catalysts with different substrates were presented in Tables 26, 27, 28, 29 and 34 in the Results and Discussion, Chapter 2.

## L. Products Isolation

### 1. General Work-up Procedure in the Hectorite System

After the hydrogenation was completed, the rhodium-hectorite was filtered off and washed thoroughly with 95% ethanol. The filtrate was evaporated *in vacuo* to give the product.

### 2. General Work-up Procedure in the Homogeneous System

#### A. Method I - 95% EtOH or MeOH as a Solvent

After the hydrogenation was completed, 1-2 g of 200-400 mesh Dowex 50W-X2 cation exchange resin in the  $H^+$  form, or 0.3-0.5 g of Na-hectorite was added to the solution (under  $N_2$ ). After the mixture was stirred for 15-30 minutes (resin) or 1-2 hours (Na-hectorite) it was filtered and the resin or clay was washed thoroughly with 95% ethanol. The filtrate was evaporated *in vacuo* to give the product.

#### B. Method II - Tetrahydrofuran as a Solvent

After the hydrogenation was completed, the solvent of the reaction mixture was removed under vacuum to give an oily residue. 5 mL of deoxygenated 95% EtOH was added to the residue and the solvent was removed again. This was repeated two more times to ensure that none of the THF solvent remained. The resulting yellow residue was dissolved in 25 mL deoxygenated 95% EtOH. The work-up procedure was then completed by following Method I.

## M. Chemical Conversions

The chemical conversions were estimated by  $^1H$  NMR. The chemical conversions of the corresponding amino acids

were larger than 97%.

#### N. Optical Yields

All optical rotations of the hydrogenated products were recorded with a Perkin-Elmer 141 automatic polarimeter and a 10 cm pathlength micro-cell. Two measurements were recorded for each sample by preparing two independent solutions. The optical yields were calculated by using the values of specific rotations of pure products which are listed on Table 38.

Table 38. Specific Rotations of Pure Amino Acid Derivatives <sup>a</sup>

Amino Acid Derivative	Specific Rotation
<i>N</i> -Acetyl-( <u>R</u> )-alanine	$[\alpha]_D^{26} +66.3^\circ$ (c 2.0, H <sub>2</sub> O)
<i>N</i> -Acetyl-( <u>S</u> )-phenylalanine	$[\alpha]_D^{26} +46.0^\circ$ (c 1.0, EtOH)
<i>N</i> -Benzoyl-( <u>S</u> )-phenylalanine	$[\alpha]_D^{26} -40.3^\circ$ (c 1.0, MeOH)
<i>N</i> -Benzoyl-( <u>S</u> )-phenylalanine ethyl ester	$[\alpha]_D^{26} -42.7^\circ$ (c 1.0, MeOH)
<i>N</i> -Acetyl-( <u>S</u> )-tyrosine	$[\alpha]_D^{27} +51.5^\circ$ (c 1.0, MeOH)
<i>O,N</i> -Diacetyl-( <u>S</u> )-tyrosine	$[\alpha]_D^{27} +45.5^\circ$ (c 1.5, MeOH)
<i>N</i> -Acetyl-3-(4-acetoxy-3-methoxyphenyl)-( <u>S</u> )-alanine	$[\alpha]_D^{20} +40.7^\circ$ (c 1.0, MeOH)

<sup>a</sup>Data were obtained from reference 9.

## APPENDIX

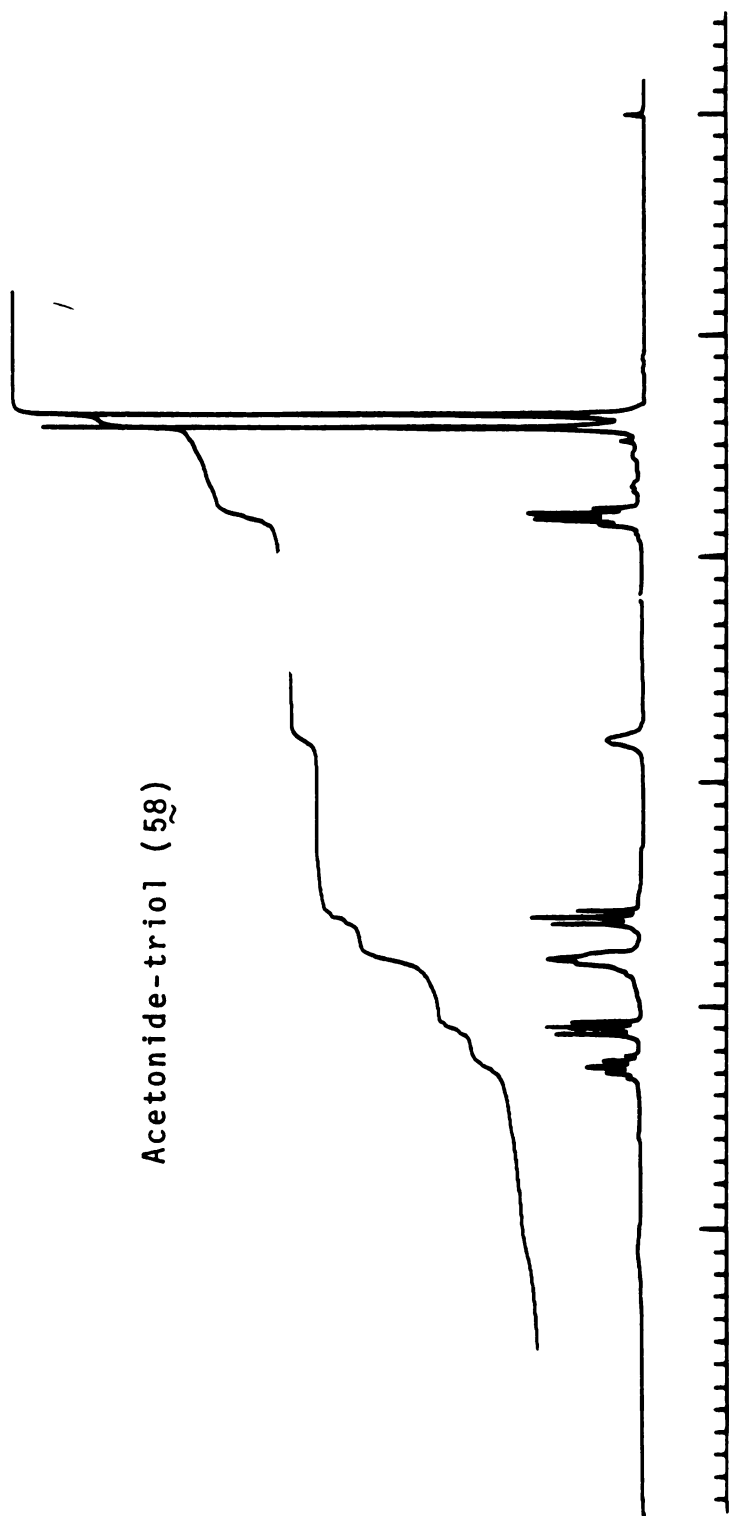
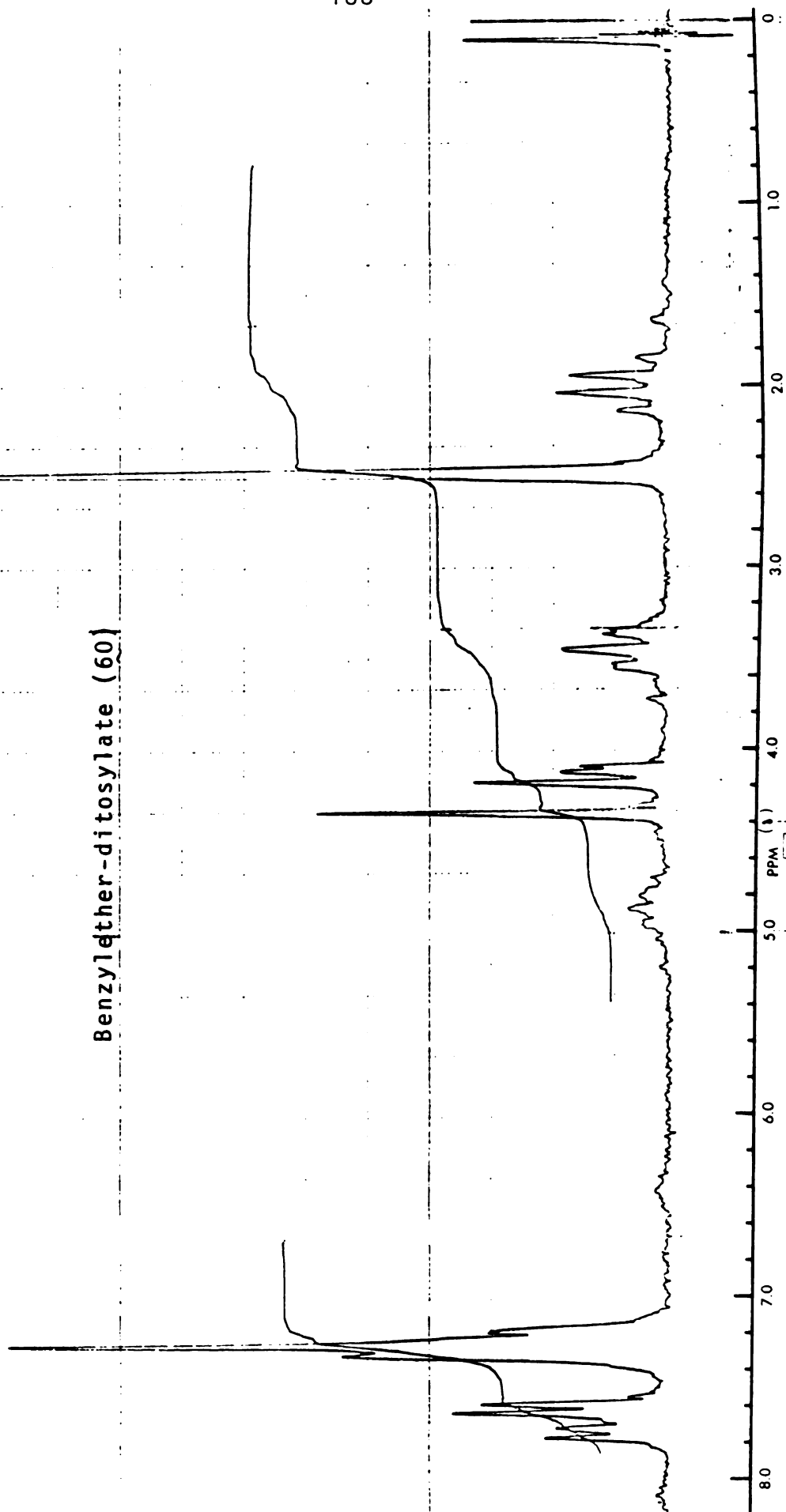


Figure 23.  $^1\text{H}$  NMR spectrum of Acetonide-triol (58) in  $\text{CDCl}_3$ , at  $25^\circ\text{C}$  (250 MHz)

## Benzylether-ditosylate (60)

Figure 24 .  $^1\text{H}$  NMR spectrum of Benzylether-ditosylate (60) in  $\text{CDCl}_3$ , at  $25^\circ\text{C}$  (60 MHz)



## Acetonide-tosylate (63)

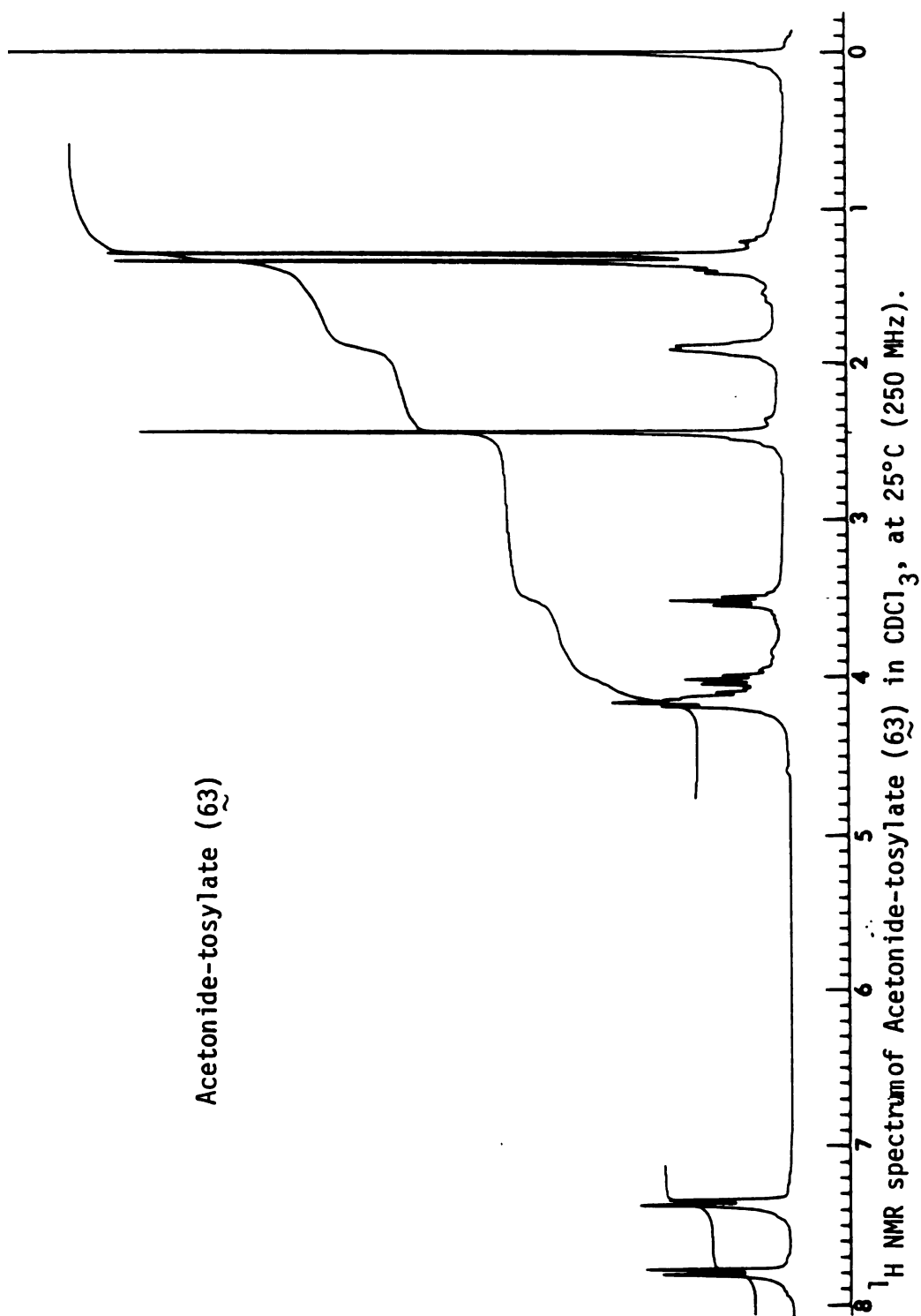


Figure 25.  $^1\text{H}$  NMR spectrum of Acetonide-tosylate (63) in  $\text{CDCl}_3$ , at  $25^\circ\text{C}$  (250 MHz).

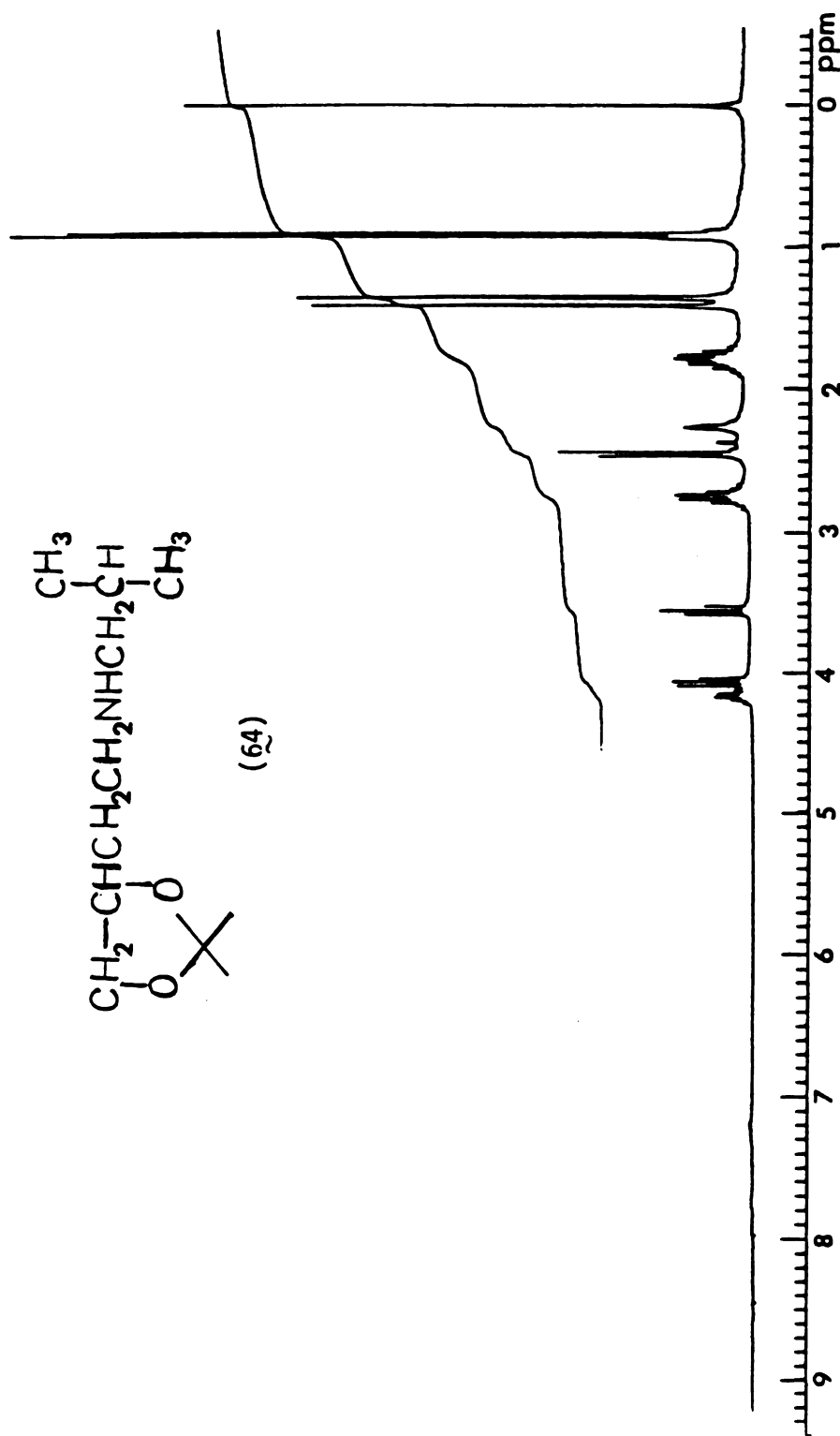


Figure 26.  $^1\text{H}$  NMR spectrum of 4-Iso-butylamino-1,2-*O*-iso-propylidene-1,2-*(S)*-butanediol (64) in  $\text{CDCl}_3$ , at  $25^\circ\text{C}$  (250 MHz).



Aminodiol (65)

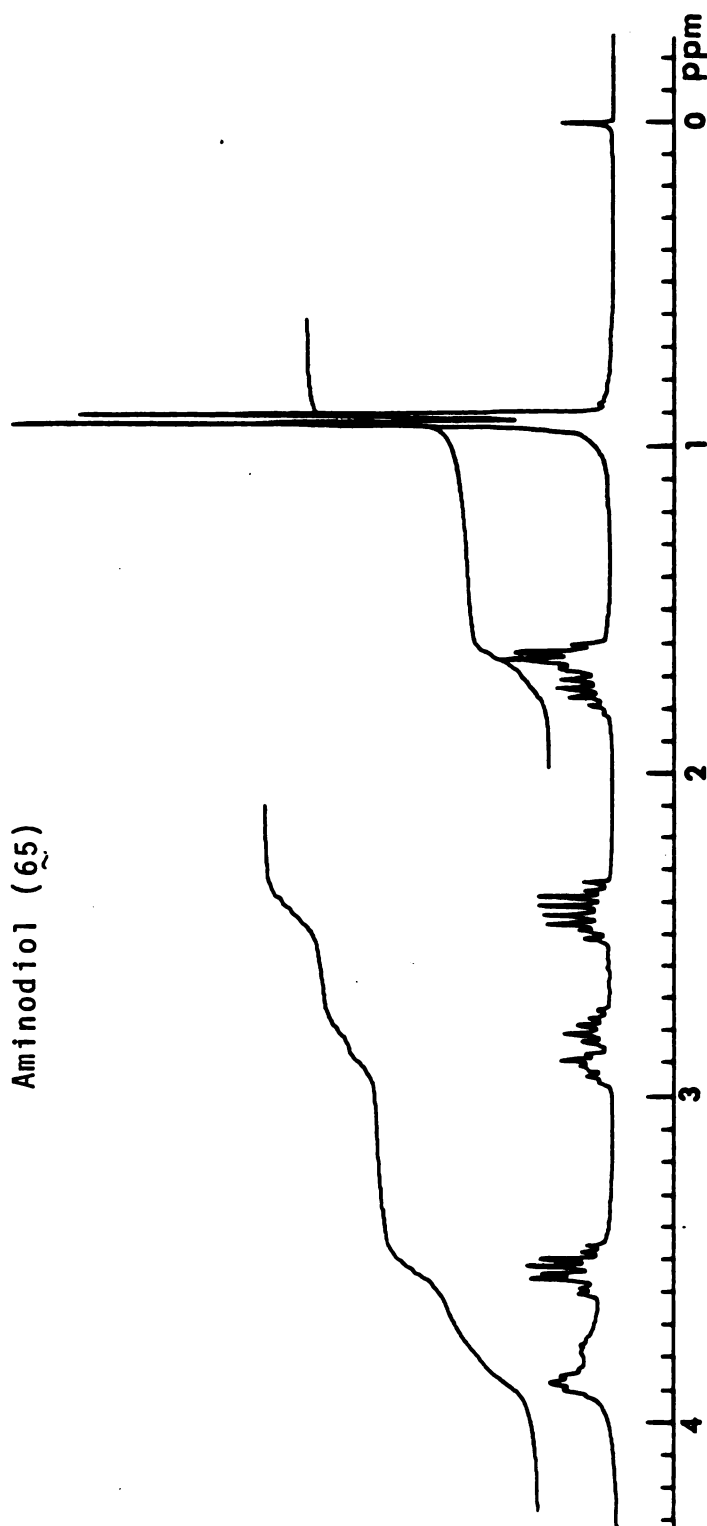


Figure 27.  $^1\text{H}$  NMR spectrum of Aminodiol (65) in  $\text{CDCl}_3$  at  $25^\circ\text{C}$  (250 MHz)

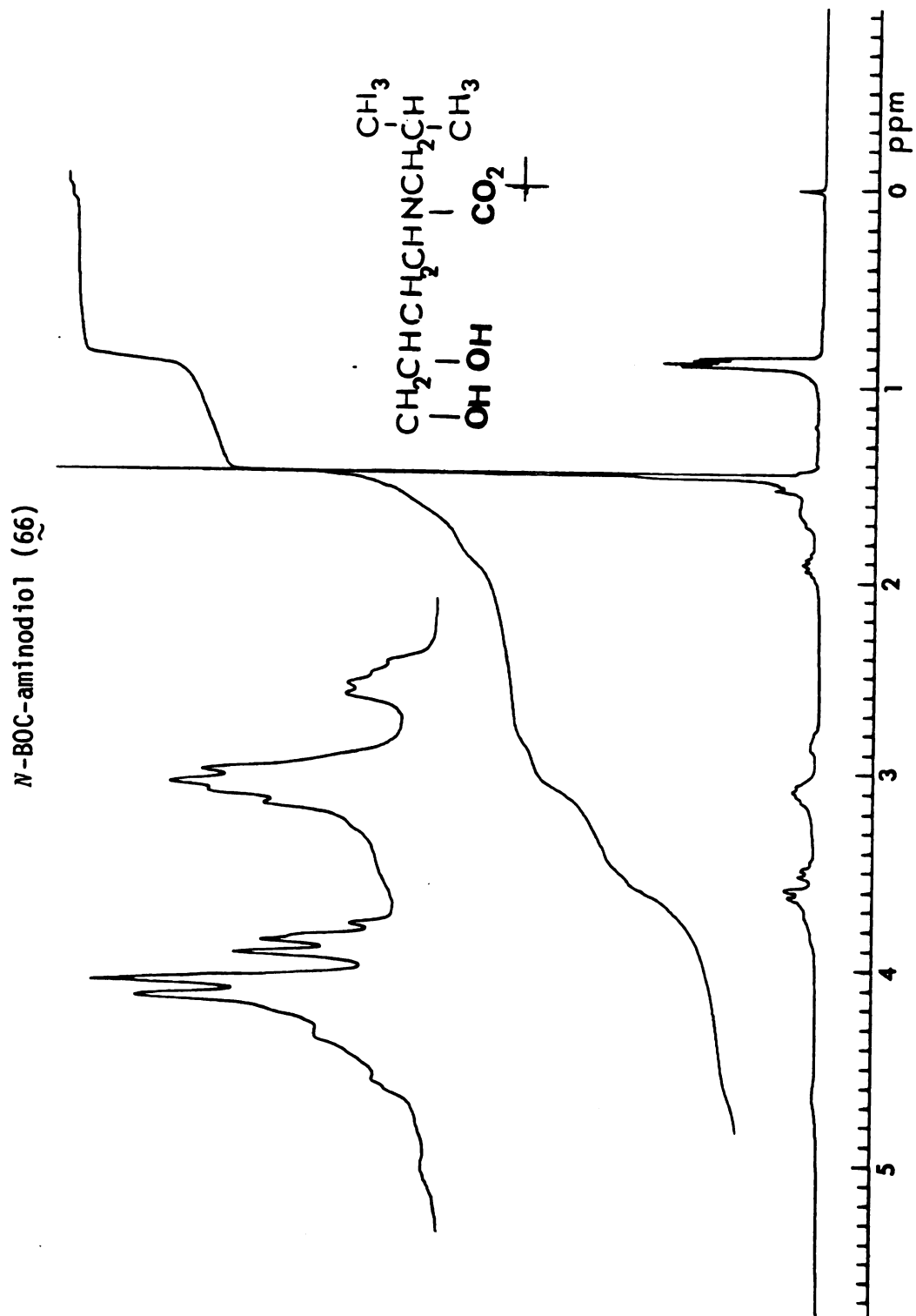


Figure 28.  $^1\text{H}$  NMR spectrum of *N*-BOC-aminodiol (66) in  $\text{CDCl}_3$ , at  $25^\circ\text{C}$  (250 MHz).

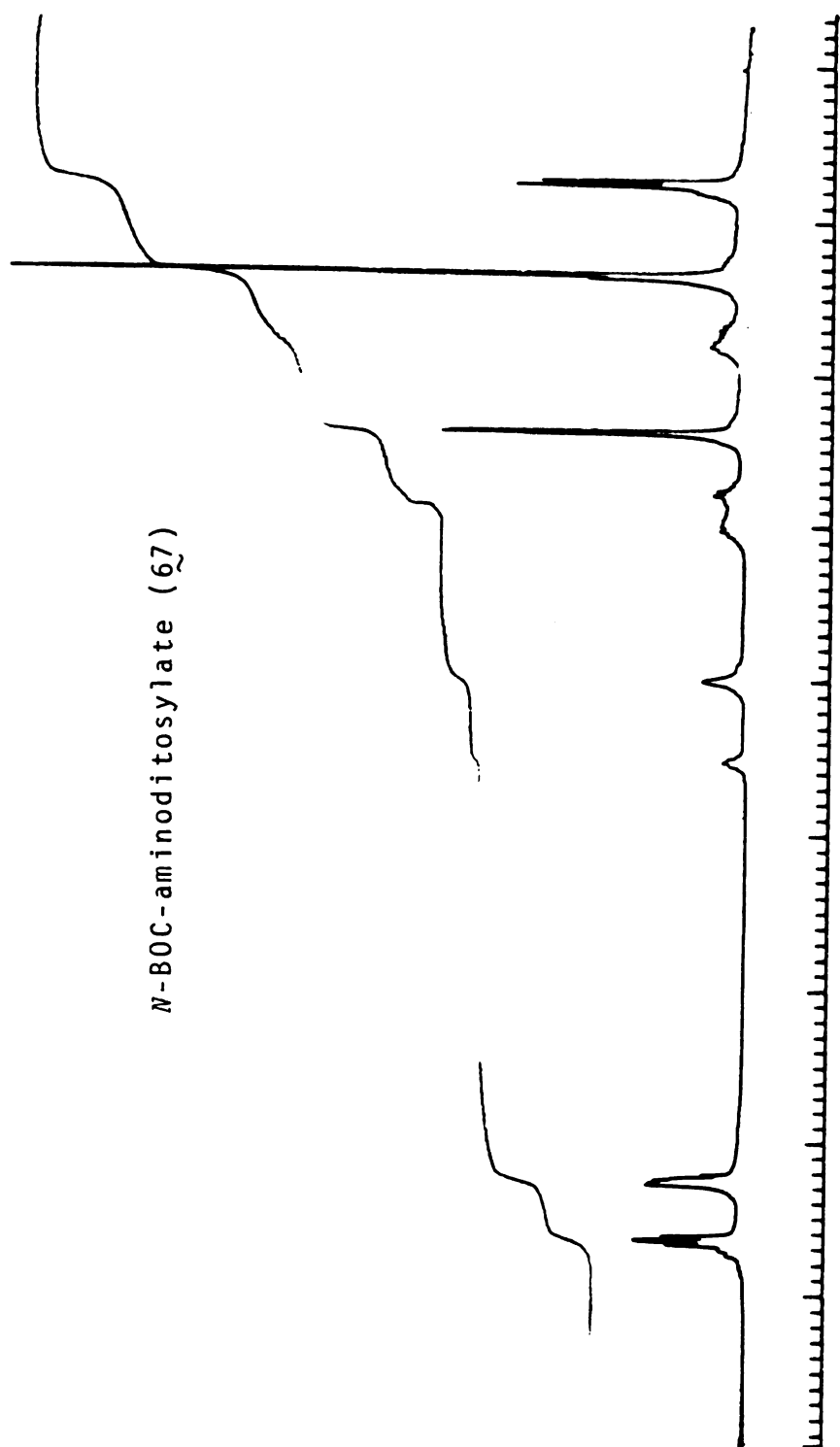


Figure 29.  $^1\text{H}$  NMR spectrum of *N*-BOC-aminoditosylate (67) in  $\text{CDCl}_3$ , at  $25^\circ\text{C}$  (250 MHz)

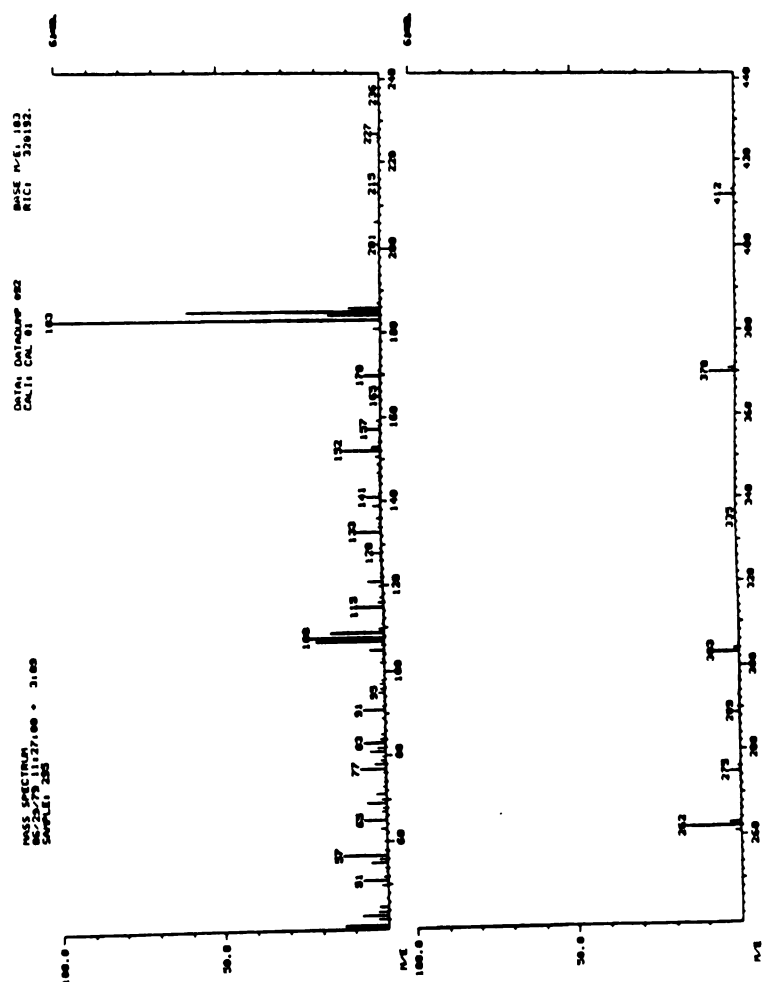


Figure 30 . Mass spectrum of (R)-Prophos (6)

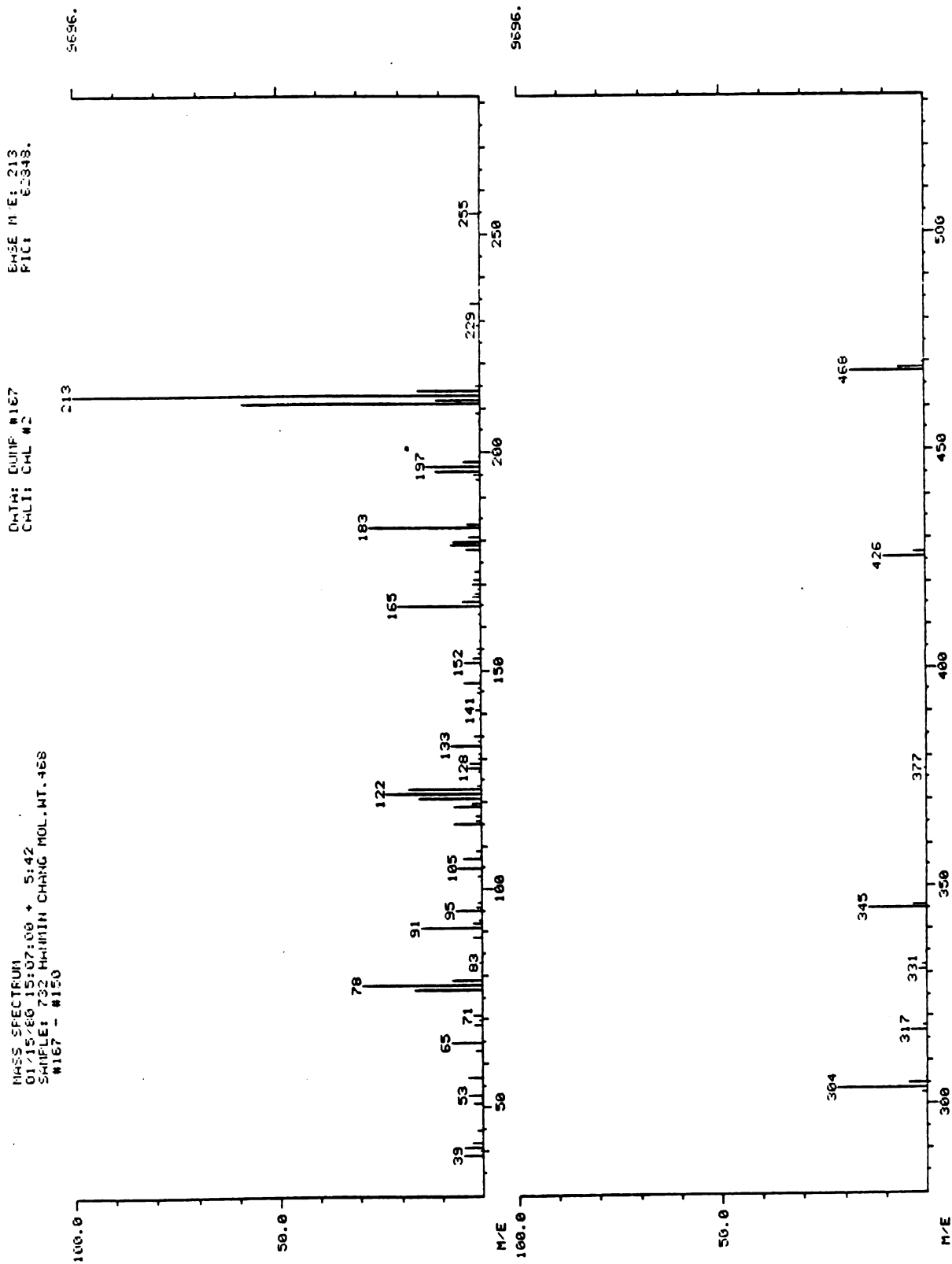
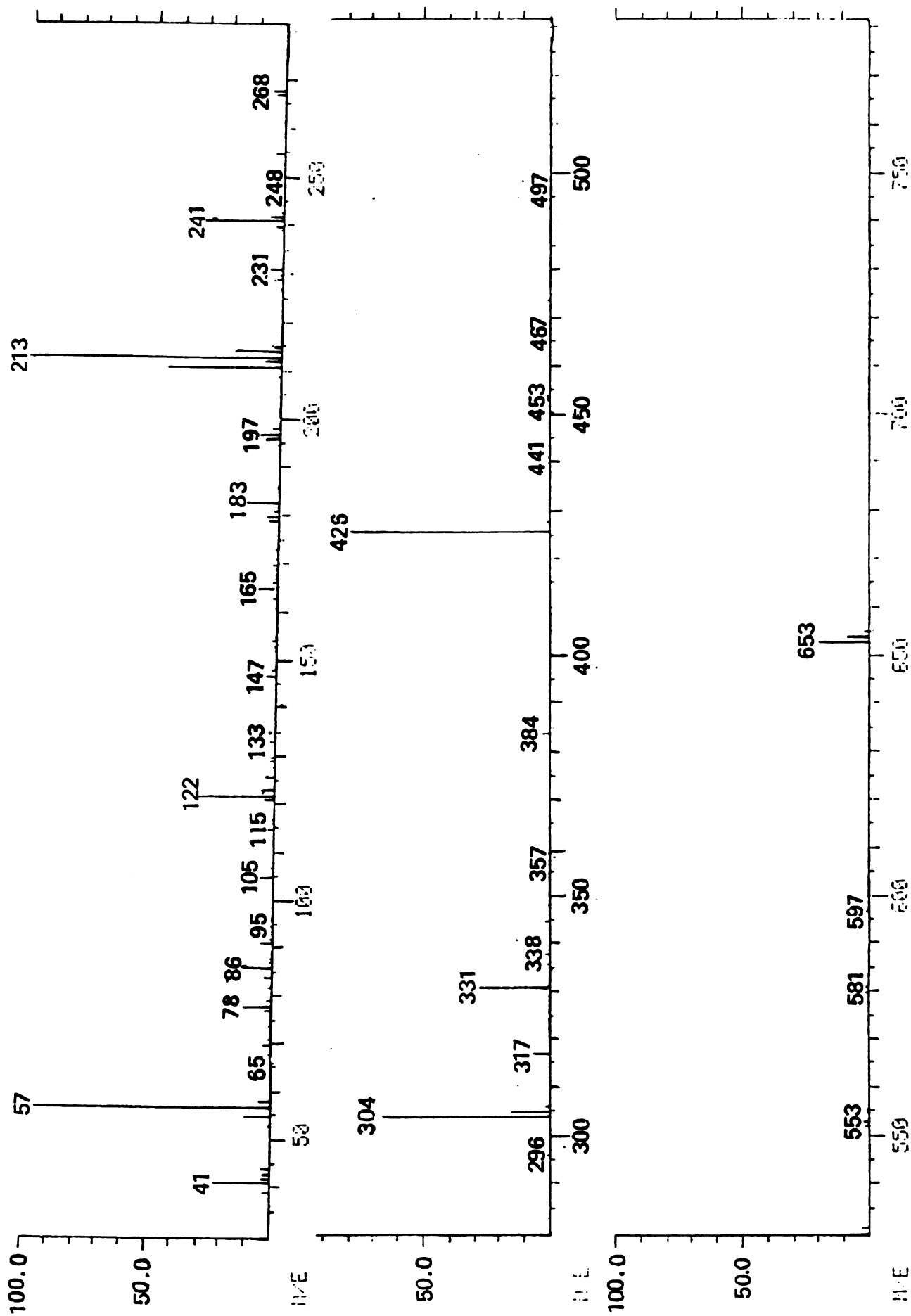
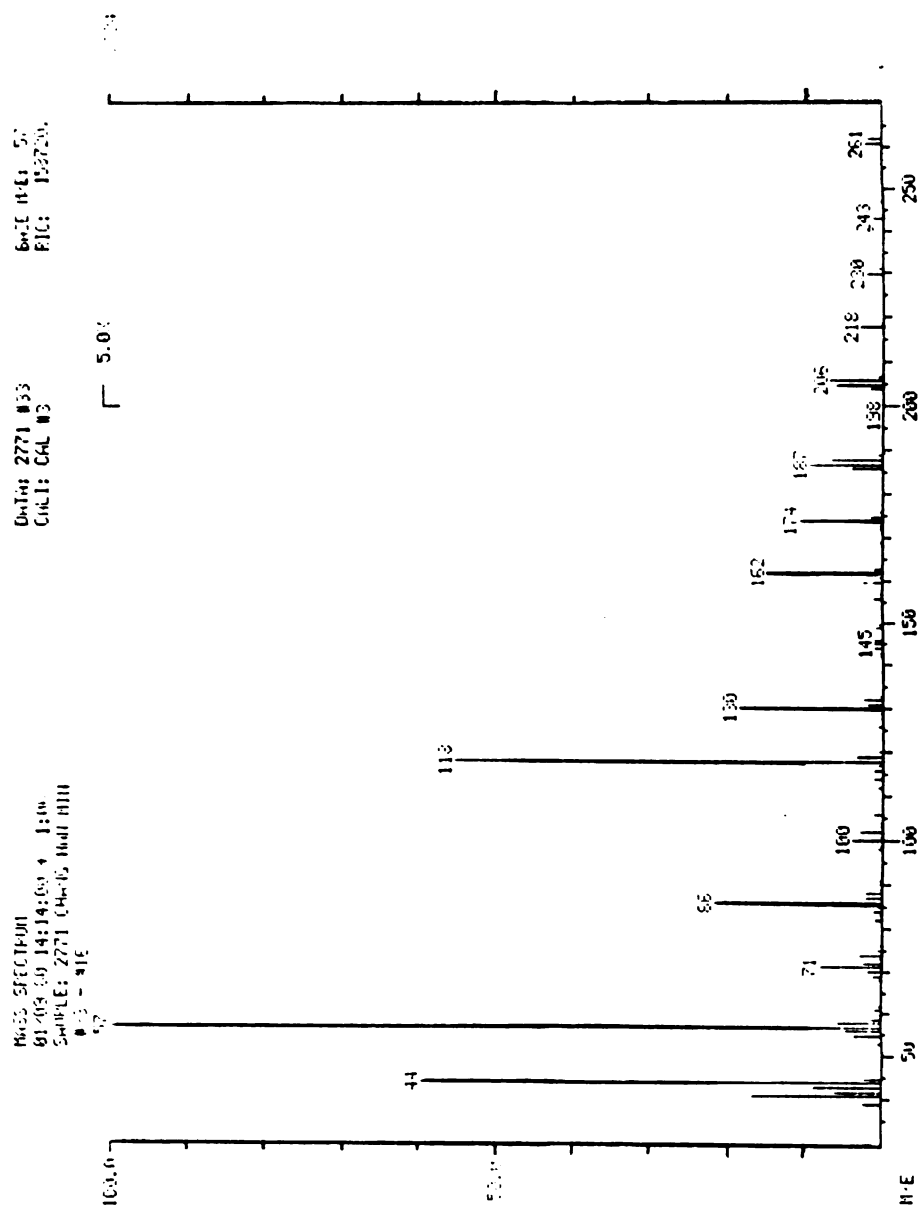


Figure 31 . Mass spectrum of (R)-4-Me-Propos (49)

Figure 32 . Mass spectrum of *N*-BOC-butaphos (53)



Figure 33. Mass spectrum of *N*-BOC-aminodiol (66)

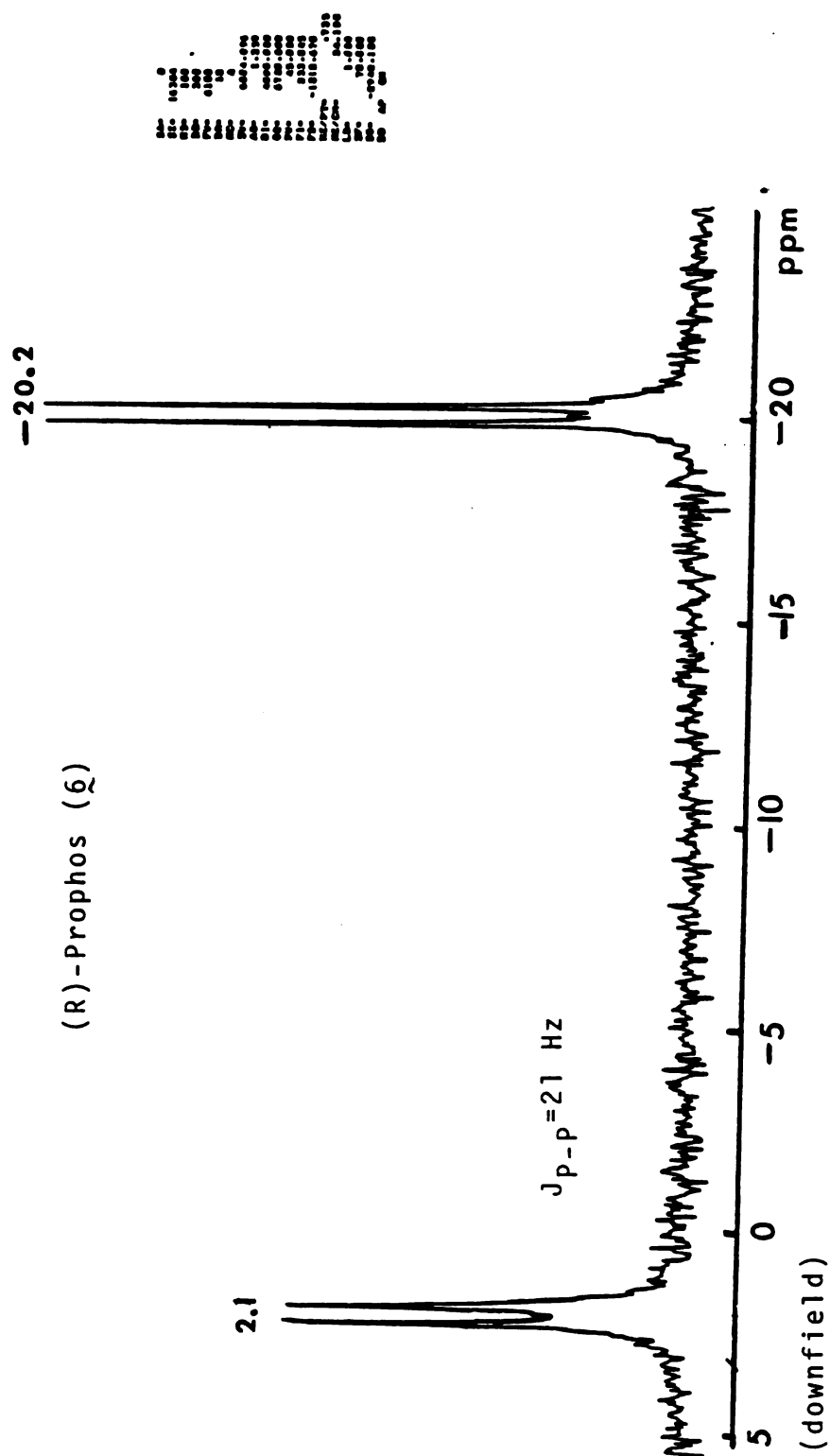


Figure 34.  $^{31}\text{P}$  NMR spectrum of (R)-Prophos ( $\tilde{6}$ ) in  $\text{CDCl}_3$  at  $25^\circ\text{C}$

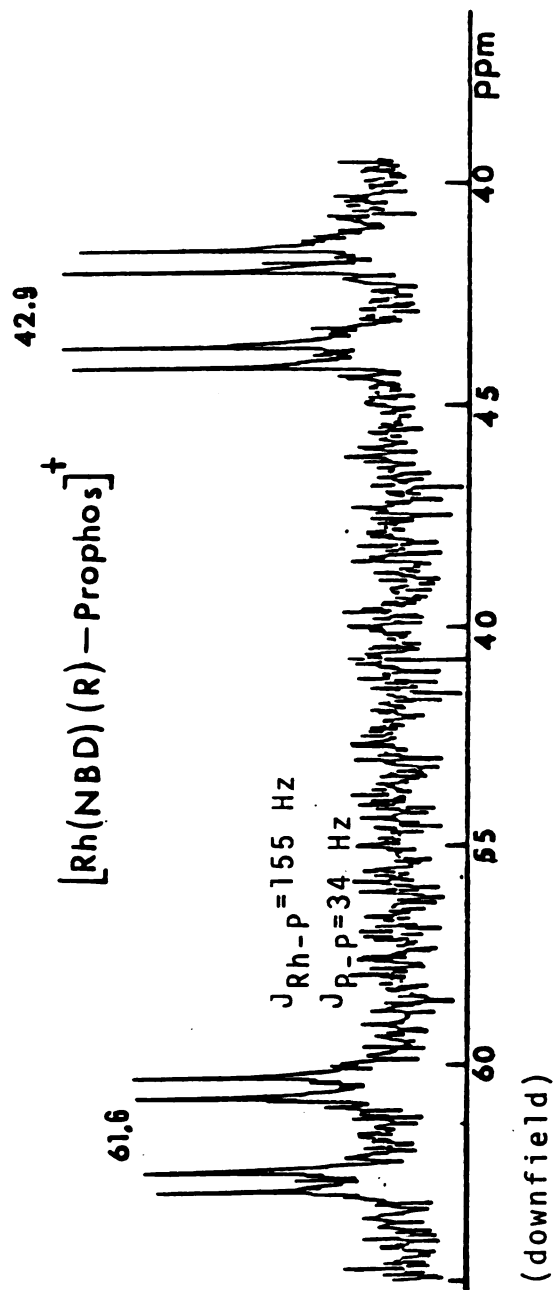


Figure 35.  $^{31}\text{P}$  NMR spectrum of 0.01 M solution of  $[\text{Rh}(\text{NBD})(\text{R})-\text{Prophos}(\text{6})]^+\text{ClO}_4^-$  in  $\text{CDCl}_3$  at  $-20^\circ\text{C}$



26.7

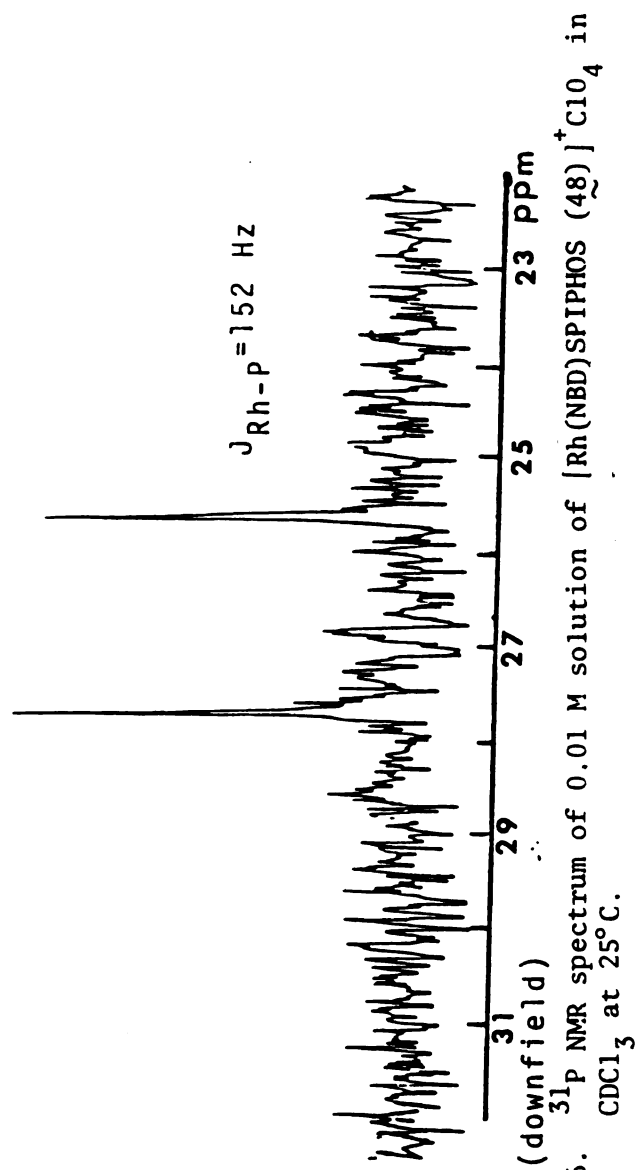


Figure 36.  $^{31}\text{P}$  NMR spectrum of 0.01 M solution of  $[\text{Rh}(\text{NBD})\text{SPIPHOS}(\tilde{48})]^+\text{ClO}_4$  in  $\text{CDCl}_3$  at  $25^\circ\text{C}$ .

- A. 44.3 ppm (dd,  $J_{\text{Rh-P}}=191$  Hz,  $J_{\text{P-P}}=36$  Hz)  
 B. 43.8 ppm, (dd,  $J_{\text{Rh-P}}=191$  Hz,  $J'_{\text{P-P}}=39$  Hz)  
 C. 33.6 ppm (dd,  $J_{\text{Rh-P}}=149$  Hz,  $J_{\text{P-P}}=36$  Hz)  
 D. 28.8 ppm (dd,  $J_{\text{Rh-P}}=149$  Hz,  $J_{\text{P-P}}=36$  Hz)  
 E. 20.2 ppm (dd,  $J_{\text{Rh-P}}=140$  Hz,  $J'_{\text{P-P}}=39$  Hz)  
 F. 15.5 ppm (dd,  $J_{\text{Rh-P}}=140$  Hz,  $J'_{\text{P-P}}=39$  Hz)

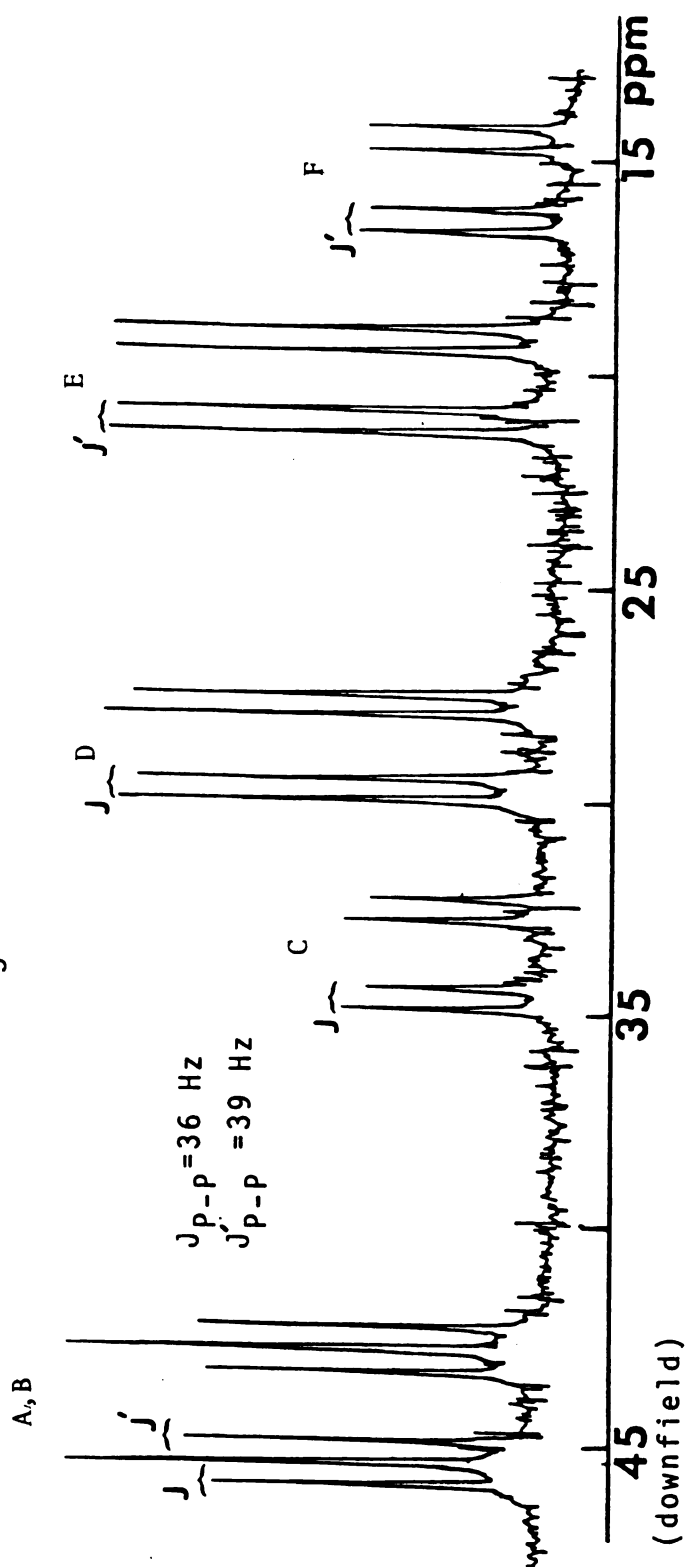
Rh SPIPHOS  $\text{PPh}_3$  Cl

Figure 37.  $^{31}\text{P}$  NMR spectrum of 0.01 M solution of Rh SPIPHOS (48)  $\text{PPh}_3$  Cl in  $\text{CDCl}_3$  at  $10^\circ\text{C}$ .

Table 39. High Resolution Mass Spectrum of (R)-4-Me-Propios  
(49)

SYMBOL	VALENCE	MASS	UL	LL
C	4	12.00000000	**	0
H	1	1.00782522	**	0
P	3	30.97376300	**	0

UL OF \*\* MEANS COMPUTER CALCULATES LIMIT.

MASS # 1      468.21459000    ACC 0.005  
 RINGS AND DOUBLE BONDS: -3.0 TO 18.0

MASS	DIFF	PPM	RDB	FORMULA
468.21358	-0.00101	2.15	16.0	C   H   P 31   34   2

Table 40. High Resolution Mass Spectrum of N-BOC-butaphos (53)

SYMBOL	VALENCE	MASS	UL	LL
C	4	12.00000000	50	38
H	1	1.00782522	60	40
O	2	15.99491410	4	0
P	3	30.97376300	4	0
N	3	14.00307440	3	0

UL OF \*\* MEANS COMPUTER CALCULATES LIMIT.

MASS # 1      653.35352000    ACC 0.005  
 RINGS AND DOUBLE BONDS: -3.0 TO 18.0

MASS	DIFF	PPM	RDB	FORMULA
653.35083	-0.00269	4.12	17.5	C   H   O   P   N 40   50   4   1   2
653.35517	0.00165	2.52	17.0	C   H   O   P   N 41   53   2   2   1

Table 41. High Resolution Mass Spectrum of Benzyl-diol (59)

SYMBOL	VALENCE	MASS	UL	LL
C	4	12.00000000	**	0
H	1	1.00782522	**	0
O	2	15.99491410	**	0

UL OF \*\* MEANS COMPUTER CALCULATES LIMIT.

MASS # 1 196.10965000 ACC 0.005  
RINGS AND DOUBLE BONDS: -3.0 TO 18.0

MASS	DIFF	PPM	RDB	FORMULA
196.10995	0.00030	1.51	4.0	C H O 11 16 3

Table 42. High Resolution Mass Spectrum of (64)

SYMBOL	VALENCE	MASS	UL	LL
C	4	12.00000000	**	0
H	1	1.00782522	**	0
N	3	14.00307440	**	0
O	2	15.99491410	**	0

UL OF \*\* MEANS COMPUTER CALCULATES LIMIT.

MASS # 1 201.17156000 ACC 0.005  
RINGS AND DOUBLE BONDS: -3.0 TO 18.0

MASS	DIFF	PPM	RDB	FORMULA
201.17020	-0.00136	6.76	2.0	C H N 7 19 7
201.17154	-0.00002	0.09	1.5	C H N O 9 21 4 1
201.17288	0.00132	6.57	1.0	C H N O 11 23 1 2
201.16752	-0.00404	20.09	-2.5	C H N O 4 21 6 3
201.16886	-0.00270	13.42	-3.0	C H N O 6 23 3 4

Table 43. High Resolution Mass Spectrum of *N*-BOC-aminodiol (66)

---

SYMBOL	VALENCE	MASS	UL	LL
C	4	12.00000000	**	0
H	1	1.00782522	**	0
N	3	14.00307440	**	0
O	2	15.99491410	**	0

UL OF \*\* MEANS COMPUTER CALCULATES LIMIT.

BASE # 2 261.19633000 ACC 0.005  
 RINGS AND DOUBLE BONDS: -3.0 TO 18.0

MASS	DIFF	PPM	RDB	FORMULA
261.19535	-0.00098	3.74	6.0	C H N 14 23 5
261.20122	0.00489	18.73	2.5	C H N 6 21 12
261.19669	0.00036	1.39	5.5	C H N O 16 25 2 1
261.19720	0.00087	3.33	-1.5	C H N O 1 21 14 2
261.19267	-0.00366	14.01	1.5	C H N O 11 25 4 3
261.19854	0.00221	8.46	-2.0	C H N O 3 23 11 3
261.19401	-0.00232	8.88	1.0	C H N O 13 27 1 4
261.19988	0.00355	13.60	-2.5	C H N O 5 25 8 4
261.20122	0.00489	18.73	-3.0	C H N O 7 27 5 5



## BIBLIOGRAPHY

# BIBLIOGRAPHY

1. (a) Morrison, J.D.; Mosher, H.S., "Asymmetric Organic Reactions", Prentice-Hall, Englewood Cliffs, New Jersey, 1971.  
(b) Scott, J.W.; Valentine, D. Jr., Science, 1974, 184, 943-952.  
(c) Valentine, D. Jr.; Scott, J.W., Synthesis, 1978, 329-356.  
(d) Apsimon, J.W.; Sequin, R.P., Tetrahedron, 1979, 69, 2797-2842.
2. (a) Morrison, J.D.; Masler, W.F.; Neuberg, M.K., Adv. Catal., 1976, 25, 81-124.  
(b) Caplar, V.; Comisso, G.; Sunjic, V., Synthesis, 1981, 85-116.  
(c) Merrill, R.E., CHEMTECH, 1981, 118-127.
3. Horner, L; Buthe, H; Siegel, H., Tetrahedron Lett., 1968, 4023-4026.
4. Horner, L; Siegel, H; Buthe, H. Angew. Chem, 1968, 80, 1034, Angew. Chem., Int. Ed. Engl., 1968, 9, 942.
5. Knowles, W.S.; Sabacky, M.J., J. Chem. Soc., Chem. Commun., 1968, 1445-1446.
6. Morrison, J.D.; Benett, R.E.; Aquiar, A.M.; Morrow, C.J.; Phillips, C., J. Am. Chem. Soc., 1971, 93, 1301-1303.
7. (a) Dang, T.P.; Kagan, H.B., J. Chem. Soc., Chem. Comm., 1971, 481.  
(b) Kagan, H.B.; Dang, T.P., J. Am. Chem. Soc., 1972, 94, 6429-6433.
8. Knowles, W.S.; Sabacky, M.J.; Vineyard, B.D., J. Chem. Soc., Chem. Comm., 1972, 10.
9. Fryzuk, M.D.; Bosnich, B., J. Am. Chem. Soc., 1977, 99, 6262-6267.
10. Fryzuk, M.D.; Bosnich, B., J. Am. Chem. Soc., 1978, 100, 5491-5494.

11. King, R.B.; Bakos, J; Hoff, C.D.; Marko, L., J. Org. Chem., 1979, 44, 1729-1731.
12. Brown, J.M.; Murrer, B.A., Tetrahedron Lett., 1979, 4858-4862.
13. Riley, D.P.; Shumate, R.E., J. Org. Chem. 1980, 45, 5187-5193.
14. Brunner, H; Pieronczyk, W., Angew. Chem., 1979, 91, 655-656; Angew. Chem., Int. Ed. Engl., 1979, 18, 620-621.
15. Samuel, O; Couffignal, R.; Lauer, M; Zhang, S.Y.; Kagan, H.B., Nouv. J. Chim., 1981, 5, 15-20.
16. Vineyard, B.D.; Knowles, W.S.; Sabacky, M.J.; Bachman, G.L.; Weinkauff, D.J., J. Am. Chem Soc., 1977, 99, 5946-5952.
17. Dang, T.P.; Poulin, J.C.; Kagan, H.B., J. Organomet. Chem., 1975, 91, 105-115.
18. Glaser, R.; Twaik, M.; Geresh, S.; Blumenfeld, J., Tetrahedron Lett., 1977, 4635-4638.
19. Achiwa, K., J. Am. Chem. Soc., 1976, 98, 8265-8266.
20. Ojima, I.; Achiwa, K., J. Chem. Soc., Chem. Commun., 1977, 428-430.
21. (a) Achiwa, K.; Kogure, T.; Ojima I., Tetrahedron Lett. 1977, 4431-4432.  
 (b) Ojima, I; Kogure, T.; Terasaki, T.; Achiwa, K., J. Org. Chem., 1978, 43, 3444-3446.
22. Hayashi, T.; Mise, T.; Mitachi, S.; Yamamoto, K.; Kumada M., Tetrahedron Lett., 1976, 1133-1134.
23. Hayashi, T.; Mise T.; Kumada M., Tetrahedron Lett., 1976, 4351-4354.
24. Hayashi, T.; Katsumura, A.; Konishi, M.; Kumada, M., Tetrahedron Lett., 1978, 425-428.
25. Ojima, I.; Kogure, T.; Achiwa, K., J. Chem. Soc., Chem. Commun., 1977, 428-430.

26. Tamao, K.; Yamamoto, H.; Matsumoto, H.; Miyake, N.; Hayashi, T.; Kumada, M., Tetrahedron Lett., 1977, 1389-1392.
27. Grubbs, R.H.; DeVries, R.A., Tetrahedron Lett., 1977, 1879-1880.
28. Miyashita, A.; Yasuda, A.; Takaya, H.; Toriumi, K.; Ito, T.; Souchi, T.; Noyori, R., J. Am. Chem. Soc., 1980, 102, 7932-7934.
29. Fiorini, M.; Giongo, G.M., J. Mol. Catal., 1979, 5, 303-310.
30. (a) Onuma, K.; Ito, T.; Nakamura, A. Tetrahedron Lett., 1979, 3163-3166.  
 (b) Hanaki, K.; Kashiwabara, K.; Fujita, J., Chem. Lett., 1978, 489-490.
31. Babievske, K.K.; Latov, V.K., Usp. Khim., 1969, 38 1009, Inch, T.D., Synthesis, 1970, 2, 466-473.  
 Izumi, Y., Angew. Chem., 1971, 83, 956-966.
32. Dumont, W.; Poulin, J.C.; Dang, T.P.; Kagan, H.B., J. Am. Chem. Soc., 1973, 95, 8295-8299.
33. Takaishi, N.; Imai, H.; Bertelo, C.A.; Stille, J.K., J. Am. Chem. Soc., 1978, 100, 264-268.
34. Achiwa, K., Chem. Lett., 1978, 905-908.
35. Baker, G.L., Dissertation, Dept. of Chem., Colorado State University, 1980, 180 pp.; Dissertation Abstracts International, Vol. 41, No.11, May 1981. Order No. 8110793.
36. Kagan, H.B.; Langlois, N.; Dang, T.P., J. Organomet. Chem., 1975, 90, 353-365.
37. (a) Halpern, J., Trans. Am. Crystallogr. Assoc., 1978, 14, 59-70.  
 (b) Chan, A.S.C.; Pluth, J.J.; Halpern, J., Inorg. Chim. Acta., 1979, 37, L477-L479.  
 (c) Chan, A.S.C.; Pluth, J.J.; Halpern, J., J. Am. Chem. Soc., 1980, 102, 5952-5954.
38. Brown, J.M.; Chaloner, P.A., J. Am. Chem. Soc., 1980, 102, 3040-3048.

39. Halpern, J. ; Riley, D.P.; Chan, A.C.S.; Pluth, J.J., J. Am. Chem. Soc., 1977, 99, 8055-8057.
40. Chan, A.C.S.; Pluth, J.J.; Halpern, J., J. Am. Chem. Soc., 1980, 102, 5952-5954.
41. (a) Ojima, I.; Kogure, T.; Yoda, N., Chem. Lett., 1979, 495-498.
- (b) Ojima, I.; Kogure, T.; Yoda, N., J. Org. Chem., 1980, 45, 4728-4739.
42. Halpern, J.; Okamoto, T.; Zakhariev, A., J. Mol. Catal., 1977, 2, 65-68.
43. Koenig, K.E.; Knowles, W.S.; J. Am. Chem. Soc., 1978, 100, 7561-7564.
44. Detellier, C.; Gelbard, G.; Kagan, H.B., J. Am. Chem. Soc., 1978, 100, 7556-7561.
45. Grim, R.E., "Clay Mineralogy", 2nd Ed., McGraw-Hill Book Company, New York, NY, 1968, pp. 77-92.
46. (a) Lahav, N.; Shani, V.; Shabtai, J., Clays and Clay Minerals, 1978, 26, 107-115.
- (b) Endo, T.; Mortland, M.M.; Pinnavaia, T.J., Clays and Clay Minerals, 1980, 28, 105-110.
- (c) Yamanaka, S.; Brindley, G.W., Clays and Clay Minerals, 1979, 27, 119-124.
- (d) Yamanaka, S.; Brindley, G.W.; Hattori, M., Clays and Clay Minerals, 1980, 28, 281-284.
47. Lussier, R.J.; Magee, J.S.; Vaughan, D.E.W.,
48. (a) Pinnavaia, T.J.; Welty, P.K., J. Am. Chem. Soc., 1975, 97, 3819-3820.
- (b) Pinnavaia, T.J.; Welty, P.K.; Hoffman, J.F., in "Proceedings of the International Clay Conference", 1975, Applied Publishing Ltd., Wilmette, Illinois, pp. 373-381.
- (c) Quayle, W.H.; Pinnavaia, T.J., Inorg. Chem., 1979, 18, 2840-2847.
49. Pinnavaia, T.J.; Raythatha, R.; Lee, J.G.S.; Halloran, J.; Hoffman, J.F., J. Am. Chem. Soc., 1979, 101, 6891-6897.

50. Raythatha, R.H.; M.S. Thesis, Dept. of Chem., Michigan State University, 1978.
51. Farzaneh, F.; Ph.D. Dissertation, Dept. of Chem., Michigan State University, 1981.
52. DeVries, R.A.; Ph.D. Dissertation, Dept. of Chem., Michigan State University, 1980.
53. Baltazzi, E.Q., Rev., Chem. Soc., 1955, 9, 150-173.
54. Herbst, R.M.; Shemin, D., "Organic Syntheses", Collect. Vol. 1; Wiley; New York, NY, 1943, p. 1-3.
55. Carter, H.E.; Risser, W.C., J. Biol. Chem., 1941, 159, 255-262.
56. Dakin, H.D., J. Biol. Chem., 1929, 82, 439-446.
57. Harrington, C.R.; McCartney, W., Biochem. J., 1927, 852-856.
58. Levy, G.C.; Nelson, G.L., "Carbon-13 Nuclear Magnetic Resonance for Organic Chemists", Wiley-Interscience, N.Y., 1972.
59. Horeau, A., Tetrahedron Lett., 1969, 3121-3124.
60. Sinou, D.; Kagan, H.B.; J. Organomet. Chem., 1976, 114, 325-337.
61. Gelbard, G.; Kagan, H.B.; Stern, R., Tetrahedron, 1976, 32, 233-237.
62. MacNeil, P.A.; Roberts, N.K.; Bosnich, B., J. Am. Chem. Soc., 1981, 103, 2273-2280.
63. Schrock, R.R.; Osborn, J.A., J. Am. Chem. Soc., 1976, 98, 2134-2143.
64. Poulin, J.C.; Dang, T.P.; Kagan, H.B., J. Organomet. Chem., 1975, 84, 87-92.
65. Masuda, T.; Stille J.K., J. Am. Chem. Soc., 1978, 100, 268-272.
66. (a) Chan, A.S.C.; Halpern, J., J. Am. Chem. Soc., 1980, 102, 838-840.  
(b) Brown, J.M.; Chaloner, P.A., J. Chem. Soc., Chem. Commun., 1980, 344-346.

67. Slack, D.A.; Baird, M.C., J. Organomet. Chem., 1977, 142, C69-C72.
68. Brown, J.M.; Chaloner, P.A., J. Am. Chem. Soc., 1978, 100, 4307-4309.
69. Eliel, E.L., "Stereochemistry of Carbon Compounds", McGraw-Hill: New York, 1962; Chapter 8.
70. Achiwa, K.; Ohga, Y.; Iitaka, Y., Tetrahedron Lett., 1978, 4683-4686.
71. Mori, K.; Takigawa, T.; Matsuo, T., Tetrahedron, 1979, 35, 933-940.
72. Morrison, J.D.; Masler, W.F., J. Org. Chem., 1974, 270-272.
73. Bianco, V.D.; Doronzo, S., "Inorganic Syntheses", Vol. XVI; McGraw-Hill Book Company, New York, NY, 1976, P. 161-163.
74. Abel, E.W.; Bennett, M.A.; Wilkinson, G., J. Chem. Soc., 1959, 3178-3182.
75. Chatt, J.; Venanzi, L.M., J. Chem. Soc. A., 1957, 4735-4741.